

UNCLASSIFIED

AD NUMBER
AD812108
NEW LIMITATION CHANGE
TO Approved for public release, distribution unlimited
FROM Distribution authorized to U.S. Gov't. agencies and their contractors; Administrative/Operational Use; 01 JAN 1967. Other requests shall be referred to Air Force office of Scientific Research, Bolling AFB, Washington, DC 20332.
AUTHORITY
AFOSR ltr, 12 Nov 1971

THIS PAGE IS UNCLASSIFIED

95 00

SOME RELATED COMPOUNDS

D D C
 RECEIVED
 APR 21 1967
 RELIVE
 BO

1 JANUARY 1967



U.S. DEPARTMENT OF COMMERCE
NATIONAL BUREAU OF STANDARDS

Best Available Copy

Distribution of this
document is ~~restricted~~

THE NATIONAL BUREAU OF STANDARDS

The National Bureau of Standards is a principal focal point in the Federal Government for assuring maximum application of the physical and engineering sciences to the advancement of technology in industry and commerce. Its responsibilities include development and maintenance of the national standards of measurement, and the provisions of means for making measurements consistent with those standards; determination of physical constants and properties of materials; development of methods for testing materials, mechanisms, and structures, and making such tests as may be necessary, particularly for government agencies; cooperation in the establishment of standard practices for incorporation in codes and specifications; advisory service to government agencies on scientific and technical problems; invention and development of devices to serve special needs of the Government; assistance to industry, business, and consumers in the development and acceptance of commercial standards and simplified trade practice recommendations; administration of programs in cooperation with United States business groups and standards organizations for the development of international standards of practice; and maintenance of a clearinghouse for the collection and dissemination of scientific, technical, and engineering information. The scope of the Bureau's activities is suggested in the following listing of its three Institutes and their organizational units.

Institute for Basic Standards. Applied Mathematics. Electricity. Metrology. Mechanics. Heat. Atomic Physics. Physical Chemistry. Laboratory Astrophysics.* Radiation Physics. Radio Standards Laboratory.* Radio Standards Physics; Radio Standards Engineering. Office of Standard Reference Data.

Institute for Materials Research. Analytical Chemistry. Polymers. Metallurgy. Inorganic Materials. Reactor Radiations. Cryogenics.* Materials Evaluation Laboratory. Office of Standard Reference Materials.

Institute for Applied Technology. Building Research. Information Technology. Performance Test Development. Electronic Instrumentation. Textile and Apparel Technology Center. Technical Analysis. Office of Weights and Measures. Office of Engineering Standards. Office of Innovation and Innovation. Office of Technical Resources. Clearinghouse for Federal Scientific and Technical Information.**

*Located at Boulder, Colorado, 80301.

**Located at 5265 Port Royal Road, Springfield, Virginia, 22171.

NAME	
DATE TYPE PLANNING JUSTIFICATION	REVIEW SECTION <input checked="" type="checkbox"/> DIST. SECTION <input type="checkbox"/> TELETYPE <input type="checkbox"/>
DISTRIBUTION/AVAILABILITY CODES DIST. AVAIL. AND/OR SPECIAL	
7	F

Best Available Copy

1493

NATIONAL BUREAU OF STANDARDS REPORT

NBS PROJECT

221-0404
221-0405
221-0426
222-0423
223-0442
223-0513
313-0430

(11) 1 January 1967

(12) 226p.

(14) NBS REPORT
NBS-9500

(6) PRELIMINARY REPORT
ON THE THERMODYNAMIC PROPERTIES OF
SELECTED LIGHT-ELEMENT AND
SOME RELATED COMPOUNDS,

(15) ARPA Order-20

(The previous reports in this series have the NBS Report Nos. 6297, 6484, 6645, 6928, 7093, 7192, 7437, 7587, 7796, 8033, 8186, 8504, 8628, 8919, 9028, and 9389.)

(16) AF-9713-02, NBS-221-0444

Technical Summary Report,
on the Thermodynamic Properties
of Light-Element Compounds

Reference: U. S. Air Force Order No. OAR ISSA 65-8

IMPORTANT NOTICE

NATIONAL BUREAU OF STANDARDS REPORTS are usually preliminary or progress accounting documents intended for use within the Government. Before material in the reports is formally published it is subjected to additional evaluation and review. For this reason, the publication, reprinting, reproduction, or open-literature listing of this Report, either in whole or in part, is not authorized unless permission is obtained in writing from the Office of the Director, National Bureau of Standards, Washington 25, D.C. Such permission is not needed, however, by the Government agency for which the Report has been specifically prepared if that agency wishes to reproduce additional copies for its own use.

(16) Charles W. ...
Thomas ...



(18) AFOSR
(19) 67-0891

U. S. DEPARTMENT OF COMMERCE
NATIONAL BUREAU OF STANDARDS

11. 24...

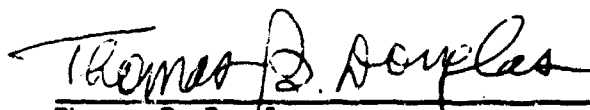
mk

ABSTRACT

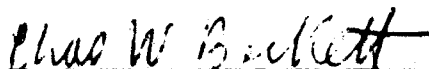
Thermodynamic and related properties of substances important in current high-temperature research and development activities are being investigated under contract with the U. S. Air Force Office of Scientific Research (USAF Order No. OAR ISSA 65-8) and the Advanced Research Projects Agency (ARPA Order No. 20). This research program is a direct contribution to the Interagency Chemical Rocket Propulsion Group, Working Group on Thermochemistry, and, often simultaneously, to other organizations oriented toward acquiring the basic information needed to solve not only the technical problems in propulsion but also those associated with ballistics, reentry, and high-strength high-temperature materials. For given substances this needed basic information comprises an ensemble of closely related properties being determined by a rather extensive array of experimental and theoretical techniques. Some of these techniques, by relating thermodynamic properties to molecular or crystal structure, make it possible to tabulate these properties over far wider ranges of temperature and pressure than those actually employed in the basic investigations.

This report presents improved values for the heats of formation and some other thermodynamic properties of a number of light-element substances -- resulting from recent NBS experimental studies (calorimetric, vaporization, and spectroscopic) and critical literature review. Methods, results, and earlier published values are discussed critically and in detail. The standard heat of formation of $\text{BF}_3(\text{g})$ was determined by direct combination of the elements in a bomb calorimeter and with an estimated error of ± 0.5 kcal mol⁻¹. $\text{OF}_2(\text{g})$ was found to be endothermic ($+5.86 \pm 0.3$ kcal mol⁻¹) from flame calorimetry on the reactions of OF_2 , O_2 , and F_2 with H_2 . The results of a precise entrainment (transpiration) study of the sublimation of $\text{AlF}_3(\text{c})$ were combined with published data to give new values for the thermodynamic properties of $\text{AlF}_3(\text{g})$ and $\text{Al}_2\text{F}_6(\text{g})$. A final revised report on high-temperature mass spectrometry of the $\text{BeO}-\text{BeF}_2$ system discusses interfering ion intensities, and evaluates the heat of sublimation of $\text{BeF}_2(\text{gl})$ and the standard heat of formation of $\text{Be}_2\text{OF}_2(\text{g})$. A quadrupole mass spectrometer appears to have shown that liquid Al_2O_3 loses oxygen and becomes non-stoichiometric, a result consistent with the earlier NBS discovery of an irreversible change in sublimed $\text{Al}_2\text{O}_3(\text{c})$. To illustrate light-element hydroxide

molecules, CsOH(g) and CsOD(g) showed high-temperature microwave spectra indicative of a linear or near-linear molecule, a low-frequency large-amplitude bending vibration producing an unusual variation in the rotational constant, and a highly ionic Cs-O bond. The dipole moment also was derived. From the current revision of NBS Circular 500, recommended values of ΔH_{f298}^0 for 39 Be-containing substances (including different states) of special interest are given, together with discussions of the underlying published data. Recent design and experimental studies have led to a proposed feasible procedure for automatic power measurement to complement the existing NBS automatic temperature measurement in precise low-temperature heat-capacity calorimetry.



Thomas B. Douglas
Project Leader



Charles W. Beckett
Assistant Division Chief for Thermodynamics
Heat Division, Institute for Basic Standards

TABLE OF CONTENTS

	<u>Page</u>
Abstract	1
 Chap. 1. <u>THE HEAT OF FORMATION OF BORON TRIFLUORIDE</u> <u>BY DIRECT COMBINATION OF THE ELEMENTS</u> (by Eugene S. Domalski and George T. Armstrong) .	
Abstract	1
1. Introduction	2
2. Materials	5
2.1 Boron	5
Table 1. Analysis of boron sample	6
Table 2. Composition of fluorine sample	8
3. Preparation of Sample Pellets	9
Table 3. Amounts of sample and losses incurred during pellet preparation (averages)	10
4. Calorimetric System	11
5. Products of Combustion	12
Table 4. Composition of residual product gases from a combustion experiment (mass spectrometric examination)	13
6. Calibration Experiments	14
7. Fluorine Combustion Experiments	15
Table 5. Boron-Teflon combustion experiments	16
8. Discussion and Results	20
9. Summary of Errors	23
Table 6. Summary of errors	24
10. Heat of Formation of Boron Trifluoride	25
References	28
 Chap. 2. <u>STUDIES ON THE AUTOMATION OF LOW-TEMPERATURE</u> <u>HEAT-CAPACITY CALORIMETRY</u> (by G. T. Furukawa)	
I. Introduction	31
Figure 1	31
II. Symbols, Abbreviations, and Definitions	33
III. General Requirements for Energy Measurements	34

TABLE OF CONTENTS (Continued)

	<u>Page</u>
III.1 Calorimeter Heater	36
III.2 Power Measurements	36
Figure 2	36
III.3 Stable Reference Voltage Sources	37
III.4 Voltmeters and Potentiometers	37
III.5 Automatic Digital Voltmeters	38
III.6 Application of Integrating Digital Voltmeters	39
IV. Self Generation of Reference Voltage for Calorimetry and Automatic Measurement of Input Energy	41
IV.1 Circuit for Power Measurements	41
Figure 3	41
IV.2 Voltage Transfer Capacitors and Their Effects on the Measurements	42
IV.3 Energy Dissipation by the Digital Voltmeter	43
IV.4 Constant Current Power Supply	43
IV.4.1 Effects of the Calorimeter Heater-Dummy Resistor Switch	43
IV.4.2 Effects of the Chopper	45
IV.4.3 Determination of the Constant Current Power Supply Current	46
IV.5 Results of Preliminary Test Experiments	46
V. Time Control of Automatic Heat-Capacity Measurements	46
VI. Conclusion	49
VII. References	49

Chap. 3. STRUCTURE OF THE ALKALI HYDROXIDES. I. MICROWAVE SPECTRUM OF GASEOUS CsOH

(by David R. Lide, Jr., and Robert L. Kuczkowski)	50
Abstract	50
Introduction	51
Experimental	52
Analysis of Spectrum	55
L-Type Doubling	61
Vibrational Energies	62
Bending Potential Function	63

TABLE OF CONTENTS (Continued)

	<u>Page</u>
Structure	65
Dipole Moment	66
Summary	67
Acknowledgment	67
References	68
Table I. Observed frequencies in CsOH	69
Table II. Observed frequencies in CsOD	70
Table III. Effective rotational constants for various vibrational states of CsOH and CsOD	71
Table IV. Variation of rotational constants with v_1	72
Table V. k -Doubling constants.	73
Table VI. Fit of $B_{0v_2}^k$ to power series	74
Table VII. Structural parameters of cesium hydroxide	75
 Chap. 4. <u>THE VAPOR PRESSURE, VAPOR DIMERIZATION, AND HEAT OF SUBLIMATION OF ALUMINUM FLUORIDE, USING THE ENTRAINMENT METHOD</u> (by Ralph F. Krause Jr. and Thomas B. Douglas)	 76
Abstract	76
Introduction	77
Entrainment Method	79
Fig. 1. Diagram of Entrainment Tubes in the Cylindrical Furnace	80
Vapor Cell Temperature	82
Test for Saturation	83
Monomeric Vapor Assumption	85
Table I. Results for Reaction 1 by Assuming Wholly Monomeric Vapor	86
Generation of Hypothetical Values	87
Entropy of Sublimation	89
Fig. 2(a). Hypothetical values of $\Delta H_{1000}^0(3)$, consistent with this work, versus arbitrary mol fraction of dimer, N_d , 1000 at selected values of ΔT and $\Delta S_{1000}^0(1)$	90

TABLE OF CONTENTS (Continued)

	<u>Page</u>
Fig. 2(b). $\Delta H_{1000}^2(1)$ vs. $N_{d,1000}$	91
Fig. 2(c). $\Delta S_{1000}^0(2)$ vs. $N_{d,1000}$	92
Recommended Values	95
Table II. Thermodynamic Values for Reactions 1, 2, and 3 at 1000°K	97
Fig. 3. Third Law values of ΔH_{1000}^0 for $AlF_3(c) = AlF_3(g)$ for several vapor pressure measure- ments corrected for dimer	99
Acknowledgments	100
 Chap. 5. <u>A MASS SPECTROMETRIC STUDY OF THE BeO-BeF₂</u> <u>SYSTEM AT HIGH TEMPERATURES</u> (by J. Efimenko)	
1. Introduction	101
2. Experimental	101
2.1 Mass Spectrometer	101
2.2 Beryllium Difluoride	101
2.3 Beryllium Oxide	102
2.4 BeO + BeF ₂	102
3. Results and Discussion	103
3.1 Beryllium Difluoride	103
3.2 Beryllium Oxide	103
Table 1. Data, BeF ₂ (s) = BeF ₂ (g)	104
Table 2. Vapor Species from BeF ₂ ·xH ₂ O + BeO During Initial Heating	106
Fig. 1. A least squares fit to the data of Table 1	107
3.3 BeO-BeF ₂ System	108
Table 3. Mass Spectrometric Temperature-Intensity Data	110

TABLE OF CONTENTS (Continued)

	<u>Page</u>
Table 4. Mass Spectrometric Temperature-Intensity Data	111
Table 5. Auxiliary Data for Computations	112
Fig. 2. Formation of Be ₂ OF ₂ (g) between 1510°K and 1890°K	113
Fig. 3. Formation of Be ₂ OF ₂ (g) between 1870°K and 2200°K	114
References	115
 Chap. 6. <u>VAPORIZATION OF REFRACTORY MATERIALS:</u> <u>ARC-IMAGE MASS SPECTROMETRY</u> (by J. J. Diamond and A. L. Drago)	
	116
 Chap. 7. <u>THE STATUS OF THE THERMOCHEMICAL</u> <u>DATA ON SOME Be COMPOUNDS</u> (by Vivian B. Parker)	
	117
I. Introduction	117
II. Discussion of Data	117
Be(c), Be(g)	117
BeO(c), BeO(g), Be ₂ O(g), (BeO) _n (g)	118
BeH(g), Be(OH) ₂ (α, tetragonal and β, orthorhombic), Be(OH) ₂ (g)	119
BeF(g)	120
BeF ₂ (c, quartz), BeF ₂ (amorphous) and BeO(c)	121
BeF ₂ (g), BeF ₂ (aq), H ₂ BeF ₄ (in conc. aqueous HF)	123
BeF ₂ (aq, in HF solutions), Be ₂ OF ₂ (g), H ₂ BeF ₄ (aq, in conc. aqueous HF), BeCl(g)	124
Table I	125
BeCl ₂ (c, α and c, β), BeCl ₂ (g)	126
BeCl ₂ (aq, dilute)	127
BeCl ₂ (aq, in 68H ₂ O + 6.38 HCl), BeCl ₂ ·4H ₂ O(c), Be ₂ Cl ₄ (g), BeBr ₂ (c), BeI ₂ (c)	128
Be ₃ N ₂ (c, α and c, β), Be ₃ C(c)	129
Be ₃ SiO ₄ (c), Be(BO ₂) ₂ (g), Be ₃ B ₂ O ₅ (c), BeOAl(g), BeO·Al ₂ O ₃ (chrysoberyl)	130
Bibliography	133
Table I. Selected Values for Some Be Compounds at 298°K	138

TABLE OF CONTENTS (Continued)

	<u>Page</u>
Chap. 8. <u>FLUORINE FLAME CALORIMETRY. II. THE</u> <u>HEATS OF REACTION OF OXYGEN DIFLUORIDE,</u> <u>FLUORINE, AND OXYGEN, WITH HYDROGEN.</u> <u>THE HEAT OF FORMATION OF OXYGEN DIFLUORIDE.</u> (by R. C. King and G. T. Armstrong) . . .	140
Abstract	140
1. Introduction	140
2. Apparatus, General Experimental Procedures, and Calibration	142
2.1 The Reaction Vessel	142
Earlier Burner Design	142
Fig. 1. Burner for Fluorine Flame Calorimetry	143
New Burner Design	144
Fig. 2. Burner for Fluorine Flame Calorimetry (New Design)	145
Fig. 3. Complete Assembly of Reaction Vessel	146
Fig. 4. Combustion Chamber and Solution Vessel	147
2.2 The Calorimetric Equipment	148
Calorimeter	148
Electrical Calibration System	149
Fig. 5. Bath Temperature Control Record	150
Flow System	152
Fig. 6. Plot Showing Variation of Current and Voltage Readings	153
Fig. 7. Flow System	154
Fig. 8. Fuel Sample Container Ignition System	156
2.3 General Experimental Procedures	157
Adjustment of the Jacket Temperature	157
Preparation of the Burner	157
Preparation of the Fuel Sample, Absorbers, and Calorimeter Can	157
Conduct of a Reaction Experiment	158
Conduct of an Electrical Calibration Experiment	159
Calculation of the Corrected Temperature Rise	159
Fig. 9. Variation of Calorimeter Temperature with Time	160

TABLE OF CONTENTS (Continued)

	<u>Page</u>
2.4 Electrical Calibrations	161
Table 1. Calibration of Calorimeter	162
3. The Reaction Experiments	163
3.1 The Oxygen Difluoride-Hydrogen Reaction	163
Analysis of the Oxygen Difluoride .	163
Fig. 10. Gas Sampling Manifold (F_2 and OF_2) . . .	165
Fig. 11. IR Spectrum of OF_2 Sample	166
Fig. 12. Manifold for Introducing OF_2 Sample Into Chromatograph . . .	167
Fig. 13. Chromatogram of OF_2 Sample on Silica Gel ($0^\circ C$)	169
Fig. 14. Chromatogram of OF_2 Sample on Silica Gel ($50^\circ C$)	170
Calorimetric Experiments	171
Analysis for the Reaction Products .	171
Table 2. Reaction Quantities of Oxygen Difluoride .	173
Tests for Corrosion of the Reaction Vessel	174
Table 3. Tests for Metal Ions in HF Solutions . . .	175
Heat Measurements for the OF_2 - H_2 Reaction	176
Corrections to the Heat Data . . .	176
Table 4. Heat Measurements (OF_2 - H_2)	177
Table 5. Corrections to Heat Measurements	178
Thermal Correction for the Corrosion of the Reaction Vessel	179
Table 6. Treatment of Heat Data (OF_2 - H_2) . . .	181
Table 7. Heat of Reaction . .	183
Heat of Reaction of Oxygen Difluoride with Hydrogen	184

TABLE OF CONTENTS (Continued)

	<u>Page</u>
3.2 The Fluorine-Hydrogen Reaction . . .	185
Analysis of the Fluorine . . .	185
Fig. 15. Manifold for Chromatographic Analysis of Impurities in Fluorine	187
Fig. 16. Chromatogram of Impurities in Fluorine on Molecular Sieves, 5A	189
Fig. 17. Chromatogram of Impurities in Fluorine on Silica Gel . . .	190
Table 8. Comparison of Chromato- graphic and Mass Spectrometric Analyses for Impurities in Fluorine . . .	191
Table 9. Analysis of Fluorine Sample . . .	192
The Calorimetric Experiments . . .	193
Analysis of the Reaction Product for Hydrogen Fluoride . . .	194
Tests for Corrosion of Combustion Chamber . . .	194
Table 10. Reaction Quantities of Fluorine . . .	195
Heat Measurements for the F_2-H_2 Reaction . . .	196
Table 11. Test for Corrosion in F_2-H_2 Experiments .	197
Table 12. Heat Measurements for the F_2-H_2 Reaction	198
Thermal Correction for the Corrosion of the Reaction Vessel . . .	199
Table 13. Corrections to the Heat Data for the F_2-H_2 Reaction . . .	200
Table 14. Treatment of the Heat Data (F_2-H_2) Reaction	201
3.3 The Oxygen-Hydrogen Reaction . . .	203
Analysis of the Oxygen . . .	203
The Calorimetric Experiments . . .	204
Fig. 18. Chromatogram of Oxygen on Molecular Sieves, 5A	205
Table 15. Reaction Quantities in Oxygen-Hydrogen Reactions . . .	206

TABLE OF CONTENTS (Continued)

	<u>Page</u>
Heat Measurements for the O_2-H_2	
Reaction	207
Table 16. Heat Measurements (O_2-H_2)	208
Table 17. Corrections to the Heat Data for the O_2-H_2 Reaction	209
The Heat of Formation of Water	210
4. The Heat of Formation of Oxygen Difluoride	211
5. The Work of Earlier Investigators	212
5.1 On the Heat of Formation of $OF_2(g)$	212
5.2 The Fluorine-Hydrogen Reaction	217
5.3 The Heat of Formation of $H_2O(l)$	218
6. Appendix	219
6.1 The Vaporization of Water from the Reaction Vessel	219
Table 18. m_{H_2O} Removed from Reaction Vessel vs. m_{H_2O} Condensed in Vessel	220
6.2 Correction for the Tempering of the Gases	221
References	224

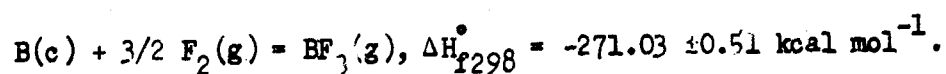
Chapter 1

THE HEAT OF FORMATION OF BORON TRIFLUORIDE BY DIRECT COMBINATION OF THE ELEMENTS¹

Eugene S. Domalski and George T. Armstrong

Abstract

The energy of combination of crystalline boron in gaseous fluorine was measured in a bomb calorimeter. The experimental data combined with reasonable estimates of all known errors may be expressed by the equation:



This result is compared with other recent work on and related to the heat of formation of boron trifluoride.

¹This research was sponsored by the Air Force Aero Propulsion Laboratory, Research and Development Division, Air Force Systems Command, Wright-Patterson Air Force Base, Ohio, under USAF Delivery Order Nr. 33(615)64-1003, and by the Air Force Office of Scientific Research under Order No. OAR ISSA 65-8.

1. Introduction

An accurate value for the heat of formation of boron trifluoride is of significant importance because this value is involved in the thermochemistry of many boron compounds.

The study of the compounds thermochemistry of boron/was for a long time hampered by difficulties in measuring a suitable reaction involving elemental boron. The heat of formation of boric oxide, for instance, was uncertain to several kilocalories per mole because of the difficulty of getting complete combustion of the element in oxygen, or of determining the amount of reaction, in the absence of complete combustion. The difficulty was apparently due to the glassy and non-volatile character of the boric oxide the formed, which tended to terminate/reaction before completion, and made the analysis of the product a complex problem.

The thermochemistry of boron was placed on a firm basis by the work of Prosen, Johnson and Pergiel [1,2]² on the decomposition and hydrolysis of diborane, and of Johnson, Miller and Prosen [3] on the heat of formation of boron trichloride from the elements. With the aid of the heats of these reactions and other data, they obtained reasonably consistent values for $\text{B O}_3(\text{c})$, $\text{H}_3\text{BO}_3(\text{c})$, $\text{B}_2\text{H}_6(\text{g})$ and $\text{BCl}_3(\text{g})$. While more recent work has suggested changes in some of the values, these changes have been small.

² Numbers in brackets refer to references at the end of this paper.

The heat associated with the direct combination of the elements in a bomb calorimeter was measured by Wise, Margrave, Feder and Hubbard [4], who found the heat of formation of $\text{BF}_3(\text{g})$

to be $-269.88 \pm 0.24 \text{ kcal mol}^{-1}$. Another study involving the direct combination of the elements by Gross, Hayman, Levi and Stuart [5] gave $-271.20 \text{ kcal mol}^{-1}$ for the heat of formation of $\text{BF}_3(\text{g})$.

More recent additional measurements by Johnson, Feder and Hubbard [6] showed that the calorimetric work of Wise, et al. [4] was correct, but re-analysis of the boron sample revealed impurities not previously taken into account. A recalculation of their earlier data gave for $\Delta H_{f298}^{\circ}[\text{BF}_3(\text{g})]$, ^{calorimetric} $-271.6 \pm 0.9 \text{ kcal mol}^{-1}$. The / measurements reported by Johnson, et al. [6] were made using a boron sample of greater purity in both a conventional-type combustion bomb and a two-chambered combustion bomb and led to a value for $\Delta H_{f298}^{\circ}[\text{BF}_3(\text{g})]$ of $-271.65 \pm 0.22 \text{ kcal mol}^{-1}$.

Research prior to the work of Wise, et al. [4] is neither sufficiently detailed nor accurate enough to derive a value for the heat of formation of BF_3 having an uncertainty less than several kilocalories per mole, and hence, has not been considered. Gmelin [7] provides a review of the earlier work on this subject for the interested reader.

that

We felt/additional confirmatory work on the heat of formation of BF_3 was needed to establish more fully the recent work of Gross, et al. [5] and Johnson, et al. [6]. In addition, we have found that work in our laboratory on the measurement of the heats of combustion of several refractory boron compounds has produced values for their heats of formation very sensitive to the auxiliary value used for the heat of formation of boron trifluoride. Some systematic errors in the calculated heats of formation may be avoided by measuring the heat of combustion of boron using a similar procedure in the same apparatus. The variations in the heat of formation of BF_3 , as reported by other investigators, are large enough to make a significant difference in the heats of formation of metallic borides if calculated from their heats of combustion in fluorine.

2.0 Materials

2.1 Boron

The sample of β -rhombohedral boron was obtained from the Eagle-Picher Company and had been

prepared by the hydrogen reduction of boron tribromide on a substrate of zone refined boron. The maximum particle size was 150 mi-

crons. The supplier reported traces of copper and silicon and a small amount of carbon in the sample. The sample was analyzed

spectrographically for metallic

impurities and quantitatively for individual metals to 0.001 percent.

A nitrogen assay was made using the Kjeldahl method and the carbon

content was determined by oxygen combustion of the sample and meas-

urement of the CO_2 formed. This measurement gave a higher carbon con-

tent than was indicated by the supplier. We preferred our carbon

analysis for the assay of our sample. The analysis for oxygen in our

boron sample was performed by both neutron activation and inert-

gas fusion methods. The oxygen analysis obtained by inert-gas fusion

is preferred over the analysis by neutron activation because of sus-

pected interference by isotopic species produced from irradiation of the

boron itself[3]. Table I summarizes the analysis of the boron sample,

showing the total boron content to be 99.68 percent by difference.

TABLE 1. Analysis of boron sample^a

Metal impurities								Total
Al	Fe	Mg	Mn	Sr	Ca	Si	Cu	
<0.001	0.079	0.002	0.014	0.002	0.010	0.012 (0.0003) ^b	- (0.0007) ^b	0.120

Non-metallic impurities				
N	O	C		
<0.005	0.088 ^c (0.161) ^d	0.11 (0.05) ^e	0.203	

Assumed presence of non-metallic impurities				
BN	B ₂ O ₃	B ₄ C		
0.009	0.128	0.506		0.643

Total boron content			99.677	
Total boron as the element				99.237

^aAnalyses presented in Table 1 were performed by the NBS Analysis and Purification Section, unless otherwise stated.

^bSupplier's analysis (Eagle-Picher Co.)

^cInert-gas fusion (Ledoux and Co.)

^dNeutron activation analysis (General Atomic)

^eSupplier's analysis for carbon in boron by the method of Kuo, Bender and Walker [9].

An x-ray diffraction pattern of the boron sample determined by the NBS Crystallography Section yielded lattice parameters in good agreement with data reported earlier. The lattice parameters were $a=10.922\text{\AA}$ and $c=23.79\text{\AA}$ (compared to $a=10.944\text{\AA}$ and $c=23.811\text{\AA}$ [10]) and the space group found was $R\bar{3}m$.

2.2 Teflon (polytetrafluoroethylene)

The Teflon film and Teflon powder ("Teflon 7") used in preparing pelleted mixtures for combustion experiments were the same as we have described in an earlier publication [11]. Here again neither the Teflon powder nor the Teflon film were modified or treated in any special way prior to use. The energy of combustion, ΔE_{303}° , of the Teflon (film and powder) was $-10,372.8 \text{ Jg}^{-1}$ [11].

The fluorine used in the heat measurements assayed at 99.40 percent F_2 . The fluorine was analyzed by absorbing the F_2 in mercury and observing the pressure and composition of the residual gases [12]. The composition of the residue was determined by examination in a mass spectrometer. Table 2 shows the results of typical analysis of a fluorine sample.

TABLE 2. Composition of fluorine sample

Constituent	Mole Percent
F_2	99.40 ^a
O_2	0.0960
N_2	0.2784
CO_2	0.0175
CF_4	0.1962
Ar	0.0083
SO_2F_2	0.0001
SiF_4	0.0003
C_2F_6	0.0023
SF_6	0.0001
C_4F_8	0.0002
C_3F_8	0.0005
C_2F_4 or cyclic C_4F_8	0.0001

^a By difference.

3.0 Preparation of Sample Pellets

The first step of the procedure used to prepare the boron sample for combustion in fluorine was to mix the sample with Teflon powder in a bag made of Teflon film. The bagged mixture was then pelleted and provided with an additional coating of Teflon (method B of our earlier work[11]). Attempts to burn pelleted mixtures of boron and Teflon powder on which no outer Teflon coating was provided (method A, [11]) resulted in spontaneous combustion of the pellet during the fluorine-loading procedure. However, if method B was used, it was possible to carry out the calorimetric experiment, and the apparent heat transfer coefficients calculated for the calorimeter in these heat measurements were comparable to that of a normal combustion experiment in which no premature reaction was taking place.

Much care is needed in keeping track of the cumulative mass of the sample as the Teflon and boron are added because some losses are always observed and their distribution significantly affects the results of the experiment.

Table 3 gives average values for the amounts of Teflon and boron used in preparing a pellet and the losses detected in the process. The sample masses were adjusted for losses in the manner previously described [11].

The densities used for the Teflon film, Teflon powder, and boron in making buoyancy corrections were 2.15, 2.16 and 2.35 g cm⁻³ [13], respectively. Weighings of pelleted mixtures and intermediate stages were made to 0.01 mg.

TABLE 3. Amounts of sample and losses incurred
during pellet preparation (averages)

1. Mass of Teflon bag, g.	0.30
2. Mass of boron in mixture, g.	0.16
3. Mass of Teflon in mixture, g.	1.88
4. Mass of Teflon coating, g.	0.70
5. Loss of Teflon in sealing bag, mg.	0.32
6. Loss of mixture in pelleting, mg.	0.30
7. Total loss in preparation, mg.	0.62

4.0 Calorimetric System

No major changes had been made in the bomb calorimeter, thermometric system or combustion bomb since our earlier work[11] which was carried out with the same apparatus. The apparatus will be discussed here only briefly.

An isothermal-jacket, stirred-water calorimeter was used; the jacket was maintained at a constant temperature near 30°C within 0.002°C. Temperature changes in the calorimeter were measured to 0.0001°C with a G-2 Mueller bridge in conjunction with a platinum resistance thermometer. Reactions were carried out in an "A" nickel combustion bomb, designed for service with fluorine, having a volume of approximately 360 ml. Two aluminum electrodes each suspended from the bomb head by a monel rod held a tungsten fuse (0.002 in. diam.) which contributed about 20 J to the combustion energy, assuming complete combustion. The quantities of boron and Teflon in the pellets were adjusted to produce a temperature rise in the calorimeter of about three degrees (27° to 30°C). For procedures dealing with the loading and emptying of the combustion bomb, and for details of the design and construction of the fluorine manifold, our earlier work should be consulted[14].

5.0 Products of Combustion

Our previous work[11,14] has established that Teflon burns in 15 to 21 atm of fluorine to carbon tetrafluoride as the only major product. Higher fluorocarbons were not detected in amounts greater than 0.02 mole percent. The product gases were analyzed in a mass spectrometer after absorption of the excess fluorine in mercury. It is interesting to note that the mass spectrometric examination of product gases from a boron-Teflon combustion experiment showed no sign of BF_3 . We suspect that under the conditions of the reaction of fluorine with mercury, an interaction of some kind takes place between BF_3 and the mercury fluoride formed during the absorption of fluorine.

A typical analysis of the residual product gases from a combustion experiment is shown in Table 4. The amounts of minor constituents found in the product gases are greater than those expected on the basis of the amounts present as impurities in the original fluorine. The increments observed in the minor constituents were probably introduced during sampling and analysis procedures and were probably not involved in the actual bomb process.

Boron trifluoride was identified as a combustion product by infrared spectrometry. Examination in the region 650 to 400 cm^{-1} of a sample of the bomb product gases containing excess/fluorine revealed the BF_3 band at 481 cm^{-1} and the CF_4 band at 630 cm^{-1} . Spectra of the evacuated cell and of BF_3 alone were taken over the region mentioned above to substantiate the identification. The cell used was 8 cm long and had polyethylene windows, 0.0625 in. thick.

TABLE 4. Composition of residual product gases from a
combustion experiment (mass spectrometric examination)

Component	Mole Percent
N_2	0.74
O_2	0.87
CO_2	0.16
CF_4	98.4
BF_3	-
SO_2F_2	0.008
SIF_4	0.026
C_2F_6	0.012
SF_6	0.008

6.0 Calibration Experiments

Twenty calibration experiments were performed in which benzoic acid (Standard Sample 391) was burned in 30 atm. of oxygen and with one mL. of distilled water in the nickel combustion bomb. Their consistency and reproducibility have been discussed in our earlier paper [11]. The average energy equivalent was calculated to be $14,803.27 \pm 0.99 \text{ J deg}^{-1}$. The uncertainty cited is the standard deviation of the mean. The energy equivalent is that of the standard initial oxygen calorimeter which included the nickel combustion bomb with 30 atm. of oxygen, a platinum crucible and fuse support wires, platinum fuse (2 cm long, 0.01 cm diam.), a type 304 stainless-steel liner, monel pellet holder, and no sample. Fastened to the bomb was a heater and ignition leads. The mass of the calorimeter vessel and water was 3750.0 grams.

Using the appropriate heat capacity data, the energy equivalent of the standard oxygen calorimeter was adjusted to the proper value for the fluorine experiments. This involved allowing for the heat capacities of 30 atm. of oxygen, one mL. of distilled water, the platinum ware, 21 atm. of fluorine, and two aluminum electrodes. The application of these corrections gave $14,805.17 \text{ J deg}^{-1}$ for the energy equivalent of the standard initial fluorine calorimeter over the temperature range used (27° to 30 °C).

7.0 Fluorine Combustion Experiments

calorimetric

The / measurements included seven experiments, which have been previously reported in detail [11], in which Teflon was burned in 21 atm of fluorine. The value listed in section 2.2 for the energy of combustion, ΔE_{303}° , was determined in these experiments. Ten heat measurements were performed in which boron-Teflon pellets were burned in 21 atm of fluorine. These measurements are summarized in Table 5. In each experiment the sample pellet was placed in the recess of an "A" nickel plate on the bottom of the bomb. The bomb was attached to the fluorine manifold and filled to 21 atm with fluorine by the usual procedure. All bomb parts (bomb base, bomb-head assembly, electrodes, liner and nickel plate) were weighed before the first experiment and after each successive experiment. The bomb parts were washed with water and dried before the weighings were made.

TABLE 5. Boron-Teflon combustion experiments

Experiment No.	1	2	3	4	5
(1a) m(sample), g	0.157378	0.153795	0.151406	0.153477	0.163715
(1b) m(Teflon), g	2.767867	2.813748	2.675968	2.717357	2.880045
(2) P(F ₂) atm.	21.2	21.6	21.4	21.6	21.4
(3) (ε), J deg ⁻¹	14,798.95	14,796.70	14,805.56	14,803.17	14,804.61
(4) Δt _c , deg	3.05494	3.06023	2.94249	2.78886	3.17645
(5) (ε) (-Δt _c), J	-45,209.9	-45,281.3	-43,565.2	-44,244.6	-47,026.1
(6) ΔE fuse, J	20.2	20.5	20.3	20.4	20.4
(7) ΔE gas, J	13.2	13.6	12.8	13.1	13.9
(8) ΔE ^o (Teflon), J	28,710.5	29,186.4	27,757.3	28,186.6	29,874.1
(9) ΔE ₃₀₃ ^o (sample), Jg ⁻¹	-104,627	-104,430	-104,189	-104,410	-104,558
Experiment No.	6	7	8	9	10
(1a) m(sample), g	0.149249	0.152208	0.153996	0.160486	0.167872
(1b) m(Teflon), g	3.243633	3.168021	2.933396	3.053495	2.807221
(2) P (F ₂) atm.	21.8	21.6	21.9	22.0	21.9
(3) (ε), J deg ⁻¹	14,803.77	14,804.26	14,799.88	14,805.01	14,803.61
(4) Δt _c , deg	3.33155	3.29647	3.14578	3.27706	3.15415
(5) (ε) (-Δt _c), J	-49,319.5	-48,801.8	-46,557.1	-48,516.9	-46,692.8
(6) ΔE fuse, J	20.4	20.4	16.9	17.4	18.5
(7) ΔE gas, J	15.8	15.4	14.3	15.1	13.9
(8) ΔE ^o (Teflon), J	33,645.6	32,861.2	30,427.5	31,673.3	29,117.7
(9) ΔE ₃₀₃ ^o (sample), Jg ⁻¹	-104,776	-104,494	-104,538	-104,751	-104,500
(10) ΔE ₃₀₃ ^o (boron sample), Jg ⁻¹	= -104,527 Jg ⁻¹				
(11) Standard Deviation of the Mean	= 54 Jg ⁻¹ = 0.14 kcal mol ⁻¹				
(12) Contribution from impurities	= 545 Jg ⁻¹ for 0.763% impurities				
(13) ΔE ₂₉₈ ^o - ΔE ₃₀₃ ^o	= 2 Jg ⁻¹				
(14) ΔE ₂₉₈ ^o (boron)	= -104,779 Jg ⁻¹ = -270.74 kcal mol ⁻¹				
(15) ΔnRT	= -115 Jg ⁻¹				
(16) ΔH ₂₉₈ ^o (boron)	= -104,894 Jg ⁻¹ = -271.03 kcal mol ⁻¹				

The numbered entries in Table 5 are as follows:

- (1a) mass of the boron mixed with Teflon in the pellet, corrected for weight loss in preparation, for recovery of unburned boron, and for a boron blank.
- (1b) mass of Teflon mixed with sample in the pellet, corrected for weight loss.
- (2) pressure of fluorine introduced into the bomb prior to combustion, corrected to 30°C.
- (3) energy equivalent of the initial calorimeter for a given experiment.
- (4) temperature change of the calorimeter, corrected for heat of stirring and heat transfer.
- (5) total energy change in the bomb process.
- (6) energy liberated by the tungsten fuse assuming the fuse burns according to the reaction: $W(c) + 3F_2(g) = WF_6(g)$

From the heat of formation of WF_6 [15], we calculate 9.44 J mg^{-1} for the energy of combustion of the fuse.

- (7) net energy correction for the hypothetical compression and decompression of bomb gases.

$$\Delta E_{\text{gas}} = \Delta E^i(\text{gas}) \Big|_0^{P_i(\text{gas})} + \Delta E^f(\text{gas}) \Big|_{P_f(\text{gas})}^0$$

- (8) standard energy of combustion per gram of Teflon at 30°C multiplied by the corrected mass of Teflon in the pellet, (1b).
- (9) standard energy of combustion per gram of the sample.
- (10) average standard energy of combustion per gram of the sample.
- (11) standard deviation of the mean of the average cited in (10).
- (12) energy contribution by impurities.
- (13) energy correction converting the reference temperature to 298°K.
- (14) standard energy of combustion of the pure substance. Contributions from impurities have been accounted for both in mass and in energy.
- (15) ΔnRT term.
- (16) standard heat of formation at 298°K.

The heat capacities at constant pressure, C_p , used in the calculation of entries (3) and (13) are as follows in $\text{cal deg}^{-1} \text{g}^{-1}$ at 25°C: boron, 0.245 [16]; and Teflon, 0.28 [17]. The heat capacities at constant volume, C_v , used in the calculation of entries (3) and (13) were 5.52 [18], 12.62 [19] and 10.04 [16] $\text{cal deg}^{-1} \text{mol}^{-1}$, respectively for fluorine, carbon tetrafluoride, and boron trifluoride at 30°C.

Washburn corrections, entry (7), were calculated following the procedure outlined by Hubbard [20] for experiments in which fluorine is used as an oxidant. The coefficients $[\partial E / \partial P]_m = -T[dE/dT]$ were found in tables compiled by Hirschfelder, Curtiss and Bird [21] using the appropriate force constants. The force constants used for fluorine, carbon tetrafluoride and boron trifluoride were those determined by White, Hu, and Johnston [22], Douslin [23] and Brooks and Raw [24], respectively. Force constants appropriate to the mixtures F_2 , CF_4 and BF_3 in the reaction products were calculated from those for the pure components.

We assumed that the metallic impurities in the boron sample were present as the elements and that the non-metals, oxygen, nitrogen and carbon were present as B_2O_3 , BN and B_4C , respectively.

In calculating the correction for the B_4C impurity in the boron sample, we have chosen $\Delta H_{298}^\circ = -97.84 \text{ kJg}^{-1}$ for the reaction: $\text{B}_4\text{C}(c) + 8\text{F}_2(g) = 4\text{BF}_3(g) + \text{CF}_4(g)$ based upon heat measurements performed in our laboratory. These latter data will be reported in more detail in a future publication.

Note that in adjusting the energy of combustion of the sample, entry (10), to the energy of combustion of pure boron, entry (14), the energy contributed by the impurities is subtracted from entry (10), and at the same time the mass of sample is reduced by the mass of the impurities. In calculating the corrections for the combustion of other impurities in the boron sample, the following heat of formation values were used and are given in kcal mol.⁻¹: B₂O₃, -304.20 [25]; BN, -60.8 [25]; MgF₂, -268.7 [26]; CaF₂, -290.3 [27]; SiF₄, -385.98 [28]; FeF₃, -235 [29]; SrF₂, -290.3 [27]; MnF₃, -238 [29]; and AlF₃, -361.0 [11].

The raw data obtained in the benzoic acid calibration experiments were programmed for the IBM 7094 computer according to procedures outlined by Shomate [30] for the computer calculation of combustion bomb calorimetric data. The energy equivalent obtained was adjusted to that of the standard initial oxygen calorimeter as described in Section 6.0. The combustion experiments were similarly programmed, however, the only valid data calculated by the computer were the corrected temperature rise, Δt_c , because the program used had not been modified to accommodate the use of fluorine as the oxidant.

Atomic weights were taken from the 1961 table of atomic weights based on $C^{12} = 12$ and adopted by the International Union of Pure and Applied Chemistry [31]. The unit of energy is the joule, and one calorie was defined as 4.1840 J.

About 500 mg of crystalline boron was transformed into boric acid solution by pyrohydrolysis³ and the solution examined by surface emission mass spectrometry for the isotopic abundance of B^{10}/B^{11} . This study resulted in the atomic weight determination of our sample of 10.812 ± 0.005 .

As a result of the good agreement with the atomic weight of boron in the Table based on $C^{12} = 12$ we have used the value $10.811 \text{ g mol}^{-1}$ from this table in our calculations.

8.0 Discussion and Results

A residue amounting to less than one mg. which was assumed to be unburned Teflon and/or carbon, was observed in heat measurements involving Teflon alone. No correction was applied to any experiment for this residue, and we assumed that the formation of the residue took place in all experiments approximately in proportion to the amount of Teflon initially present. The heat of combustion per gram of Teflon would be constant and the error due to residue formation would be eliminated when the energy due to the combustion of Teflon in the pelleted mixture was subtracted from the total energy released in the combustion.

³ The authors are grateful to M. W. Lerner and L. J. Pinto, U. S. A. E. C. New Brunswick Laboratory, New Brunswick, New Jersey, for performing this task.

After a boron-Teflon combustion experiment, a larger residue was than when only Teflon was burned amount of found, which necessitated determining the/unburned boron and also finding a method for gathering the residue from the nickel support plate. The mass of the residue was obtained by weighing the plate before and after the experiment. The average mass found from these weighings was three mg.

The residue was taken up from the support plate by mixing and rubbing Na_2CO_3 into the residue with a spatula. To determine the amount of boron, the residue mixed with Na_2CO_3 was fused and put into solution with dilute acid. The pH of the solution was adjusted, mannitol added, and the liberated acid titrated with base. The mass of unburned boron found in the residues by this analysis ranged from 0.5 to 1.1 mg. To determine the reliability of the above procedure, control experiments were performed in which crystalline boron was mixed with Na_2CO_3 and the mixture was analyzed for boron using the same procedure. As a result of the control experiments a correction factor was applied to the boron recovered from the residues. Analysis of residues mixed with Na_2CO_3 were made by the NBS Analysis and Purification Section.

We attempted to assign a composition to the residue even though the mass was subject to effects difficult to estimate such as reaction of the support plate with fluorine, hygroscopicity of the residue, and spattering of molten tungsten onto the plate from the ignition process. Our estimate for the boron blank, boron recovery, unburned Teflon, and tungsten account for about two thirds of the mass of the combustion residue. The remainder could be attributed to one of the above effects, but in the absence of definite information no adjustment was made for it.

A test made to determine whether the presence of boron affected the residue of Teflon, indicated a negligible effect. was analyzed and the results showed an amount

A boron-Teflon combustion residue/for carbon,/ amount

comparable to the carbon content of residues formed from burning Teflon alone. A test for weight changes of pellets on exposure to fluorine indicated a slow weight increase, which was not fully reversed on evacuation. A pellet which has been exposed to fluorine and later exposed to moist air showed additional small weight gains, indicating a hygroscopicity resulting from the exposure to fluorine. These effects were small and slow, and no corrections were applied for them. However, they have been taken into account in assessing possible errors.

9.0 Summary of Errors

We have tried to estimate the over-all experimental uncertainty for the heat of formation of $\text{BF}_3(\text{g})$ determined as a result of this investigation. Table 6 lists the errors considered in making the estimate. We have used the loss of sample found during the pelletizing operation as a guide in estimating the error incurred in preparing a pellet (see Table 3, line 6). From this source we estimate an error of 0.10 percent. The two oxygen analyses were 0.161 and 0.088 percent and the two carbon analyses were 0.05 and 0.11 percent. The effect that the differences of the analyses would have upon the heat data introduces an error of 0.06 percent. An error from the reaction of the sample in the bomb prior to ignition was estimated at 0.03 percent. This was based upon the assumption that pre-reaction occurring in the bomb prior to ignition was not more than 5 J hr^{-1} as suggested by mass increments of pelleted mixtures upon exposure to fluorine. We assumed that the determination of unburned boron was not in error by more than 0.1 mg (0.06 percent) and that the additional error in estimating the total composition of the combustion residue is similarly 0.06 percent. Since the carbon in the boron combustion residue was comparable to the carbon from the combustion of Teflon alone, no error has been attributed to the uncertainty in residue left by the combustion of Teflon.

TABLE 6. Summary of errors

Description of errors	Magnitude of error expressed in percent of ΔH_{298}° for boron
1. weighing pellet	0.01
2. loss during sample preparation	0.10
3. analysis of impurities	0.06
4. reaction prior to ignition	0.03
5. determining the amount of unburned boron	0.06
6. determining the composition of the combustion residue	0.06
7. fuse energy	0.01
8. bomb corrosion	0.01
9. calibration experiments	0.01
10. energy of combustion of Teflon [16]	0.03
11. boron combustion experiments	0.12
12. atomic weight of boron	0.05
13. total error (percent)	0.19 ^a

^a(This is equivalent to 0.51 kcal mol⁻¹)..

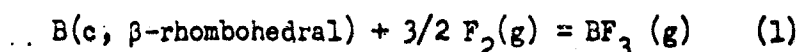
Errors due to the weighing of the pellet, fuse energy, and bomb corrosion were estimated at 0.01 percent. Estimates of uncertainties arising from the benzoic acid calibration experiments, Teflon combustion experiments and combustions of boron-Teflon mixtures were made by multiplying the percent standard deviations of the means of the experiments by the appropriate factors for the Student t distribution at the 95 percent confidence level. Finally, we suggest that the error present in the determination of the atomic weight is 0.05 percent as a result of our experimental findings given in Section 7.0.

The total percent error in this study was found by taking the square root of the sum of the squares of the individual errors cited.

10.0 Heat of Formation of Boron Trifluoride

On the basis of the calorimetric data given

in Table 5, we calculate for the standard heat of reaction (1),

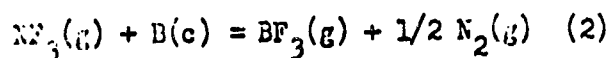


and, hence, the standard enthalpy of formation of boron trifluoride at 298°K, $-271.03 \pm 0.14 \text{ kcal mol}^{-1}$. The latter uncertainty is the standard deviation of the mean. We estimate our over-all experimental uncertainty to be $0.31 \text{ kcal mol}^{-1}$.

Our value for the enthalpy of formation of $\text{BF}_3(\text{g})$ is in good agreement with the result reported by Gross, et al. [5] and differs from the result reported by Johnson, et al. [6] by approximately our over-all uncertainty.

Johnson, et al. [6] have used some recent work by Gunn [32] on the solution of BF_3 in conc $\text{HF}(\text{aq})$, Good and Månsson [33] on the combustion of boron in oxygen in the presence of excess aqueous HF , their own data on $\Delta H_{f298}^\circ[\text{BF}_3(\text{g})]$, and other appropriate auxiliary data to derive a value for $\Delta H_{f298}^\circ[\text{HF} \cdot 3\text{H}_2\text{O}(\text{aq})] = -76.78 \text{ kcal mol}^{-1}$. Insertion of our value for $\Delta H_{f298}^\circ[\text{BF}_3(\text{g})]$ into this cycle, gives $-76.58 \text{ kcal mol}^{-1}$ for $\Delta H_{f298}^\circ[\text{HF} \cdot 3\text{H}_2\text{O}(\text{aq})]$. Both our work and that of Johnson, et al. [6] agree in showing that the heats of formation for aqueous solutions of HF should be more negative than those suggested by Wagman, et al. [34], but less negative than those indicated by Cox and Harrop [35]. In this respect they substantiate our similar finding on the heat of formation of $\text{HF}(\text{aq})$ as derived from several other reactions in our study of the heat of formation of CF_4 [11].

Ludwig and Cooper [36] reported for the heat of reaction (2),



$\Delta H_{298}^\circ = -239.7 \pm 1.2 \text{ kcal mol}^{-1}$. Combining our data on $\Delta H_{298}^\circ [\text{BF}_3(\text{g})]$ with the heat of reaction (2), we calculate for $\Delta H_{298}^\circ [\text{NF}_3(\text{g})]$,

$-31.33 \text{ kcal mol}^{-1}$. Although this is in good agreement with the heat of

formation of $\text{NF}_3(\text{g})$; $-31.44 \text{ kcal mol}^{-1}$ reported by Sinke [37], the

merits of the agreement are dubious because of the large uncertainty

associated with the heat of reaction (2).

References

- [1] E. J. Prosen, W. H. Johnson and F. Y. Pergiel, J. Research NBS 61, 247-250 (1958).
- [2] E. J. Prosen, W. H. Johnson, and F. Y. Pergiel, J. Research NBS 62, 43-7 (1959).
- [3] W. H. Johnson, R. G. Miller and E. J. Prosen, J. Research NBS 62, 213-217 (1959).
- [4] S. S. Wise, J. L. Margrave, H. M. Feder, and W. N. Hubbard, J. Phys. Chem. 65, 2157-9 (1961).
- [5] (a) P. Gross, C. Hayman, P. L. Levi, and M. C. Stuart, Fulmer Research Institute Report R. 146/4/23, Nov. 1960, (b) C. Hayman, private communication, April, 1966.
- [6] G. K. Johnson, H. M. Feder and W. N. Hubbard, J. Phy. Chem. 70, 1-6 (1966).
- [7] Gmelin's "Handbuch der anorganische Chemie", System Nummer 13, Deutscher Verlag, Verlag Chemie G. M. B. H., (a) Hauptband, Leipzig-Berlin, (1962), pages 113-116; (b) Ergänzungsband Weinheim/Bergstrasse, (1954), page 171.
- [8] (a) G. H. Andersen, General Atomic, San Diego, California, private communication, March, 1966. (b) Kaman Nuclear, Technical Note (TN-105), 10 June 1965.
- [9] C. Kuo, G. T. Bender, and J. M. Walker, Anal. Chem. 35, 1505-9 (1963).
- [10] J. L. Hoard and A. E. Newkirk, J. Am. Chem. Soc. 82, 70-6 (1960).
- [11] E. S. Domalski and G. T. Armstrong, J. Research NBS 71A, (1967).
- [12] G. T. Armstrong and R. S. Jessup, J. Research NBS 64A, 49-59 (1960).
- [13] A. E. Newkirk, "Preparation and Chemistry of Elementary Boron", in Borax to Boranes, Advances in Chemistry Series, No. 32, American Chemical Society, Washington, D. C., 1961.
- [14] E. S. Domalski and G. T. Armstrong, J. Research NBS 69A, 137-147 (1965).

References

- [15] O. E. Myers and A. P. Brady, J. Phys. Chem. 64, 521-4 (1960).
- [16] W. H. Evans, NBS, private communication, January 1, 1961.
- [17] W. D. Good, D. W. Scott, and G. Waddington, J. Phys. Chem. 60, 1080-9 (1956).
- [18] W. H. Evans, J. Hilsenrath and H. W. Woolley, NBS, private communication, July 1, 1960.
- [19] Dow Chemical Company, JANAF Thermochemical Tables, PB 168 370 (Clearinghouse for Federal Scientific and Technical Information, Springfield, Virginia, 1965).
- [20] W. N. Hubbard, "Fluorine Bomb Calorimetry", Chapter 6, Experimental Thermochemistry, Vol II, H. A. Skinner, Editor, (Interscience Publishers, Inc., New York, 1962).
- [21] J. O. Hirschfelder, C. F. Curtiss, and R. B. Bird, "Molecular Theory of Gases and Liquids", (John Wiley and Sons, Inc., New York, Copyright 1954, Second Printing 1964).
- [22] D. White, H. Hu, and H. L. Johnston, J. Chem. Phys. 24, 1149-52 (1953).
- [23] D. R. Douslin, paper No. 11, pp. 135-46, "PVT Relations and Intermolecular Potentials for Methane and Carbon Tetrafluoride" in Progress in International Research on Thermodynamics and Transport Properties, J. F. Masi and D. H. Tsai, Editors, (Academic Press, New York, 1962).
- [24] G. L. Brooks and C. J. G. Raw, Trans. Faraday Soc. 54, 972-4 (1958).
- [25] D.D. Wagman, W.H. Evans, I. Hallow, V.B. Parker, S.M. Bailey, and R.H. Schumm, NBS Technical Note 270-2, May 6, 1966.
- [26] E. Rudzitis, H. M. Feder, and W. N. Hubbard, J. Phys. Chem. 68, 2978-81 (1964).
- [27] F. D. Rossini, D. D. Wagman, W. H. Evans, S. Levine, and I. Jaffe, "Selected Values of Chemical Thermodynamic Properties", NBS Circular 500, (U.S. Government Printing Office, Washington, D.C., 1952).

References

- [28] S. S. Wise, J. L. Margrave, H. M. Feder, and W. N. Hubbard, *J. Phys. Chem.* 6, 815-21 (1963).
- [29] L. Brewer, L. A. Bromley, P. W. Gilles, and N. Lofgren, "The Thermodynamic Properties of the Halides", paper 6, *Chemistry and Metallurgy of Miscellaneous Materials: Thermodynamics*, L. L. Quill, Editor, (McGraw-Hill Book Company, Inc., New York, 1950).
- [30] C. H. Shomate, "Computer Calculations of Combustion Bomb Calorimetric Data", Technical Progress Report 327, NOTS TP 3286, U. S. Naval Ordnance Test Station, China Lake, California, August 1963.
- [31] A. E. Cameron and E. Wichers, *J. Am. Chem. Soc.* 84, 4175-97 (1962).
- [32] S. R. Gunn, *J. Phys. Chem.* 69, 1010-5 (1965).
- [33] W. D. Good and M. Mansson, *J. Phys. Chem.* 70, 97-104 (1966).
- [34] D. D. Wagman, W. H. Evans, I. Halow, V. P. Parker, S. M. Bailey and R. H. Schumm, NBS Technical Note 270-1, October 1, 1965.
- [35] J. D. Cox and D. Harrop, *Trans. Faraday Soc.* 61, 1328-37 (1965).
- [36] J. R. Ludwig and W. J. Cooper, *J. Chem. Eng. Data* 8, 76-7 (1963).
- [37] G. C. Sinke, *J. Phys. Chem.* 71, 359-360 (1967).

Chapter 2

STUDIES ON THE AUTOMATION OF LOW-TEMPERATURE HEAT-CAPACITY CALORIMETRY

G. T. Furukawa

I. Introduction

Heat capacity is determined in the incremental heating method from a series of observations as illustrated in Figure 1.

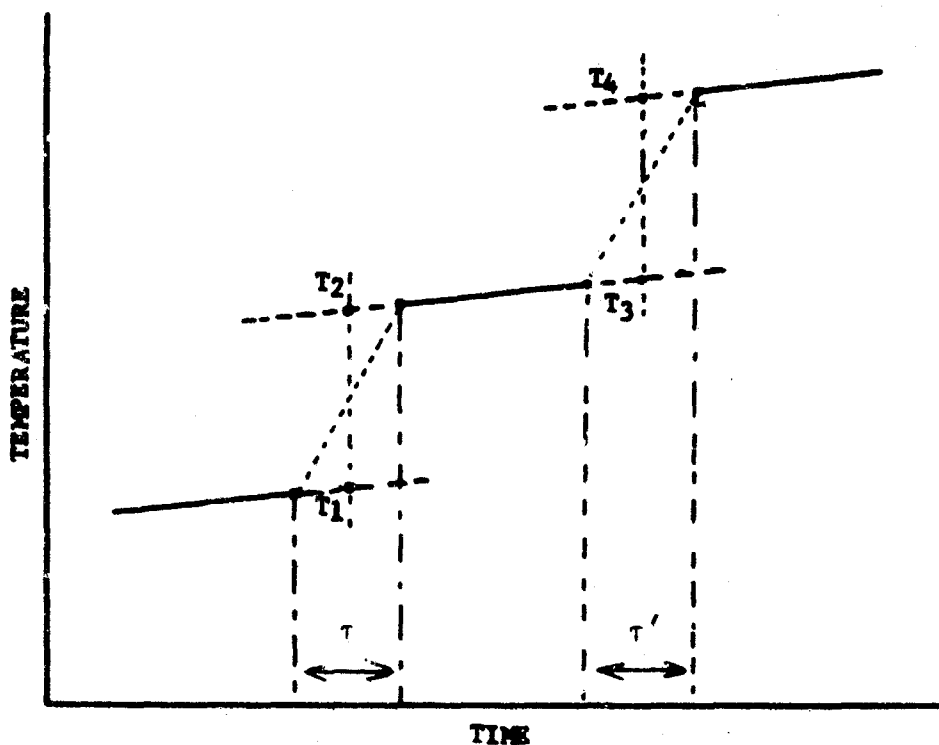


FIGURE 1

Perfect thermal isolation is not achieved even in the most carefully designed low-temperature adiabatic calorimeter used for heat-capacity measurements. This is manifested by the continuously changing temperatures of the calorimetric system under conditions considered adiabatic. Corrections must be applied for the energy transfer between the calorimetric system and its surroundings that occurs during the course of an experiment. Because of the relatively high degree of thermal isolation of low temperature adiabatic calorimeters, the steady-state temperature-time curves before and after any heating interval are essentially linear.

The assumption is made that during the heating interval the heat transfer is the average of the steady-state rates before and after heating. This corresponds to the extrapolation of the steady-state temperature-time curves for the fore- and after-periods to the middle of the heating period as shown in Figure 1. The temperature increments corresponding to the measured energy increments introduced are $T_2 - T_1$ and $T_4 - T_3$.

The observations shown in Figure 1 represent equally the processes in reaction calorimetry and in heats of mixing calorimetry. In all these experiments temperature-time curves are determined. In Bunsen calorimetry the equivalent volume-temperature curves are determined directly or indirectly, for example, through the change in the mass of mercury contained in the system. In heat-capacity experiments the input energy is known from direct measurements and the corresponding temperature increment determined from the temperature-time curves. In heats of reaction or mixing experiments the heat capacity of the system is known from calibration and temperature increment caused by the energy release of the process is determined from the temperature-time curves. The methods used to determine the temperature increment in reaction calorimetry and in heat of mixing calorimetry are very similar to the method just described for the heat-capacity measurements [1].

The temperature-time observations and the calculations of temperature increments associated with energy increments depicted in Figure 1 have now been automated for low-temperature heat-capacity measurements. Automatic observations of temperatures equal in precision to standard manual methods of platinum resistance thermometry have been performed in this laboratory since May 1964. Computer methods have been developed for making calibration corrections for the bridge resistances used, for the plotting of the observations, for calculating the temperatures associated with resistances extrapolated to the midpoint of heating intervals, and for estimating the standard deviations of the extrapolated temperatures.

Methods for the automatic measurement of energy increments introduced into the calorimeter and methods for the automation of the heat-capacity measurement process have, in the meantime, been under investigation. The goal for the accuracy of electrical energy measurements was set at 0.001 percent. Preliminary test experiments have been performed to check out certain methods. This report is an account of the studies made in which procedures and methods for realizing automatic energy measurements are described. The discussions presented in this report progress in evolutionary steps, starting from the development of the basic and adjuvant equipment for attaining the final automatic energy measurements. Much of the discussions on the evolutionary steps have been made brief in order to proceed quickly to the proposed method for automatic energy measurements.

II. Symbols, Abbreviations, and Definitions

The symbols, terminology, and abbreviations used in this report are defined in this section.

- foreperiod = period prior to the start of energy input during which accurate temperatures are made to evaluate the heat leak and the "initial" temperature.
- afterperiod = period following the termination of energy input during which accurate temperature measurements are made to evaluate the heat leak and the "final" temperature. When energy increments are introduced successively, the afterperiod of one energy increment is the foreperiod of the next energy increment (See Figure 1).
- initial temperature = temperature corrected for heat leak by extrapolating the foreperiod curve ahead to the middle of the heating period, corresponds to the "temperature" prior to introducing heat. (e.g., T_1 and T_3 of Figure 1).
- final temperature = temperature corrected for heat leak by extrapolating the afterperiod curve back to the middle of the heating period, corresponds to the "temperature" after introducing heat. (e.g., T_2 and T_4 of Figure 1).
- sampling time = time required to complete a measurement, e.g., voltage.
- voltmeter = the instrument will be referred to in a very restricted sense. The essential difference between this instrument and the digital voltmeter is only that the latter is automatic and the former is manually operated and the balance visually observed. The features of the instrument include:
- self-contained precision power supply, derived usually from 110 V ac, for generating voltages for comparison which are manually selectable
 - high input impedance amplifier detector and meter for indication of balance.

operate time	= time interval from relay coil energization to the performance of a particular functions. In this study, operate time = time interval from the end of one function to the beginning of another function.
standard resistor	= stable resistor of known magnitude.
dummy resistor	= auxiliary resistor, of resistance close to that of the calorimeter heater, through which the current is diverted when not flowing through the calorimeter heater in order to maintain the power supply load constant.
J	= joule
P	= power = $J \text{ sec}^{-1}$ = watt
Hz	= Hertz = cycles per second
R	= resistor or its magnitude
R_s	= standard resistor or its magnitude
R_c	= calorimeter heater or its magnitude
R_D	= dummy resistor or its magnitude
E	= voltage
E_s	= voltage developed across the standard resistor
E_{Ref}	= voltage of stable reference voltage source
E_c	= voltage developed across the calorimeter heater
i	= current through the calorimeter heater
C	= capacitor or capacitance
SW_1	= switch for transferring the current to either R_c or R_D
SW_e	= switch for connecting the voltage measuring equipment to R_c or R_D
F	= Farad
m	= 10^{-3} (milli)
μ	= 10^{-6} micro

W = energy

T = time interval of heating, defined in seconds.

k = voltage to frequency conversion rate =
 counts per volt per second.

N = M = counts on the integrating digital voltmeter.

DVM = digital voltmeter, automatically measures the
 voltage.

BBM = break-before-make action of a double throw
 switch or relay (corresponds to Form C).

MBB = make-before-break action of a double throw
 switch or relay (corresponds to Form D).

III. General Requirements for Energy Measurements

III.1 Calorimeter Heater

With the use of a constant current power supply, the voltage change across the calorimeter heater is directly related to the temperature coefficient of resistance of the heater wire. Shorter sampling times and time intervals between measurements are required for measuring rapidly changing voltages. Instruments tending to meet these requirements become, in general, less accurate. A study was made to find heater wires of low temperature coefficient of resistance over the temperature range used (10 to 380°K). The resistance of alloy wires of about 75% Ni and 20% Cr plus other elements, depending upon the manufacturer, has been found to change only 0.9 percent over the range 10 to 380°K [2]. At the usual heating rate of 1 deg/min and at constant current, the average voltage change across a heater constructed from such wires would only be about 0.002 percent per min. The accurate measurement of voltages changing at such low rates should be relatively easy to achieve.

III.2 Power Measurements

The electrical power dissipated in the calorimeter heater is determined from the relation:

$$P = E_c i \quad (1)$$

where E_c and i are the instantaneous voltage across and current through the heater. A typical calorimeter heater circuit is illustrated in Figure 2. The upper voltage limit of most manual high-precision potentiometers is about 2 volts. The heater voltage can be 20 volts or higher. A voltage divider is, therefore, required at terminals a and b (Figure 2) to perform the measurements. Part of the current that flows through the standard resistor R_s (used for determining the current) now flows through the voltage divider, the relative magnitude depending upon the ratio of the resistance of the heater to that of the voltage divider.

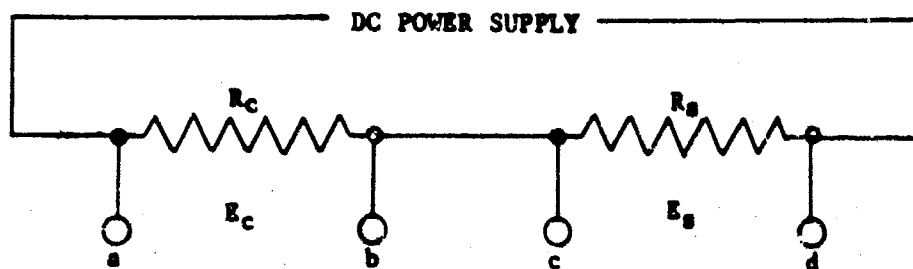


FIGURE 2

In low-temperature calorimeters the leads from the heater are necessarily long and of small gauge and to minimize heat conduction a large portion of the lead wires are temperature controlled. The resistance and the change in resistance with temperature of the leads must, therefore, be considered in the determination of the actual power developed in the calorimeter heater. A method using a voltage divider of exceptionally high resistance plus a sensitive detector of high input impedance can minimize or make negligible the effect of the voltage divider. A procedure for making direct measurements of the heater voltage without the voltage divider would be an even better choice. The present study has been directed toward the latter method.

III.3 Stable Reference Voltage Sources

The use of a voltage divider can be avoided by balancing out or biasing most of the heater voltage by means of a known constant voltage source and by measuring the relatively small difference by means of the potentiometer. The internal resistance of the voltage source must be low enough and that of the detector high enough to achieve the desired sensitivity and accuracy. Reference voltage sources up to 100 volts are available with 0.001 percent or higher stability over a period of a day and longer and with six to seven decades of resolution. With the potentiometer for measuring the difference, the high degree of resolution is not required. The prerequisite of a reference voltage source would be high stability and reproducibility of the voltage for a particular dial setting. Any deviation from the nominal dial setting can be readily corrected by calibration, if the above requirements are met.

III.4 Voltmeters and Potentiometers

The design of reference voltage sources with six to seven decade resolution has led directly to the instrumentation of "voltmeters" and potentiometers which incorporate with the manually variable reference voltage source a high impedance detector with a meter output for visual indication of balance. Most of these instruments have multiple ranges and some are capable of detecting an unbalance of $0.01\mu\text{V}$. In the upper voltage range the instruments are capable of measuring the heater voltage directly. The input impedance of many of these instruments must, however, be carefully examined, for in some ranges the input impedance could be low enough that the calorimeter heater may become excessively loaded and approach the voltage divider condition referred to earlier. Instruments of up to 10^{10} ohm input impedance in the 0.1, 1, 10, and 100 volt full scale ranges, which are most useful for heater voltage measurements, are available in which 0.005 percent accuracy are claimed. Their accuracy can perhaps be improved by calibration.

III.5 Automatic Digital Voltmeters

Numerous automatic digital voltmeters (DVM), based on a variety of design principles, are available that are capable of measuring the heater voltage directly to within 0.01 percent or to 0.005 percent under favorable conditions. Systems having input impedances up to 10^9 or 10^{10} ohms are available so that excessive loading of the calorimeter heater can be avoided. Basically, two methods are used in DVM for measuring the voltages. The first is closely related to the manual voltmeter or potentiometer. Voltages are generated in the instrument by switching in a resistance network or by other methods (e.g., integration of a reference voltage in an integrating circuit) and compared until a null balance is attained. The voltage readout corresponds to the switch positions or to the count of time pulses in the case of the integration method of voltage generations.

The second method used in DVM involves integration of the unknown voltage. In one design the unknown voltage is integrated by means of a high gain amplifier system until an equality with a reference voltage is attained at which time the capacitor is instantly discharged and the integration resumed. In another design the voltage is integrated for a fixed time and at the end of the time the input instantly switched to a reference voltage and the capacitor discharged at a known constant rate. In the first case the repetition rate (voltage to frequency conversion) is the measure of the voltage. In the second case, the time to discharge the capacitor is the measure of the voltage. In both designs any 60 Hz interference is essentially cancelled out by performing the integrations at integral numbers of 60 Hz cycles.

By using a stable reference voltage for balancing a large portion of the heater voltage and by using the lowest range of the digital voltmeter, a higher accuracy can be obtained. The absolute voltage accuracy of the reference voltage source and the digital voltmeter must, however, be compatible. For example, consider the case where 20.2000 volts across the calorimeter heater are partially balanced by 20.0000 volts from the stable reference voltage source. The reading of 0.2 volt to ± 0.0001 volt requires an accuracy of 0.05 percent from the DVM but demands an accuracy of 0.0005 percent for the reference voltage source. These figures are not outside of the capabilities of such instruments. Hence, the method is limited by the absolute constancy and accuracy of the reference voltage source.

An instrument based on the above principle is now available. The accuracy claimed for the instrument is 0.005 percent of the reading or 0.0005 percent of the full scale reading, whichever is worse, with a sampling time of about 1 sec. The input impedance is 10^7 ohms. The accuracy may be improved by better control of the reference voltage source.

III.6 Application of Integrating Digital Voltmeters

A number of DVM based on the voltage to frequency conversion technique described earlier are available. This method yields the average voltage for a given time interval of measurement which is, depending upon the instrument and operating mode, 1 sec or less. If the sensitivity and stability of the main voltage to frequency converter unit is compatible with a $10 \mu\text{V}$ accuracy and if the conversion rate is 10^5 counts per volt per second, then the average voltage during the 1-sec interval could be determined to 1 part in 10^5 , provided that the attenuators or amplifiers used have a linearity and accuracy at least as good. The performance of the instruments that are available at the present time are not quite as good.

The integrating DVM is ideally suited for calorimetry. The total energy introduced into the calorimeter is given by:

$$W = \int_0^{\tau} E_c i dt, \quad (2)$$

where E_c is the instantaneous voltage across the calorimeter heater, τ the time interval of heating, and i the current. If the current is maintained constant,

$$W = i \int_0^{\tau} E_c dt. \quad (3)$$

The quantity within the integral is obtained directly by the integrating DVM. If k (counts per volt per second) is the voltage to frequency conversion rate, then

$$\int_0^{\tau} E_c dt = \frac{N\tau}{k} = \frac{N}{k}, \quad (4)$$

where N is the total count for τ secs of heating. The automatic measurement of the input energy can be performed by adding overflow counters to the integrating DVM to extend the count and by means of a suitable system for simultaneous switching on and off of the calorimeter heater and the DVM. The integrating DVM can also be connected at all times to the calorimeter heater (i.e., at terminals a and b, Figure 2) and the switching on of the heater current be made coincident with the simultaneous resetting and starting of the DVM. The stopping of the DVM should then be coincident with the switching off of the heater current. The accumulated count of the DVM over a known time interval with zero current through the heater yields information on the error to be expected in the accumulated count during the heating period.

An important feature of the method is indicated by eq (4). The time interval τ of integration by the DVM and that of heating need only be the same and it need not be measured at all. Very precise and simultaneous triggering is needed, however, to achieve equality of the time intervals within the desired limits (better than 1×10^{-5}).

The time base for the voltage to frequency conversion rate k must be consistent with the standard time on which the current i is based. Standard cells and the standard time base are both needed to check k .

To obtain a higher accuracy, an integrating DVM can be used to integrate the voltage difference ($E_c - E_{Ref}$) between that of the calorimeter heater and a stable reference voltage source. (Another method will be described later for generating reference voltages.) If E_{Ref} is the stable reference voltage, the total energy input at constant current is:

$$W = i \int_0^T [E_{Ref} + (E_c - E_{Ref})] dt \quad (5)$$

$$= iE_{Ref}\tau + i \int_0^T (E_c - E_{Ref}) dt \quad (6)$$

If the accumulated count on the DVM is M ,

$$i \int_0^T (E_c - E_{Ref}) dt = iM/k \quad (7)$$

and

$$W = i(E_{Ref}\tau + M/k) \quad (8)$$

Equation (8) shows that in this method the time interval, τ , must be measured precisely in terms of the standard time. The stable reference voltage source and the DVM can be left connected at all times to the calorimeter heater, provided the resistance of the system is high enough to have negligible power dissipation in the calorimeter heater during the off period. If the reference voltage source is set at 20 volts and the resistance of the circuit is 10^{10} ohms (input impedance of DVM) the current will be 2×10^{-9} amp and the power dissipated in a 100-ohm calorimeter heater will be only 4×10^{-16} watt. In this method the DVM would be reset and on standby until started and stopped coincidentally with the switching on and off, respectively, of the heater current.

IV. Self Generation of Reference Voltage for Calorimetry and Automatic Measurement of Input Energy

IV.1 Circuit for Power Measurements

The reference voltage source for biasing a large portion of the calorimeter heater voltage can be generated directly in the calorimeter circuit by means of a reliable constant current power supply and a standard resistor. (Constant current power supplies yielding currents constant to 1 or 2 parts in 10^6 are available.) Figure 3 illustrates a circuit arrangement for the method.

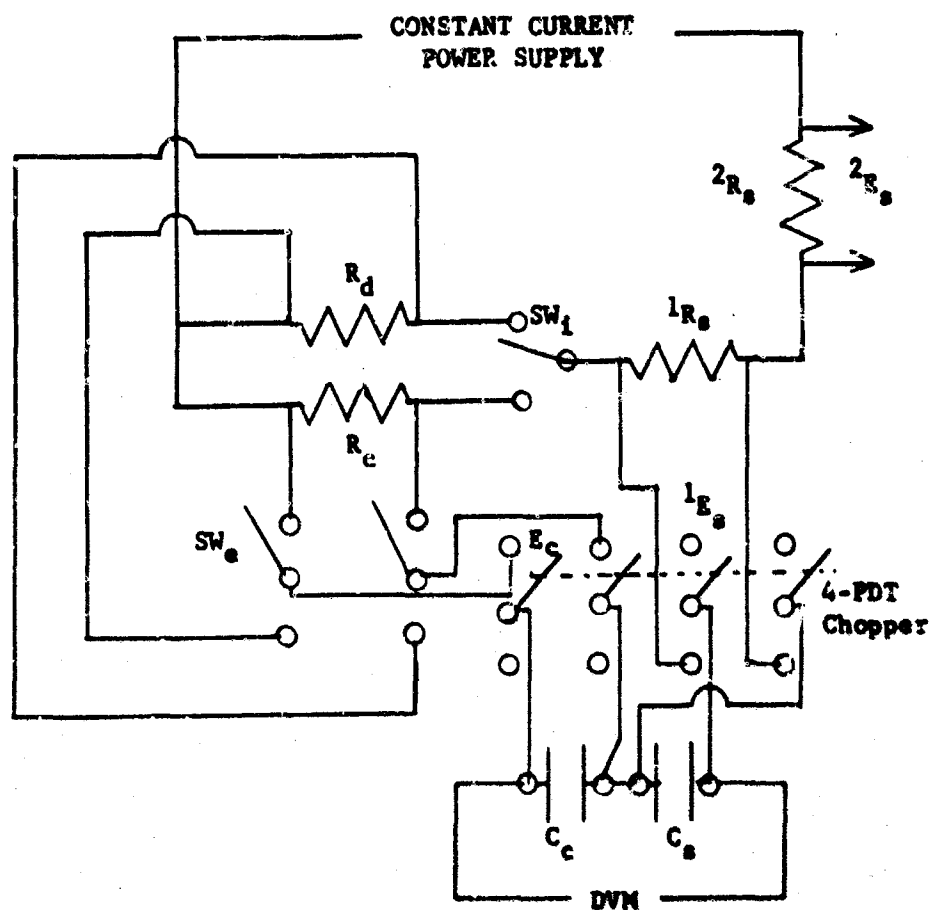


FIGURE 3

At a known constant current, the voltage 1E_S developed across the standard resistor 1R_S is known and constant. The degree of stability and magnitude of the current, i , can be determined by monitoring the voltage 2E_S across another standard resistor 2R_S of a value within the range suitable for measuring occasionally on a manual potentiometer or for biasing the standard cell voltage and recording the small difference continuously on a strip-chart recorder.

The voltage E_C across the calorimeter heater and the voltage 1E_S are transferred alternately in opposition onto the high-grade polystyrene capacitors C_C and C_S , respectively, by means of a 4-pole double-throw chopper (4-PDT). The two pairs of the chopper contacts are operated 180° out of phase with the break-before-make (BBM) arrangement. The voltage differences ($E_C - ^1E_S$) across C_C and C_S are measured by means of an automatic DVM. The power developed in the calorimeter heater is given by:

$$P = i \left[^1E_S + (E_C - ^1E_S) \right] \quad (9)$$

IV.2 Voltage Transfer Capacitors and Their Effects on the Measurements

If R_C and 1R_S are about 100 ohms each and the capacitors are 10 μ F each, the time constant of each RC circuit is 1 msec. When the chopper is operated at 25 Hz with one-third "dwell time" for each pair, the dwell time for each pair of contacts is 13.3 time-constants (13.3 msec). This dwell time is long enough to transfer onto the capacitors all except 2×10^{-6} of the voltages developed across the resistors. If a DVM with an input impedance of 10^{10} ohm is used, the time constant of its circuit will be 5×10^{-4} secs. For a 1-sec sampling time, this will correspond to the reduction of the voltage difference on the capacitors by 2×10^{-5} . This would seem somewhat unfavorable, but in the same second each capacitor will be recharged 25 times and at each time, even if each of the capacitors were completely discharged, charged to within 2×10^{-6} of the voltages across R_C and 1R_S . Since only a small fraction of the charge difference on the capacitors is discharged even during a 1-sec sampling time, the voltages on the capacitors represent closely those across the resistors.

The energy stored in a capacitor is:

$$W = 0.5CE^2 \text{ J} = 0.5Q^2/C \text{ J}, \quad (10)$$

with C in farads, Q in coulombs, and E in volts. When $C = 10 \mu\text{F}$ and $E = 20$ volts, $W = 0.002 \text{ J}$. Except at the lower temperatures (below 40°K),

this energy is negligible compared to the energy dissipated in the calorimeter heater, R_C . Actually, at the lower temperatures, the energy stored in the capacitors will be smaller since lower operating voltages are used. In practice, the capacitor, C_C , could be charged through a "dummy" resistor prior to switching to the calorimeter heater (see Figure 3). The energy transferred to the capacitor during the measurement will, therefore, be much smaller than the total stored energy considered above.

Good quality polystyrene capacitors have 10^6 megohm- μ F resistance. The loss of energy through leakage in such capacitors would be 4×10^{-9} watt ($E = 20$ volts, $C = 10 \mu$ F), which is negligible.

IV.3 Energy Dissipation by the Digital Voltmeter

If the DVM discharges 2×10^{-5} of the charge corresponding to the voltage difference ($E_C - E_S$) in 1 sec and E_C and E_S are within 1 percent, then E_C is reduced by 1×10^{-7} and E_S is increased by 1×10^{-7} in 1 sec because approximately one-half of the total voltage change occurs in each capacitor. (Reference is made to voltage and charge interchangeably since $E = Q/C$.) Since $W = 0.5CE^2$ joule, approximately 2×10^{-10} W joule of energy in the capacitor C_C is dissipated per second. This also means that the energy dissipated in the calorimeter heater each second is less by the above amount. Again, with $C = 10 \mu$ F and $E_C = 20$ volts, this corresponds to 4×10^{-10} watt or with $R_C = 100$ ohms the ratio of powers dissipated in the heater and by the DVM is 10^{10} . Hence, the power dissipated by the DVM is negligible.

The input capacitance of 200 pF or smaller is typical for integrating DVM. The amount of energy absorbed by the DVM would also be negligible.

IV.4 Constant Current Power Supply

Another consideration in the measurement of energy developed in a calorimeter heater is the time constant of the constant current power supply. The effects of the switching of current connections between the calorimeter heater and the dummy resistor and of the switching of the chopper on the power supply have been examined.

IV.4.1 Effects of the Calorimeter Heater-Dummy Resistor Switch

Most of the modern constant current power supplies have a time constant of a few microseconds. Power supplies of 1-msec time constant are, however, adequate for most applications and in many respects are more desirable. In switching from the dummy resistor to the calorimeter heater, a BEM switch action will cause the power supply to experience

momentarily an open circuit and to react to increase its output voltage. The operate time of dry reed relays is about 1 msec and that of mercury relays about 4 msec. If the open circuit condition is kept to a few tenths of a millisecond, a power supply of 1 msec time constant would increase its output voltage relatively little (about 18 percent of the final value). A longer open circuit condition would allow time for the power supply to increase its output voltage accordingly.

If the case is considered of a power supply of maximum output voltage of 100 volts and with 200 μ F capacitance in its output circuit, the total energy stored is 1 joule when enough time is allowed to reach the maximum voltage condition. If the operating voltage is 40 volts, most of the 0.84 J of "excess energy" will be dissipated in the calorimeter circuit, including R_C , L_{Rg} , and R_g , in the first few msec after switching on. If one-half of the excess energy is dissipated in the calorimeter heater and is not accounted for by the measuring equipment, a significant error may arise depending upon the total energy dissipated in the heater during the whole heating period. In measurements at low temperatures, the excess energy could very easily be greater than the apparent measured energy. For a switch of a given speed, the maximum voltage condition will be attained more rapidly by faster acting power supplies. The problem may be circumvented partially by operating close to the maximum voltage and using auxiliary resistors in the circuit; less of the excess energy would then be dissipated in the calorimeter heater. Obviously, the power supply should never be allowed to reach the overload or the unstable condition.

If the switch is operated with the MBB action, the dummy resistor and the calorimeter heater will momentarily be in parallel at both the beginning and the end of a heating period. The reaction of the power supply corresponds to that of rapid exponential discharge or decay at the instant of parallel connection and the relatively slower exponential build-up situation following the connection to either the calorimeter heater or the dummy resistor. The effect from the MBB action of the switch at the end of a heating period is negligible if the "make" period is about 0.2 msec. At the beginning of a heating period an interval corresponding to 11 time constants will be required to recover to within 1×10^{-5} of the decay caused by the momentarily parallel connection. This corresponds at most to the energy of about one time constant times the difference between the full and the decayed power levels. Depending on the total length of the heating period, this amount of energy may be significant with the slower power supply of 1-msec time constant but not with a power supply of a few μ sec time constant.

These considerations suggest that MBB switch action is preferred in high precision calorimetry. When the operate time of the calorimeter heater switch is about 0.1 msec, the switch action may be BEM with the slower 1-msec power supply but must definitely be MBB with the faster 1- μ sec power supply. The choice is not, however, of great concern if the operating time of the switch were very much faster than the time constant of the power supply. The choice of BEM action will depend on how rapidly and how much the excess energy would be built up during the open circuit period, and the choice of MBB action will depend on how rapidly the recovery occurs after the termination of the parallel connection period. The effect of the "make" period of the MBB switch can be reduced by operating the constant current power supply at maximum voltage with auxiliary resistors in series to achieve the desired level of current in the calorimeter heater.

Constant voltage/constant current power supplies have recently become available with automatic "crossover" so that full control can be retained with load resistances from infinity to zero. Load resistances from infinity to the crossover resistance are under constant voltage control and load resistances less than the crossover resistance under constant current control. Since the voltage and current values can be independently selected, the crossover resistance can be located anywhere on the voltage-ampere range of the power supply. When such a power supply of μ sec time constant is operated with the crossover resistance slightly above the calorimeter circuit resistance, the BEM action can become tolerable for the calorimeter heater switch.

IV.4.2 Effects of the Chopper

When the chopper is operated at 25 Hz with one-third of the total time in the break condition and one-third for the dwell times of each pair of chopper contacts, the break period between dwell times is one-sixth of a cycle or 0.7 msec. At the instant of the beginning of the dwell period of one pair of chopper contacts there will be a load change corresponding to the amount of discharge (energy loss) that occurred during the two-thirds of a cycle or 26.7 msec not in contact. As pointed out in a previous paragraph, the total discharge by the DVM during a period of 1 sec is only 10^{-7} of E_C when E_C and E_S differ by 1 percent. The change in E_C during 26.7 msec is, therefore, negligible and correspondingly the load change at the instant of the start of a dwell period will be negligible. The load change at the start of the break period will also be negligible. Since the dwell time is 13.3 msec, if any load change did occur there should be essentially complete recovery even with a 1-msec power supply. The conclusion from these considerations is that if the input impedance of the DVM is as high as 10^{10} ohms, the chopper will have negligible effect on the power supply.

IV.4.3 Determination of the Constant Current Power Supply Current

The current corresponding to the dial settings of the power supply can be calibrated. The repeatability of the current for a particular dial setting can be tested by the same method used in calibration. Auxiliary switches may be either attached directly to the dials or manually set to the calibrated current value for automatic recording. The current should be continuously monitored on a strip-chart recorder. Experience shows that our present laboratory unit is constant to 2×10^{-6} for a day or longer.

IV.5 Results of Preliminary Test Experiments

The usual high precision, time-tested manual method and the automatic DVM method just described were compared in a series of relatively limited power measurements in a calorimeter. The DVM and related equipment were borrowed from the manufacturer. The nominal input impedance of the DVM system was 10^{10} ohms. The results obtained by the two methods were essentially the same.

Since the resistance of the standard resistor R_S should be close to that of the calorimeter heater R_C (100 ohms), the power dissipated in R_S at the level of the highest calorimeter heater current (about 0.2 ampere) will, therefore, be higher than the recommended level of an ordinary standard resistor. The design of a special standard resistor capable of stable operation at suitable higher power levels has been investigated and has been found feasible. The resistor will be relatively large in size for exposing a large surface for heat dissipation (about 4 watts) and will be constructed of a wire of the temperature coefficient of less than 100 ppm/°C at the thermostatted temperature of about 30°C. The preliminary series of test experiments mentioned earlier using the DVM method was limited by the restriction on the operating power level of the ordinary standard resistors that were used.

Another series of experiments were performed in which the reference voltage E_S of eq (9) was supplied by a separate stable reference voltage source. This series of experiments is represented by eq (8) (Section III.6). The chopper and the capacitors obviously were not needed. The heat-capacity results obtained were within the precision of present manual methods.

V. Time Control of Automatic Heat-Capacity Measurements

As shown earlier in Figure 1, the start of a heating period occurs at the instant of the termination of the foreperiod. Similarly, the start of the afterperiod occurs at the instant of the termination of the heating period. In experiments where energy increments are introduced successively, the after period becomes the foreperiod of the next heating

interval. The control of two time intervals, the fore- or the after-period (the off period of the heater) and the heating interval (the on period of the heater), can simply be accomplished by means of a dual range electronic preset counter that is capable of resetting itself and recycling at the end of the second time interval. The preset counter should be precise enough to obtain the time interval of heating directly from its preset counts.

A procedure for automatic heat-capacity measurements and the control functions required of the dual range preset counter are given below. A digital clock of about 0.1 sec precision will be needed to record the running time at which each X and Y counts occur.

1. Test and check out:
 - (a) coolant level, vacuum and automatic adiabatic controls for the calorimeter
 - (b) calibration on the integrating DVM for zero and standard cell readings
 - (c) constant current supply current
 - (d) 4-PDT chopper
 - (e) resistance of dummy resistor (R_D)
 - (f) reading of the voltage difference between R_D and R_S using the DVM.
2. Start the automatic bridge.
 - (a) check readings on a standard resistor
 - (b) switch over to the calorimeter thermometer
 - (c) when the bridge begins to track the thermometer, start recording the resistance values and set the criteria for readout.
3. Decide on the suitable time intervals (counts) for the off and on periods of the calorimeter heater.
4. Set the preset counter for X counts of the off period and Y counts of the (Y-X) counts of the on period of the calorimeter heater.
5. Start the preset counter.
6. At the instant of the coincidence of the X count the following should take place simultaneously:

- (a) switch on the calorimeter heater
 - (b) switch on the integrating DVM
 - (c) record running time of the X coincidence
7. The bridge can be allowed to track the relatively rapid temperature changes that are occurring or stopped coincidentally with the X count.
8. At the instant of the coincidence of the Y count the following should occur simultaneously:
- (a) switch off the calorimeter heater
 - (b) switch off the integrating DVM
 - (c) reset the Y count and start the count towards X
 - (d) record the running time of Y coincidence
 - (e) start the bridge if previously stopped coincidentally with the X count.
9. Record the following data:
- (a) accumulated count on the DVM
 - (b) current i
 - (c) X and Y
10. Reset the DVM.
11. Go to 6.

As the temperature of the calorimeter increases the energy increment must be increased so that the temperature change would be a reasonable size. The adjustment of the preset counts X and Y and of the power supply current should be done before the X count is reached. If the current supply has not stabilized by the time close to the new X count setting, the preset counter could be switched to the stand-by position. The temperature readings will proceed quite independently and unaffected.

Initially, auxiliary electronic counters should be coupled to the start-stop pulses of the DVM and the calorimeter switch to check their equality as required in eqs (4), (7), and (8) of Section III.6. The X and Y coincidences may be sequentially numbered, but the running time records will be adequate to identify them. The running time records will be used to merge the temperature and energy measurement data.

VI. Conclusion

The method outlined should permit us to make automatic measurements of heat capacity. Instruments to which references were made are constantly being improved, but the general procedure for automating the measurements could in principle be as outlined above.

VII. References

- [1] R. S. Jessup, J. App. Phys. 13, 128 (1942).
- [2] G. T. Furukawa, M. L. Reilly, and W. G. Saba, Rev. Sci. Instr. 35, 113 (1964).

Chapter 3

STRUCTURE OF THE ALKALI HYDROXIDES. I. MICROWAVE SPECTRUM OF GASEOUS CsOH^+

David R. Lide, Jr., and Robert L. Kuczkowski*

National Bureau of Standards, Washington, D. C.

ABSTRACT

The microwave spectra of gaseous CsOH and CsOD have been studied in a high-temperature spectrometer. The spectrum indicates a linear or near-linear molecule with a large-amplitude, low-frequency bending vibration. A large number of excited states involving the bending mode and the Cs-O stretching mode have been identified. The rotational constant B_v shows an unusual variation as the bending mode is excited; the cause is not yet understood. The Cs-O bond length is found to be $2.40 \pm 0.01 \text{ \AA}$ and the O-H distance is probably about 0.97 \AA . The electric dipole moment is $7.1 \pm 0.5 \text{ D}$. Relative intensity measurements indicate a Cs-O stretching frequency of about 400 cm^{-1} and a bending frequency in the neighborhood of 300 cm^{-1} . All of the evidence supports a highly ionic cesium-oxygen bond.

†This research was supported by the U. S. Air Force Office of Scientific Research.

*NBS-NRC Postdoctoral Research Associate 1964-66. Present address:

Department of Chemistry, University of Michigan, Ann Arbor, Michigan.

INTRODUCTION

There is very little information on the vapors of alkali metal hydroxides. At relatively high temperatures the saturated vapors above liquid KOH and NaOH appear to be largely monomeric, according to vapor pressure measurements.¹ At lower temperatures mass spectrometric studies^{2,3} of NaOH, KOH, RbOH, and CsOH indicate the presence of both monomer and dimer species, with the dimer predominating in NaOH and KOH. There appears to be no direct information on the molecular structure of the vapor-phase species. The structure of the monomers raises interesting questions, in particular as to whether the molecules are bent or linear. Since the alkali hydroxides may be regarded as prototypes of a class of inorganic molecules in which hydroxyl groups are attached by highly ionic bonds, information on their structure is of general importance in high-temperature chemistry.

A number of efforts have been made to detect microwave and infrared spectra of gaseous alkali hydroxides. However, the results have been negative, except for one report of weak infrared bands in NaOH, KOH, and RbOH vapor.⁴ We have now succeeded in detecting the microwave spectrum of CsOH; a brief account of this spectrum, as well as that of KOH, have already been reported.⁵ The full details of the CsOH spectrum are presented here.

EXPERIMENTAL

The spectrum of cesium hydroxide was observed in a high-temperature microwave spectrometer which has been described previously.⁶ Some modifications were necessary for the studies on CsOH. The ceramic spacers were removed from the waveguide in the hot region because of attack by the alkali/hydroxide vapor. The waveguide was therefore supported by mica or teflon spacers near each end; the reduced rigidity caused no problems. The stainless steel waveguide was lined with thin silver sheet in order to reduce chemical attack. Although the CsOH spectrum could be observed weakly in a bare stainless-steel guide, the silver-lined waveguide proved much more satisfactory. The sample trays were also made of silver. There was gradual attack on the quartz vacuum jacket, but a number of runs could be made before replacement was necessary.

Samples of cesium hydroxide obtained from commercial sources were held under vacuum at 100-200°C for several hours in an effort to remove as much water as possible. The temperature was then slowly raised until the CsOH lines appeared, which usually occurred by 500°C. Most measurements were made in the range 500-600°C. There was considerable evolution of gas during the experiments, and continuous pumping was necessary. Even so, the total pressure in the hot region was probably of the order of 0.1 mm Hg during the measurements.

One major problem caused considerable difficulty in all of these experiments. During the course of a run a finite conductivity gradually developed between the Stark electrodes. This caused a deterioration of

the shape of the square-wave modulation and a corresponding broadening of the Stark components. Furthermore, it led to an amplitude modulation of the microwave power which eventually obscured the desired signals completely. It was finally shown by several experiments that the trouble was due to thermionic emission from the Stark plates. There was evidently some decomposition of the CsOH vapor leading to deposition of metallic cesium on the silver surface. At the operating temperature the thermionic current across the waveguide was significant, and this of course produced a modulation of the microwave power at the Stark frequency.

Various attempts were made to reduce the thermionic emission by treating the waveguide surface, but none were very successful. The difficulties appeared to be less severe when the waveguide was carefully cleaned before a run; however, it must be admitted that the variables responsible for good or bad runs are still not well understood. It was found practical to carry out measurements very quickly before the emission became prohibitive, particularly if the temperature was held as low as possible. Lines with second-order Stark effects were measured first, since they required modulation voltages of several hundred V/cm. When conditions became too bad to observe these lines, attention was turned to lines which could be seen with weaker modulation fields. Through this rather tedious process the necessary data were eventually accumulated.

Certain very weak lines with second-order Stark effects could never be seen clearly with Stark modulation. A double-resonance procedure was used for these lines.⁷ The $J = 1 \rightarrow 2$ transition was saturated by a klystron which was amplitude modulated at 80 kc/sec, and the $J = 2 \rightarrow 3$ transition was observed with a second klystron which was scanned in the usual way. There was little difficulty in saturating the CsOH transitions with ordinary laboratory klystrons.

Samples of CsOD were prepared by dissolving CsOH in an excess of 98% D₂O with subsequent drying. Two cycles were sufficient to give a CsOD sample of sufficient isotopic purity to obtain a strong spectrum. Since the isotope shift is quite large, there was no problem of overlapping of the CsOH and CsOD spectra.

The line widths in the cesium hydroxide spectrum were unusually large. Under the best operating conditions the half-widths at half-maximum were the order of 0.5 Mc/sec. It is possible that unresolved nuclear quadrupole hyperfine structure contributes to the widths; however, this is unlikely to be the major contribution, because there was no significant variation of width with rotational transition. A more probable explanation is excessive pressure broadening resulting from the unavoidable high pressure of decomposition products in the absorption cell. One might expect the line-width parameter to be quite high both for self-broadening of CsOH and broadening by water.

ANALYSIS OF SPECTRUM

The spectrum of cesium hydroxide vapor consists of complex groups of lines separated by intervals of about 11,000 Mc/sec. These groups clearly correspond to successive $J \rightarrow J+1$ transitions of a linear or near-linear molecule. There can be little doubt that this spectrum is due to monomeric CsOH. It is difficult to imagine reaction products which would give a spectrum of the type observed. Furthermore, the same spectrum is found when either silver or stainless steel surfaces are exposed to the CsOH. Polymeric species of CsOH are probably too symmetric to have a microwave spectrum, and in any event their spectral patterns would be quite different from that observed. Finally, the deuterium isotope shift is consistent with the assignment to CsOH, as discussed below. Therefore, in spite of the difficult chemical problems, there is overwhelming evidence that we have obtained the spectrum of CsOH.

The first question which arises in attempting to assign the spectrum is the geometry of CsOH. A rigid non-linear model would give the characteristic spectral pattern of a near-prolate asymmetric rotor. Because of the small mass of the hydrogen atom, the asymmetry would be very small whatever the value of the CsOH angle. The spectral pattern of a $J \rightarrow J+1$, μ_a -type transition should therefore consist of a cluster of lines, probably not completely resolved, corresponding to states of $K_{-1} = 0, 2, 3$, etc.; there would also be a pair of $K_{-1} = 1$ lines symmetrically placed with respect to this central cluster. Weaker groups of lines with a similar pattern would be expected from excited vibrational states. In the case of a linear molecule there would be a single strong line from the ground vibrational state plus weaker

satellites from excited states. However, it is clear that the energy-level pattern for a bent molecule must merge smoothly into the pattern for a linear molecule as the angle is varied toward 180° . Thus there must be an intermediate region where the energy levels do not conform to either bent or linear models, and where the customary spectral patterns do not apply. This "quasi-linear" case^{8,9} must also be considered, in addition to the linear and bent extremes.

The observed spectra of CsOH and CsOD are not completely consistent with the patterns expected from either the bent or linear models. However, the patterns are definitely closer to the linear extreme (although the quasi-linear situation cannot be excluded), so that it is more convenient to use notation appropriate to a linear molecule. This will be done in the present paper, but it does not imply that the equilibrium configuration is proved to be linear.

We shall designate the vibrational state by the usual notation for a linear triatomic molecule, $v_1 v_2^l v_3$. The v_1 quantum number refers to the normal mode v_1 , which is almost a pure Cs-O stretching vibration, while v_2 refers to the degenerate bending mode. The O-H stretching mode, designated by the quantum number v_3 , presumably has a frequency, ω_3 , of at least 3000 cm^{-1} ; excited states of v_3 will therefore not be sufficiently populated to contribute to the spectrum at the present operating temperature of $500\text{--}600^\circ\text{C}$. However, comparison with related molecules suggests that ω_1 and ω_2 are both less than kT , so that several excited states involving v_1 and v_2 should be well-populated. The symmetry of the excited states is determined by the quantum number l . In the usual manner we designate states of $l = 0, 1, 2, 3, \dots$ as $\Sigma, \pi, \Delta, \Phi, \dots$,

respectively. For simplicity of notation we shall regard l as an unsigned quantum number; in the case of the π states, which are split by first-order l -doubling, we designate the state of higher energy by l_+ and the lower by l_- .

The $J = 1 \rightarrow 2$, $2 \rightarrow 3$, and $3 \rightarrow 4$ transitions have been studied in CsOH; the most complete measurements were made in the $J = 2 \rightarrow 3$ region. In CsOD only the $J = 2 \rightarrow 3$ transitions were measured. In accordance with the notation which has been adopted, the large number of lines in each region have been assigned to various vibrational states of a linear molecule. The lines were readily sorted into Σ , π , and Δ states on the basis of their qualitative Stark effects. The Stark effects also helped in pairing the l -doublets from π states. One Φ state was tentatively assigned in CsOH; although the Stark effects of Φ and Δ states are similar, the Φ state could be recognized by the appearance of a line in the $J = 3 \rightarrow 4$ region without a corresponding absorption in the $J = 2 \rightarrow 3$ region. Similarly, the assignment of Δ states was confirmed by the absence of lines from these states in the $J = 1 \rightarrow 2$ region.

The measured frequencies for CsOH and CsOD are given in Tables I and II, respectively. The assignment of vibrational states will be discussed below. Within the uncertainty of the measurements the observed frequencies are directly proportional to $J+1$, which implies that the energy levels are accurately proportional to $J(J+1)$. We can therefore define an effective rotational constant $B_{v_1 v_2 v_3}^l$ (or, more concisely, B_v) for each vibrational state which contributes to the spectrum. The B_v value was calculated from each line from the equation $B_v = \nu/2(J+1)$,

and the results were appropriately averaged. For the π states the usual expression for the l_+ and l_- components,

$$v = 2 B_v (J+1) \pm \frac{1}{2} q (v_2+1) (J+1),$$

was used to calculate B_v and q . Although centrifugal distortion has been ignored, a calculation based on a reasonable set of assumed molecular constants indicates that its effect should not be detectable in the present measurements and that its neglect results in an error of less than 0.05 Mc/sec in the derived B_v values. The values of B_v obtained in this way are summarized in Table III.

It was not easy to arrive at a unique assignment of vibrational states in the cesium hydroxide spectrum. The available evidence included regularities in the frequency pattern, qualitative observations of relative intensities, and the symmetry of the vibrational states as determined from Stark effects. By considering all this evidence in some detail, an assignment has been reached which seems far more probable than any alternatives. This assignment is indicated in Tables I-III. We feel that there is strong evidence for the overall correctness of this interpretation of the spectrum, although it is possible that some details are in error. The main arguments supporting the assignment will now be discussed.

In each $J \rightarrow J+1$ region one intense line from a Σ state is observed which must clearly be assigned to the ground vibrational state, 00^0_0 . A somewhat weaker pair of l -doublets is readily assigned to the first π state, 01^1_0 . A weaker, but still quite prominent line from a Δ state

can be assigned as 02^20 . The qualitative intensities leave little doubt that this part of the assignment is correct, since all other lines of corresponding symmetry are decidedly weaker.

While the assignment of these low-lying states is relatively straightforward, the weaker lines present more problems. In a normal linear molecule with no perturbations the rotational constants should be expressible to a good approximation as

$$B_{v_1 v_2 v_3} = B_e - \alpha_1 (v_1 + \frac{1}{2}) - \alpha_2 (v_2 + 1) - \alpha_3 (v_3 + \frac{1}{2}).$$

Since we can safely assume that $v_3 = 0$ for all observed states, we might hope to explain all the satellite lines in terms of two parameters, α_1 and α_2 . When the B_v values of CsOH are examined, one repeating interval of about 33 Mc/sec is found. The symmetry of the states which are involved shows that this interval must be identified with successive excitation of v_1 . This forms the chief basis for the assignment of the v_1 quantum numbers in Table III. In Table IV the increments in B_v for unit change in v_1 are listed. The agreement is seen to be very good except for the Δ states of CsOH, where a somewhat smaller interval is found. This could be an indication of the significance of higher order terms in the expansion of B_v , or possibly of Fermi resonance among the Δ levels. Unfortunately, there is not enough information to make a definite decision on the latter possibility. The intervals observed in CsOD are also listed in Table IV; here there is no anomaly in the Δ levels.

The data in Table IV fix the values of α_1 as

$$\alpha_1 (\text{CsOH}) = 33.3 \pm 0.2 \text{ Mc/sec}$$

$$\alpha_1 (\text{CsOD}) = 29.3 \pm 0.2.$$

This is a quite reasonable magnitude for α_1 ; it may be compared with $\alpha_e = 35.2 \text{ Mc/sec}$ in CsF .¹⁰ Furthermore, the deuterium isotope shift of about 12% agrees well with a rough calculation based on the usual expressions for the α 's of a linear triatomic molecule.¹¹

No well-defined interval which can be identified with α_2 appears in the spectrum. Thus it must be concluded that the dependence of B_v on v_2 is strongly non-linear. Furthermore, the failure to observe close pairs of lines from Σ and Δ states indicates a strong dependence on B_v on l . The assignment of v_2 quantum numbers is therefore based principally on the observed relative intensities and on the presumption of a smooth variation of B_v with v_2 . It will be noted from Table III that, according to this assignment, the B_v values for CsOD first decrease but later increase as v_2 increases. This rather surprising behavior is clearly indicated by the qualitative relative intensities; no acceptable alternative assignment is available.

It is noted that states through $v_2 = 6$ are observed except the $v_2 = 5$ state. Although lines from $05^1 0 \pi$ should be inherently stronger than those from the $06^2 0 \Delta$ state, experimental considerations led to an effectively greater sensitivity for detecting Δ states (see above). Thus the $05^1 0$ lines appeared to be just below the threshold of detectability.

A question might be raised concerning the possible influence of vibrational perturbations on the assignment. This possibility has been carefully considered, but there is no positive evidence of significant perturbations. A Coriolis resonance is possible between $10^0 0$ and $01^1 0$ and similar pairs of levels. However, this would lead to anomalous J-dependent terms in the energy, while it has been found that all features in the observed spectrum follow a $J(J+1)$ energy dependence. A Fermi resonance between the $10^0 0$ and $02^0 0$ levels also seems unlikely; attempts to explain the spectrum on this hypothesis do not lead to a satisfactory assignment. In fact, the normal behavior of the B_v values for all levels of $v_1 \leq 3$ (Table IV) argues against any significant Fermi resonances (except possibly in the Δ levels of CsOH). Finally, the best estimates of the vibrational energies (see below) do not suggest any close coincidences which could lead to perturbations. In particular, the $02^0 0$ and $10^0 0$ levels appear to be separated by about 200 cm^{-1} .

ℓ -TYPE DOUBLING

A check on the assignment of the π states is provided by the ℓ -doubling constant q . The q values calculated by the use of Eq. (1) are summarized in Table V. There is, of course, some question about the validity of Eq. (1), in view of the peculiar variation of B_v with v_2 . Nevertheless, the q values are seen to be reasonably consistent. In CsOH there is an increase in q with increasing v_1 , which is not so prominent in CsOD. Also, q (CsOD) appears slightly smaller than q (CsOH)

while the usual harmonic approximation¹¹ for a linear triatomic molecule would predict it to be about 10% larger. The interpretation of these results is not yet clear.

VIBRATIONAL ENERGIES

The assignment of vibrational states in the cesium hydroxide spectrum has now been placed on a reasonably solid foundation. It would be desirable to obtain further support for this interpretation by determining the vibrational energies from quantitative intensity measurements. Unfortunately, the experimental problems place a severe limitation on the use of intensity measurements for quantitative purposes. The Stark-modulation difficulties which were discussed earlier made it impossible to obtain reliable relative intensities for states of different symmetry. Even with states of the same symmetry the uncertainties were higher than usual because of the accumulation of various experimental problems. The only lines on which reliable measurements could be made were those from the 00^0_0 , 10^0_0 , and 02^0_0 states. A series of measurements of these lines gave the following vibrational energy differences for CsOH:

$$\begin{aligned}E_{10^0_0} - E_{00^0_0} &= 400 \pm 80 \text{ cm}^{-1} \\E_{02^0_0} - E_{00^0_0} &= 600 \pm 120 \text{ cm}^{-1} \\E_{02^0_0} - E_{10^0_0} &= 200 \pm 60 \text{ cm}^{-1}\end{aligned}$$

The uncertainties take into account the scatter of the intensity measurements and the uncertainty in the sample temperature. However, it must be pointed out that the measurements were done under very

difficult conditions, and the possibility of other systematic errors cannot be excluded.

Since the data in Table IV suggest no unusual amount of anharmonicity in the ν_1 mode, we can conclude that $\omega_1 \approx 400 \text{ cm}^{-1}$. This may be compared to $\omega_e = 352 \text{ cm}^{-1}$ in CaF . In the case of ν_2 the assumption of harmonic spacing is more questionable, but if valid it leads to $\omega_2 \approx 300 \text{ cm}^{-1}$. Another estimate of ω_2 can be obtained from the l -doubling constant. If we again make the rather dubious assumption that q can be interpreted by the usual expression for a linear triatomic molecule,¹¹ we obtain $\omega \approx 270 \text{ cm}^{-1}$ from the observed q for the $01^1 0$ state of CaOH . These estimates of ω_2 must be strongly qualified because of the uncertain character of the bending potential in CaOH (see below); nevertheless, this appears to be the first experimental information on the bending frequency of an OH group which is attached through a highly ionic bond.

BENDING POTENTIAL FUNCTION

The major question still open is the meaning of the peculiar variation of B_v as the bending mode is excited. These data should provide useful information on the nature of the bending potential function if they can be properly interpreted. We do not yet have the answer to this question but will point out certain interesting features of the data.

An examination of the $B_{v_2} l_0$ values shows that they can be fit quite accurately to a power series. A good fit is obtained, in fact, including only terms in (v_2+1) , $(v_2+1)^2$, and l^2 . The result of a least

squares fit with these terms is given in Table VI. The coefficients determined from the fit are:

$$\begin{aligned} \text{CsOH: } B_{0v_2} l_0 &= 5518.74 - 18.95 (v_2+1) + 1.207 (v_2+1)^2 - 1.615 l^2 \\ \text{CsOD: } B_{0v_2} l_0 &= 4999.23 - 3.08 (v_2+1) + 0.542 (v_2+1)^2 - 0.830 l^2 \end{aligned} \quad (2)$$

When the least-squares calculation was carried out with an additional term in $(v+1)^3$, only a negligible improvement in the overall fit resulted, and the coefficient of the $(v+1)^3$ term was not statistically determined. There is, of course, no proof that a power series of this type gives the best analytical representation of the data. However, it is rather striking that such a good fit results for both CsOH and CsOD, and that the quadratic term makes a major contribution while higher terms are apparently negligible.

The tentatively assigned $03^3 0 \frac{1}{2}$ state was omitted from this fit. The constants in Eq. (2) predict a B_v value 4.2 Mc above the observed. This discrepancy could result from an incorrect assignment, although no other line was detectable near the predicted position. Alternatively, higher order terms in the expansion may become important when $l > 2$. A reasonably good fit can be obtained for all the data, including the $\frac{1}{2}$ state, if a term in l^4 is included and the other parameters are readjusted. However, it seems undesirable to extend this empirical approach at the present stage.

Any attempt to equate the coefficients in Eq. (2) with the usual spectroscopic parameters α_2 , γ_{22} , etc. is open to question. However, it is worth pointing out that the coefficient of (v_2+1) is negative

for CsOH and CsOD, while for all known linear triatomic molecules it is positive. Furthermore, this constant is reduced by a factor of six by deuterium substitution, a much larger change than could occur in a normal linear molecule. Finally, the large contribution of the quadratic term relative to the linear term, while higher-order contributions are negligible, is difficult to rationalize with the usual theory of vibration-rotation interactions.

The source of these anomalies is not yet clear. An obvious suggestion is the presence of a small potential maximum at the linear configuration; i.e., a quasi-linear molecule of the type discussed by Thorsen and Nakagawa⁸ and by Dixon.⁹ While this possibility cannot be excluded, it does not appear, by qualitative arguments, to lead to the correct isotope effect. Another possibility is a highly anharmonic potential function with a linear equilibrium configuration. Finally, it is not out of the question that some of the anomalies are simply due to the very large amplitude of the bending vibration. It seems clear that the usual formulation of rotation-vibration interactions, which is based on infinitesimal amplitudes and rectilinear motion, is quite inadequate for handling a molecule such as CsOH. This point is now under investigation.

STRUCTURE

Although the equilibrium configuration of cesium hydroxide has not been definitely established, some information on the structure can be derived from the spectroscopic data. If one assumes a linear

molecule, the rotational constants of CsOH and CsOD allow determination of the Cs-O and O-H distances. Table VII gives the results obtained when this calculation is carried out in two ways. The first method uses the observed ground state constants, B_{00}^0 , for CsOH and CsOD. The second calculation makes use of the leading term in Eq. (2), which may be regarded as a quasi-equilibrium rotational constant; i.e., a rotational constant in which the effects of the bending mode have been removed by extrapolation to zero amplitude, while the zero-point contribution of the stretching modes remains. It is seen that the Cs-O distance is not greatly affected by the method of calculation; we can thus take it to be determined as 2.40 ± 0.01 Å. On the other hand, the O-H distance is suspiciously short when ground-state constants are used, but a more reasonable value is obtained when the extrapolated " B_e " is used. This appears to be another manifestation of the very large amplitude of the bending mode. Even in the ground vibrational state, the bending amplitude is so large that the average projection of the O-H bond on the Cs-O axis, which is roughly what is determined by this calculation, is significantly shorter than the O-H bond length itself.

DIPOLE MOMENT

Considerable difficulty was experienced in making quantitative Stark measurements on CsOH. However, fairly reliable measurements were obtained on the $M = 1 \rightarrow 2$ component of the $J = 1 \rightarrow 2$ transition of the ground vibrational state. The measurements were limited to the field strength range of 400-500 V/cm because of excessive broadening at higher fields (see above); frequency displacements ranged from 9.5 to 16.0 Mc/sec. The field strength was calibrated by measuring the Stark effect¹² of

the $J = G - 1$ transition of ${}^7\text{Li}^{35}\text{Cl}$ at the same temperature used in the CsOH experiments. The Stark effect was calculated on the assumption of a linear molecule. The dipole moment obtained in this way is

$$\mu = 7.1 \pm 0.5 \text{ D.}$$

SUMMARY

The microwave spectrum of cesium hydroxide shows that the molecule is linear, at least in an average sense, although it is not yet clear whether the equilibrium configuration is linear or not. The amplitude of the bending vibration is very large and its frequency is probably in the neighborhood of $250\text{--}350 \text{ cm}^{-1}$ (but there could be a high degree of anharmonicity). The Cs-O distance is $2.40 \pm 0.01 \text{ \AA}$, and the frequency of the Cs-O stretching mode ν_1 is about 400 cm^{-1} . These are fairly close to the values in diatomic CsF (2.345 \AA and 352 cm^{-1} , respectively).¹⁰ Furthermore, the vibration-rotation interaction constant α_1 has about the same value as in CsF, and the dipole moment of 7.1 D compares with 7.87 D in CsF.¹³ All of this evidence suggests that the Cs-O bond in CsOH is very similar to the bond in CsF. We may thus picture the CsOH molecule as having a highly ionic bond between Cs^+ and OH^- and a rather weak bending force constant.

Further spectroscopic work on the alkali hydroxide molecules is in progress and will be reported later.

ACKNOWLEDGMENT

The authors wish to acknowledge several helpful discussions with F. X. Powell concerning the experimental problems.

REFERENCES

1. K. K. Kelley, U. S. Bureau of Mines Bulletin 383 (1935). H. Von Wartonberg and P. A. Albrecht, Z. Electrochem. 27, 162 (1921).
2. R. C. Schoonmaker and R. F. Porter, J. Chem. Phys. 28, 454 (1958); 31, 830 (1959).
3. R. F. Porter and R. C. Schoonmaker, J. Phys. Chem. 62, 234 (1958).
4. L. H. Spinar and J. L. Margrave, Spectrochim. Acta 12, 244 (1958).
5. R. L. Kuczkowski, D. R. Lide, and L. C. Krisher, J. Chem. Phys. 44, 3131 (1966).
6. D. R. Lide, J. Chem. Phys. 42, 1013 (1965).
7. R. C. Woods, A. M. Ronn, and E. B. Wilson, Rev. Sci. Instr. 37, 927 (1966).
8. W. Thorson and I. Nakagawa, J. Chem. Phys. 33, 994 (1960).
9. R. W. Dixon, Trans. Faraday Soc. 60, 1363 (1964).
10. S. E. Veazey and W. Gordy, Phys. Rev. 138, A1303 (1965).
11. See, e.g., F. Dorman and C. C. Lin, J. Mol. Spectry. 12, 119 (1964).
12. D. R. Lide, P. Cahill, and L. P. Gold, J. Chem. Phys. 40, 156 (1964).
13. J. W. Trishka, J. Chem. Phys. 25, 784 (1956).

Table I. Observed frequencies^a in CsOH (in Mc/sec)

State	J = 1 - 2	J = 2 - 3	J = 3 - 4
00 ⁰ 0	22004.4	33006.6	44008.2
01 ¹ 0, ℓ_+	21952.1	32928.1	43904.2
01 ¹ 0, ℓ_-	21920.6	32880.7	43840.3
02 ⁰ 0	21889.7	32834.6	
03 ¹ 0, ℓ_+	21875.3	32813	
10 ⁰ 0	21871.8	32807.0	
02 ² 0		32795.8	43728.1
11 ¹ 0, ℓ_+	21821.0	32733.0	
04 ⁰ 0		32726.5	
03 ¹ 0, ℓ_-	21809.7	32715.5	
04 ² 0		32687.8	43583
11 ¹ 0, ℓ_-	21786.6	32678.6	
03 ³ 0			43548.3
06 ² 0		32631.8	43509.3
12 ⁰ 0		32630.1	
12 ² 0		32619.8	43492.7
13 ¹ 0, ℓ_+	21743	32614	43483.6
20 ⁰ 0		32607.5	43475.4
21 ¹ 0, ℓ_+	21689.6	32534.7	43378.4
13 ¹ 0, ℓ_-			43346.4
14 ² 0		32504	43336.2
21 ¹ 0, ℓ_-	21652	32477.2	
22 ² 0		32438.4	43250.6
22 ⁰ 0		32427	
30 ⁰ 0		32406.2	
24 ² 0		32320.1	43092.6
32 ² 0		32253.8	

^aFrequencies quoted to the nearest 0.1 Mc/sec are believed to be accurate to ± 0.3 Mc/sec; the uncertainty in the remaining frequencies is ± 1 Mc/sec.

Table II. Observed frequencies^a of CsOD (in Mc/sec)

State	J = 2 → 3
06 ² 0	30034.7
03 ¹ 0, l_+	30027.2
04 ⁰ 0	30000.3
01 ¹ 0, l_+	29991.6
00 ⁰ 0	29981.0
04 ² 0	29979.9
02 ⁰ 0	29973.8
02 ² 0	29954.4
01 ¹ 0, l_-	29946.1
03 ¹ 0, l_-	29928.8
11 ¹ 0, l_+	29815.4
10 ⁰ 0	29805.4
14 ² 0	29803.1
12 ² 0	29776.4
11 ¹ 0, l_-	29768.1

^aUncertainty is believed to be ± 0.3 Mc/sec.

Table III. Effective rotational constants for various vibrational states of CsOH and CsOD.^a

State	B_v (CsOH)	B_v (CsOD)
00 ⁰ Σ	5501.08	4996.83
01 ¹ 0 π	5484.07	4994.81
02 ⁰ Σ	5472.43	4995.64
02 ² 0 Δ	5465.97	4992.40
03 ¹ 0 π	5460.65	4996.32
03 ³ 0 π	5443.54	
04 ⁰ Σ	5454.4	5000.06
04 ² 0 Δ	5447.95	4996.65
06 ² 0 Δ	5438.65	5005.78
10 ⁰ Σ	5467.90	4967.57
11 ¹ 0 π	5451.0	4965.29
12 ⁰ Σ	5438.35	
12 ² 0 Δ	5436.63	4962.73
13 ¹ 0 π	5427.0	
14 ² 0 Δ	5417.0	4967.18
20 ⁰ Σ	5434.50	
21 ¹ 0 π	5417.64	
22 ⁰ Σ	5404.5	
22 ² 0 Δ	5406.36	
24 ² 0 Δ	5386.62	
30 ⁰ Σ	5401.04	
32 ² 0 Δ	5375.6	

^a Those values given to the nearest 0.01 Mc/sec are believed to be uncertain by no more than ± 0.10 Mc/sec. Values given to one decimal place may be in error by as much as 0.3 Mc/sec.

Table IV. Variation of rotational constants with v_1

v_2^l	$B_{0v_2^l 0} - B_{1v_2^l 0}$	$B_{1v_2^l 0} - B_{2v_2^l 0}$	$B_{2v_2^l 0} - B_{3v_2^l 0}$
CsOH:			
0^0	33.18	33.40	33.46
1^1	33.1	33.3	
2^0	34.08	33.8	
2^2	29.34	30.27	30.73
3^1	33.7		
4^2	30.9	30.4	
CsOD:			
0^0	29.26		
1^1	29.52		
2^2	29.67		
4^2	29.47		

Table V. *L*-Doubling constants.

State	q (CsOH)	q (CsOD)
01^1_0	7.90	7.59
03^1_0	8.19	8.20
11^1_0	8.8_2	7.88
13^1_0	8.6_7	
21^1_0	9.49	

Table VI. Fit of $B_{0v_2^0}$ to power series.^a

State	CsOH		CsOD	
	Calc $B_{0v_2^0}$	Obs-Calc	Calc $B_{0v_2^0}$	Obs-Calc
00 ⁰ 0	5500.99 Mc/sec	0.09	4996.79	0.04
01 ¹ 0	5484.05	0.02	4994.81	0.00
02 ⁰ 0	5472.74	-0.31	4995.77	-0.13
02 ² 0	5466.28	-0.31	4992.45	-0.05
03 ¹ 0	5460.60	0.05	4996.36	-0.04
04 ⁰ 0	5454.14	0.26	4999.89	0.17
04 ² 0	5447.68	0.27	4996.57	0.08
06 ² 0	5438.74	-0.09	5005.82	-0.04

Table VII. Structural parameters of cesium hydroxide.

	From B_{000}^O	From ^{137}Ba
$r(\text{CsO})$	2.403 \AA	2.395 \AA
$r(\text{OH})$	0.920	0.969

^a5518.74 and 4999.23 Mc/sec for CsOH and CsOD, respectively, as obtained from Eq. (2).

THE VAPOR PRESSURE, VAPOR DIMERIZATION, AND HEAT OF SUBLIMATION
OF ALUMINUM FLUORIDE, USING THE ENTRAINMENT METHOD¹

Ralph F. Krause Jr. and Thomas B. Douglas

National Bureau of Standards, Washington, D. C. 20234

ABSTRACT

The vapor pressure P of anhydrous aluminum fluoride was measured at eight temperatures between 1194 and 1258°K by an entrainment method. The standard deviation of P from a least square fit was 0.15%, and systematic uncertainties of 0.4% in P and 1 deg in T were estimated. If the vapor were assumed to be completely monomeric and ideal, this fit would yield Second Law values and their standard deviations at 1000°K of $\Delta H^\circ = 69.64 \pm 0.06$ kcal and $\Delta S^\circ = 45.48 \pm 0.06$ eu for



However, corresponding Third Law values were found sufficiently lower as to indicate that the saturated vapor could be treated as ideal only by taking into account the occurrence of some dimerization,



P was considered as the sum of the monomeric and twice the dimeric vapor pressure, and smooth values of P and dP/dT at 1225°K were determined. The other two independent thermodynamic quantities necessary to define reactions 1 and 2 were taken as (a) the standard entropy of reaction 1 derived from published spectroscopic and

¹This work was supported by the Advanced Research Projects Agency under Order No. 20 and by the Air Force Office of Scientific Research under Contract No. ISSA-65-8.

crystalline heat capacity data, and (b) the mol fraction of dimer as newly evaluated from two published mass-spectrometric studies. The final results at 1000°K along with their uncertainties were $\Delta H^\circ = 68.94$ kcal and $\Delta S^\circ = 44.80 \pm 0.4$ eu for reaction 1, and $\Delta H^\circ = -56 \pm 5$ kcal and $\Delta S^\circ = -41 \pm 5$ eu for reaction 2. Owing to the precision and accuracy of this entrainment data, these values are believed to be more reliable than those previously recommended.

INTRODUCTION

As part of a program of research to determine accurately the thermodynamic properties of substances that are important to high temperature applications like chemical propulsion, a new apparatus was constructed to apply the entrainment method for measuring equilibria between solid and vapor. The high stability of anhydrous aluminum fluoride AlF_3 and the ease of obtaining a sample of fairly high purity made it suitable for precise measurements.

Even though several investigators²⁻¹³ had measured the vapor

² W. Olbrich, Dissertation, Breslau, Tech. Hochschule (1928).

³ O. Ruff and L. LeBoucher, Z. Anorg. Allgem. Chem. 219, 376 (1934).

⁴ I. I. Maryshkin, Zh. Fiz. Khim. 13, 528 (1939).

⁵ P. Gross, C. S. Campbell, P. J. C. Kent, and D. L. Levi, Discussions Faraday Soc. 4, 206 (1948).

⁶ W. P. Witt, Thesis, Oxford Univ. (1959).

⁷ W. P. Witt and R. F. Barrow, Trans. Faraday Soc. 55, 730 (1959).

⁸ A. M. Evseev, G. V. Pozharskaya, A. N. Nesmeyanov, and Ya. I. Gerasimov, Zh. Neorg. Khim. 4, 2196 (1959).

- ⁹ M. M. Vetyukov, M. L. Elyushtein, and V. P. Poddymov, *Izv. Vysshikh. Uchebn. Zavedenii, Tsvetn. Met.* 2, 126 (1959).
- ¹⁰ D. L. Hildenbrand and L. P. Theard, Aeronutronic Rept. No. U-1274, Newport Beach, Calif., (June 15, 1961).
- ¹¹ D. L. Hildenbrand, Private Commun., (March 6, 1967).
- ¹² P. E. Blackburn, Arthur D. Little Rept., Cambridge, Mass., (May 31, 1965).
- ¹³ Hon Chung Ko, M. A. Greenbaum, J. A. Elauer, and M. Farber, *J. Phys. Chem.* 69, 2311 (1965).

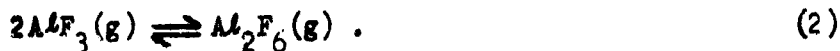
pressure of AlF_3 , predominantly from 890 to 1100°K or from 1370 to 1570°K, most of their results were too imprecise to contribute to an evaluation of the composition of the saturated vapor. Each had derived a ΔH° for



by assuming the vapor to be completely monomeric. However, a mass-spectrometric study by Porter and Zeller¹⁴ indicated that the saturated

-
- ¹⁴ R. F. Porter and E. E. Zeller, *J. Chem. Phys.* 33, 858 (1960).

vapor at 1000°K sustains appreciable dimerization,



Also, the mol fraction of dimer in the saturated vapor increases with temperature because a mass-spectrometric study by Büchler¹⁵ showed that

-
- ¹⁵ A. Buchler, Arthur D. Little Rept., Cambridge, Mass., (Sept. 30, 1962).

ΔH° of reaction 1 is less than that for



Consequently, if each of the preceding vapor pressure measurements were considered to reflect the presence of both the monomer and the dimer, a corrected ΔH° of reaction 1 would be less than a Second Law value derived by assuming the vapor to be completely monomeric, and greater than a corresponding Third Law value; moreover, the difference between these uncorrected Second and Third Law values would increase with temperature. Nevertheless, an inspection of all of these uncorrected heats for reaction 1 showed no such trend, but rather a scattering.

The aim of this paper is to show how far the use of our precise sublimation data can go toward defining the thermodynamic properties of sublimation and dimerization of AlF_3 at temperatures where the vapor pressure is appreciable.

ENTRAINMENT METHOD

The entrainment method used in this work involved the flowing of argon gas through a high temperature vapor cell, holding a sample of anhydrous AlF_3 . The sublimed sample was condensed downstream while the carrier gas was collected in a tank. Saturation was closely approximated by using an appropriate geometry of the vapor cell and flow of the gas mixture.

The vapor cell and condenser were separate sections of the same Pt/10% Rh composite tube as shown in Figure 1. The detachable cap prevented accidental spilling of the sample from the cell. The exit of the cell was connected to the condenser by a capillary tube of 5 cm length

$$\Delta H_{1000}^{\circ}(1) \text{ (kcal) for } \text{AlF}_3(\text{c}) = \text{AlF}_3(\text{g})$$

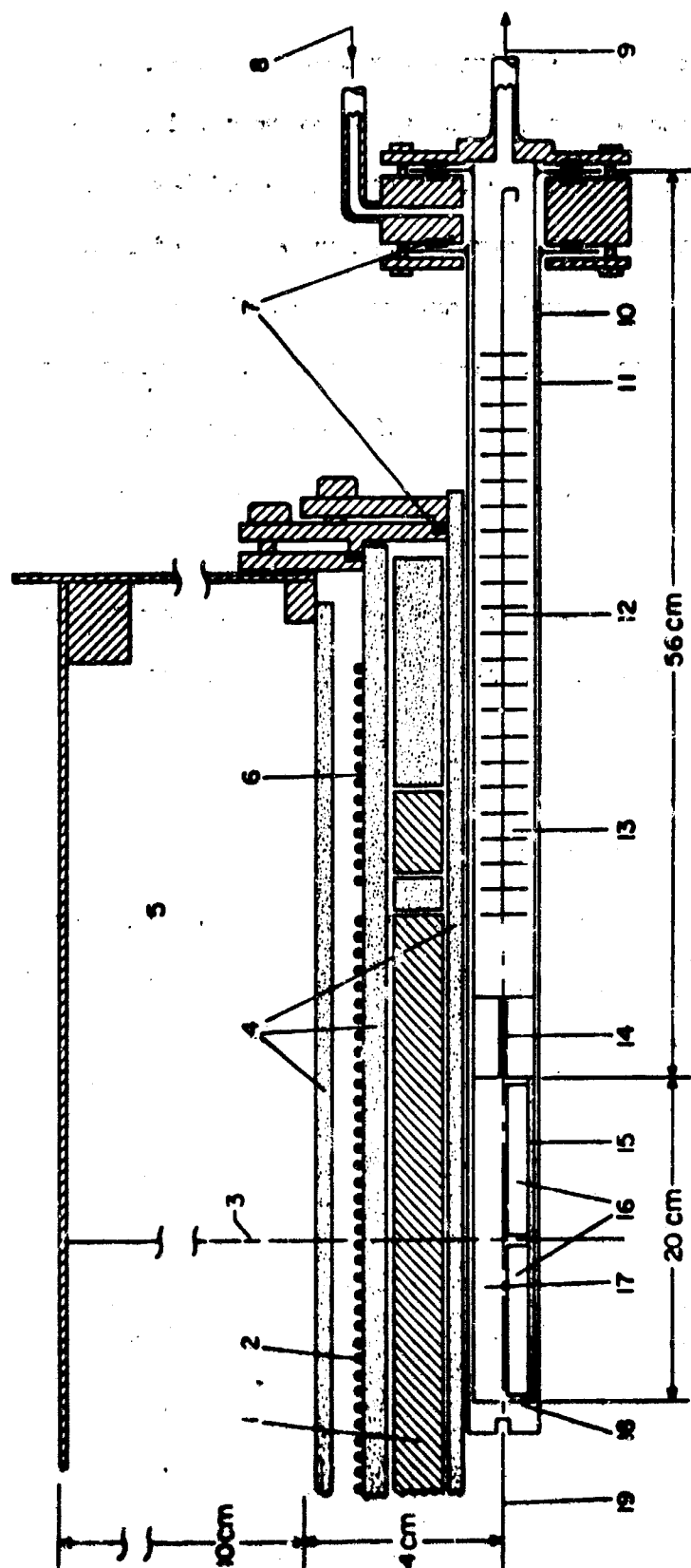


Figure 1. Diagram of Entrainment Tubes in the Cylindrical Furnace:

(1) nickel core, (2) Pt/20% Rh main heater, (3) cross-sectional center, (4) alumina tubes, (5) insulation, (6) an end heater, (7) Teflon gaskets, (8) argon input, (9) argon output, (10) Pt/10% Th composite tube, (11) Pt/20% Rh housing, (12) perforated discs, (13) condenser, (14) capillary tube, (15) alumina sled, (16) sample boats, (17) vapor cell, (18) detachable entrance cap, and (19) longitudinal axis. Note that vertical and horizontal scales differ.

and 1 mm inside diameter. Applying Merten's¹⁶ diffusion study indicated

¹⁶ U. Merten, J. Phys. Chem. 63, 443 (1959).

geometry
that this/allowed negligible diffusion of the sample vapor through the capillary tube at the gas flows employed in this work.

The crystalline sample of anhydrous AlF_3 , obtained through the courtesy of The Aluminum Company of America, had been sublimed at 1050°C in a nickel retort. A spectrographic analysis reported 0.01 to 0.1% Mg; 0.001 to 0.01% Ca, Cu, Fe, Mn, Ni, and Si; and 10^{-4} to 10^{-3} % Cr and V. Triplicate chemical analyses reported from 67.61 to 68.00% F and from 32.13 to 32.17% Al, compared to the theoretical values of 32.130% Al. The mass of sublimed sample, roughly 200 mg, was taken as the mean of the condenser gain and the boat loss with an average deviation of 0.3%. The boat loss was the weight change of the loaded boats minus 1 to 6 mg of sample accidentally spilled in the cell. Since the boat loss was observed to be less than 0.2 mg for several experiments at zero gas flow, no correction for diffusion or distillation of the sample was warranted; nevertheless the condenser gain was consistently less than the boat loss. Apparently the condenser was not 100% efficient; nevertheless this difference was near the weighing uncertainty of the 137 g composite tube.

Preliminary to the argon flow, the atmosphere of air which was held in the vapor cell prior to its installation in the furnace was reduced to 10^{-4} torr while the vapor cell was being heated to 500°C. Next, 99.996% pure argon, dried by anhydrous $Mg(ClO_4)_2$, was carefully introduced into the flowpath until its pressure was equal to barometric pressure.

Finally, after the vapor cell was heated to its operational temperature, an additional 3 to 4 hours at zero gas flow was required to attain a steady temperature. The total pressure of the gas mixture in the vapor cell was taken as the time average of the continuously recorded barometric pressure plus a head pressure of 0.6 to 1.2 torr. The volume of argon was measured with an accuracy of 10 ml by a calibrated gasometer whose displacement of 14 to 28 liters was corrected for differences in the initial and final barometric pressure and room temperature.

VAPOR CELL TEMPERATURE

Usually being the greatest single source of error in vapor pressure measurements, the temperature of the vapor cell was measured with special care¹⁷, using Pt and Pt/10% Rh thermocouples. As shown in Figure 1

¹⁷ W. F. Roeser and H. T. Wensel, J. Res. Nat. Bur. Std. 14, 247 (1935).

a nickel core in an atmosphere of nitrogen served to reduce any temperature gradient in the vapor cell which was centered within an alumina tube of a wire-wound resistance furnace. Three thermocouples were inserted longitudinally into the walls of the nickel core; two had fixed differential junctions and the third had variable immersion to observe the temperature profile. A fourth was inserted along the furnace axis with its junction in the well near the vapor cell entrance. A fifth was placed aside to check periodically the stability of the others. The thermocouples were calibrated by the NBS Temperature Section to an accuracy of ± 0.5 deg at 1000°C.

Some preliminary experiments showed that if the temperature gradient were negative in the direction of the gas flow through the vapor cell, the sample vapor would condense prematurely and plug the capillary tube. To prevent this deposit each of three heaters were manually adjusted by an autotransformer to give the same temperature at the entrance and exit of the vapor cell and at the exit of the capillary tube. Instead of a zero temperature gradient, however, a steady profile was observed to decrease about 2 deg for the first 5 cm along the length of the vapor cell, to increase linearly about 2 deg for the remaining 15 cm of the cell, and to be close to zero through the capillary tube. Besides, the axis temperature was observed to be 0.05 to 0.3 deg lower than that in the nickel core at the same cross-section.

The temperature of an experiment was taken as the time average of the vapor cell exit whose temperature range was 1 or 2 deg. An automatic recorder continuously registered the thermocouple emf relative to that of a Diesselhorst potentiometer with a precision equivalent to 0.05 deg. A systematic uncertainty of 1 deg in T was estimated; that of 0.4% in P obtained from eq 6 was considered negligible compared to $dP/PdT = 2.3\%/deg$ derived from eq 7.

TEST FOR SATURATION

Since diffusion of the sample vapor through the capillary tube was shown to be negligible, a test for saturation would be the linearity, extrapolated through the origin, of the flow of sample mass q versus the average flow of the gas mixture y at a given cell temperature.

When \underline{v} was varied by a factor of two, this test was satisfied within accidental error as shown by the very close agreement without trend of each of the four successive pairs in the sixth column of Table I.

Another test for the degree of saturation was applied by considering the mass of sample lost in each of two successive boats in the vapor cell with a temperature gradient. The ratio of the weight loss of the second boat to that of the first was observed as 0.03 ± 0.005 for \underline{v} near 120 ml/min and 0.04 ± 0.005 for \underline{v} near 60 ml/min; the uncertainty resulted from accidentally spilling some sample from either boat for each assembly. The partial pressure \underline{p} of the sample was assumed to increase with the distance \underline{x} beyond the start of the first boat at a given \underline{v} according to

$$dp/dx = k(P-p) + AD(d^2p/dx^2)/v, \quad (4)$$

where \underline{k} is a constant, \underline{A} is the cross-sectional area, and \underline{D} is the inter-diffusion coefficient of the gas mixture. If there were no temperature gradient and \underline{p} were zero at zero \underline{x} , integration of eq 4 would yield a degree of unsaturation at the exit of the vapor cell less than 0.1%. Nevertheless, the vapor pressure \underline{P} at distance \underline{x} was assumed to be represented by

$$P = P_0(1 + b\underline{x}) \quad (5)$$

where \underline{P}_0 is the vapor pressure at the start of the first boat, $\underline{b} = dT/dx$, and $\underline{a} = dP/PdT$. Assuming the observed \underline{b} , integration of eq 4 combined with eq 5 yielded a degree of unsaturation less than 0.4%.

MONOMERIC VAPOR ASSUMPTION

If the sample vapor were assumed to be wholly monomeric and ideal, our entrainment data, represented simply by the two constants of a Second Law treatment, could be compared to the corresponding Third Law treatment to reveal whether our data are incompatible with this preliminary assumption. Using a form of Dalton's Law,

$$P = P_T / (1 + M_n/w) , \quad (6)$$

the vapor pressure P was calculated from the entrainment data:

P_T the total gas pressure, n the number of moles of collected argon, w the mass of sublimed AlF_3 , and M the molecular weight of its monomer.

The resulting P at eight independently measured temperatures are tabulated in Table I.

Applying a Second Law analysis, this data for reaction 1 was fitted by least squares with a standard deviation of 0.15% to determine the coefficients ΔS_C° and ΔH_C° at $T_C = 1225^\circ K$ in

$$R \ln P = \Delta S_C^\circ - \Delta H_C^\circ/T + \Delta C_P^\circ [\ln (T/T_C) + (T_C - T)/T] \quad (7)$$

where $\Delta C_P^\circ = -2.67R$ at T_C was assumed to be constant over our temperature range. Both $\Delta S_{1000}^\circ(1)^{18}$ and $\Delta H_{1000}^\circ(1)$ in Table I were obtained by

¹⁸ Hereafter a definite temperature ($^\circ K$) will be indicated by a subscript, a specific reaction by the number in parentheses, and the standard deviation by the given tolerance unless otherwise stated.

1 calorie = 4.1840 joules.

temperature conversion using heat capacities from the literature as discussed later.

Table I: Results for Reaction 1 by Assuming Wholly Monomeric Vapor

Entrainment Data				II Law		III Law	
No. ^a	T (°K)	q(obs) (mg/min)	v(obs) (ml/min)	P (mm)	$(P-P_{II})/P_{II}$ (%)	$\Delta H_{1000}^{\circ}(1)$ (kcal)	$(P-P_{III})/P_{III}$ (%)
1	1194.0	0.1441	112.1	1.500	0.07	68.84 ₂	-0.7
2	1194.7	0.0781	59.90	1.523	-0.10	68.84 ₆	-0.9
3	1212.1	0.2385	122.5	2.011	0.11	68.83 ₀	-0.2
4	1217.5	0.1342	61.50	2.619	0.00	68.82 ₉	-0.2
5	1236.9	0.3875	115.1	4.070	-0.30	68.82 ₅	0.0
6	1233.8	0.1948	61.65	3.810	0.09	68.81 ₇	0.3
7	1252.5	0.5869	124.3	5.778	0.08	68.80 ₅	0.8
8	1257.5	0.3226	62.23	6.441	0.03	68.80 ₄	0.8
$\Delta S_{1000}^{\circ}(1)$ (eu) ^b				45.48 ± 0.05		44.80	
$\Delta H_{1000}^{\circ}(1)$ (kcal) ^b				69.64 ± 0.06		68.82 ± 0.02	

^a Chronological sequence: 3, 7, 5, 1, 4, 8, 6, and 2.

^b See footnote 18.

In addition, $\Delta H_{1000}^{\circ}(1)$ was determined by a Third Law treatment of each (P, T) pair according to

$$\Delta H_{1000}^{\circ}(1) = T[-\Delta(G^{\circ}-H_{1000}^{\circ}/T) - R \ln P] . \quad (8)$$

The results along with their mean are listed in Table I. Each $-\Delta(G^{\circ}-H_{1000}^{\circ}/T)$ of eq 8 and the Third Law $\Delta S_{1000}^{\circ}(1)$ were independently evaluated from the previously mentioned literature from which we realized the dominant uncertainty in the Third Law $\Delta H_{1000}^{\circ}(1)$ to result from that of the spectroscopic entropy of the monomeric gas.

Besides the two previously mentioned mass-spectroscopic studies, the results of the monomeric vapor assumption indicate that the saturated vapor can be treated as ideal only by taking into account the occurrence of some dimerization of reaction 2. The Third Law values of $\Delta H_{1000}^{\circ}(1)$ in Table I exhibit the characteristic trend decreasing with increasing T . Also, the Second Law $\Delta H_{1000}^{\circ}(1)$ in Table I is appreciably greater than the corresponding Third Law $\Delta H_{1000}^{\circ}(1)$. Later we shall examine the extent that our systematic error in T and the error in the Third Law $\Delta S_{1000}^{\circ}(1)$ have upon this trend and discrepancy.

GENERATION OF HYPOTHETICAL VALUES

A set of thermodynamic properties which are sufficient to define reactions 1, 2, and 3 in the temperature range from 1000 to 1500°K were sought to be consistent with our entrainment data and to appear in best agreement with other pertinent published data. Only two of these three reactions are independent; moreover, since the high-temperature heat capacities of all the species have been determined experimentally or may be inferred with sufficient accuracy, just four additional independent quantities must be known.

Two of these four quantities were derived solely from our data: namely, the smoothed values of $P_{1225} = (3.115)10^{-3}$ atm and $(dP/dT)_{1225} = (7.154)10^{-5}$ atm/deg given by eq 7. Having to look elsewhere for the other two, we chose $\Delta S_{1000}^0(1)$ and the mol fraction of dimer in the saturated vapor, $N_{d,1000}$. Both $\Delta S_{1000}^0(1)$ and $N_{d,1000}$ were allowed to assume arbitrary values selected to cover a reasonable range of uncertainty; in addition a third parameter, $\Delta T = (T_{\text{true}} - T_{\text{abs}})$, was introduced to reflect the effects of a possible systematic error in our temperature measurements on P_{1225} and $(dP/dT)_{1225}$. In this way we generated hypothetical sets of values for $\Delta H_{1000}^0(1)$, $\Delta S_{1000}^0(2)$, $\Delta H_{1000}^0(2)$, and $\Delta H_{1000}^0(3)$ using an IBM 7094 computer programed in, Omnitab¹⁹.

¹⁹ J. Hilsenrath, G. G. Ziegler, C. G. Messina, P. J. Walsh, and R. J. Herbold, Omnitab, Nat. Bur. Std. Handbook 101 (1966).

Since P was determined by the monomeric vapor assumption of eq 6, its resolution into the partial pressures of monomer and dimer must satisfy

$$P = P_m + 2 P_d \quad (9)$$

Thus, at a given temperature a set of values of P and N_d correspond to definite values of P_m and P_d , which were assumed to be related to properties of reaction 1 or 3 respectively by

$$P_i = \exp[(\Delta S^0/R) - (\Delta H^0/RT)] \quad (10)$$

The relationship among reactions 1, 2, and 3 is obviously exemplified by

$$\Delta H^{\circ}(2) = \Delta H^{\circ}(3) - 2\Delta H^{\circ}(1) . \quad (11)$$

In making temperature conversions of the ΔS° and ΔH° of reactions 2 or 3 between 1000 and 1225°K, the gas species involved were assumed to have equipartitional heat capacities.

The results of these calculations are represented graphically in Figures 2(a), 2(b), and 2(c), where $\Delta H_{1000}^{\circ}(3)$, $\Delta H_{1000}^{\circ}(1)$, and $\Delta S_{1000}^{\circ}(2)$, respectively, are plotted versus $N_{d,1000}$ at selected values for $\Delta S_{1000}^{\circ}(1)$ and ΔT .

ENTROPY OF SUBLIMATION

As one of the four quantities mentioned above, $\Delta S_{1000}^{\circ}(1)$ was evaluated after consulting the literature for the usual Third Law data and examining refinements which proved significant compared to the relatively high reliability that we believe the two quantities from our data have. King²⁰ had measured precisely the heat capacity of the crystal

²⁰ E. G. King, J. Am. Chem. Soc. 79, 2056 (1957).

from 55 to 298°K. Being in good agreement with O'Brien and Kelley²¹, Douglas and Ditmars²² measured the relative enthalpy of the crystal from

²¹ C. J. O'Brien and K. K. Kelley, J. Am. Chem. Soc. 79, 5616 (1957).

²² T. B. Douglas and D. A. Ditmars, J. Res. Nat. Bur. Std. 71A, (1967).

273 to 1173°K. The uncertainty in the entropy of the crystal arises from estimated uncertainties of 0.08 eu/mole from the low-temperature measurements and 0.04 eu/mole from the high-temperature measurements.

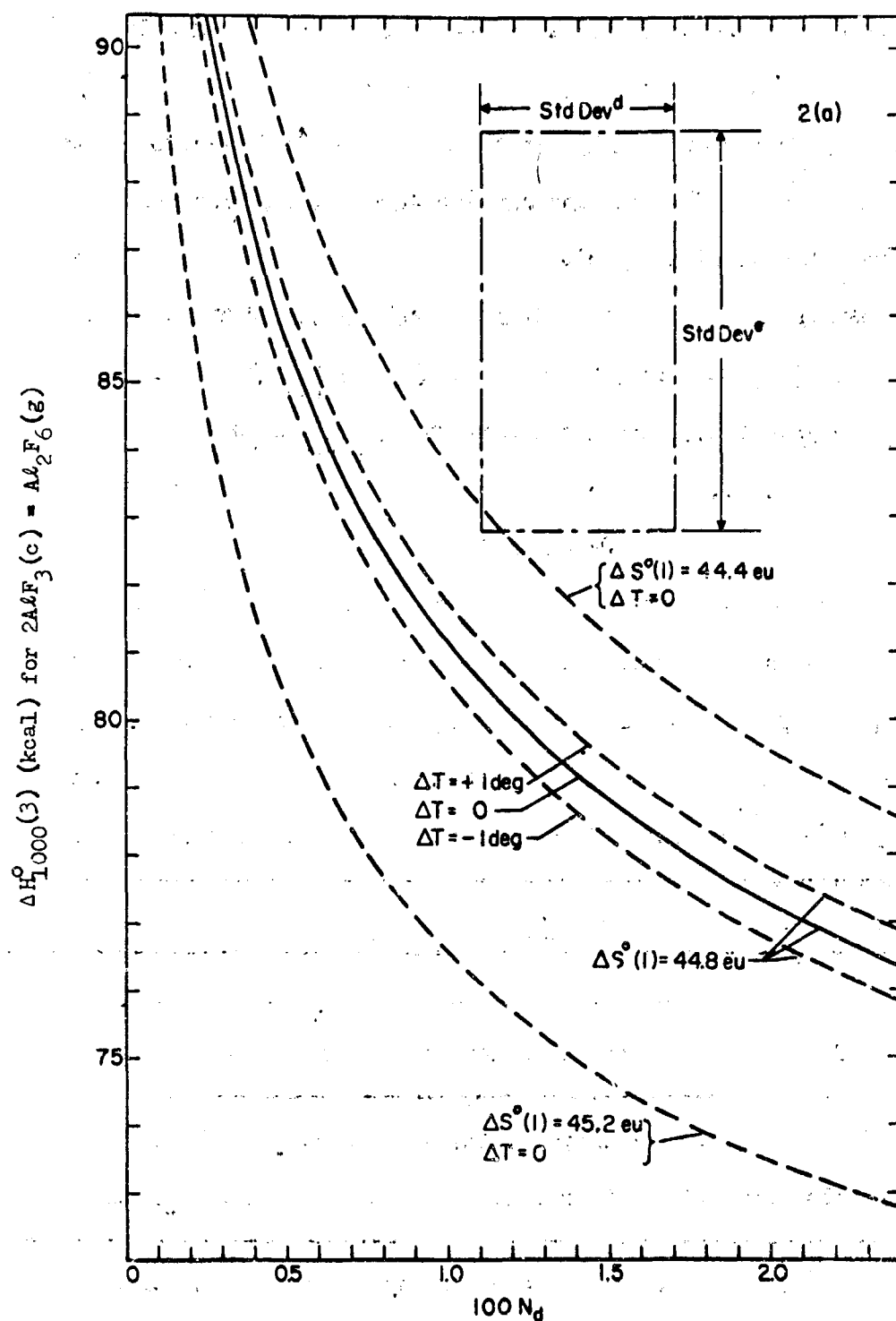


Figure 2. Hypothetical Values of: (a) $\Delta H_{1000}^{\circ}(3)$, (b) $\Delta H_{1000}^{\circ}(1)$, and (c) $\Delta S_{1000}^{\circ}(2)$, consistent with this work, versus arbitrary mol fraction of dimer $N_{\text{d},1000}$ at selected values of ΔT and $\Delta S_{1000}^{\circ}(1)$. See next two pages.

^dMass-spectrographic work by Porter and Zeller¹⁴ which gave $N_{\text{d},1000} = 0.014 \pm 0.003$.

^eMass-spectrographic work by Blichler¹⁵ which gave $\Delta H_{1000}^{\circ}(3) = 85.8 \pm 3 \text{ kcal}$.

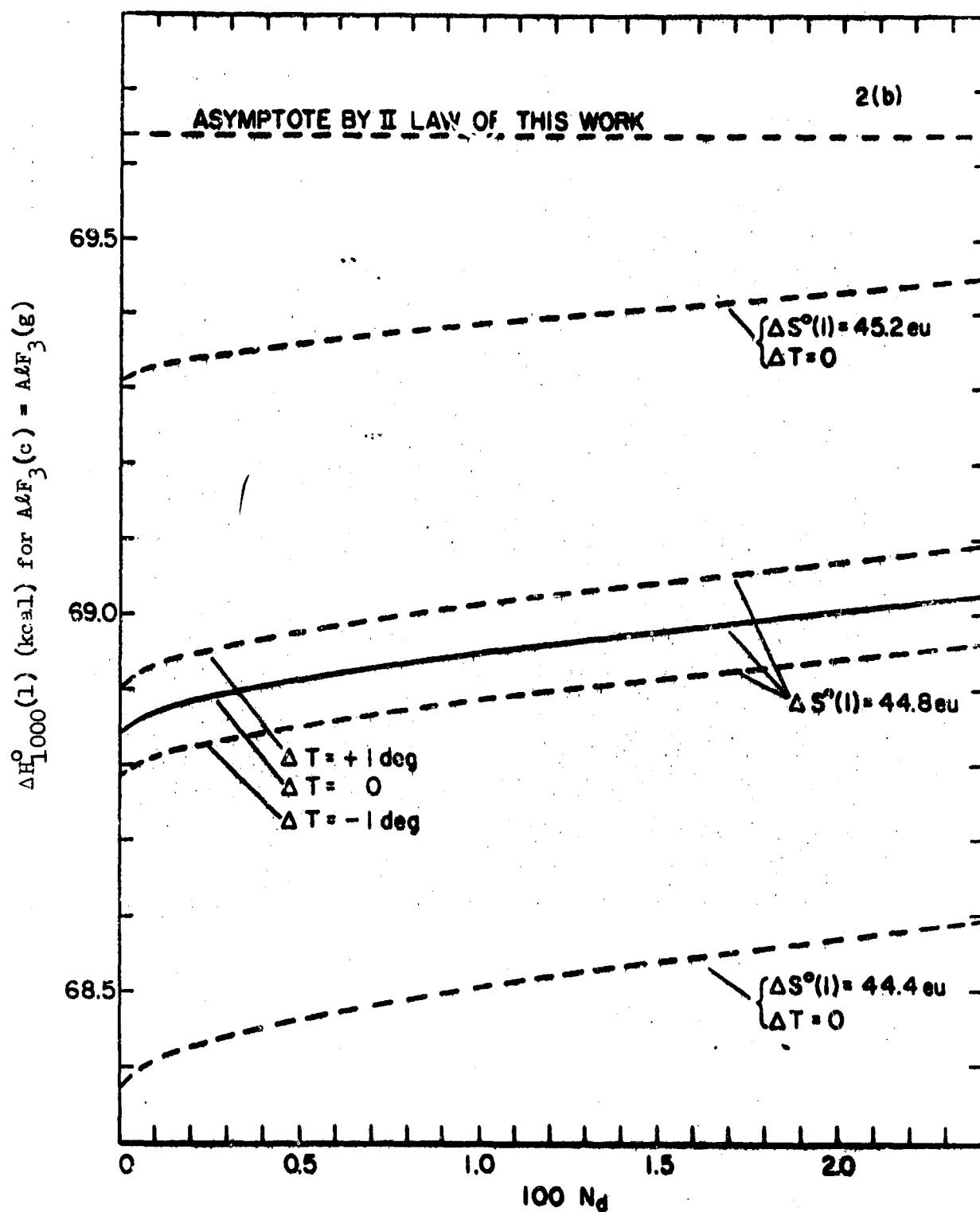


Figure 2(b)

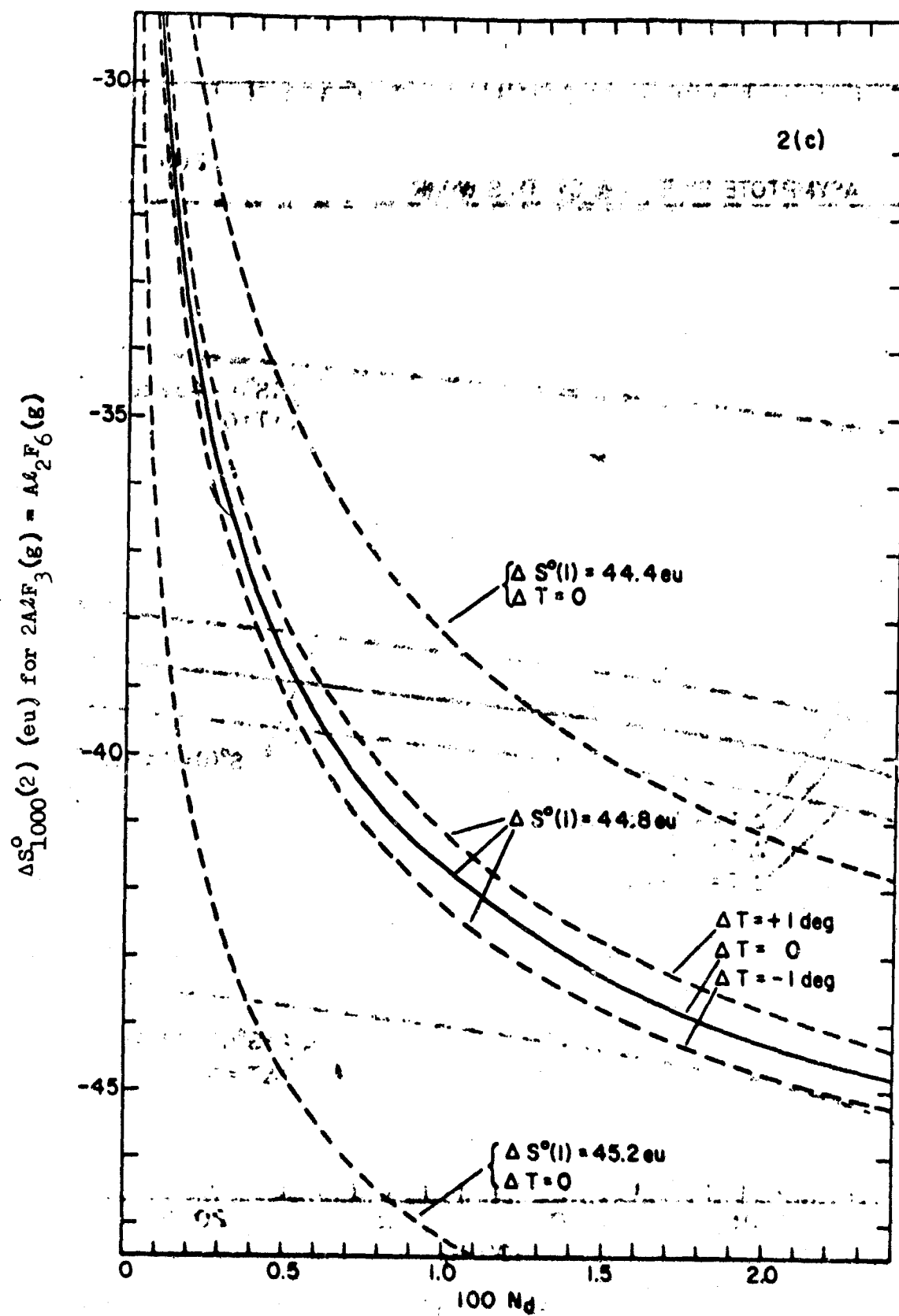


Figure 2(c)

The entropy of the ideal monomeric gas was established within narrow limits by applying the harmonic oscillator, rigid rotor approximation (HRR) to the published spectroscopic data. Analogous to the better known boron fluoride BF_3 , the AlF_3 molecule was assumed to have planar symmetry D_{3h} . An electron diffraction study by Akishin *et al.*²³ had

²³ P. A. Akishin, N. G. Rambidi, and E. Zasorin, *Kristallografiya* 4, 186 (1959).

given the Al-F bond distance as 1.63 Å. Since Lide²⁴ had shown the

²⁴ D. R. Lide Jr., *J. Chem. Phys.* 38, 2027 (1963).

corresponding distance in aluminum monofluoride to be 1.654 Å by microwave spectroscopy and since the bond distance in BF_3 is 0.03 Å higher than that in BF , we adopted 1.66 ± 0.03 Å for that of AlF_3 .

A molecule of this symmetry has four fundamental vibrational frequencies (ν_1 , ν_2 , ν_3 , and ν_4), the last two being doubly degenerate. Linevsky²⁵ recently made infrared measurements on the matrix-isolated

²⁵ M. J. Linevsky, *Space Sci. Lab. Rept.*, Philadelphia, Penn., (Nov. 30, 1964).

vapor down to near 180 cm^{-1} . Being most definitive, his results in argon were adopted here while his range of peaks in krypton and xenon are given in parentheses: ν_2 , 266 (251-266); ν_3 , 940 (921-947); and ν_4 , 251 (243-255) cm^{-1} . Using a double oven to superheat the saturated vapor by 300 to 400 deg, he observed a marked attenuation of other saturated-vapor

bands, supposedly attributable to the dimer. He considered that his assignment of ν_3 and ν_4 was confirmed by the fact that the matrix appeared to remove the degeneracy from the two bands assigned to these two modes. Similar to Linevsky, Snelson²⁶ reported 300, 965, and 270 cm^{-1}

²⁶ A. Snelson, Private Commun., (Feb. 8, 1967).

for ν_2 , ν_3 , and ν_4 respectively. Also, direct infrared observations of the high temperature vapor have been reported. Büchler²⁷ found 297, 935,

²⁷ A. Büchler, Arthur D. Little Rept., Cambridge, Mass., (June 30, 1962).

and 263 cm^{-1} for ν_2 , ν_3 , and ν_4 respectively. McCorry et al²⁸ found

²⁸ L. D. McCorry, R. C. Paule, and J. L. Margrave, J. Phys. Chem. 67, 1086 (1963).

945 cm^{-1} for ν_3 .

Since ν_1 is infrared inactive, an adopted value of 646 cm^{-1} was calculated from the other three adopted frequencies by a three-term quadratic potential for a planar XY_3 molecule²⁹. We compared this value of ν_1 with

²⁹ G. Herzberg, Infrared and Raman Spectra of Polyatomic Molecules, D. Van Nostrand Co., N. Y. (1945) p. 177.

that given alternatively by another more empirical method. Assuming that the symmetric stretching force constant is greater in AlF_3 than in AlF by the same amount compared to BF_3 and BF , namely 11%, ν_1 was estimated to be 658 cm^{-1} for AlF_3 .

We attempted to realize the extent of an anharmonicity and stretching correction for the entropy of the gas at 1000°K. The formula derived by Mayer and Mayer³⁰ for diatomic molecules gives +0.1 eu for

³⁰ J. E. Mayer and M. G. Mayer, Statistical Mechanics, John Wiley and Sons, N. Y. (1940) p. 165.

AlF at 1000°K. Assuming that the anharmonicity is comparable and that only the stretching modes for AlF₃ contribute, led to the belief that the correction would be approximately +0.2 eu/mole. On the other hand, neglecting anharmonicity and stretching, an uncertainty in the entropy of the monomeric gas was estimated to be ±0.4 eu/mole.

Incidentally, our vapor pressure data set for the entropy of the monomeric gas an upper limit which is 0.8 eu/mole higher than the adopted value. This maximum value is obtained by assuming the adopted entropy of the crystal to be too high by 0.1 eu/mole and the dimer content of the saturated vapor to be zero. With the same assumptions, a Second Law treatment applied to the vapor pressure data reported by Witt⁶, whose precision is comparable to ours as shown in Figure 3, would indicate an upper limit that is 0.2 eu/mole higher than the adopted value. That his limit is smaller than ours is in keeping with the fact that dimerization of the saturated vapor is less extensive in his temperature range than in ours.

RECOMMENDED VALUES

A final choice of values adequate to define completely reactions 1, 2, and 3 at high temperatures can be made by locating a point on any one of Figures 2(a), 2(b), or 2(c). Such a choice is most simply made from

Figure 2(a) since this graph plots the two quantities directly evaluated from mass spectrometric studies reported in the literature. These two experimental values, $\Delta H_{1000}^{\circ}(3) = 85.8 \pm 3$ kcal from Büchler's¹⁵ Second Law treatment of his data and $N_{d,1000} = 0.014 \pm 0.003$ from Porter and Zeller's¹⁴ data, locate a point which is at the center of the dashed rectangle, whose size corresponds to the two respective standard deviations.

Unfortunately, the center of this rectangle is at some distance from the solid curve, which is the curve corresponding to our data and the adopted value of $\Delta S_{1000}^{\circ}(1)$. It is then a matter of judgment as to how best to compromise this discrepancy. In view of the superior precision of our data, corresponding to a spread several times smaller than the distance between the two innermost dotted curves, we decided to require that the finally selected point lie on the solid curve. Next, two points on the curve were chosen, one agreeing exactly with the mean reported value of $\Delta H_{1000}^{\circ}(3)$ and the other agreeing exactly with the mean reported value of $N_{d,1000}$. The true value of $N_{d,1000}$ was assumed to lie between the abscissae of these two points. Furthermore, lacking information as to the relative systematic errors associated with the reported values of $\Delta H_{1000}^{\circ}(3)$ and $N_{d,1000}$, we selected approximately the mean of the two abscissae as a recommended value for $N_{d,1000}$ with an uncertainty determined by these two extremes.

This recommended value of $N_{d,1000}$ along with the solid curves of Figure 2 and eq 11, gives the recommended values of the other quantities as listed in Table II. (An extra digit is retained to preserve internal consistency.) On the basis of our earlier discussion, uncertainties of

Table II: Thermodynamic Values for Reactions 1, 2, and 3 at 1000°K

	$\Delta H^\circ(1)$ (kcal)	$\Delta S^\circ(1)$ (eu)	$\Delta H^\circ(2)$ (kcal)	$\Delta S^\circ(2)$ (eu)	$\Delta H^\circ(3)$ (kcal)	N_d
Previous Work	67.3 ± 3^a	44.12^b	-48 ± 3^c	-32 ± 3^c	85.8 ± 3^a	0.0114 ± 0.003^c
This Work	68.94	44.80	-56.2	-41.3	81.7	0.0091
Uncertainty						
from δN_d	± 0.03		± 3	± 3	± 3	± 0.004
from $\delta \Delta S^\circ(1)$	± 0.4	± 0.4	± 4	± 4	± 4	
from $\Delta T = \pm 1$ deg	± 0.06		± 0.6	± 0.6	± 0.6	
Overall	± 0.4	± 0.4	± 5	± 5	± 5	± 0.004

^a Reference 15. ^b Reference 31. ^c Reference 14. The value reported for $\Delta H^\circ(2)$ depends upon $\Delta S^\circ(2) = -32$ eu, which had been assumed by analogy.

³¹ D. R. Stull et al., JANAF Thermochemical Tables, Dow Chemical Co., Midland, Mich., (Sept. 30, 1965).

± 0.004 in $N_{d,1000}$, ± 0.4 eu in $\Delta S_{1000}^{\circ}(1)$, and ± 1 deg in ΔT were somewhat arbitrarily assumed; the uncertainties in each quantity in Table II corresponding to these separate magnitudes can readily be deduced from the curves of Figure 2, and are tabulated along with an overall uncertainty from the three sources. Also, several values resulting from previously published investigations are given in Table II for comparison.

The precision of our entrainment data was amply demonstrated by its comparison to that of some other investigations.^{2,3,6,8,10,11,12} After each reported vapor pressure was corrected for dimerization by the recommended values of $\Delta H^{\circ}(2)$ and $\Delta S^{\circ}(2)$ in Table II, $\Delta H_{1000}^{\circ}(1)$ was calculated by eq 8 and plotted in Figure 3 at the temperature of its measurement. The consistency of our points contrasts with the scattering of most of the others. Only the results of Witt⁶ agree rather closely with ours except for a systematic discrepancy equivalent to about 1 degree in measuring temperature. Nevertheless, even if his data has the same precision as ours, it could do much less toward evaluating dimerization; for N_d is much smaller at his temperatures than at ours.

While our precise entrainment data have not made it possible to assign smaller uncertainties to the individual quantities listed in Table II than those previously cited, it should be pointed out that these quantities are now much more precisely related to one another than the overall assigned tolerance of any that one might suggest. As a result, future precise measurement of one or possibly two other judiciously chosen properties of the aluminum fluoride system should be sufficient to permit fixing precise values for all these quantities.

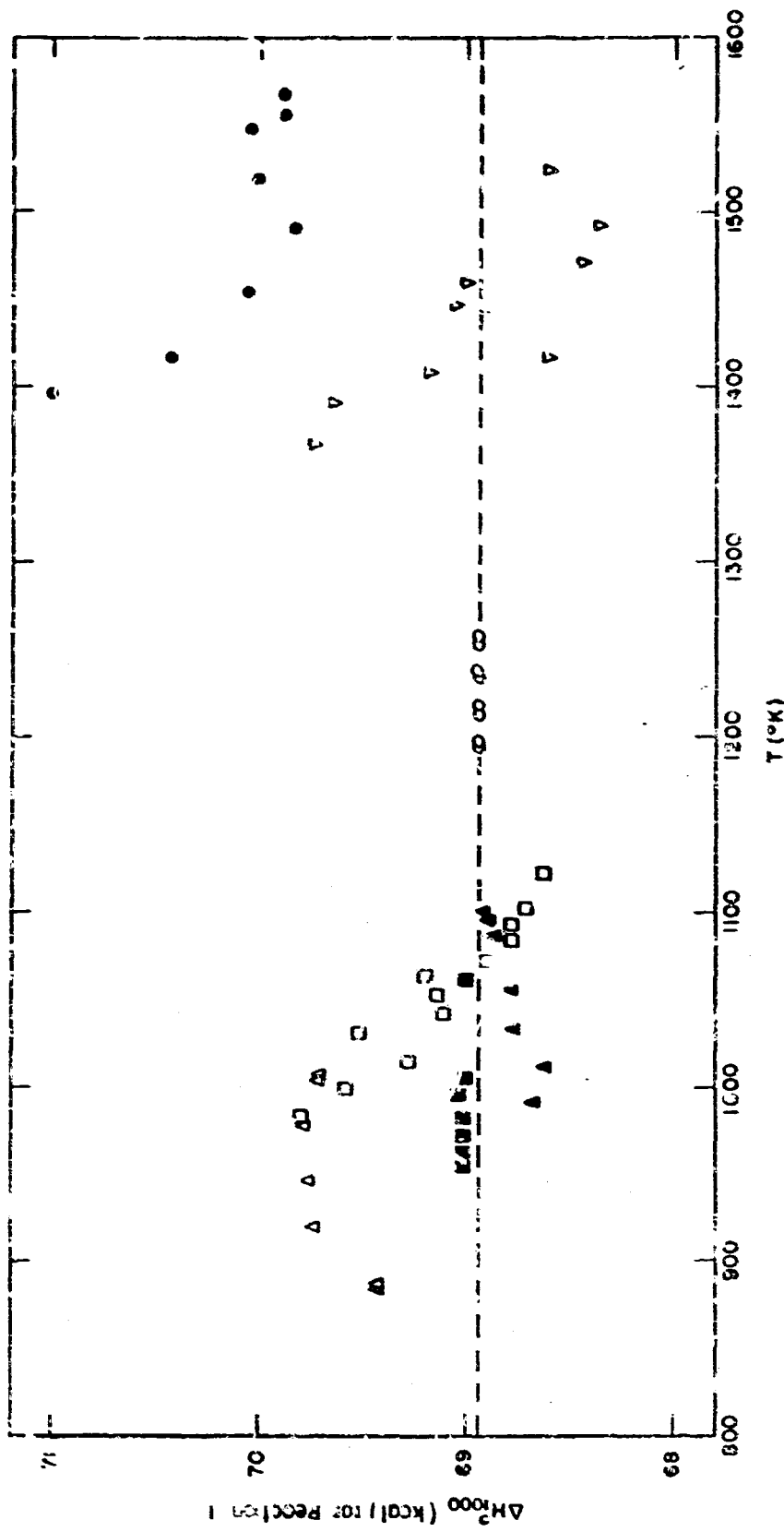
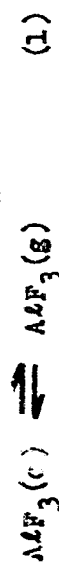


Figure 3. Third Law Values of ΔH_{1000}° for



from several vapor pressure measurements corrected for dimer: Olbrich² ●; Ruff and Le Boucher³, V; Witt⁶, ■; Evseev et al.⁸, □; Haldenbrand and Theard¹⁰, Δ; Blackburn¹², Δ; and this work, ○. Haldenbrand¹¹ reported an additional 108 values whose mean $\Delta H_{1000}^{\circ} = 68.29 \pm 0.16$ kcal. Note that each ΔH_{1000}° was derived using $\Delta S_{1000}^{\circ} = 14.50$ eu for reaction 1.

There are numerous other substances besides aluminum fluoride for which the status of the data available for evaluating the thermodynamics of evaporation and vapor association is similar. Invariably, the various types of data are related complexly, and hence inconsistencies among them are not easy to evaluate. We believe that such parametric plots as Figure 2(2) offer perhaps the clearest and most objective means of establishing what the inconsistencies are, how sensitive they are to errors in the various types of data, and whether there are one or more sets of fundamental thermodynamic quantities which appear to fit all the available data within the respective experimental reliabilities.

ACKNOWLEDGMENTS

The initial development of the entrainment apparatus was carried out by A. C. Victor. We thank E. J. Maienthal and R. A. Paulson for their chemical analyses of the sample, and appreciate the helpful advice of D. R. Lide, Jr. and S. Abramowitz in evaluating the spectroscopic data. George Long, of the Aluminum Company of America, kindly supplied the sample.

A MASS SPECTROMETRIC STUDY OF THE BeO-BeF₂ SYSTEM
AT HIGH TEMPERATURES

J. Efimenko

1. INTRODUCTION

This is a final report, including revisions, of the study of the BeO-BeF₂ reaction made in this laboratory. The study was initiated to provide thermodynamic data, previously unavailable, for the vapor-condensed state reaction of these two compounds.

At first the individual compounds were examined spectrometrically. Although the mass spectra of BeF₂ [1,2] and BeO [3,4] had been obtained by others, it was advisable to establish the mass positions, fragments and other characteristics with the same instrument to be used for the system. This is of importance in order to distinguish a product of reaction from impurities, etc. At the same time it was possible to obtain data of intrinsic interest on solid BeF₂.

2. EXPERIMENTAL

2.1. Mass Spectrometer

The instrument used in this research was based on the design of Chupka and Inghram [5] and was built by Nuclide Analysis Associates (State College, Pennsylvania). It is classified as a 12-inch radius of curvature, 60° sector, directional focusing instrument. This early design has the Knudsen cell source section positioned 60° from the vertical and the generated molecular beam is coaxial with the ion beam produced. This mass spectrometer design is described in detail in reference 5. A modification was made to the vacuum pumping system by replacing the two-inch mercury vapor pump on the Knudsen cell chamber with a six-inch mercury pump.

2.2. Beryllium Difluoride

For the vaporization of beryllium difluoride small effusion cells fabricated from molybdenum and nickel were employed. Each was of half-inch outside diameter, one inch high with a one-sixteenth inch wall thickness and a one-half millimeter diameter cylindrical orifice in the cover. Heating was accomplished by radiation from a concentric, cylindrical helix about the effusion cell. The temperature sensed with a Pt-PtRh (10%) thermocouple fastened into a hole in the bottom of the cell was taken to be the vaporization temperature. It was not possible to determine the temperature gradient along the cell but no condensation of BeF₂ was visible on the top half of the effusion cells at the conclusion of an experiment.

Beryllium difluoride was obtained from Brush Beryllium Company and was partly dehydrated by heating to 400°C for 12 hours. A sample of this material had been ground and passed through 20-50 mesh. The x-ray pattern made at NBS of the BeF_2 sample did not show a high degree of crystallinity. The detectable pattern could be attributed to the hexagonal form. Chemical analyses at NBS indicated less than 0.01% N present. The beryllium difluoride specimens were not water free.

2.3. Beryllium Oxide

Beryllium oxide was volatilized from a tungsten effusion cell, three-fourths inch outside diameter, one and one-fourth inch long, one-eighth inch wall thickness with an orifice in the cover, one millimeter in diameter. The cell was heated by a regulated electron bombardment unit (Cambridge Products Corp.) and a Leeds and Northrup optical pyrometer was employed to obtain the temperature present in a radial hole near the bottom of the cell.

The cell was filled three-fourths full with the oxide which was in the form of a very fine powder.

2.4. $\text{BeO} + \text{BeF}_2$

Due to the large difference in volatility of these two compounds, a modified reaction cell was devised. The low melting BeF_2 was contained in a tantalum tube attached into the bottom of a molybdenum effusion cell. One tantalum tube was 6.3 mm outside diameter, 0.375 mm wall thickness and 79 mm long. The second tantalum tube employed was 150 mm in length. The effusion cell containing a granulated beryllium oxide was heated by electron bombardment and the temperature gradient established along the tube insured that no BeF_2 would condense elsewhere. A deep hole located radially in the thick molybdenum cell bottom was used to indicate the reaction region temperature with an optical pyrometer. A Pt-PtRh (10%) thermocouple spotwelded to the tantalum tube bottom monitored the temperature of the BeF_2 source.

The experimental condition was modified by attaching the 150 mm tantalum tube to the same effusion cell. This allowed the relative concentrations of the reactants to be altered in the effusion chamber by establishing a different temperature for the beryllium difluoride.

The BeO used in this part was a low density solid prepared at NBS. A spectrochemical analysis performed by the NBS Spectrochemical Analysis Section indicated amounts found by weight per cent - > 10, Be; 0.01-0.001, Al, Si; < 0.001, Ba, Ca, Cu, Mg, Mn, Pb; questionable trace, Cr, Sn; not found, Ag, As, Au, B, Bi, Cd, Ce, Co, Ni.

3. RESULTS AND DISCUSSION

3.1. Beryllium Difluoride

Experimental data are presented in table 1 and in the form of a $\log P \cdot T$ vs $1/T$ plot in figure 1. The curve was fitted by a least squares treatment. The slope of this curve gives a sublimation enthalpy, $\Delta H_{\text{sub}}^\circ = 55.35 \pm 0.53$ kcal/mol. Reduction to absolute zero reference state was made using table A-51 (NBS Report No. 8504) and table B-58 (NBS Report No. 8186), $\Delta H_f^\circ = 56.28 \pm 0.53$ kcal/mol. A tabulation of literature sublimation enthalpies are listed in JANAF Thermochemical Data Tables [6] under beryllium difluoride and the values which were considered acceptable by the compilers ranged from 54.0 to 57.0 kcal/mol for second law calculations and 54.14 to 55.36 for third law results. Some difference between those results and the work done in this laboratory may exist because the specimen used in this work was mainly glassy. However, as mentioned in reference 6, the enthalpy difference between glassy and crystalline beryllium difluoride is most likely of the order of one or two kcal per mol. It should be noted that the reference temperature for the NBS reports is absolute zero whereas that for the JANAF tables is 298°K.

A mass spectrometric calibration was not carried out with the effusion cells used for BeF_2 as vapor pressure data already were available through absolute measurements [2,8-12].

Initial heating of hygroscopic BeF_2 produced copious amounts of ions, m/e 18, 19, 20 and some transient species. Those listed in table 2 illustrate from an exploratory experiment, with a layer of BeO on top of some BeF_2 , the ions produced. In all experiments a large background intensity at m/e 28 (CO^+ , N_2^+) prevented reliable intensity measurements for $(\text{BeF})^+$.

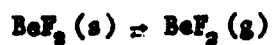
3.2. Beryllium Oxide

The vapor species from the oxide appeared in the following mass positions: $m/e = 9, 16, 75, 32, 25, 50$ in decreasing order of intensity at approximately 2100°C. The positive ions corresponding to these masses are Be^+ , O^+ , $(\text{BeO})_3^+$, O_2^+ , $(\text{BeO})^+$, $(\text{BeO})_2^+$, which check with results of previous investigators [3]. A more detailed study of BeO will be presented at a future date.

In this experiment at the high temperature, part of the beryllium ion intensity showed a behavior often referred to as "photoeffect" [7] or "anomalous ion effect" with this instrument. This effect may be a factor in the discrepancy between mass spectrometric and Knudsen weight loss measurements for the decomposition pressures of BeO . Mass spectrometric results are valid only if the ions are formed by electron impact in the ionization source. The routine use of a shutter alone to differentiate the ions issuing from the effusion cell and originating in background gases does not detect the "anomalous" effect.

Table 1

DATA



Index No.	T, °K	I_{47}^+ (1 volt) (scale)	T	$10^3/T$
1	721	1.60	1153	1.3870
2	723	1.60	1157	1.3831
3	724	1.70	1232	1.3812
4	749.1	6.00	4495	1.3349
5	749.7	6.40	4798	1.3339
6	754.4	7.50	5658	1.3256
7	780.3	24.3	18960	1.2816
8	780.1	24.3	18960	1.2819
9	783.2	27.3	21380	1.2768
10	781.1	26.1	20390	1.2802
11	781	24.9	19450	1.2804
12	780	24.3	18950	1.2821
13	795.1	47.0	37370	1.2577
14	796	48.0	38210	1.2563
15	796.5	50.0	39830	1.2555
16	778	23.0	17890	1.2853
17	778	23.3	18130	1.2853
18	777.5	22.8	17730	1.2862
19	776	20.1	15600	1.2887
20	753.5	6.90	5199	1.3271
21	753	6.75	5083	1.3280
22	714	0.55	678	1.4006
23	714	0.90	643	1.4006
24	745.5	4.80	3578	1.3414
25	745.7	4.75	3542	1.3410
26	747.1	5.10	3810	1.3385
27	748.8	6.40	4792	1.3355
28	786.0	29.5	23190	1.2723
29	785.4	29.0	22780	1.2732
30	818.9	111.0	90900	1.2212
31	790.1	38.0	30020	1.2657
32	789.1	38.0	29990	1.2673
33	787.9	38.0	29940	1.2692
34	785.5	34.2	26860	1.2731
35	762.2	12.8	9756	1.3119
36	768	13.5	10370	1.3021
37	760	13.8	10600	1.3021
38	767	13.8	10580	1.3038
39	767	13.5	10350	1.3038
40	777	21.5	16710	1.2870
41	738	3.65	2694	1.3550
42	735	3.45	2536	1.3605

Table 1, continued

Index No.	T, °K	I_{47}^+ (1 volt) (scale)	$I^+ T$	$10^3/T$
43	705	0.66	465	1.4184
44	710	0.80	568	1.4085
45	746	5.15	3842	1.3405
46	737	3.35	2469	1.3569
47	730	2.75	2008	1.3699
48	776	23.7	18390	1.2887
49	772	19.8	15290	1.2953

Table 2

Vapor Species from $\text{BeF}_2 \cdot x\text{H}_2\text{O} + \text{BeO}$
During Initial Heating

m/e	Probable Species	T, °K
18	$(\text{H}_2\text{O})^+$	
20	$(\text{HF})^+$	
23	$(\text{Na})^+$	
26	$(\text{BeOH})^+$	< 1700
27	$(\text{BeOH}_2)^+$	low
36	$(\text{HOF})^+$	< 1700
38	$(\text{F}_2)^+$	
44	$(\text{BeOF})^+$	low
47	$(\text{BeF}_2)^+$	
64	$(\text{BeOHF}_2)^+$	< 1800
72	$(\text{Be}_2\text{OF}_2)^+$	> 1600
75	$(\text{BeO})_2^+$	> 1350

Where no temperature values are given, the intensities were detected only below the optical pyrometer scale, i.e., 700°C.

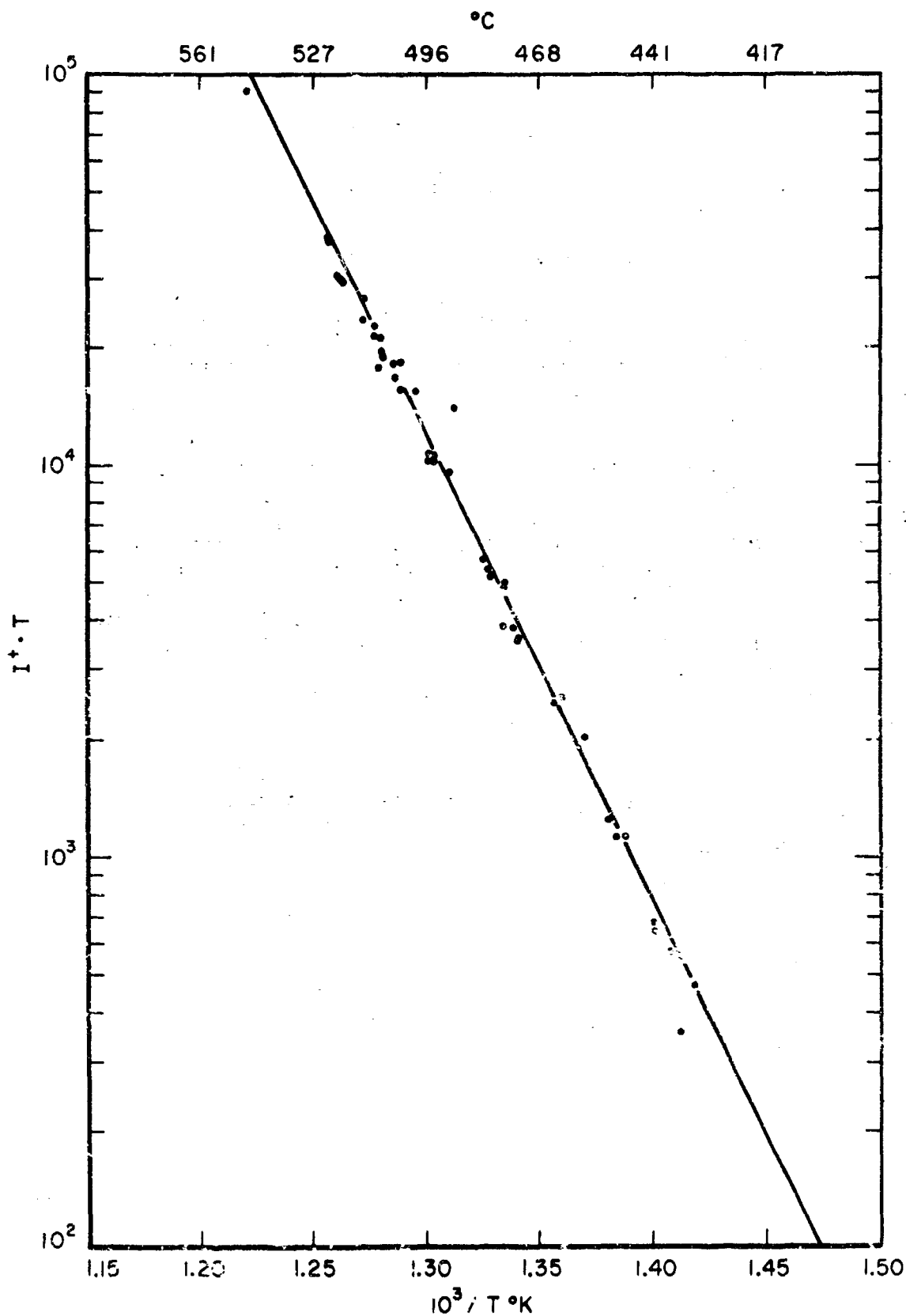
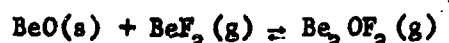


FIGURE 1: The curve is a least squares fit to the data of Table 1. The heat of sublimation obtained from this curve is 55.35 ± 0.53 kcal/mol for the arithmetic mean temperature, 755°K .

3.3. BeO-BeF₂ System

The presence of Be₃OF₂ in the temperature region above 1600°K permits examination of the equilibrium:



Data from the first set of experimental conditions, computed equilibrium constants and reaction enthalpies referred to absolute zero are shown in table 3, also similar information resulting from higher temperature observations is given in table 4. Auxiliary data and the sources are presented in table 5. The reaction enthalpy was obtained also by plotting the ratios of ion intensities A , as $\log A$ vs $1/T$, illustrated in figures 2 and 3. Least squares computations determined the slopes for the experimental points and their standard deviations. These slopes were used to give the reaction enthalpies, $\Delta H_{1730}^\circ = 39.25 \pm 3.5$ kcal/mol and $\Delta H_{2035}^\circ = 40.68 \pm 0.86$ kcal/mol. These enthalpies were corrected to absolute zero reference state, giving $\Delta H_0^\circ = 40.50 \pm 3.5$ kcal/mol and 42.62 ± 0.86 kcal/mol from which one has a mean value 41.56 ± 1.8 kcal/mol. The values of the reaction enthalpies shown in tables 3 and 4 give a mean value, $\Delta H_0^\circ = 42.6$ kcal/mol. Using the mean enthalpy obtained from the slopes, $\Delta H_0^\circ = 41.56$ kcal/mol and the heats of formation from table 5, the heat of formation of Be₃OF₂(g) was computed, $\Delta H_{0f}^\circ = -283.3$ kcal/mol.

The ion intensity ratios were converted to equilibrium constants with the aid of a silver calibration value obtained experimentally and ionization cross-sections shown in table 5. The expressions shown in (1), (2), and (3) were employed to obtain the desired thermodynamic quantities from the experimental data.

$$P_i = \frac{I_i^+}{S_i(T)} \quad (1)$$

$$S_i = S_s \frac{\sigma_i}{\sigma_s} \cdot \frac{\gamma_i}{\gamma_s} \cdot \frac{T_s}{T_i} \quad (2)$$

$$\log K_T = - \frac{\Delta H_T^\circ}{2.303 R} \left(\frac{1}{T} \right) + C \quad (3)$$

- I_i^+ = positive ion intensity of specie i
- P_i = partial pressure
- S_i = mass spectrometric sensitivity for specie i

S_r = mass spectrometric sensitivity for calibrating specie, Ag^+
 σ_i, σ_s = ionization cross sections for i and s
 Y_i, Y_s = multiplier efficiency for i and s
 T_i, T_s = absolute temperatures
 K = equilibrium constant
 ΔH_T° = reaction enthalpy at temperature T
 R = gas constant

Although Be_2OF_2 may be formed by reaction between BeF_2 and one or more of the polymers of $BeO(g)$, the reaction postulated is considered to give the greatest contribution because of the low intensities of the beryllium oxide vapor molecules even at the high temperatures of the experiment. The reaction with solid BeO does not occur to a large extent as evidenced by the magnitude of the equilibrium constant. Analysis by x-ray diffraction of the BeO solid before and after reaction with BeF_2 indicated no new phases, only a BeO phase with a slight contamination of molybdenum oxide.

Due to the uncommon design of the Knudsen effusion cell, a check was made for equilibrium conditions. The data in table 3 were obtained using a large concentration of $BeF_2(g)$ in the reaction zone. Then the concentration of $BeF_2(g)$ was decreased by replacing the short tantalum tube with a longer one as described in section 2.4. and the data in table 4 was obtained. Both straight line plots shown in figures 3 and 4 show that the Mass Action Law was obeyed. These two experimental variations also indicate that the flow rate of $BeF_2(g)$ to the reaction cell was not a limiting factor. The interior of the Knudsen cell was carefully baffled, requiring the $BeF_2(g)$ to execute a reverse flow path before leaving the effusion cell. Its intensity was taken as a measure of its concentration in this reaction.

Spectrochemical analysis indicated two elements that might cause interference with the identification of the product determined, Be_2OF_2 . The beryllia contained Si and Al as contaminants in the range 0.01-0.001 weight per cent each. Silicon was present probably as the oxide. In a reducing environment a possibility exists that $(Si_2O)^+$ would have been generated at high temperature. In the presence of an excess of fluoride it is more likely that $(SiOF)^+$ should have appeared at m/e 73. The experimental heating times were lengthy and impurities generally decreased with time but the observed product, $(Be_2OF_2)^+$, increased with temperature and did not decrease with time. Aluminum in the form of its oxide might react in the presence of water vapor to produce $(Al_2OH_2)^+$ under proper high temperature environment. After extended pumping and gentle heating the ion intensity of water decreased greatly but this had no effect on the ion intensity of $(Be_2OF_2)^+$.

Ionization of the vapor species with electrons of 70 ev energy must cause some fragmentation. Since the equilibrium constant for this reaction depended only on the ratio of product and reactant, each to the

Table 3

Mass Spectrometric Temperature - Intensity Data

Index No.	T, °C	T, °K Corr.	I_{72}^+ Volt	I_{42}^+ Volt	$K \times 10^3$	ΔH°
4	1285	1570	0.013	7.3	0.908	41.9
5	1307	1592.5	0.011	6.6	0.852	42.9
1	1337	1623	0.025	6.7	1.90	41.1
13	1343	1629	0.017	5.7	1.52	42.0
6	1383	1670	0.040	8.4	2.43	41.4
3	1425	1713	0.081	15.0	3.06	41.7
12	1431	1719	0.081	20.4	2.04	43.0
7	1465	1753	0.126	19.2	3.35	42.3
2	1500	1789	0.530	50.8	5.32	41.5
11	1522	1811	0.470	52.0	4.61	42.6
8	1530	1819	0.470	42.0	5.72	41.9
10	1548	1838	0.700	61.0	5.86	42.2
9	1600	1891	1.200	80.0	7.66	42.4

Table 4

Mass Spectrometric Temperature - Intensity Data

Index No.	T, °C	T, °K _{Corr.}	I_{2+}^+ Volt	I_{47+}^+ Volt	$K^* \times 10^2$	ΔH_0°
28	1738	2032	0.050	1.98	1.29	43.3
21	1740	2034	0.024	0.87	1.40	43.0
22	1740	2034	0.020	0.74	1.35	43.2
23	1783	2077	0.029	0.86	1.72	43.0
24	1820	2110	0.075	1.41	2.71	41.8
27	1825	2119	0.138	3.40	2.07	43.2
25	1855	2150	0.108	2.37	2.32	43.2
26	1875	2169	0.228	4.00	2.91	42.5
43	1582	1872	0.009	0.75	0.61	43.0
42	1640	1937	0.019	1.08	0.90	42.8
31	1655	1947	0.017	0.99	0.91	42.9
32	1700	1992	0.032	1.38	1.18	42.9
41	1713	2013	0.040	1.62	1.26	43.0
33	1750	2045	0.051	1.68	1.55	42.8
40	1760	2054	0.087	2.85	1.55	43.0
34	1785	2079	0.093	2.64	1.80	42.9
39	1810	2105	0.110	2.82	2.00	43.0
35	1829	2125	0.153	3.50	2.23	42.9
38	1838	2134	0.153	3.40	2.30	43.0
36	1857	2153	0.273	4.30	3.24	41.9
37	1898	2195	0.295	4.90	3.07	42.8

The chronological sequence of experimental measurements is recorded by the index numbers. Equilibrium constants, K^* are computed from the data; the ΔH_0° values, heat of reaction at absolute zero, were computed from free energy functions. In table 4, data with index nos. 21-28 and index nos. 31-43 were taken at a day interval. The data of table 4 were taken 6 months after the data of table 3.

Table 5

Auxiliary Data for Computations

Value		Source
Window Transmissivity, $5.00 \pm 0.63 \times 10^{-8}$		Author
Relative Ionization Cross-sections,		ref. 2
Be ,	6.31	
O ,	3.29	
F ,	1.85	
Standard Heat of Formation		
	ΔH_f° kcal/mol	$\Delta H_{f,98}^\circ$ kcal/mol
BeO(s)	-142.28	-143.1 \pm 4
BeF ₂ (g)	-182.55	-182.9 \pm 5
		NBS Report 6928, July 1960, Table C-2
Enthalpy of Reaction		
$\Delta H_{f,98}^\circ$	42.22 kcal/mol	computed
ΔH_f°	41.56 kcal/mol	computed
$\Delta H_{f,98}^\circ$	40.68 \pm 0.80 kcal/mol	this work
Enthalpy and Free Energy Functions		
BeO(s)	NBS Report 6484 July, 1959	Table 2-8
BeF ₂ (s,l)	NBS Report 8186 Jan., 1964	Table B-58, revised
BeF ₂ (g)	NBS Report 8504 July, 1964	Table A-51, revised
Be ₂ OF ₂ (g)	NBS Report 8186 Jan., 1964	Table A-86

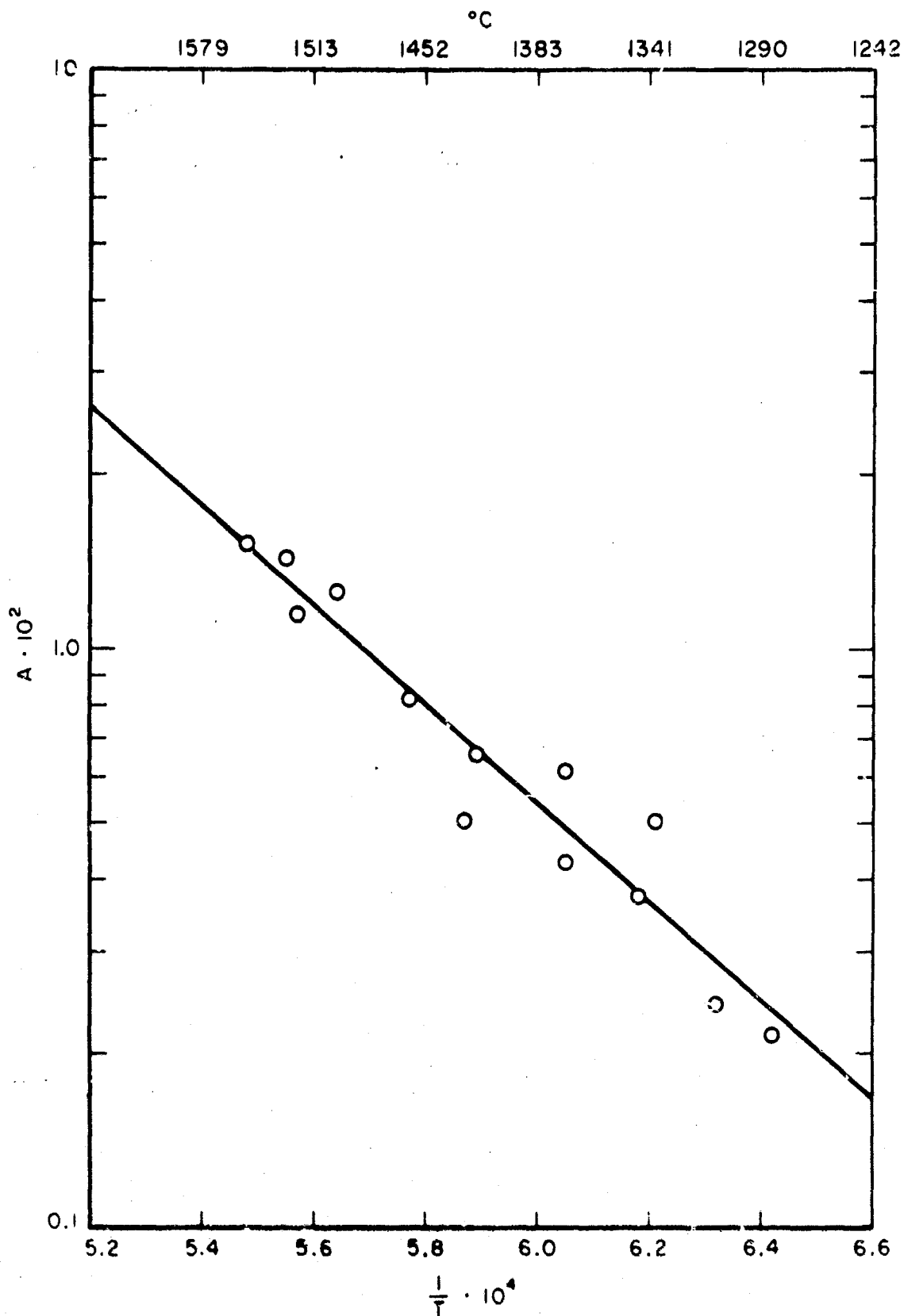


FIGURE 2: Formation of BeO(g) between 1510°K and 1890°K
 $\Delta H_{780}^\circ = 39.25 \pm 1.5 \text{ kcal/mol}$

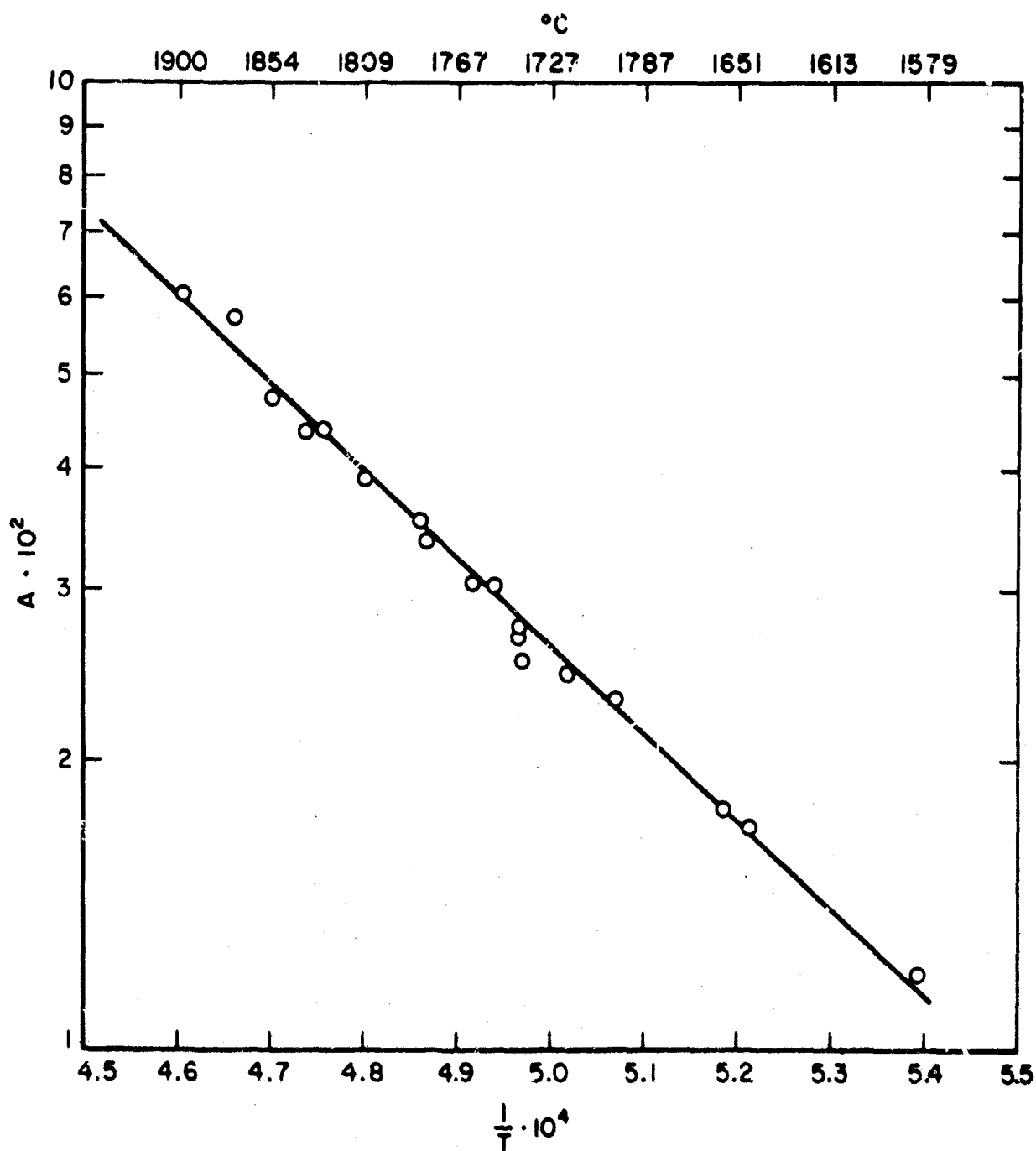


FIGURE 3: Formation of $\text{Be}_2\text{O}_2(\text{g})$ between 1870°K and 2200°K
 $\Delta H_{\text{f,298}}^\circ = 40.68 \pm 0.86 \text{ kcal/mol}$

same power, errors due to fragmentation and erroneous ionization cross sections tend to be minimal. However, the value of the slope is not dependent on the absolute value of the intensities and is free of the above uncertainties. Although there is question that some additive ionization cross sections may be too high [13], no simple advancement has been made over the additivity rule.

References

- [1] Berkowitz, J. and Chupka, W. A., Ann. N. Y. Acad. Sci. 79, 1073-1078 (1960).
- [2] Hildenbrand, D. L. and Theard, L. P., J. Chem. Phys. 42, 3230-3236 (1965).
- [3] Chupka, W. A., Berkowitz, J., and Giese, C. F., J. Chem. Phys. 30, 827-834 (1959).
- [4] Theard, L. P. and Hildenbrand, D. L., J. Chem. Phys. 41, 3416-3420 (1964).
- [5] Chupka, W. A. and Inghram, M. G., J. Phys. Chem. 59, 100-104 (1955).
- [6] JANAF Thermochemical Tables, Dow Chemical Co., Midland, Michigan, August 1965; BeF₂ table, June 30, 1964.
- [7] Inghram, M. G. and Drowart, J., "High Temperature Technology," McGraw-Hill Book Co., New York, pp. 224 (1960).
- [8] Greenbaum, H. A., Foster, J. N., Avin, M. L., and Farber, M., J. Phys. Chem. 67, 36-40 (1963).
- [9] Sense, K. A. and Stone, R. W., J. Phys. Chem. 62, 453 (1958).
- [10] Khandamirova, N. E., Evseev, A. M., Pozhorskaya, G. V., Borisov, E. A., Nesmeyanov, A. N., and Gerasimov, Ya. I., Zhur. Neorg. Khim. 4, 2192 (1959).
- [11] Novoselova, A. V., Muratov, F. Sh., Reshetnikova, L. P., and Gordeev, I. V., Vestnuk. Moskov. Univ., Ser. Mat. Mekh. Astron. Fiz. Khim. 13, 181 (1958).
- [12] Ozhigov, E. P. and Zatsarin, A. I., Trudy Dol'nevost. Filiala. Akad. Nauk SSSR, Ser. Khim. 1961, 24-34 (1961).
- [13] Pottier, R. F., J. Chem. Phys. 44, 916-922 (1966).

Chapter 6

VAPORIZATION OF REFRACTORY MATERIALS: ARC-IMAGE MASS SPECTROMETRY

J. J. Diamond and A. L. Dragoo

The E.A.I. Quad 200, a quadrupole mass spectrometer manufactured by Electronic Associates, Inc. has been set up to permit the use of arc-image heating to melt and vaporize alumina. Pumping was accomplished by a sorption pump and a small ion pump, resulting in a background pressure of about 10^{-6} Torr during the vaporization of the alumina.

Due to the very unfavorable geometry of the set-up, the mass spectrum of the direct beam from the molten alumina was not detectable above the background. However, the peak due to mass number 32 was observed to gradually build up during the heating until it was a major peak, and to rapidly disappear when the alumina was solidified and cooled.

We interpret the observation as follows. Prior published work has indicated that alumina vaporizes primarily to Al and O, with minor amounts of Al_2O and AlO . Our own prior work has shown that the Al and O recombine on the glass walls of the working chamber to form Al_2O_3 . The buildup of the O_2 peak is direct evidence of the fact that some of the O forms O_2 rather than Al_2O_3 . Hence the Al_2O_3 formed must be slightly non-stoichiometric, or if stoichiometric must contain some Al metal or Al suboxides.

The observation, reported in a previous report in this series, that differential thermal analysis of Al_2O_3 condensed from the vapor shows an irreversible exothermic double peak at 320 and 340°C, is consistent with this conclusion.

Chapter 7

THE STATUS OF THE THERMOCHEMICAL DATA ON SOME Be COMPOUNDS

by Vivian B. Parker

I. Introduction

As part of the revision of NBS Circular 500 "Selected Values of Chemical Thermodynamic Properties", we have completed a review of the available data on all beryllium compounds. We present here a summary of values selected from this review for substances pertinent to the Light Element Thermodynamics Program. We are including also a brief discussion of the sources from which these values have been calculated. It is hoped that this report will indicate areas in which additional research is required. We will appreciate it if data that have been overlooked or errors in the values are brought to our attention before the results are published.

All auxiliary data and constants used in the calculations are given in the first two parts of NBS Technical Note 270 [1]. Caution should be exercised if these values must be combined with data taken from other compilations or sources, in order to avoid errors caused by a lack of consistency between the tables.

II. Discussion of Data

Be(c) This is taken as the standard state. The thermal functions were taken from the evaluation of Hultgren et al. [2]. Since their review high temperature enthalpy measurements (in range 600 - 2200°K) have been made by Kantor et al. [3]. These measurements are in good agreement with Hultgren's estimated values.

Be(g) The ΔH_{subl} , 298°K = 78.0 kcal/mole has been taken from the evaluation of Hultgren et al. [2] as have the thermal functions of the ideal monatomic gas. More recent vapor pressure measurements by Greenbaum

et al. [4] lead to a Third Law value in good agreement with this; Kortum et al.'s [5] measurements do not. An unpublished value of Hildenbrand, Hall and Ju cited by Hildenbrand and Murad [6] is also in good agreement.

BeO(c) See $\text{BeF}_2(\text{c, quartz})$ and $\text{BeF}_2(\text{amorp})$. Since the selections of ΔH_f° for BeF_2 and BeO were made simultaneously, the discussion of BeO will be found under BeF_2 .

BeO(g) Herzberg [7] gives the ground state as $1\Sigma^+$ and tabulates the spectroscopic data; Thrush [8] confirms $1\Sigma^+$ as the ground state. The Dow Chemical Company [9] gives the thermal functions, calculated from the data in the above sources, but Brewer and Trajnor [10] point out that at the higher temperatures the state having the major effect upon the thermodynamic calculations will be the 3Π , for which there is no information. We have therefore used the thermal functions only as an approximate guide in calculating ΔH_f° of BeO(g) from the mass spectrometric study of Chupka, et al. [11] on the vapor above BeO(c) . They reported $\Delta E_0^\circ = 104.4$ for $\text{BeO(g)} \rightarrow \text{Be(g)} + \text{O(g)}$ and $\Delta E_0^\circ = -11.39$ for $\text{BeO(g)} + \text{O(g)} \rightarrow \text{Be(g)} + \text{O}_2(\text{g})$. These reactions lead to $\Delta H_f^\circ = 32$ and 30 kcal/mole, respectively. See Herzberg [7] and Gaydon [12] for their interpretations of the dissociation limit.

Be₂O(g) Theard and Hildenbrand [13] from mass spectrometric Knudsen effusion experiments have shown the existence of $\text{Be}_2\text{O(g)}$ in the equilibrium vapor above BeO(c) at temperatures around 2300°K . Using their estimated functions for $\text{Be}_2\text{O(g)}$ we obtain $\Delta H^\circ = 332$ kcal for $2\text{BeO(c)} \rightarrow \text{Be}_2\text{O(g)} + \text{O(g)}$, 141 kcal for $(\text{BeO})_2(\text{g}) \rightarrow \text{Be}_2\text{O(g)} + \text{O(g)}$, and -17 kcal for $2\text{BeO(g)} \rightarrow \text{Be}_2\text{O(g)} + \text{O(g)}$.

(BeO)_n(g) Chupka, et al. [11] from their mass spectroscopic study of the vapor above BeO(c) have shown the existence of $(\text{BeO})_n$ ($n = 2, 3, 4, 5, 6$)(g). Using the estimated thermal functions for $(\text{BeO})_n$ from the Dow Chemical Co. [9], we obtain $\Delta H_{\text{subl}} = 182$ kcal/mol for $(\text{BeO})_2(\text{g})$, 175.5 for $(\text{BeO})_3(\text{g})$, 192 for $(\text{BeO})_4(\text{g})$, 211 for $(\text{BeO})_5(\text{g})$ and 223 for $(\text{BeO})_6(\text{g})$. ΔH_f° $(\text{BeO})_2(\text{g})$ was adjusted, however, from the calculated -108 kcal, to -102 kcal for the reasons cited by the Dow Chemical Co. [9].

BeH(g) Gaydon [12] gives $D_0^\circ = 2.3$ ev. Evans [14] has calculated the thermal functions from the spectroscopic data given by Herzberg [7]. The Dow Chemical Co. [15] calculations are in essential agreement.

Be(OH)₂(α , tetragonal and β , orthorhombic) Bear and Turnbull [16] measured the heats of solution of Be(c), Be(OH)₂(c, α) and Be(OH)₂(c, β) in 22.6% aqueous HF at 294°K. By difference we obtain, at 298°K, $\Delta H = -79.83$ for Be(c) + 2H₂O(lq) \rightarrow Be(OH)₂(c, β) + H₂(g) and $\Delta H = -79.10$ for Be(c) + 2H₂O(lq) \rightarrow Be(OH)₂(c, α) + H₂(g), or $\Delta H_f(c,\beta) = -216.5$ kcal/mol and $\Delta H_f(c,\alpha) = -215.7$ kcal/mol. Fricke and Wüllhorst [17] measured the heats of solution of BeO(c), Be(OH)₂(c,stable) and Be(OH)₂(c,metastable) in 11.59% aqueous HF. By difference we obtain $\Delta H = -2.52$ kcal for BeO(c) + H₂O(lq) \rightarrow Be(OH)₂(c,stable) and $\Delta H = -1.78$ kcal for BeO(c) + H₂O(lq) \rightarrow Be(OH)₂(c,metastable) or $\Delta H_f^\circ(c,\text{stable}) = -215.8$ and $\Delta H_f(c,\text{metastable}) = -215.1$ kcal. Similarly, Matignon and Marchal [18, 19] measured the heats of solution of BeO(c) and an unspecified form of Be(OH)₂(c) in 30% aqueous HF at 289°K. By difference, corrected to 298°K, we obtain BeO(c) + H₂O(lq) \rightarrow Be(OH)₂, $\Delta H = -3.2$ or ΔH_f Be(OH)₂ = -216.4 kcal. Fricke and Severin [20] measured the equilibrium water vapor pressures over Be(OH)₂(β). At 403°K, $\Delta H = 15.5$ kcal/mol H₂O(g). This results in $\Delta H_f^\circ = -216.5$ kcal in agreement with Bear and Turnbull. We have accepted the values obtained from Bear and Turnbull's measurements.

The Dow Chemical Co. [9] gives $S^\circ(c,\beta) = 12.6$ eu, as an estimate based on a comparison of the chlorides of Be, Mg, and Ca. This value appears reasonable and results in $\Delta G_f^\circ(c,\beta) = -195.7$ kcal. From Sillen and Martell [21] we obtain $\log K_s = -21.5$ for (c, β) and -21.1 for (c, α), so that $\Delta G^\circ = +0.55$ for $\beta \rightarrow \alpha$ or $\Delta G_f^\circ(c,\alpha) = -195.1$ kcal/mol and $S^\circ(c,\alpha) = 13.4$ cal/deg mol.

Be(OH)₂(g) Altman [22] reviews and discusses the experimental data on the reaction, BeO(c) + H₂O(g) \rightarrow Be(OH)₂(g). Using the K_p 's from the study of Young [23] in the temperature range 1700-1820°K we obtain, using the estimated thermal functions of the Dow Chemical Co. [9], a Second Law value for $\Delta H^\circ = 44.1$ kcal and a Third Law value $\Delta H^\circ = 41.4$ kcal; resulting in $\Delta H_f^\circ = -158.7$ and -161.4 kcal/mol, respectively. Similarly from

Grossweiner and Seifert's [24] data between 1473°K to 1873°K, we obtain $\Delta H = 43.0$ and 42.8 kcal, respectively or $\Delta H_f^\circ = -159.8$ and -160.0 kcal. From Hutchison and Malm [25], $\Delta H^\circ = 47.3$ and 47.9 kcal or $\Delta H_f^\circ = -155.5$ and -154.9 kcal. Altman also cites the measurements of Elliot [26] and Berkman and Simon [27] which, when corrected to the Dow Chemical Co. thermal functions, result in Third Law values of 45.7 and 43 kcal for ΔH° , or $\Delta H_f = -157.1$ and -159.8 kcal, respectively. More recent measurements by Blauer, et al. [28] at four temperatures in the range 1570 to 1810°K , using the low pressure molecular flow reaction method result in a Third Law $\Delta H^\circ = 35.2$ or $\Delta H_f = -167.6$ kcal.

Douglas [29] also reviews the data on the thermodynamic properties of gaseous hydrates of BeO. He points out that under the conditions of the transpiration measurements the hydrate product of the reaction of BeO(c) with H_2O is all or predominantly $\text{Be}(\text{OH})_2(\text{g})$ below 1850°K but that the possibilities of small amounts of other hydrates, $(\text{Be}^\circ)_n \cdot \text{H}_2\text{O}(\text{g})$ being formed cannot be dismissed.

BeF(g) Greenbaum et al. [4], by the molecular flow effusion method have determined the equilibrium for the reaction, $\text{BeF}_2(\text{g}) + \text{Be}(\text{c}, \text{liq}) \rightarrow 2\text{BeF}(\text{g})$ in the temperature range $1420^\circ\text{K} - 1675^\circ\text{K}$. The Second Law and Third Law values for ΔH°_{298} are 97.0 and 89.6 kcal/mol, respectively, resulting in $\Delta H_f = -46.3$ and -53.0 kcal. Hildenbrand and Murad [6] used a mass spectrometer to study high-temperature equilibria among vapor species produced by the fluorination of elemental beryllium with CaF_2 and BF_3 in a Knudsen effusion cell. For the reaction $\text{Be}(\text{g}) + \text{BeF}_2(\text{g}) \rightarrow 2\text{BeF}(\text{g})$ we obtain Third Law ΔH°_{298} values of 27.7 , 28.6 and 29.9 kcal/mol, from the Be- BF_3 system, the Be- CaF_2 system and the Be-Al- CaF_2 systems, respectively, or an average $\Delta H_f^\circ = -41.5$ kcal. Second Law ΔH° values for the first two systems are 26.8 and 30.2 kcal/mol, respectively, or an average $\Delta H_f = -41.6$ kcal. Also from the Be-Al- CaF_2 system for the reaction $\text{Be}(\text{g}) + \text{AlF}(\text{g}) \rightarrow \text{BeF}(\text{g}) + \text{Al}(\text{g})$, from two values for K at 1423° and 1443°K we obtain a Third Law $\Delta H_f = -54.3$ kcal. We have taken $\Delta H_f^\circ = -41.5$ kcal or $D_0^\circ = 5.96$ ev. This is in good agreement with Hildenbrand and Theard's [30] estimate of $D_0^\circ = 6.0$ ev. Gaydon [12], Herzberg [7] and Tatevskii, et al. [31] give 4.0 , 5.4 and 8.0 ev, respectively.

The thermal functions were taken from the Dow Chemical Co. [15]. They were calculated using the constants given by Herzberg [7]. The thermal functions calculated by Evans et al. [32] using the spectroscopic constants of Tetevskii et al. [31] as interpreted by Woolley [33] are in perfect agreement. The ground state is $2s^2$.

$\text{BeF}_2(\text{c, quartz})$, $\text{BeF}_2(\text{amorphous})$ and $\text{BeO}(\text{c})$ As pointed out earlier, the evaluation and selection of values for BeF_2 and $\text{BeO}(\text{c})$ were made simultaneously since the direct determinations of ΔH_f for both compounds were discordant; the final values had to be decided on the basis of the interconnecting ΔH° for the reaction of $\text{BeO}(\text{c})$ with HF to form BeF_2 .

The discussion of the independent determinations for $\text{BeO}(\text{c})$ follow.

The heat of combustion of $\text{Be}(\text{c})$ was determined by Moose and Parr [34], (temperature unspecified), Roth, Burger, and Siemonsen [35], at 293°K, Neuman, Kroger and Kunz [36] at 292°K, Mielenz and v. Wartenberg [37] at 298°K and Cosgrove and Snyder [38] at 300.4°K. The ΔH_f° 's are -134.4, -147.3, -145.3, -136.2 and -143.1 kcal, respectively.

Matignon and Marchal [39] have measured the heats of solution of $\text{Be}(\text{c})$ and $\text{BeO}(\text{c})$ in 30% HF solutions, as have Copaux and Philips [40]. By difference, we obtain for the reaction $\text{Be}(\text{c}) + \text{H}_2\text{O}(\text{liq}) \rightarrow \text{BeO}(\text{c}) + \text{H}_2(\text{g})$, $\Delta H = -70.9$ and -62.1 kcal/mole, or $\Delta H_f = -139.2$ and -130.4 kcal, respectively.

Neumann, Kroger, and Kunz [36] measured the $\Delta H^\circ_{\text{comb}}$ of Be_3N_2 (crystal form unspecified) to form $\text{BeO} + \text{N}_2$ to be -300.6 kcal/mole $\text{Be}_3\text{N}_2(\text{c})$. Neumann, Kroger and Haebler [41] directly determined $\Delta H_f^\circ \text{Be}_3\text{N}_2$ to be -134.1 kcal. Combining these two reactions we obtain $\Delta H_f^\circ \text{BeO}(\text{c})$ to be -144.9 kcal.

From the cell measurements of Smirnov and Chukreev [42], in the temperature range 955° to 1313°K we obtain a Second Law $\Delta H^\circ = -94.56$ and a Third Law $\Delta H^\circ = -93.73$ kcal/mole for $\text{Be}(\text{c}) + 1/2 \text{CO}_2(\text{g}) \rightarrow \text{BeO}(\text{c}) + 1/2 \text{C}(\text{graph})$ or $\Delta H_f^\circ = -141.6$ and -140.8 kcal, respectively.

From the above values for $\Delta H_f^\circ \text{BeO}(\text{c})$ we would tentatively say the "best" value is that of Cosgrove and Snyder [38] although they did not determine the completeness of the reaction.

We turn now to the measurements on BeF_2 . Taylor et al. [43] measured the

heat of the α , quartz form from 8° to 300°K and have also determined H° - $H_{273^\circ K}$ between 300° and 1200°K. They have also determined the ΔH_{soln} of both the α , quartz form and the glassy form in acetic acid-sodium acetate solutions to be -3.64 and -4.76 kcal/mole, respectively. This leads to a ΔH_{trans} (quartz \rightarrow glass) = 1.12 kcal.

Good [44] reports ΔH_f° (amorphous) = -242.9 kcal. Assuming the amorphous and glassy states are the same, ΔH_f° (α , quartz) = -244.0 kcal. P. Gross [45] reports ΔH° = -84.0 kcal for $\text{Be}(c) + \text{PbF}_2(c) \rightarrow \text{Pb}(c) + \text{BeF}_2(\text{gl})$ which results in $\Delta H_f^\circ(\text{amorph})$ = -242.7 and $\Delta H_f^\circ(\text{quartz})$ = -243.8 kcal. Churney and Armstrong [46], in describing their own work, also review the earlier results on BeF_2 . They cite the unpublished measurements of J. Simmons which lead to $\Delta H_f^\circ \text{BeF}_2(c)$ = -257.0. Their own measurements on the combustion of $\text{Be}(c)$ with F_2 lead to two values for $\Delta H_f^\circ(\text{amorphous})$, one with a ΔH_f° = -246.3 kcal with an estimated systematic error from +0.2 to -1.8 kcal/mole, and the other with ΔH_f° = -244.2 with an estimated systematic error of +0.3 to -1.5 kcal/mole. These values result in $\Delta H_f^\circ(c)$ = -247.4 and -245.3 kcal/mole.

Kolesov, et al. [47] measured the heats of solution at 294°K of $\text{BeO}(c)$ and a crystal form of BeF_2 which they called β , cristobalite. Their reactions corrected to 298°K yield: $\Delta H_f^\circ \text{BeO}(c) - \Delta H_f^\circ \text{BeF}_2(c) = +99.26$ kcal. If we use our tentative selection of $\Delta H_f^\circ \text{BeO}(c) = -143.1$ we obtain $\Delta H_f^\circ \text{BeF}_2(c) = -242.4$ kcal, which in view of Churney and Armstrong's, Good's, and Gross' values, appears too positive (we are making the assumption that the β , cristobalite BeF_2 Kolesov specifies would be equivalent to the quartz form). If we reverse the selection and take $\Delta H_f^\circ \text{BeF}_2(c) = -245.3$ we obtain $\Delta H_f^\circ \text{BeO}(c) = -146.0$. Referring now to our earlier discussion on the values for $\text{BeO}(c)$ we now have:

Roth, et al. [35]	-147.3
Neumann, et al. [36]	-145.3
Cosgrove and Snyder [38]	-143.1
Neumann, et al. [36, 41]	-144.9
Kolesov, et al. [47]	-146.0

We have selected $\Delta H_f^\circ \text{BeO(c)} = -145.0$ and $\Delta H_f^\circ \text{BeF}_2\text{(c)} = -245.3$ kcal.

The thermal functions for BeO(c) were obtained from the Dow Chemical Company [8].

$\text{BeF}_2\text{(g)}$ The estimated thermal functions used in the calculations were obtained from the Dow Chemical Company [48].

The following table shows the vapor pressure measurements reported for $\text{BeF}_2\text{(c, liq)}$, the temperature range of measurements and the Second and Third Law values for $\Delta H^\circ_{\text{subl}}$.

Investigator	Temp. Range °K	Second Law ΔH°	Third Law ΔH°
Cantor [49]	1146°-1372°	56.03	55.70
Khandamirova [50]	846°-950°	58.7	56.07
Sense and Stone [51]	1075°-1293°	55.37	55.65
Sense, Snyder and Clegg [52]	1019°-1076°	60.8	55.58
	1075°-1241°	55.9	
Hildenbrand and Theard [30]	821°-942°	55.98	55.40
Blauer, et al. [53]	713°-795°	58.1	53.70
Greenbaum, et al. [54]	823°-1053°	56.66	54.85
Efimenko [55]	755°	56.8	
Novoselova, et al. [56]	1040°-1376°	52.3	55.2

From these values we obtain $\Delta H^\circ = 55.7$ kcal or $\Delta H_f^\circ \text{(g)} = -189.6$ kcal/mol.

Greenbaum, et al. [57] by the differential torsion method obtained the K's for the equilibrium $\text{BeO(c)} + 2\text{HF(g)} \rightarrow \text{BeF}_2\text{(g)} + \text{H}_2\text{O(g)}$ in the temperature range 943° to 1243°K. The Second and Third Law ΔH° are 22.2 and 26.5 kcal, respectively or $\Delta H_f^\circ = -194.6$ and -190.3 kcal/mol.

Hildenbrand and Theard [30] determined the K's of $\text{BeF}_2\text{(g)} + 2\text{Al(c)} \rightarrow \text{Be(c)} + 2\text{AlF(g)}$ in the range 897 to 946°K by the torsion method. The Third Law $\Delta H^\circ = 59.3$ or $\Delta H_f = -182.7$ kcal. The Second Law value = 62.6 or $\Delta H_f = -186.0$ kcal.

$\text{BeF}_2\text{(aq)}$ and H_2BeF_4 (in conc. aqueous HF) Petersen [58] reported $\Delta H = -32.6$ kcal for $\text{BeCl}_2\text{(aq)} + 2\text{AgF} \rightarrow 2\text{AgCl(c)} + \text{BeF}_2\text{(aq)}$, or $\Delta H_f^\circ = -249.8$ kcal. Also from his reactions $2\text{HF}_{300} + \text{H}_2\text{O} + \text{BeCl}_{2600} \rightarrow \text{soln.}$; $\Delta H = -4.87$ kcal, and $2\text{HCl}_{300} + \text{BeF}_2\text{(aq)} \rightarrow \text{soln.}$; $\Delta H = +1.22$, we obtain $\Delta H_f^\circ \text{BeF}_2\text{(aq)} = -250.3$ kcal.

BeF₂(aq, in HF solutions) See H₂BeF₄(aq, in concentrated aq HF).
 Be₂OF₂(g) Efimenko [52] reported $\Delta H_f^\circ = 42.6$ kcal for BeO(c) + BeF₂(g)
 \rightarrow Be₂OF₂(g) or $\Delta H_f^\circ = -291$ kcal/mol.

Mann [60] estimated the molecular constants of Be₂OF₂(g); Evans [61] calculated the ideal gas thermal functions.

H₂BeF₄(aq, in concentrated aqueous HF) BeF₂ in HF solutions is a mixture with complex ion formation. Very little is known about the equilibrium processes and their respective heats of formation and the effect of varying the concentration of H₂O and HF upon the complex ions. This makes it virtually impossible to correct to a common basis; this is accentuated by, in many cases, the lack of details concerning the total number of moles of HF and H₂O reacting with Be(c), BeO(c), Be(OH)₂, and BeF₂(c) to form the aqueous mixture. There were two possibilities in treating the data: 1. to call the species aqueous BeF₂ and to correct, where possible or necessary, for the dilution of HF; and 2. to call the species something which relates the concentration of HF to BeF₂ more directly, and to correct on that basis. We have called this species H₂BeF₄. This by no means solves the dilemma. The values arrived at for H₂BeF₄ at specific H₂BeF₄/HF/H₂O ratios do however show more clearly the problems involved. A comparison of the values arrived at for the two treatments follows. (X refers to an unknown number of moles of HF·nH₂O present. It is not to be considered constant.) See Table 1.

BeCl(g) Potter [66] reported $\Delta H_f^\circ = 14.1 \pm 2.2$ kcal/mol from the reaction Be(g) + AlCl(g) \rightarrow BeCl(g) + Al(g) and 13.0 ± 2.9 kcal from Be(g) + BeCl₂(g) \rightarrow 2BeCl(g). The auxiliary ΔH_f° values used are not given.

Hildenbrand, et al. [67], from the mass spectral intensities in the HCl-BeO system, report $K_{2140^\circ K} = .062$ for BeCl₂(g) + Be(g) \rightarrow 2BeCl(g). This results in $\Delta H_{298}^\circ = 31.1$ kcal or $\Delta H_f^\circ = +12$ kcal/mol.

Greenbaum, Arin, Wong and Farber [68] determined the K's for BeCl₂(g) + Be(liq) \rightarrow 2BeCl(g) in the range 1573° - 1723°K. Second and Third Law Treatments result in $\Delta H^\circ = 96.3$ and 88.7 kcal, respectively or $\Delta H_f^\circ = 5$ and 2 kcal/mol.

TABLE I.

INVESTIGATOR	REACTANTS	ΔH° kcal/mol	ΔH° BeF ₂ aq kcal/mol	Total no. moles HF + H ₂ O in final solution	ΔH° H ₂ BeF ₄ aq kcal/mol	Total no. moles HF + H ₂ O in final solution
Matignon and Marchal [18, 19]	BeO(c) + X(HF + 3.3 H ₂ O)	-22.4	-251.1	X(HF + >3.3 H ₂ O)	-403.1	X(HF + >3.3 H ₂ O)
	Be(OH) ₂ (c) + X(HF + 3.3 H ₂ O)	-20.1	-251.2	X(HF + >3.3 H ₂ O)	-403.2	X(HF + >3.3 H ₂ O)
Mulert [62]	Be(OH) ₂ ppt + X(HF + 4.4 H ₂ O)	-20.3	-250.5	X(HF + >4.4 H ₂ O)	-402.8	X(HF + >4.4 H ₂ O)
Copeaux and Phillips [63, 64]	BeO(c) + X(HF + 3.3 H ₂ O)	-20.3	-249.0	X(HF + >3.3 H ₂ O)	-401.0	X(HF + >3.3 H ₂ O)
Bear and Turnbull [16]	Be(c) + 679(HF + 3.80 H ₂ O)	-101.0	-252.5	677(HF + 3.81 H ₂ O)	-404.0	675(HF + 3.82 H ₂ O)
	Be(c) + 360(HF + 8.14 H ₂ O)	-101.45	-253.7	358(HF + 8.19 H ₂ O)	-406.0	356(HF + 8.25 H ₂ O)
	Be(c) + 901(HF + 2.59 H ₂ O)	-100.5	-252.3	899(HF + 2.597 H ₂ O)	-405.0	897(HF + 2.602 H ₂ O)
Kolesov, Popov and Skuratov [47]	BeO(c) + 342(HF + 3.801 H ₂ O)	-24.25	-252.4	340(HF + 3.826 H ₂ O)	-403.6	338(HF + 3.849 H ₂ O)
Armstrong and Goyle [65]	Be(c) + 6.465(HF + 3.308 H ₂ O)	-99.52	-251.0	4.465(HF + 4.800 H ₂ O)	-403.2	2.465(HF + 8.677 H ₂ O)

Gaydon [11] gives $D_0^\circ = 69$ kcal/mol. Novikov and Tunitskii [69] obtained $D_0^\circ = 36,555$ cm⁻¹ for the ground state but did not accept it. From an evaluation of the data they obtained $D_0^\circ = 5.9$ e.v. for X_Σ^{2+} state. The Dow Chemical Company [70] reevaluated Novikov and Tunitskii's data and showed that the linear extrapolation for $D_0^\circ = 36,555$ cm = 104.5 kcal is good. This results in $\Delta H_f^\circ = 1.7$ kcal.

The thermal functions were calculated by [70] from Novikov and Tunitskii's data. Their values are in agreement with those calculated by Evans, Hilsenrath, and Woolley [32] who used slightly different constants.

BeCl₂(c, α) and (c, β) The Dow Chemical Company [71] has tabulated the thermal functions of the α and β forms from the original measurements of McDonald and Oetting [72] on the α' and β form. The α form was assumed to be identical to α' .

Johnson and Gilliland [73] determined $\Delta H^\circ = -118.0$ kcal for the direct reaction $\text{Be}(c) + \text{Cl}_2(g) \rightarrow \text{BeCl}_2(c)$. However the crystal form of BeCl_2 was not identified.

Thompson et al. [74] measured the heats of solution of $\text{Be}(c)$ and $\text{BeCl}_2(c)$ and $\text{BeCl}_2(50\% \alpha$ and $50\% \beta)$ according to [71] in aqueous HCl. By difference we obtain $\Delta H^\circ = -43.70$ for $\text{Be}(c) + 8.381 (\text{HCl} + 8.114 \text{H}_2\text{O}) \rightarrow \text{BeCl}_2(\alpha, \beta) + \text{H}_2(g) + 6.381 (\text{HCl} + 10.654 \text{H}_2\text{O})$ or $\Delta H_f^\circ (\alpha, \beta) = -117.88$ kcal. Since $\Delta H^\circ = 1.5$ for $\beta \rightarrow \alpha$, we obtain $\Delta H_f^\circ (\alpha) = -117.2$ and $\Delta H_f^\circ (\beta) = -118.5$ kcal. Gross, et al. [75] reported the direct determination of $\Delta H_f^\circ \alpha' = -117.1$ kcal/mol.

From the cell data of Markov and Delmarskii [76] we obtain $\Delta H_f^\circ \alpha = -117.9$ kcal/mol.

The data of Mielenz and v. Wartenberg [37] and Liemonsen [77] are not in agreement.

BeCl₂(g) The Dow Chemical Company [71] estimated the thermal functions used here in calculating the Second and Third Law ΔH_f° from the vapor pressure measurements on the liquid and crystal. In cases where it was not clear whether the crystal form used was α or β , $\Delta H_{\text{subl}}^\circ$ was calculated for both $\beta \rightarrow$ gas and $\alpha \rightarrow$ gas and then used to obtain ΔH_f° . These are shown in the following table.

Investigator	Temp. range °K		$\Delta H_f^\circ \text{ BeCl}_2(\text{g})$ kcal/mol	
			2nd Law	3rd Law
Fischer, et al. [78]	638° - 673°	1f β	-82.6	-87.4
		1f α	-81.0	-87.3
	677° - 710°		-84.0	-87.7
Ko, et al. [79]	640° - 854°	from α , liq		-84.2
Greenbaum, et al. [60]	471° - 511°	1f β	-84.6	-85.9
		1f α	-83.1	-85.4
	441° - 600°	1f β	-84.9	-86.2
		1f α	-83.4	-85.8
Hildenbrand, et al. [67]	461° - 504°	β	-85.4	-87.5
Rahlfis and Fischer [81]	513° - 677°	1f β	-87.2	-87.5
		1f α	-85.6	-87.3
	679° - 731°		-86.2	-87.6
Sheiko and Feshchenko [82]	573° - 673°	1f β	-86.5	-87.0
		1f α	-84.9	-86.8
	693° - 753°		-86.4	-87.1

We have taken $\Delta H_f^\circ = -85.7$.

$\text{BeCl}_2(\text{aq, dilute})$ Thomsen [83] reported $\Delta H^\circ_{292} = -6.66$ kcal for $\text{BeSO}_4(400 \text{ H}_2\text{O}) + \text{BaCl}_2(400 \text{ H}_2\text{O}) \rightarrow \text{BaSO}_4(\text{ppt}) + \text{BeCl}_2(800 \text{ H}_2\text{O})$ and $\Delta H^\circ_{292} = -9.15$ kcal for $\text{BaCl}_2(400 \text{ H}_2\text{O}) + \text{H}_2\text{SO}_4(400 \text{ H}_2\text{O}) \rightarrow \text{BaSO}_4(\text{ppt}) + 2\text{HCl}(400 \text{ H}_2\text{O})$. By difference, we obtain $\Delta H^\circ_{298} = 2.9$ kcal for $\text{BeSO}_4(400 \text{ H}_2\text{O}) + 2\text{HCl}(400 \text{ H}_2\text{O}) \rightarrow \text{BeCl}_2(800 \text{ H}_2\text{O}) + \text{H}_2\text{SO}_4(400 \text{ H}_2\text{O})$. Using $\Delta H_f^\circ \text{ BeSO}_4(400 \text{ H}_2\text{O}) = -307.34$, we obtain $\Delta H_f^\circ \text{ BeCl}_2(400 \text{ H}_2\text{O}) = -171.3$ kcal. Matignon and Marchal [18, 19] reported $\Delta H^\circ_{293} = -6.97$ kcal for $\text{BeSO}_4(110 \text{ H}_2\text{O}) + \text{BaCl}_2(110 \text{ H}_2\text{O}) \rightarrow \text{BeCl}_2(220 \text{ H}_2\text{O}) + \text{BaSO}_4(\text{ppt})$. Using Thomsen's ΔH° for the reaction of $\text{BaCl}_2(400 \text{ H}_2\text{O}) + \text{H}_2\text{SO}_4(400 \text{ H}_2\text{O})$ and correcting for the dilution difference and to 298°K we obtain $\Delta H^\circ_{298} = 2.70$ kcal for $\text{BeSO}_4(110 \text{ H}_2\text{O}) + 2\text{HCl}(400 \text{ H}_2\text{O}) \rightarrow \text{BeCl}_2(220 \text{ H}_2\text{O}) + \text{H}_2\text{SO}_4(400 \text{ H}_2\text{O})$. Since $\Delta H_f^\circ \text{ BeSO}_4(110 \text{ H}_2\text{O}) = -306.79$ kcal, we obtain $\Delta H_f^\circ \text{ BeCl}_2(220 \text{ H}_2\text{O}) = -170.9$ kcal. Matignon and Marchal [19] also reported $\Delta H^\circ_{289} = -12.3$ kcal for $\text{BeCl}_2(\text{aq}) + 2\text{NaOH}(\text{aq}) \rightarrow \text{Be}(\text{OH})_2(\text{ppt}) + 2\text{NaCl}(\text{aq})$, and $\Delta H = -13.65$

for $\text{Be}(\text{OH})_2(\text{ppt}) + 2\text{HCl}(200 \text{ H}_2\text{O}) \rightarrow \text{BeCl}_2(\text{aq}) + 2\text{H}_2\text{O}(\text{liq})$. Using ΔH_f° $\text{Be}(\text{OH})_2(\text{fresh ppt}) = -214.6 \text{ kcal}$ we obtain $\Delta H_f^\circ = -172.3$ and -171.1 kcal , respectively. They also measured $\Delta H_{\text{soln}}^\circ, 289^\circ\text{K} = -51.1 \text{ kcal}$ for the crystal. This results in $\Delta H_f^\circ \text{BeCl}_2(\text{aq}) = -168.8$ if α' $\text{BeCl}_2(\text{c})$ or -170.0 if β . Pollok [84] also reported $\Delta H_{\text{soln}}^\circ$. This results in $\Delta H_f^\circ(\text{aq}) = -161.7$ if α was used or -163.0 if β .

$\text{BeCl}_2(\text{aq})$, in $68 \text{ H}_2\text{O} + 6.38 \text{ HCl}$ Thompson, Sinko, and Stull [74] reported $\Delta H_{\text{soln}}^\circ \text{BeCl}_2(0.5 \alpha'$ and $0.5 \beta)$ in $[6.381 \text{ HCl} + 67.98 \text{ H}_2\text{O}] = -45.91 \text{ kcal}$.

$\text{BeCl}_2 \cdot 4\text{H}_2\text{O}(\text{c})$ Biltz and Messerknecht [85] measured the heats of solution of $\text{BeCl}_2(\text{c})$ and $\text{BeCl}_2 \cdot 4\text{H}_2\text{O}(\text{c})$ in HCl . They reported $\Delta H = -44.1$ and -2.9 kcal , respectively. Assuming the BeCl_2 used was a mixture of the two forms, we obtain $\Delta H_f^\circ = -432.3 \text{ kcal}$. They also reported $\Delta H = -83.0 \text{ kcal}$ for $\text{BeCl}_2(\text{c}) + 4\text{H}_2\text{O}(\text{g}) \rightarrow \text{BeCl}_2 \cdot 4\text{H}_2\text{O}(\text{c})$, or $\Delta H_f^\circ = -432.0 \text{ kcal}$.

$\text{Be}_2\text{Cl}_4(\text{g})$ Hildenbrand, et al. [67] from a mass spectroscopic investigation of the vapor pressure of $\text{BeCl}_2(\text{c}, \beta)$ reported $\Delta H_{500^\circ\text{K}} = 33.0 \text{ kcal}$ for $\text{BeCl}_2(\text{c}) \rightarrow \text{BeCl}_2(\text{g})$ and $\Delta H_{500^\circ\text{K}} = 35.8 \text{ kcal}$ for $2\text{BeCl}_2(\text{c}) \rightarrow \text{Be}_2\text{Cl}_4(\text{g})$, or $\Delta H_{500^\circ\text{K}} = -30.2$ for $2\text{BeCl}_2(\text{g}) \rightarrow \text{Be}_2\text{Cl}_4(\text{g})$. This results in $\Delta H_f = -202 \text{ kcal}$.

Ko et al. [79] reported $\Delta H_{471^\circ\text{K}} = 32.2 \text{ kcal}$ for $\text{BeCl}_2(\alpha, \text{c}) \rightarrow \text{BeCl}_2(\text{g})$ and $\Delta H_{663^\circ} = 35.1 \text{ kcal}$ for $2\text{BeCl}_2(\alpha, \text{c}) \rightarrow \text{Be}_2\text{Cl}_4(\text{g})$. Then $\Delta H_{298}^\circ = -30 \text{ kcal}$ for $2\text{BeCl}_2(\text{g}) \rightarrow \text{Be}_2\text{Cl}_4(\text{g})$ or $\Delta H_f = -201 \text{ kcal/mol}$. The Dow Chemical Company [71] estimated the thermal functions.

$\text{BeBr}_2(\text{c})$ Biltz and Messerknecht [85] reported $\Delta H_{\text{soln}}^\circ \text{BeBr}_2(\text{c})$ in $\text{HCl} \cdot 8.8 \text{ H}_2\text{O} = -55.7 \text{ kcal}$ and similarly $\Delta H = -44.1 \text{ kcal}$ for $\text{BeCl}_2(\text{c})$ in HCl . Assuming BeCl_2 to be a mixture of α and β forms we obtain $\Delta H_f \text{BeCl}_2$ in $\text{HCl} \cdot 8.8 \text{ H}_2\text{O} = -162.0 \text{ kcal/mole}$. Assuming that the effect of Br^- for Cl^- is about the same as for infinite dilution we obtain $\Delta H_f^\circ \text{BeBr}_2$ in $\text{HCl} \cdot 8.8 \text{ H}_2\text{O} = -140.2 \text{ kcal/mol}$ and $\Delta H_f^\circ \text{BeBr}_2(\text{c}) = -84.5 \text{ kcal/mol}$.

$\text{BeI}_2(\text{c})$ Biltz and Messerknecht [85] reported $\Delta H_{\text{soln}}^\circ \text{BeI}_2(\text{c})$ in $\text{HCl} \cdot 8.8 \text{ H}_2\text{O} = -62.5 \text{ kcal}$. Using the same procedure as for $\text{BeBr}_2(\text{c})$ we obtain $\Delta H_f^\circ \text{BeI}_2$ in $\text{HCl} \cdot 8.8 \text{ H}_2\text{O} = -108.5 \text{ kcal}$ and $\Delta H_f^\circ \text{BeI}_2(\text{c}) = -46.0 \text{ kcal/mol}$.

Be₃N₂(c,α) and c,β) From Neumann, Kröger, and Kunz [36] we obtain $\Delta H = -300.6$ for $\text{Be}_3\text{N}_2 + 3/2 \text{C}_2 \rightarrow 3\text{BeO(c)} + \text{N}_2(\text{g})$ or $\Delta H_f^\circ = -134.4$ kcal/mol. Neumann, Kröger and Haebler [86] reported from direct reaction of Be with N₂, $\Delta H_f^\circ = -135.7$ kcal/mol. Hoenig [87] measured the decomposition pressure of $\text{Be}_3\text{N}_2(\text{c}) \rightarrow 3\text{Be(g)} + \text{N}_2(\text{g})$ from 1640°K to 1950°K, by the Knudsen and Langmuir methods. The best Third Law value for $\Delta H^\circ = 370.5$ kcal was obtained using the thermal functions relative to 298°K calculated by the Dow Chemical Company [15] from the C_p measurements of Douglas and Payne [88] and an estimated $S^\circ_{298} = 12$ e.u. This results in $\Delta H_f^\circ = -136.5$ kcal. However Douglas and Payne estimate $S^\circ = 8.1$ e.u. which would make $\Delta H^\circ = 377.5$ kcal and $\Delta H_f^\circ = -143.5$ kcal/mol. Yates, Greenbaum, and Farber [89] measured the decomposition pressure in the range 1450-1650°K. The Third Law $\Delta H_f^\circ = -140.3$ kcal/mol, using $S^\circ_{298.1} = 8.1$ e.u.

Gross, et al. [75] calorimetrically measured the ΔH° 's of the following reactions at 298°K:

1. $\text{Be}_3\text{N}_2(\alpha, \text{cubic}) + 3\text{Cl}_2(\text{g}) \rightarrow 3\text{BeCl}_2(\alpha') + \text{N}_2(\text{g}); \Delta H^\circ = -210.3$ kcal.
2. $3\text{Be(c)} + 2\text{NH}_3(\text{g}) \rightarrow 3\text{H}_2(\text{g}) + \text{Be}_3\text{N}_2(\text{c}, \alpha); \Delta H^\circ = -118.4$ kcal.
3. $\text{Be}_3\text{N}_2(\beta, \text{hexagonal}) + 3\text{Cl}_2(\text{g}) \rightarrow 3\text{BeCl}_2(\alpha') + \text{N}_2(\text{g}); \Delta H^\circ = -214.6$ kcal.
4. $\text{Be(c)} + \text{Cl}_2 \rightarrow \text{BeCl}_2(\alpha'); \Delta H^\circ = -117.1$ kcal.

From the above reactions we arrive at $\Delta H_f^\circ(\alpha, \text{cubic}) = -140.6$ kcal/mol and $\Delta H_f^\circ(\beta, \text{hexagonal}) = -136.5$ kcal/mol.

Be₂C(c) Pollock [90] measured the decomposition pressure of Be₂C in the range 1430° to 1669°K by the Knudsen technique. Using the estimated thermal functions of the Dow Chemical Company [91] we obtain Second and Third Law ΔH° values of 91.4 and 88.8 kcal, respectively for $1/2 \text{Be}_2\text{C} \rightarrow \text{Be(g)} + 1/2 \text{C(c)}$ or $\Delta H_f^\circ = -21.6$ and -26.8 kcal/mol. Muratov and Novoselova [92] measured the equilibrium CO(g) from 1808°K to 2003°K for the process $\text{BeO(c)} + 3/2 \text{C(graph.)} \rightarrow 1/2 \text{Be}_2\text{C(c)} + \text{CO(g)}$. Second and Third Law ΔH° are 98.0 and 97.3 kcal or $\Delta H_f^\circ = -41.1$ and -42.6 kcal/mol. Earlier measurements by Muratov and Novoselova [93] in the range 1673°K to 1953°K yield $\Delta H_f^\circ = -53.5$ kcal/mol. Motzfeldt [94] used the static method to measure the CO pressure from 1780°K to 2320°K. Second and

Third Law ΔH_f° 's are -24.8 and -31.2 kcal/mol.

Earlier data have been reviewed by [91].

Be₂SiO₄(c) Furukawa and Reilly [95] reevaluated the low temperature Cp data of Kelley [96]. The Dow Chemical Company [71] estimated the high temperature thermal functions.

Holm and Kleppa [97, 98] measured the ΔH_{soln} of Be₂SiO₄(c), BeO(c), and SiO₂(c, quartz) in a melt of 9PbO·3CdO·4B₂O₃ at 968°K. The values are $\Delta H = 7.95, 3.45, \text{ and } -3.64$ kcal, respectively which result in $2\text{BeO}(c) + \text{SiO}_2(\text{quartz}) \rightarrow \text{Be}_2\text{SiO}_4(c)$, $\Delta H_{968} = -4.69$ kcal. Corrected to 293°K, $\Delta H^\circ = -4.6$ kcal, or $\Delta H_f^\circ = -512.3$ kcal/mol.

Be(BO₂)₂(g)

Blackburn and Buchler [99] investigated the vaporization process in the BeO-B₂O₃ system by the Knudsen effusion method using the vacuum balance and a mass spectrometer, and by differential thermal analysis. They obtain $\Delta H_{1500^\circ\text{K}} = 22$ kcal for $\text{BeO}(c) + \text{B}_2\text{O}_3(g) \rightarrow \text{Be}(\text{BO}_2)_2(g)$. Using the estimated thermal functions for Be(BO₂)₂(g) from the Dow Chemical Company [71] we obtain $\Delta H_{298} = 22.8$ kcal or $\Delta H_f^\circ = -324$ kcal/mol.

Be₃B₂O₆(c) Blackburn and Buchler [99] reported $\Delta H_{1500^\circ\text{K}} = -23$ kcal for $3\text{BeO}(c) + \text{B}_2\text{O}_3(\text{liq}) \rightarrow \text{Be}_3\text{B}_2\text{O}_6(c)$. We have assumed that ΔH_{298}° for $3\text{BeO}(c) + \text{B}_2\text{O}_3(c) \rightarrow \text{Be}_3\text{B}_2\text{O}_6(c) = -19.4$ kcal or $\Delta H_f^\circ = -759$ kcal/mol.

Gross [100] reported $\Delta H_{\text{soln}}^\circ$ of 3BeO·B₂O₃(c, 25°C) in aqueous HF at 75°C = -110.07±0.4 kcal and that of the corresponding mixture = -123.38±0.14 kcal. This results in $\Delta H_{298} = -13.31$ kcal/mol for $3\text{BeO}(c) + \text{B}_2\text{O}_3(g) \rightarrow 3\text{BeO} \cdot \text{B}_2\text{O}_3(c)$ or $\Delta H_f^\circ = -748.2$ kcal/mole.

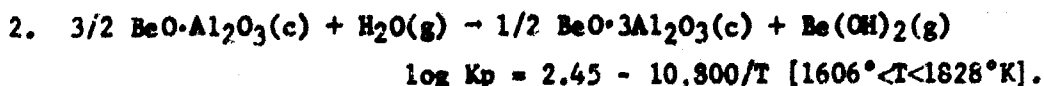
BeOAl(g) Efimenko and Horton [101] recalculated the results of their mass spectroscopy study of the vapor species in equilibrium with Al₂O₃·BeO. From their given pressures for the range 2150°K to 2570°K we obtain a Third Law $\Delta H_{298} = -221.1$ kcal for $\text{Al}(g) + \text{Be}(g) + \text{O}(g) \rightarrow \text{AlOBe}(g)$ or $\Delta H_f^\circ = -5.6$ kcal/mol. The Second Law $\Delta H_f^\circ = -2.8$ kcal. The thermal functions used were calculated by Evans [14] from the estimated molecular constants of Mann [102].

BeO·Al₂O₃(chrysoberyl) Furukawa and Saba [103] measured the heat capacity from 16° to 380°K and calculated the thermodynamic properties. Dittmars and Douglas [104] measured the high temperature relative enthalpies

and tabulated the thermodynamic functions up to 2150°K.

Holm and Kleppa [97] measured the ΔH_{soln} at 968°K of BeO(c) , $\text{Al}_2\text{O}_3\text{(c)}$, $\text{BeO} \cdot \text{Al}_2\text{O}_3\text{(c)}$ and $\text{BeO} \cdot 3\text{Al}_2\text{O}_3\text{(c)}$, in the melt of $9\text{PbO} \cdot 3\text{CdO} \cdot 4\text{B}_2\text{O}_3$. From their results we obtain $\Delta H_{968^\circ\text{K}} = -4.0 \pm 0.3$ kcal for $\text{BeO(c)} + \text{Al}_2\text{O}_3\text{(c)} - \text{BeO} \cdot \text{Al}_2\text{O}_3\text{(c)}$.

Young [22] reported for the following reactions:



$$\log K_p = 1.55 - 9,450/T \quad [1626^\circ < T < 1791^\circ\text{K}]$$

then for $\text{BeO(c)} + \text{Al}_2\text{O}_3\text{(c)} \rightarrow \text{BeO} \cdot \text{Al}_2\text{O}_3\text{(c)}$

$$\Delta H_{1700^\circ\text{K}}^\circ = -4.9 \text{ kcal}, \quad \Delta G^\circ = -3.2 \pm 1.4 \text{ kcal and} \\ \Delta S = -1.0 \text{ e.u.}$$

If we correct Holm and Kleppa's $\Delta H_{968^\circ\text{K}}$ to 1700°K we obtain $\Delta H_{1700^\circ\text{K}}^\circ = -4.4 \pm 0.3$. Since this value for ΔH and Young's value for ΔG are more accurate than the ΔH from the Clausius-Clayeyron equations, we may use $\Delta H_{1700^\circ\text{K}}^\circ = -4.4 \pm 0.3$ and $\Delta G^\circ = -3.2 \pm 1.4$ to obtain $\Delta S = -0.7$ in agreement with the $\Delta S = 0.11$ obtained from the calorimetric S° values of Furukawa and Saba and the relative enthalpy measurements of Dittmars and Douglas. We have therefore accepted the tabulated thermodynamic functions for $\text{BeO} \cdot \text{Al}_2\text{O}_3\text{(c)}$ with $S_{298}^\circ = 15.84$ and $\Delta S_{1700^\circ\text{K}} = 0.11$ for the above reaction and have used a weighted average from Holm and Kleppa's ΔH and Young's ΔG to obtain $\Delta H_{298}^\circ = -4.12$ or $\Delta H_{298}^\circ = -549.2$ kcal/mol.

$\text{BeO} \cdot 3\text{Al}_2\text{O}_3\text{(c)}$ Furukawa and Saba [105] measured the heat capacity from 15 to 390°K and tabulated the thermodynamic properties. Dittmars and Douglas [104] measured the high temperature relative enthalpies and tabulated the thermodynamic functions up to 2150°K.

As in the case of $\text{BeO} \cdot \text{Al}_2\text{O}_3\text{(c)}$, we obtain from Holm and Kleppa's [97] ΔH° 's $\text{BeO(c)} + 3\text{Al}_2\text{O}_3\text{(c)} \rightarrow \text{BeO} \cdot 3\text{Al}_2\text{O}_3\text{(c)}$. $\Delta H_{968^\circ\text{K}}^\circ = 2.9 \pm 0.5$ kcal which corrected to 1700°K becomes $\Delta H = 3.66 \pm 0.5$. From Young's measurements we obtain $\Delta G_{1700}^\circ = -2.7 \pm 2.2$ kcal, $\Delta H = -0.8$ kcal and $\Delta S = +1.7$ e.u. Since Young's ΔG° and Holm and Kleppa's ΔH are the two more accurate values we may use them to calculate a more accurate $\Delta S_{1700^\circ\text{K}}^\circ = 4.3 \pm 1.5$ e.u.

The $\Delta S^\circ_{1700^\circ\text{K}}$ derived using the calorimetric S° of Furukawa and Saba and the relative enthalpy measurements of Dittmars and Douglas is +2.97 e.u. As Holm and Kleppa point out there is a possibility of a zero point entropy due to random mixing of the Be^{+2} and Al^{+3} but the evidence is not conclusive. We have therefore accepted the thermal functions but have increased the uncertainty of S° to cover this possibility. Using $\Delta S^\circ_{1700} = 3.0$ and Young's $\Delta G_{1700} = -3.7 \pm 2.2$ kcal we obtain a $\Delta H^\circ = +1.3 \pm 2.2$ kcal. Using a weighted average of this value and that of Holm and Kleppa, we obtain $\Delta H^\circ_{1700^\circ\text{K}} = 3.2$ kcal, $\Delta H^\circ_{298} = 2.3$ kcal and $\Delta H^\circ_f = -1344.2$ kcal/mol.

BIBLIOGRAPHY

1. D. D. Wagman, W. H. Evans, I. Halow, V. B. Parker, S. Bailey, and R. Schumm, Selected Values of Chemical Thermodynamic Properties, National Bureau of Standards Technical Notes 270-1 and 270-2 (U.S. Gov't)
2. R. R. Hultgren, R. L. Orr, P. D. Anderson, and K. K. Kelley, Selected values of thermodynamic properties of metals and alloys, 963 pp. (John Wiley and Sons, Inc. (1963)).
3. P. B. Kantor, R. M. Krasovitskaya and A. N. Kisel', Fiz. Metal i Metalloved. 10, 635 (1960).
4. M. A. Greenbaum, R. E. Yates, M. L. Arin, et al., J. Phys. Chem. 67, 703 (1963).
5. G. P. Kortun, A. A. Kruglykh and V. S. Pavlov, Izvest. Akad. Nauk SSSR, Met. i Gorn. Delo 1964, 177-9.
6. D. L. Hildenbrand and E. Murad, J. Chem. Phys. 44, 1524 (1966).
7. G. Herzberg, Molecular spectra and molecular structure. I. Spectra of diatomic molecules, 2nd ed., (D. Van Nostrand Co., New York, London (1950)).
8. B. A. Thrush, Proc. Chem. Soc. 1960, 339.
9. Dow Chemical Company - JANAF Thermochemical Tables, Sept. 30, 1963.
10. L. Brewer and S. Trajmor, J. Chem. Phys. 36, 1585 (1962).
11. W. A. Chupka, J. Berkowitz and J. F. Giese, J. Chem. Phys. 30, 927 (1959).
12. A. G. Gaydon, Dissociation energies and spectra of diatomic molecules, (Chapman and Hall, Ltd., London, (1953)).
13. L. P. Theard and D. L. Hildenbrand, J. Chem. Phys. 41, 3416 (1964).
14. W. H. Evans, NBS Report 8504, p. 123 (July 1, 1964).
15. Dow Chemical Company - JANAF Thermochemical Tables, March 31, 1963.
16. I. J. Bear and A. G. Turnbull, J. Phys. Chem. 69, 2828 (1965).
17. R. Fricke and B. Wüllhorst, Z. anorg. u. allgem. Chem. 205, 127 (1932).
18. C. Matignon and G. Marchal, Compt. rend. 181, 859 (1925).
19. C. Matignon and G. Marchal, Bull. soc. chim. France [4], 39, 167 (1926).

20. R. Fricke and H. Severin, Z. anorg. u. allgem. Chem. 205, 287 (1932).
21. L. G. Sillen and A. E. Martell, Stability constants of metal-ion complexes, Chem. Soc. London, Spec. Publ. No. 17, 754 pp. (London, 1964).
22. R. L. Altman, J. Chem. Eng. Data 8, 534 (1963).
23. W. A. Young, J. Phys. Chem. 64, 1003 (1960).
24. L. I. Grossweiner and R. L. Seifert, J. Am. Chem. Soc. 74, 2701 (1952).
25. C. A. Hutchison and J. G. Malm, J. Am. Chem. Soc. 71, 1338 (1949).
26. G. R. B. Elliot, U.S.AEC UCRL Rept. 1831, 52 pp. (June 1952).
27. M. G. Berleman and S. L. Simon, U.S.AEC ANL-4177, 22 pp. (July 15, 1948).
28. J. Blauer, M. A. Greenbaum, and M. Farber, J. Phys. Chem. 70, 973 (1966).
29. T. B. Douglas, CPIA Publication No. 108 I, 27 (June 1966)).
30. D. L. Hildenbrand and L. P. Theard, J. Chem. Phys. 42, 3230 (1965).
31. V. M. Tatevskii, L. N. Tunistiskii and M. M. Novikov, Optika i Spektroskopiya 5, 520 (1958).
32. W. H. Evans, J. Hilsenrath and H. W. Woolley, NBS Rept. 6928, A1 (July 1, 1960).
33. H. W. Woolley, NBS Rept. 6928, 41 (July 1, 1960).
34. J. E. Moose and S. W. Parr, J. Am. Chem. Soc. 46, 2656 (1924).
35. W. A. Roth, E. Bürger, and H. Siemonsen, Z. anorg. u. allgem. Chem. 239, 321 (1938).
36. B. Neumann, C. Kröger, and H. Kunz, Z. anorg. u. allgem. Chem. 218, 379 (1934).
37. W. Mielenz and H. v. Wartenberg, Z. anorg. u. allgem. Chem. 116, 267 (1921).
38. L. A. Cosgrove and P. E. Snyder, J. Am. Chem. Soc. 75, 3102 (1953).
39. C. Matignon and G. Marchal, Compt. rend. 183, 927 (1926).
40. H. Copaux and E. Philips, Compt. rend. 176, 579 (1923).
41. S. Neumann, C. Kröger, and H. Haeblar, Z. anorg. u. allgem. Chem. 204, 381 (1932).

42. M. V. Smirnov and N. Ya. Chukreev, Zhur. Neorg. Khim. 3, 2445 (1958) .
43. A. R. Taylor and T. E. Gardner, U.S. Bureau of Mines Rept. Invest. 6664, 15 pp. (1965).
44. W. D. Good, Private Communication, March 18, 1965.
45. P. Gross, Private Communication, November 2, 1966.
46. K. L. Churney and G. T. Armstrong, NBS Report 8919, p. 175 (July 1, 1965).
47. V. P. Kolesov, M. M. Popov, and S. M. Skuratov, Zhur. Neorg. Khim. 4, 1233 (1959).
48. Dow Chemical Company - JANAF Thermochemical Tables, June 30, 1964.
49. S. Cantor, J. Chem. Eng. Data 10, 237 (1965).
50. N. E. Khandamirova, A. M. Evseev, G. Pozharskaya, et al., Zhur. Neorg. Khim. 4, 2192 (1959).
51. K. A. Sense and R. W. Stone, J. Phys. Chem. 62, 453 (1958).
52. K. A. Sense, M. J. Snyder, and J. W. Clegg, J. Phys. Chem. 58, 223 (1954).
53. J. A. Blauer, M. A. Greenbaum, and M. Farber, J. Phys. Chem. 69, 1069 (1965).
54. M. A. Greenbaum, J. Foster, M. L. Arin, and M. Farber, J. Phys. Chem. 67, 36 (1963).
55. J. Efimenko, NBS Report 8033, 55 (July 1, 1963).
56. A. V. Novoselova, F. Sh. Muratov, L. P. Reshatnikova, and I. V. Gordeev, Vestnik Moskov. Univ., Ser. Mat., Mekh., Astron., Fiz. i Khim. No. 6, 181-190 (1958).
57. M. A. Greenbaum, M. L. Arin, and M. Farber, J. Phys. Chem. 67, 1191 (1963).
58. E. Petersen, Z. physik. Chem. 5, 259 (1890).
59. J. Efimenko, NBS Report 8504 (July 1, 1964).
60. D. E. Mann, NBS Report 8186, 118 (January 1, 1964).
61. W. H. Evans, NBS Report 8186, Table A-86 (Jan. 1, 1964).
62. O. Mulert, Z. anorg. Chem. 75, 198 (1912).

63. H. Copaux and C. Philips, Compt. rend. 176, 579 (1923).
64. H. Copaux and C. Philips, Compt. rend. 171, 630 (1920).
65. G. T. Armstrong and C. F. Coyle, NBS Report 8919, 144 (July 1, 1965).
66. N. D. Potter, CPIA Publication No. 108 I, 89-97 (June 1966).
67. D. L. Hildenbrand, L. P. Theard, E. Murad, and F. Ju, Aeronutronic Final Tech. Report., Publication No. U-3068, Contract AF04(611)-8523, ARPA Order 348-62, 83 pp. (April 1, 1965).
68. M. A. Greenbaum, M. L. Arin, M. Wong, and M. Farber, J. Phys. Chem. 68, 791-795 (1964).
69. M. M. Novikov and L. N. Tunitskii, Optika i Spektroskopiya 8, 752 (1960).
70. Dow Chemical Company - JANAF Thermochemical Tables, March 31, 1964.
71. Dow Chemical Company - JANAF Thermochemical Tables, June 30, 1965.
72. R. A. McDonald and F. L. Oetting, J. Phys. Chem. 69, (11) 3839 (1965).
73. W. H. Johnson and A. A. Gilliland, J. Research Natl. Bur. Standards 65A, 59 (1961).
74. C. J. Thompson, G. C. Sinke and D. R. Stull, J. Chem. Eng. Data 7, 380 (1962).
75. P. Gross, C. Hayman, P. D. Greene, and J. T. Bingham, Trans. Faraday Soc. 62, 2719 (1966).
76. B. F. Markov and Yu. K. Delimarskii, Zhur. Fiz. Khim. 31, 2589 (1957).
77. H. Siemonsen, Z. Elektrochem. 55, 327 (1951).
78. W. Fischer, T. Petzel, and S. Lauter, Z. anorg. u. allgem. Chem. 333, 226 (1964).
79. H. C. Ko, C. Selph, M. A. Greenbaum, and M. Farber, CPIA Publication No. 108I, 79-87 (June 1966).
80. M. A. Greenbaum, R. E. Yates and M. Farber, J. Phys. Chem. 67, 1802 (1963).
81. O. Rahlfs and W. Fischer, Z. anorg. u. allgem. Chem. 211, 349 (1933).
82. I. N. Sheiko and V. G. Feshchenko, A.E.C. Tr. (6193/6194) Eng. Trans. of Ukrain Khim. Zhur. 28, 478 (1962).

83. J. Thomsen, Thermochemische Untersuchungen, Vols. I, II, III, and IV (J. A. Barth, Leipzig, 1882-1886).
84. J. H. Pollok, J. Chem. Soc. 85, 603 (1904).
85. W. Biltz and C. Messerknecht, Z. anorg. u. allgem. Chem. 148, 157 (1925).
86. B. Neumann, C. Krüger and H. Haebler, Z. anorg. Chem. 204, 81 (1932).
87. C. L. Hoenig, USAEC, UCRL-7521, 131 pp. (1964).
88. T. B. Douglas and W. H. Payne, NBS Report 7587, 44 (July 1, 1962).
89. R. E. Yates, M. A. Greenbaum, and M. Farber, J. Phys. Chem. 68, 2682 (1964).
90. B. D. Pollock, J. Phys. Chem. 63, 587 (1959).
91. Dow Chemical Company - JANAF Thermochemical Tables, June 30, 1963.
92. F. Sh. Muratov and A. V. Novoselova, Doklady Akad. Nauk S.S.S.R. 143, 599 (1962).
93. F. Sh. Muratov and A. V. Novoselova, Doklady Akad. Nauk S.S.S.R. 129, 334 (1959).
94. K. Motzfeldt, Acta Chem. Scand. 18, 495 (1964).
95. G. Furukawa and M. L. Reilly, NBS Report 7587, 101 and 169 (July 1, 1962).
96. K. K. Kelley, J. Am. Chem. Soc. 61, 1217 (1939).
97. J. L. Holm and O. J. Kleppa (preprint of article submitted to Acta Chem. Scand. June 1966, received courtesy D. Dittmars, NBS).
98. J. L. Holm and O. J. Kleppa, Inorg. Chem. 5, 698 (1966).
99. P. E. Blackburn and A. Bückler, J. Phys. Chem. 69, 4250 (1965).
100. P. Gross, Private Communication, Jan. 13, 1967.
101. J. Efimenko and W. S. Horton, NBS Report 9028, 59 (Jan. 1, 1966).
102. D. E. Mann, NBS Report 8504, 85 (July 1, 1964).
103. G. T. Furukawa and W. G. Saba, J. Research Natl. Bur. Standards 69A, 13 (1965).
104. D. A. Dittmars and T. B. Douglas, NBS Report 9028, 80 (Jan. 1, 1966).
105. G. T. Furukawa and W. G. Saba, NBS Report 9028, 45 (Jan. 1, 1966).

TABLE I.
Selected Values for Some Be Compounds at 298°K

Compound	State	ΔH_f° kcal/mol	ΔG_f° kcal/mol	S° cal/deg mol
Be	c	0	0	2.28
Be	g	78.0	69.0	32.544
BeO	c	-145.0	-138.0	3.38
BeO	g	31.		
Be ₂ O	g	-18.		
(BeO) ₂	g	-102.		
(BeO) ₃	g	-260.		
(BeO) ₄	g	-388.		
(BeO) ₅	g	-514.		
(BeO) ₆	g	-647.		
BeH	g	76.6	69.3	42.21
Be(OH) ₂	c, α	-215.7	-195.1	13.4
Be(OH) ₂	c, β	-216.5	-195.7	12.6
Be(OH) ₂	g	-160.		
BeF	g	-41.5	-48.3	49.15
BeF ₂	c, quartz	-245.3	-234.0	12.75
BeF ₂	glass	-244.2		
BeF ₂	g	-189.6		
BeF ₂	aq	-250.0		
Be ₂ OF ₂	g	-291.		
H ₂ BeF ₄	aq (in conc. HF)	-404.0		
BeCl	g	2.	-5.	52.0
BeCl ₂	c, α	-117.2	-106.5	19.76
BeCl ₂	c, β	-118.5	-107.3	18.12
BeCl ₂	g	-85.7		
BeCl ₂	aq, dilute	-171.1		
Be ₂ Cl ₄	g	-202.		
BeCl ₂ ·4H ₂ O	c	-432.2		
BeBr ₂	c	-84.5		
BeI ₂	c	-46.0		

Compound	State	ΔH_f° kcal/mol	ΔG_f° kcal/mol	S° cal/deg mol
Be ₃ N ₂	c,cubic	-140.6		
Be ₃ N ₂	c,hexag.	-136.5		
Be ₂ C	c	-26.		
Be ₂ SiO ₄	c	-512.3	-485.0	15.37
Be(BO ₂) ₂	g	-324.		
Be ₃ B ₂ O ₆	c	-748.2		
BeOAl	g	-5.		
BeO·Al ₂ O ₃	c,chrysoberyl	-549.2	-520.0	15.84
BeO·3Al ₂ O ₃	c	-1344.2	-1270.9	42.0

Chapter 8

FLUORINE FLAME CALORIMETRY. II. THE HEATS OF REACTION OF OXYGEN DIFLUORIDE, FLUORINE, AND OXYGEN, WITH HYDROGEN. THE HEAT OF FORMATION OF OXYGEN DIFLUORIDE.^a

R. C. King and G. T. Armstrong

Abstract

The heat of formation of oxygen difluoride, $\Delta H_{f298.15}^0$ [$\text{OF}_2(\text{g})$] was determined to be $+5.86 \pm 0.30$ kcal mol⁻¹. The value was obtained by combining the heats of reaction of oxygen difluoride, fluorine, and oxygen with hydrogen. The heats of reactions were measured by means of fluorine flame calorimetry. Other heat-of-formation data derived from the study are $\Delta H_{f298.15}^0$ [$\text{HF} \cdot 50 \text{ H}_2\text{O}$] = -76.68 ± 0.05 kcal mol⁻¹, and $\Delta H_{f298.15}^0$ [H_2O] = -68.32 ± 0.03 kcal mol⁻¹.

1. Introduction

The gaseous inorganic fluorine compounds of oxygen and the halogens such as OF_2 , ClF_3 , O_3F_2 , O_2F_2 , and BrF_3 are very reactive, combining with most other compounds and elements. Because of the lack of large enough quantities of pure materials, their extreme reactivity, the lack of suitable methods for reliable analyses, and the non-existence of corrosion-resistant materials for apparatus construction, few properties of these compounds have been measured accurately. The thermochemical data are especially lacking. Yet, while the lack of accurate thermochemical data persists, important uses are being discovered for these substances. Like fluorine, they are powerful oxidizing agents and are commonly used for fluorination. Some of the compounds are considered to be ingredients for the high-energy propellant and explosive systems; the others are potential reagents for chemical reactions at extremely low temperatures. Most of the compounds are easily liquefiable. Some, like OF_2 , though very reactive, require a larger activation energy than would fluorine for the same reaction. This property makes it more useful than fluorine in areas where materials compatibility may be a problem. Bromine trifluoride is also used as an electrolytic solvent. In most cases, accurate thermochemical data are required for calculations based on uses of these substances.

^a For Paper I in this series, see G. T. Armstrong and R. S. Jessup, Journal of Research, NBS, 64A, 49 (1960).

For the purpose of providing reliable heat-of-formation data for this group of compounds, a new flame calorimetric apparatus has been set up in this laboratory. It is planned that this apparatus will be used for studying heats of reactions involving some of the above compounds, in addition to reactions of fluorine with other gases. The first compound of a series to be studied is oxygen difluoride (OF_2).

Several earlier attempts have been made to determine the heat of formation of oxygen difluoride. Von Wartenberg and Klinkott [1]¹ reacted oxygen difluoride separately with (1) KOH (in excess KOH aq. 40%), (2) $6\text{KI} + 2\text{HF}$ (in excess. aq. solution), and (3) HBr (in excess HBr aq. 45%). From these reactions they derived the heat of formation of oxygen difluoride and reported an average value. Near the same time, Ruff and Menzel [2] measured the heats of three different reactions: (1) $\text{F}_2\text{O}(\text{g}) + 2\text{H}_2(\text{g}) + 2\text{NaOH}$ (xs aq. 20%); (2) $\frac{1}{2}\text{O}_2(\text{g}) + 2\text{H}_2(\text{g})$; and (3) $\text{F}_2(\text{g}) + \text{H}_2(\text{g}) + 2\text{NaOH}$ (xs aq. 20%). By studying the latter two reactions, Ruff and Menzel had hoped to obtain in the same apparatus the auxiliary data needed for deriving the heat of formation of oxygen difluoride from their first reaction. More recently, Bistee, et al. [3] reacted oxygen difluoride with hydrogen in a combustion bomb to which was initially added water for solution of the product hydrogen fluoride. In various reviews [4,5,6] the data from these three studies have been recalculated, using the most recent auxiliary data available for the reactions studied. However, these recalculations do not reconcile the differences between the heat-of-formation values derived. Presently, the reported values of $\Delta H_{298.15}^\circ [\text{OF}_2]$ are +7.6 [1,4], +4.7 [2,5] -4.4 [3,6], and -5.2 kcal mol⁻¹ [7].

The earlier thermochemical studies involving this compound confirm the belief held since the time of its discovery [8], that its heat of formation is small, possibly positive. Therefore, it would be desirable to determine its heat of formation from a reaction that involves a small heat of reaction. Unfortunately, reactions involving oxygen difluoride which evolve small heat effects lead to multiple products which are not readily recovered and separated for quantitative analysis. This problem exists for reactions with gaseous reactants and products as well as for those in the aqueous phase. Under ordinary conditions, oxygen and fluorine do not combine directly to form oxygen difluoride. In most reactions, leading to product hydrogen fluoride, the corrosiveness of the hydrogen fluoride can also introduce a sizeable uncertainty in the derived thermochemical data. In designing the experiments in the present study, these and other complications were considered carefully.

¹ Figures in brackets indicate literature references at the end of this paper.

The reactions undertaken for the present study are those of oxygen difluoride, fluorine, and oxygen with hydrogen, by means of flame calorimetry. Flame calorimetry is particularly suitable for studying reactions involving only gaseous reactants. Similar to the reasoning of Ruff and Menzel, it was felt that the measurements on the fluorine-hydrogen and oxygen-hydrogen reactions would provide the auxiliary data needed for calculating the heat of formation of the oxygen difluoride. Although this investigation is not intended to be a definitive study of the F_2-H_2 and O_2-H_2 reactions, the heats of these auxiliary reactions can be compared with data already available in the literature.

Many procedures were used in common for the three reactions. However, because of the various methods of analysis used, and because of the need for a description of the different problems encountered, a section is devoted to describing the experiments and results for each system.

2.0 Apparatus, General Experimental Procedures and Calibration

2.1. The Reaction Vessel

2.1.1. Earlier Burner Design

Because of the corrosiveness of the product hydrogen fluoride, both in the gaseous and aqueous phases, it was found that special attention had to be given to the design of the reaction vessel for this study. In the first of many preliminary experiments, oxygen difluoride was reacted in a hydrogen atmosphere in a Monel burner. This burner was similar in design to the one previously used at the National Bureau of Standards [9]. The earlier burner design is shown in Figure 1.

The burner tested for these experiments differed from the earlier design (1) in being constructed of Monel instead of copper, and (2) in having a simpler entry passageway for the atmosphere gas. In a burner of this design the fuel (F_2O) enters opening A and the atmosphere (H_2) is introduced through annular opening B. The reaction product(s) along with the excess hydrogen exit the reaction chamber at D. In the early experiments of the current study it was found that after burning the desired amount of OF_2 in H_2 most of the product H_2O remained in the burner chamber, saturated with HF , while the remainder of the HF was either in the vapor phase above the solution, or had been carried from the burner in the effluent atmosphere.

Such a state of the reaction products introduces many complications to efforts to determine the amounts of the reaction products. Because of these problems a new burner was designed in which the products, hydrogen fluoride and water, can be collected inside of the reaction vessel in the calorimeter.

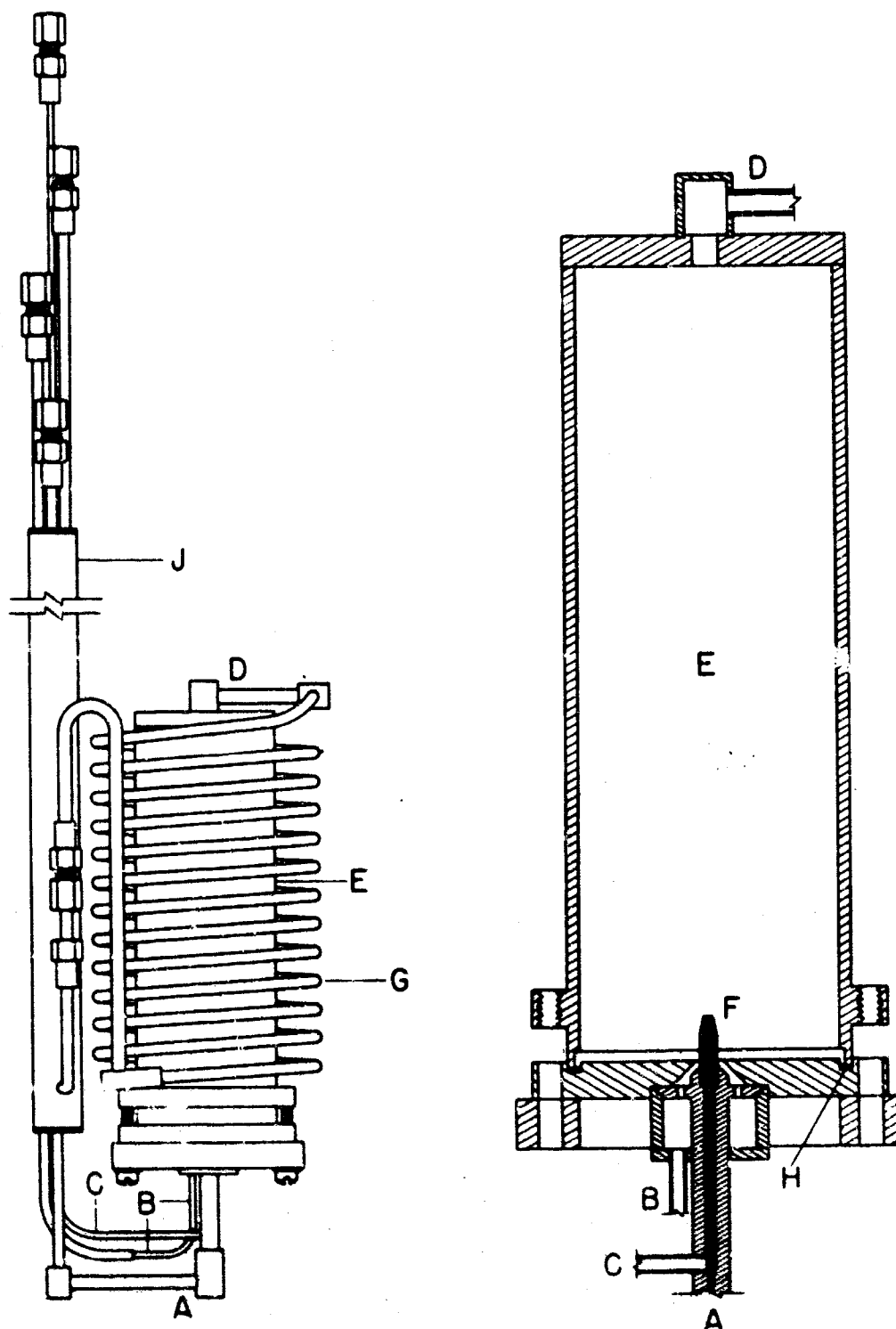
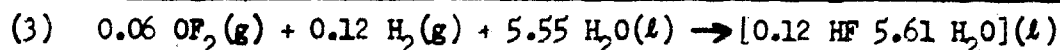
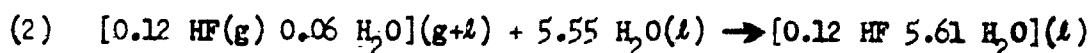
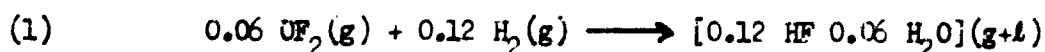


Figure 1. -- Burner for Fluorine Flame Calorimetry

A, B, C, fuel, fluorine, and helium flow lines;
D, combustion chamber exit; E, burner chamber;
F, burner tip; G, monel coil; H, Teflon gasket;
J, Heat interchanger for incoming and outgoing
gases.

2.1.2. New Burner Design

In a general way the new burner design may be described as a two-chambered reaction vessel (Figure 2). In the upper chamber (A) the oxygen difluoride and hydrogen (excess) are mixed and ignited, producing a flame. In the lower chamber (B) the products are dissolved in a known volume of water, producing a solution of determinable concentration. The excess hydrogen removes the product HF and H₂O from the upper chamber into the lower chamber. A gas dispersion system forces the gas mixture as fine bubbles through the aqueous solution and causes complete removal of the HF from the flowing hydrogen. Using the OF₂-H₂ system as an example, the reaction in equation (1) takes place in the upper chamber and equation (2) shows the reaction occurring in the solution chamber. The overall reaction for which the heat effect is measured is given by equation (3). Quantities shown are actual amounts used in the experiments.



Dissolving the HF in water in the calorimeter causes the heat of formation of oxygen difluoride obtained to depend on the heat of formation of the aqueous solution of HF, rather than on gaseous HF.

With the exception of the primary solution chamber, B, the burner is composed almost entirely of Monel and soldered with silver at all of the permanent joints. In a manner similar to that in the earlier burner, the gases are brought to the burner from the exterior of the calorimeter by Monel tubes passing through heat exchanger, C, through which also pass the exit gases. The outlet, E, on the primary solution vessel connects to a smaller solution vessel which can be seen in the foreground in a photograph of the burner in Figure 3. The effluent gases leaving the secondary solution chamber at F pass through a helix of thin-wall Monel tubing, D, before passing through the heat exchanger.

Details of the combustion chamber, A, are shown in Figure 4. The body which is cup-shaped is made of Monel, 1.25 in. O.D., and 2 in. high, with 0.0625 in. wall. The dimensions of the combustion chamber were chosen so that shortly after the reaction (i.e., after the flame is extinguished) all of the remaining products (H₂O and HF) can be flushed from the combustion chamber into the solution vessel. The inlet tubes for the reacting gases, the igniter, and the flame tip are all attached to the lid of the combustion chamber. On the outer side of the lid, the tubing is 0.125 in. O.D., 0.010 in. wall Monel. On the inside, the tubing leading to the flame tip, D, is 0.0625 in. O.D., 0.010 in. wall. The fuel is introduced through inlet C, and what may

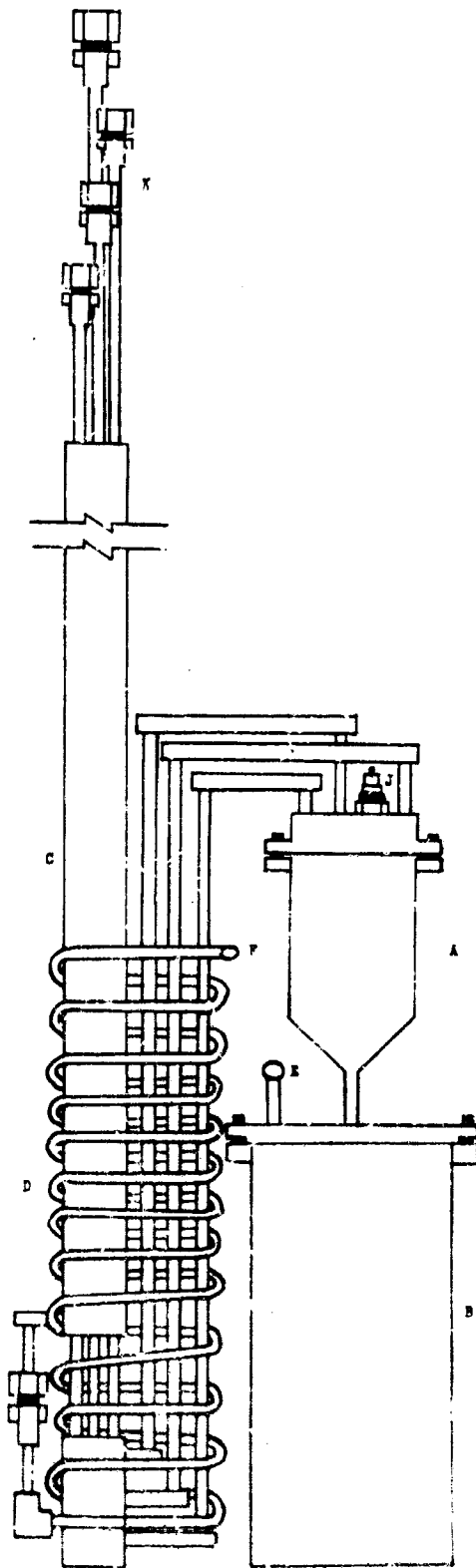
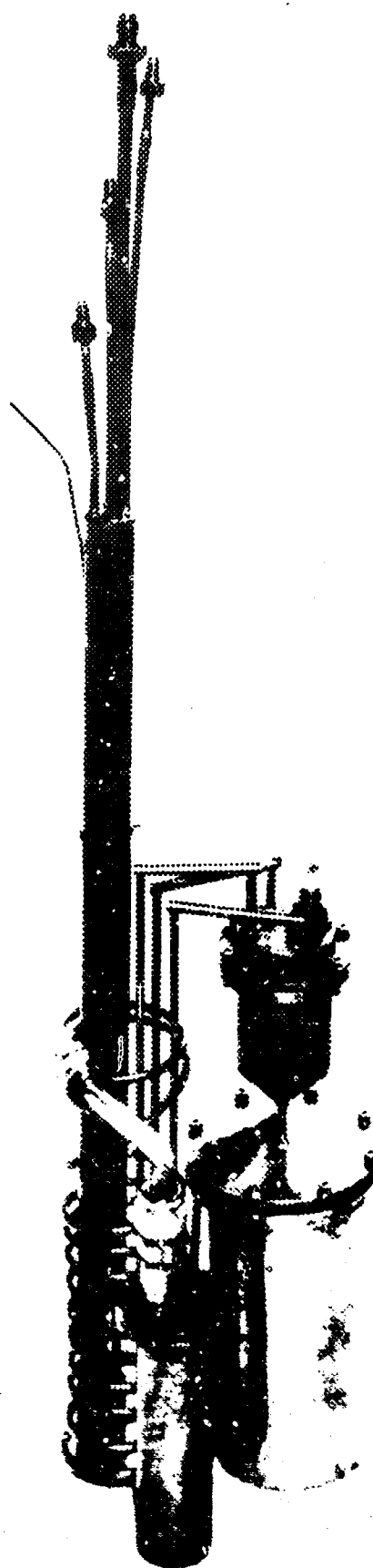


Figure 1. - Apparatus for Fluorine Flame Calorimetry (New Design)



the 1990s, the number of people in the world who are under 15 years of age is expected to increase from 1.1 billion to 1.5 billion. The number of people aged 65 and over is expected to increase from 200 million to 400 million. The number of people aged 15 and over is expected to increase from 3.5 billion to 4.5 billion. The number of people aged 15 and over is expected to increase from 3.5 billion to 4.5 billion. The number of people aged 15 and over is expected to increase from 3.5 billion to 4.5 billion.

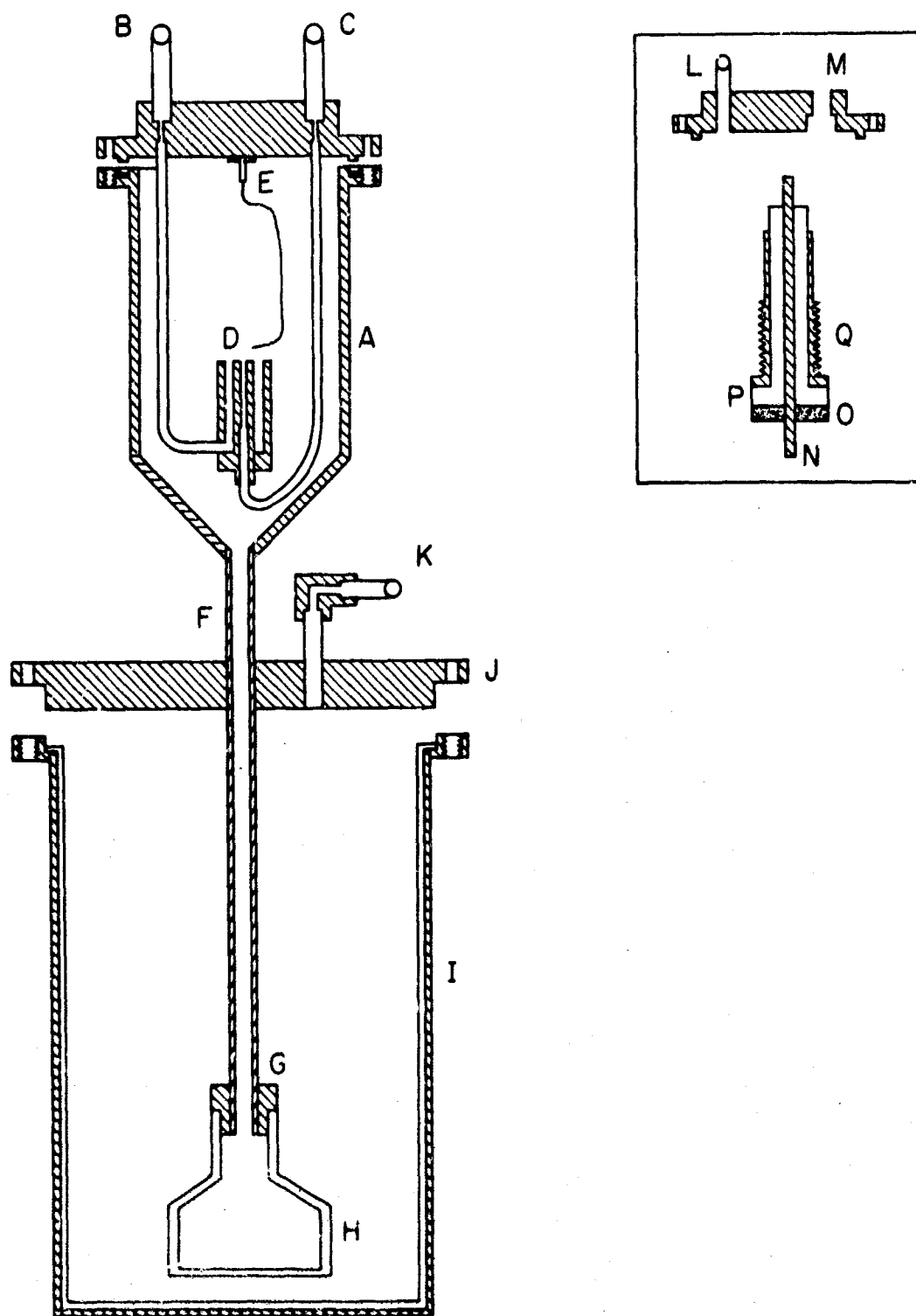


Figure 1 -- Combustion Chamber and Solution Vessel

be called the primary atmosphere enters through inlet B. Additional atmosphere is introduced through inlet L. The orifice at D through which the fuel enters is 0.050 in. The secondary atmosphere entering through inlet L serves two-fold: (1) it provides additional atmosphere for the reaction; and (2) it helps to flush the products down into the solution chamber. The joint between the cover and the combustion chamber is made by a 0.030 in. thick Teflon gasket placed in the groove on the flange of the cup.

At M is the opening for the high voltage electrode used for initiating the reaction. The electrode is a Monel-Teflon unit as shown in the insert in Figure 4. A calcium fluoride disc (0.095 in. thick), O, placed over the electrode serves as a heat sink. The Monel sheath, Q, surrounding the Teflon insulation, P, also helps to cool the Teflon. A three-in. piece of 0.010 in diam. nickel wire, E, is attached to the electrode at N, and positioned over the flame tip, D.

The tube, F, leading into the solution chamber is platinum with 0.125 in. O.D. and 0.013 in. wall thickness. The end of the tube is fitted with a polyethylene cap having a porous lower surface and connected with a small Teflon adapter, G. The cover to the solution chamber is of nickel-plated steel.

The primary solution vessel is two in. O.D., four in. high, with a 0.032 in. wall thickness. The cylinder is made of nickel-plated copper. The flange, which has threaded holes, is nickel plated steel. The container has a Teflon liner which also has a 0.032 in. wall. The flange on the liner makes the seal when the vessel is closed.

For an experiment the primary solution vessel contains 100 cc. demineralized water. The volume of the secondary vessel is 30 cc. During an experiment it contains 20 cc. of water. This secondary solution removes any HF from the effluent gas that may be carried over from the primary solution. Since the secondary solution is so dilute it also assures that upon leaving the burner the effluent gas flows through a solution whose vapor pressure is essentially unchanged during the experiment. In the main solution vessel, the liquid is pure water during the fore-period, and contains about two weight percent HF in the final drift. The vapor pressure of water over this solution is 23.46 mm. HF at 25°C [10], whereas it is 23.77 mm. Hg over the pure water. The vapor pressure of HF over the solution is 0.048 mm. Hg at 25°C.

2.2. The Calorimetric Equipment

2.2.1. Calorimeter

The calorimeter is one of several in this laboratory incorporating modifications of the Dickinson design [11]. The modifications are

briefly described by Prosen, et al. [12]. This calorimeter is usually referred to as the submarine type, since the constant-temperature enclosure can be raised and lowered in the surrounding water bath. The calorimeter can is separated from the enclosure by a $\frac{1}{2}$ -inch air space. The calorimeter is supported by three metal pegs and has a volume of 5.5 liters. The lid has three holes for bringing out the platinum resistance thermometer, the leads to the electrical calibration heater, and the flow lines to the reaction vessel. These holes coincide with three tubes in the shield cover. The reaction vessel and most of the heat exchanger are immersed in the stirred water of the calorimeter. The water is stirred at a rate of 300 r.p.m. The reaction vessel was placed on a small brass platform, supported by three small cones. This positioned the bottom of the reaction vessel about $1/4$ inch above the bottom of the calorimeter can.

In the customary manner, temperature measurements were made with a calibrated platinum resistance thermometer, used in conjunction with a G-2 Mueller bridge and a high-sensitivity galvanometer [13]. A displacement of 0.5 mm on the galvanometer scale represented 10 micro-ohms on the bridge or one-tenth millidegree. At 0°C, the thermometer has a resistance of 25.4668 ohms.

The temperature of the jacket water was kept constant at 32°C by an automatic regulating system consisting of a thermistor sensing element, linear D.C. microvolt amplifier, strip-chart recorder (-5 to +5 mv.), current-adjusting-type controller, and a 50-watt magnetic power amplifier [14]. The jacket bath is equipped with two heaters, a 14-ohm heater for raising jacket temperature to 32°C, and a 131-ohm heater for temperature control. A 500 ma meter is connected between the magnetic amplifier and the control heater. The thermistors form two arms of a Wheatstone bridge circuit of which the two remaining arms are formed by adjustable temperature-insensitive resistors. Each thermistor arm of the bridge consists of four bead thermistors of about 1000 ohms each. The thermistors are encased in flattened thin-wall copper tubing in the water bath. A 1.5 volt mercury cell supplies a current of 0.040 ma to the bridge. The current is kept very small to keep self heating of the thermistor elements below .001°C. Figure 5 shows a portion of the record of the variation of the jacket temperature with time. The temperature was usually controlled to better than $\pm .0015^\circ\text{C}$.

2.2.2. Electrical Calibration System

The heating coil was made from B&S gauge No. 30 Advance wire covered with a double layer of glass insulation. The wire was covered with baked glass impregnated spaghetti to insure complete insulation from the copper sheath in which it was enclosed. The sheath was of

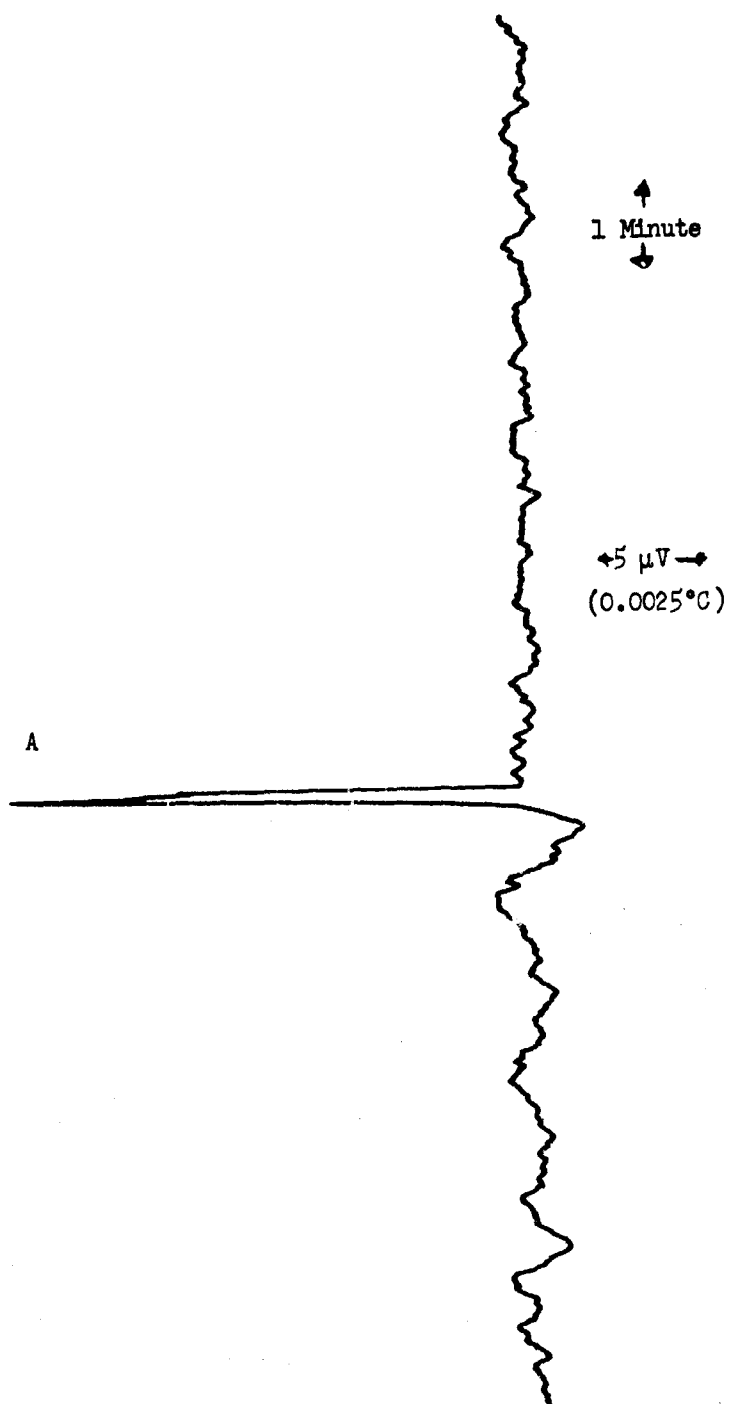


Fig. 5 BATH TEMPERATURE CONTROL RECORD

Spike at (A) is interference signal caused by high voltage sparking

0.010" wall soft copper tubing, flattened onto the resistance wire up to a distance of about four inches from the tubing ends. The flattened tubing was coiled on a one-inch o.d. tube, to form a coil of about six inches long. The current leads were of 22 gauge copper wire and were soldered to the heater wire, so that the junction was positioned about six inches inside the end of the tubing. This placed the junction about four inches under the surface of the water in the calorimeter. The coiled heater was suspended from a small copper plug, provided with two 1/8 inch holes for the ends of the heater sheath. The tubing ends were cemented in place, flush with the upper end of the plug. The plug fitted quite snugly into a ring mounted on the calorimeter lid. To further secure the plug, a small screw fastened it to the ring. Ginnings and West [15] have discussed a method for attaching the potential leads so that there is negligible disturbance in the current leads due to the attachment of the potential leads. The first potential lead was soldered to the current lead just inside of the copper sheath. This positioned this junction at the physical boundary of the calorimeter, in fairly good thermal contact with the calorimeter. The three leads were then brought up to a 1/16" thick, three-inch o.d. copper plate; the second potential lead was soldered on at the point where the current lead contacted the copper plate. Then all four wires were coiled on the lower side of the plate and cemented firmly in place. This placed them in good thermal contact with the plate. For positioning the copper plate, the lower side of the lid of the submarine well was counter-drilled to 1/16". Soldered onto the upper side of the copper plate was a threaded brass ring. A bakelite rod, drilled with four holes for the heater leads and made to fit closely in the tube on the submarine lid, was held by the brass ring. The opposite end of the bakelite rod was threaded, so that, once the copper plate was positioned in the groove on the lower side of the submarine lid, it could be firmly pulled up against the lid, to insure good thermal contact between the heater leads and the submarine boundary. The heater and lead connectors are permanently attached to the calorimeter lid.

The power for the electrical energy calibration was obtained from a precision regulated power supply (Alpha Scientific Laboratories, Inc., Model 103-5A). The unit has a maximum output power of about 500 watts with a current range from 0-5 amps and a voltage range from 0-103 volts. The supply can be operated in the voltage or current mode.

We found that with the parameters and switching arrangement of our apparatus, operation in the current mode gave more constant current and voltage readings. The double pole-double throw switch, which connected the heater and a dummy heater of similar resistance alternately into the circuit, posed a problem in the calibrations. When the power supply is open-circuited, as when interchanging the dummy and calorimeter heaters, a large voltage builds up across the capacitors. When the connection is again made this transient voltage disappears quite rapidly,

too quickly to be measured with the ordinary procedure for taking the voltage and current readings. In a separate investigation [17] the magnitude and decay time of this transient voltage was observed with an oscilloscope. Depending on the length of the heating period, it may be significant in calibration experiments. For these experiments, it is assumed that this transient effect does not significantly affect the accuracy of the calibrations, since the heating periods were usually sixteen minutes long. For later calibrations, the double pole-double throw switch will be replaced by a make-before-break switch.

Figure 6 shows the observed current and voltage readings. Current and voltage readings were made on alternate minutes. The diagram shows that for both sets of measurements, the regulation improves about four minutes after initiating heating.

The time interval for the electrical heating was measured with a Beckman Universal EPUT and Timer, which gave the time readings to 10^{-5} second. The throwing of the switch to send energy into the calorimeter simultaneously initiated the timing. The alignment of the knife edges of the switches with their respective clip receptacle was carefully checked. In blank experiments, the accuracy of the time intervals given by the timer was approximately checked against the time intervals using the one-second standard frequency signal at the National Bureau of Standards.

Other equipment used in measuring the electrical energy input consisted of a 0.01 ohm standard resistor, a volt box with a ratio of 20,000 to 20 ohms, a thermostated standard cell, and a Wolff Diesselhorst potentiometer. Osborne, Stimson, and Ginnings observed a seasonal variation in the calibration on this potentiometer [16]. They devised a special circuit to avoid this problem. The same circuit was used in the present calibrations. Also, additional details on the calibration circuit are given by Churney and Armstrong [17]. The resistors, potentiometer, and standard cells were calibrated at the National Bureau of Standards.

2.2.3. Flow System

The gas flow system is similar to the one used previously for flame calorimetric work at the National Bureau of Standards [9]. Figure 7 shows the arrangement of the parts of the flow system for the calorimetric experiments. Preceding the calorimeter, there are three principal flow lines which connect to the three inlet ports on the burner (Fig. 3). These three lines are used for (1) the primary atmospheric gas (H_2), which makes up the larger amount of gas, (2) the secondary atmospheric gas (H_2), and (3) the fuel gas. In all experiments conducted in this study, hydrogen was the reactant in excess, and is therefore referred to as the atmosphere. The helium source is

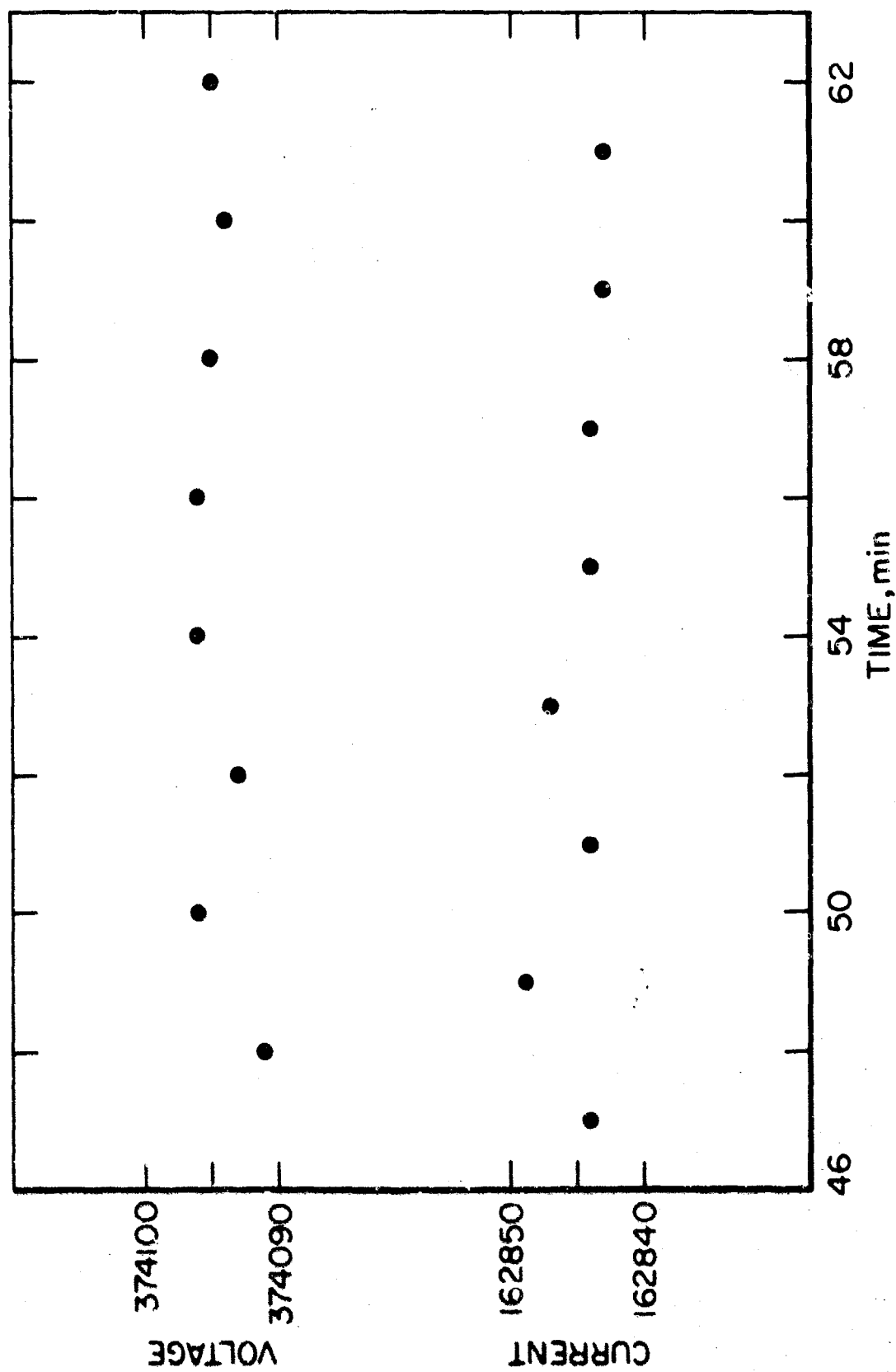


Figure 6 -- Plot Showing Variation of Current and Voltage Reading

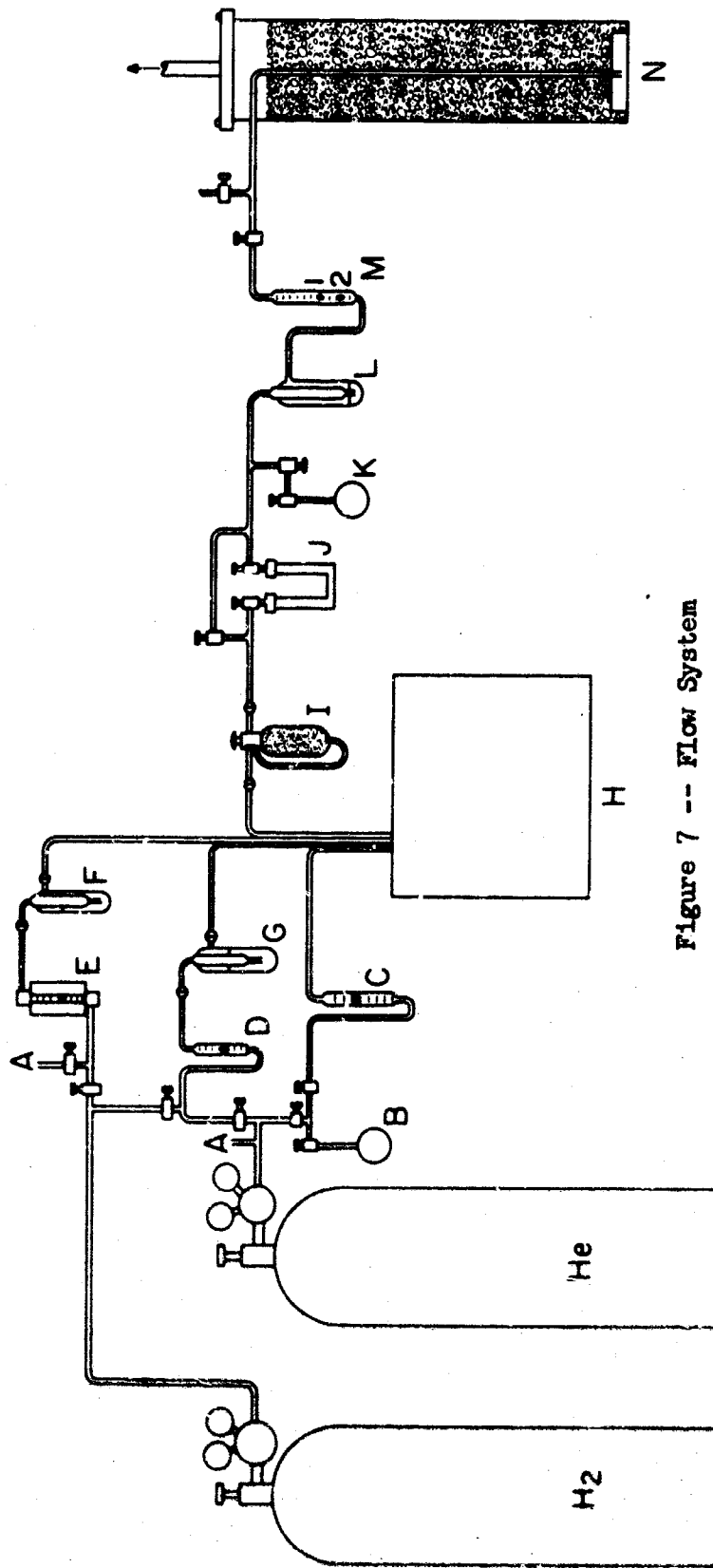


Figure 7 -- Flow System

- | | |
|--------------------------------|-------------------------------|
| A. Flow Inlet (Helium) | H. Calorimeter |
| B. Fuel sample Bulb | I. Absorber ($Mg(ClO_4)_2$) |
| C. Flowmeter (fuel) | J. Absorber (NaF) |
| D. Flowmeter, (atmosphere, II) | K. Sampling Bulb |
| E. Flowmeter, (atmosphere, I) | L. Bubbler (Kel-F oil) |
| F. Bubbler (Water) (I) | M. Flowmeter (Effluent gas) |
| G. Bubbler, (Water) (II) | N. Absorber (soda-lime) |

available and connected up so that any or all of the flow lines can be flushed with helium at any time.

The fuel line begins with the sample bulb at B. More detail of this weighable bulb is shown in Figure 8. It is specially constructed for resistance to corrosive gases. The three-inch sphere is assembled from thin-wall (0.015" wall) Monel hemispheres which are welded to a thicker equatorial support ring. The stem is approximately 4" long of 3/16" o.d. Monel tubing. The stem reduces to 1/8" o.d. thin-wall so that small valves can be connected. The valves used were obtained from the Dibert Valve and Fitting Co. Both Monel and stainless steel 316 valves with Teflon packing were found to be satisfactory. Including valve, a typical bulb weighs approximately 150 grams. The bulbs were weighed on a 300-gram-capacity Mettler balance.

The float type flowmeter in the fuel line is equipped with two floats, one of tantalum and the other of stainless steel. Not shown in the diagram is an absorber of magnesium perchlorate placed immediately after the helium cylinder. Pre-drying of the helium is desired for the helium that enters the fuel line, but as will be explained later dried helium is not needed for the hydrogen lines. It is to be noted that the flowmeter is the only intervening item in the fuel line between the fuel source and the flame tip where the fuel and hydrogen are reacted.

Both hydrogen lines include a float-type flowmeter and weighable bubblers. Each bubbler is Pyrex and, including water, weighs about 69 grams. The purpose of the bubbler is to saturate the hydrogen with water to compensate for the water removed from the reaction vessel by the effluent hydrogen. This point is discussed more fully in the appendix.

The calorimeter is shown at H without detail. The items after the calorimeter used in these experiments are the absorption bulb, I, containing magnesium perchlorate; the sample bulb, K; the bubbler, L; and the flowmeter, M. The absorption bulb removes water from the effluent hydrogen. The sample bulb is used to extract samples of the effluent gas for analyses. In contrast to the fuel sample bulb, these spherical bulbs have no special weight restrictions. The ones used were of Monel, assembled from commercially available spheres (20-gauge wall). The stems were .250 in. o.d. When prepared for use, this bulb is evacuated. Therefore, the bubbler containing Kel-F oil serves two purposes: (1) it prevents suction of air into the sample bulb while the effluent gas is being sampled, and (2) it is a visual indication of the flow of gas through the calorimeter. The final flowmeter is mostly of value as an indication that the reaction is taking place. When the reaction is not occurring a higher flow of hydrogen exits the reaction vessel and the float registers at position 1, for example. Upon initiation of the flame, some of the hydrogen is reacted and the products are

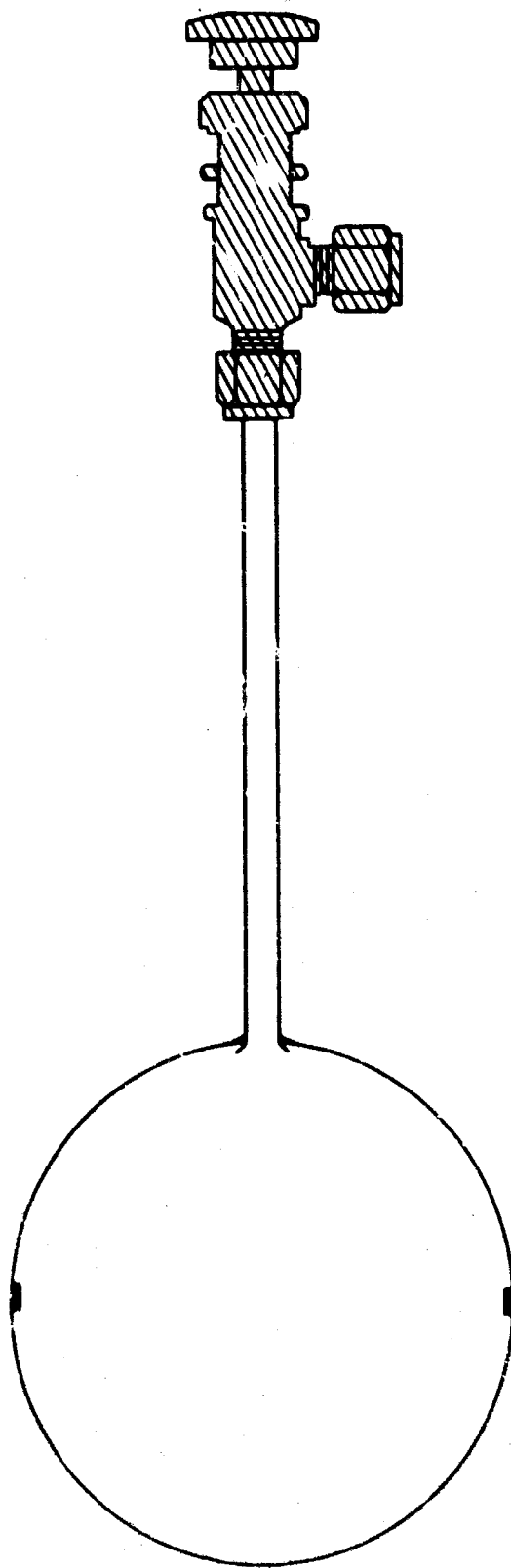


Figure 8 -- FUEL SAMPLE CONTAINER

condensed in the calorimeter. Therefore, less hydrogen leaves the calorimeter and the float registers at position 2. When the reaction is halted the flame is extinguished and the hydrogen flow returns to normal. Therefore, during the initial and final drift periods the float is at position 1 and during the reaction it registers at 2. The soda-lime absorber (N) was not used in the calorimetric experiments, but was used in disposing of unwanted fluorine and oxygen difluoride while filling sample bulbs. It also serves as an absorber if the flame does not ignite as planned.

2.2.4. Ignition System

A high voltage coil (previously removed from an automobile) was obtained from the Transportation Section of the National Bureau of Standards. It was connected through a 6-volt transformer and a toggle switch was connected in the 110 volt line. For the experiment the high voltage lead was connected to the lead shown in the photograph in Figure 3. The toggle switch was thrown at the appropriate time to initiate the sparking for igniting the reaction gas mixture.

2.3. General Experimental Procedures

2.3.1. Adjustment of the Jacket Temperature

The first step in the calorimetric procedure is to adjust the temperature of the jacket to 32°C. Once it is established that the temperature is being controlled satisfactorily, preparations for the experiment are continued.

2.3.2. Preparation of Burner

For the three systems investigated, the burner was subjected to varying amounts of conditioning which will be described under the separate sections on the reactions. However, in general, preparation of the reaction vessel consists of (1) positioning the sparking wire over the flame tip, D, (Figure 4), (2) charging the solution chambers with water, and (3) assembling the burner. After positioning the sparking wire, the primary solution vessel is filled with 100 cc of demineralized water and covered immediately. Note that the cover for the primary solution vessel is attached to the gas inlet tube to which also is connected the cup of the combustion chamber. Next, the second solution vessel is charged with 20 cc water, covered and connected to the primary solution vessel and cooling helix. At this point, the burner is ready to be positioned in the calorimeter.

2.3.3. Preparation of Fuel Sample, Absorbers, and Calorimeter Can

The fuel sample bulbs are always filled prior to the calorimetric experiment, using a procedure described for each fuel. Similarly, the bubblers and magnesium perchlorate absorber are charged in advance.

Immediately after preparing the burner, each of these items is weighed to 0.1 mg. On a 6 kg balance the weight of the calorimeter can, with water, is adjusted to 5950 grams, ± 0.5 mg. This weight also includes the support for the reaction vessel. Immediately the burner is placed in the calorimeter and the calorimeter is covered with its lid from which is suspended the calibration heater. A small strip of neoprene is placed around the heat exchange tube of the burner to close the calorimeter opening and prevent evaporation of water from the calorimeter. The calorimeter is now placed in the enclosure (submarine) and lowered into the jacket bath. The fuel bulb, bubbler and absorber are connected into flow lines. In about five minutes the temperature of the jacket bath has equilibrated back to 32°C.

2.3.4. Conduct of a Reaction Experiment

The flow lines are first purged with helium to remove any air present. A flowing hydrogen atmosphere is then established in the primary and secondary atmosphere lines. Using the calibration heater the temperature of the calorimeter is adjusted to 29°C. Once the temperature of the calorimeter has equilibrated and the desired hydrogen flow rate is established, initial drift period readings are begun. Though the fuel line is initially flushed with helium, no gas is flowing through the fuel line during this period. After a fore drift period of about 20 minutes, the reaction is initiated by simultaneously initiating the sparking and releasing the fuel from the sample bulb. The high-voltage sparking is discontinued when there is certainty that the fuel has ignited. This is usually after 10 to 15 seconds of sparking. Increase in the rate of the temperature rise of the calorimeter and the decrease in the flow rate of effluent gas are the main signals that the reaction is taking place smoothly. In most experiments, the reaction was continued until a 2.5-degree temperature rise had been achieved, at a rate of about 0.20° per minute. This usually required a 15 to 18 minute reaction period. As will be discussed more later, it was feared that a faster rate of reaction would have resulted in either melting of the burner tip or more extensive corrosion of the combustion chamber. After achieving the desired temperature rise, the fuel sample bulb is closed and the fuel remaining in fuel line is flushed into burner with helium. The helium flow is reduced and continued in the fuel line for the remainder of the experiment, while hydrogen flows through the other lines. The reason for continuing the helium flow is to prevent back-up of the products into the fuel line in case of no gas flow. However, it was later realized that helium flow in the fuel line up to and during the final drift period is not necessary. After the reaction experiments, the solution in the primary solution vessel is transferred, with washings, to a weighed 250-cc polyethylene bottle. The secondary solution (20 cc) is also recovered for titration.

2.3.5. Conduct of an Electrical Calibration Experiment

The procedure for conducting the calibration experiments is very similar to that used for the reaction experiments. The solution vessels contained 100 and 20 cc water, respectively. A hydrogen flow through the bubblers is maintained at a comparable rate as used for the reactions. The helium flow in fuel line constitutes the main difference in the gas flow for the calibration and reaction experiments. In the calibrations, a small flow of helium is maintained in fuel line throughout the experiment. In the reaction, as pointed out above, helium flow is started in fuel line when it is needed to purge the fuel from the flow line.

Figure 9 compares the variation of calorimeter temperature with time for an electrical calibration experiment and for a combustion (oxygen difluoride-hydrogen) reaction. Some "overshooting" is observed in the calibration curve. Also, for the combustion reaction, "overshooting" was observed, however, considerably less than for the calibration. This "overshooting" is presumed to be due to the position of the produced heat effect relative to the platinum resistance thermometer.

2.3.6. Calculation of the Corrected Temperature Rise

All of the values for the corrected temperature rise were calculated by an IBM 7094 computer, with a computer program developed by Shomate [18]. For the calculation, it was necessary to give the computer the following data: (1) dial corrections for the Mueller bridge; (2) time and resistance readings taken during the fore-drift, reaction, and final drift periods of the experiment; and (3) constants for the platinum resistance thermometer. This program was originally developed for use in bomb calorimetry experiments. A comparison between values for some hand-calculated and computer-calculated values, showed that the program could be used in calculating some parts of the data for flame (flow) experiments. For flow experiments, the useful data obtained include the corrected temperature rise; the conversion factor, $\frac{dR}{dT}$, the corrected resistance change, ΔR_{corr} ; the initial and final drifts; the cooling constant; and the initial and final temperatures for the reaction period.

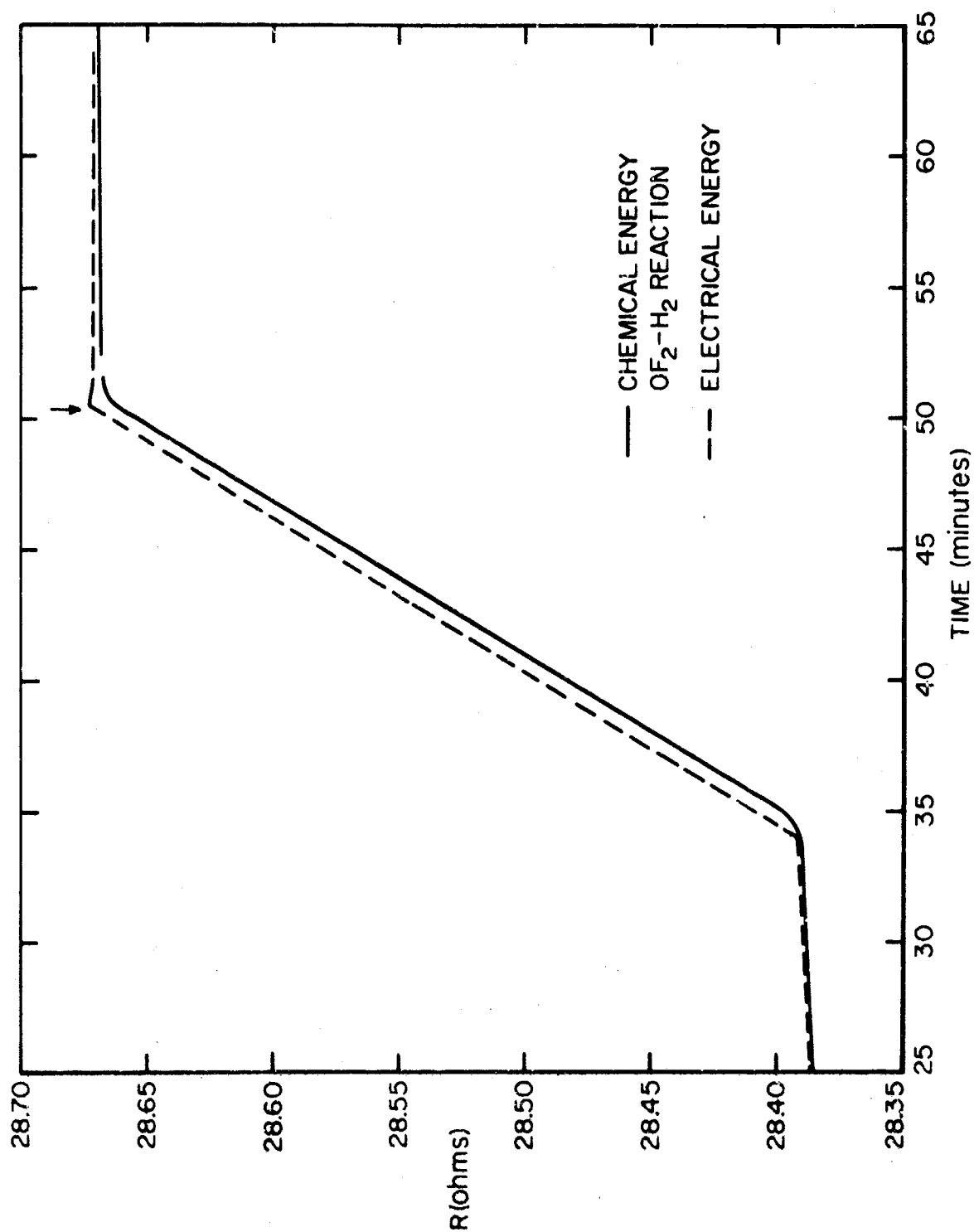


Figure 9 -- Variation of Calorimeter Temperature with Time

2.4. Electrical Calibrations

A total of ten calibration experiments were performed. The first three were considered preliminary, carried out for the purpose of coordinating procedures used between the two persons conducting the calibration experiments. The results from the remaining seven experiments are given in Table 1. These are an uninterrupted series of experiments, carried out between two sets of oxygen-difluoride-hydrogen reaction experiments. Given in the table are the experiment number, the initial temperature of the calorimeter, t_i ; the final temperature of the calorimeter, t_f ; the average temperature, t_{av} ; the corrected resistance increase, ΔR_{corr} ; and the corresponding corrected temperature rise, Δt_{corr} . The lower part of the table gives the measured current, voltage, time, total electrical energy, and energy equivalent of the calorimeter. The average value found for the energy equivalent was $21887.9 \text{ J } (^{\circ}\text{C})^{-1}$ with a standard deviation of the mean (seven experiments) of 0.006%.

Table 3

Calibration of Calorimeter

Expt. No.	t_i °C	t_f °C	$t_{av.}$ °C	ΔR corr. ohm	$\frac{dR}{dt}$ ohms (°C) ⁻¹	Δt corr. °C
15	28.98	31.76	30.37	.275193	.1005763	2.73616
16	28.96	31.77	30.36	.277000	.1005764	2.75413
17	29.00	31.77	30.38	.273928	.1005757	2.72350
18	29.01	31.77	30.39	.272626	.1005756	2.71066
19	28.98	31.77	30.37	.275739	.1005761	2.74159
20	23.97	31.79	30.38	.278886	.1005760	2.77289
21	29.18	31.78	30.48	.257158	.1005728	2.55693

Expt. No.	Current amp	Voltage	Time sec	Electrical Energy J	Energy Equivalent τ (°C) ⁻¹
15	1.626616	37.394856	984.85712	59876.0	21333.2
16	1.627697	37.437788	939.15986	60276.8	21336.0
17	1.627063	37.423601	979.20620	59624.4	21391.7
18	1.627920	37.428044	974.07658	59320.7	21334.2
19	1.627699	37.438458	984.87412	60016.3	21391.2
20	1.628170	37.448274	995.61232	60704.6	21392.2
21	1.628186	37.428167	918.80547	55964.0	21337.2

Mean

standard dev. of the mean 1.4 (.006%)

3.0 The Reaction Experiments

3.1 The Oxygen Difluoride-Hydrogen Reaction

3.1.1 Analysis of the Oxygen Difluoride

The oxygen difluoride sample was obtained from the General Chemical Division of the Allied Chemical Corporation. This gas is generally produced by bubbling fluorine into a two percent solution of sodium hydroxide. By special selection from the production lines, the oxygen difluoride supplied for these experiments was of higher purity than is ordinarily available.

According to the supplier's analysis which accompanied the cylinder, the gas contained in weight percent: OF_2 , 99.25; O_2 , 0.69; CO_2 , 0.06; and 0.01 volume percent CF_4 . These analyses were obtained by a gas chromatographic method developed by Kesting *et al.* [19,20]. The CF_4 content was estimated from an infrared spectrum. In addition to this information, these authors made available to us complete details of their procedures and also information obtained from their investigation of iodimetry and infrared spectroscopy as possible methods of analysis for oxygen difluoride. A comparison of the results from their repeated analyses using the three methods was made, and it was found that the gas chromatographic method yielded both the most precise and the most accurate results.

Their chromatographic equipment consisted of a Perkin Elmer Model 154 chromatograph equipped with a Micro Tek 7 part gas sampling valve. Silica gel of 40-60 mesh was used for column material. The conditions were: column length - 1 meter (1/4" o.d.) copper tubing, column temperature - 25 °C (isothermal) carrier gas - helium, flow rate - 50 cc/min, detector - thermal conductivity cell, detector voltage - 8 volts, and sample size - 1 cc.

The OF_2 sample, for analysis was extracted directly from the cylinder. The chromatographic peaks for oxygen difluoride, oxygen, and carbon dioxides were calibrated. It was found that peak area percent for these fractions was very nearly equal to volume percent. Using a mercury absorption technique which they developed, they found no free fluorine in the gas.

For the calorimetric experiments in our study, the oxygen difluoride was not used directly from the source cylinder. For this reason and also because of the importance of the analysis to the accuracy of the calorimetric data, the oxygen difluoride was re-analyzed in this laboratory, using procedures similar to those described by Kesting *et al.* [19,20].

The manifold for filling the sample bulbs is shown in Figure 10. This manifold was used for filling sample bulbs with fluorine and oxygen difluoride. Only those items used for oxygen difluoride sampling are mentioned in this discussion. For these experiments the oxygen difluoride was not subjected to any further purification. Directly to the source cylinder was connected a one-piece multiple-valving system obtained from the Matheson Company. With the nitrogen source (A), traps C, F, and I, and valves 2, 8, and 12 closed off, the sample bulb and flow lines were evacuated. Valves 3, 4, and 5 were closed and the OF₂ cylinder was opened by a remote control. Valve 3 was slightly opened. Valve 4 was opened long enough to allow one atmosphere of gas to expand into the open lines and sample bulbs. After about 20 minutes the cylinder was closed, valves 10 and 11 were opened, and the system was evacuated through soda-lime trap, F. Valve 10 was then closed. The valves to the sample bulbs were closed. The OF₂ cylinder was opened and by slowly opening valves 3, 4, 7, 9, and 13, gas from the cylinder was allowed to bleed through the soda-lime trap (I) until all connecting lines were adequately passivated. Valves 4 and 13 were then closed. Note now that the fore-pressure on valve 4 is 400 p.s.i.g., the same as in the source cylinder. The valves to sample bulbs were then opened and the bulbs were repeatedly (3 times) filled with OF₂ (20 p.s.i.g.) and then emptied through trap I. After this manipulation, they were filled to 100 p.s.i.g. The cylinder valve and valve 13 were then closed and opened, respectively. The over-pressure of OF₂ was then absorbed in the soda lime trap. Valve 5 was then opened and the line flushed with nitrogen through the soda lime trap. The lines were then evacuated through trap F and the nitrogen-flushing repeated. At this point the sample bulbs were removed.

For qualitative identification, an infrared absorption spectrum was made on the sample [21,22]. The IR cell was Pyrex with silver chloride windows. The windows were clamped in place and sealed to the cylindrical cell with Kel-F O-rings. This spectrum is shown in Figure 11. On the basis of information in the literature references, the absorption band at 1300 cm⁻¹ can be attributed to CF₄.

The chromatographic procedure for quantitative analysis of the oxygen difluoride sample is similar in most respects to that recommended by Kesting *et al* [19,20]. Our chromatographic equipment consisted of an F & M Model 500 which was already equipped with an electrically heated oven for the column, a detector (thermal conductivity cell), and a strip-chart recording potentiometer (-0.2 to + 1.0 mv).

Figure 12 shows the manifold for introducing the OF₂ sample into the chromatograph. The sample bulb was simply connected in the carrier gas loop which was provided with a bypass. After attaching the sample bulb, the sample loop (between valves 1 and 2) is flushed with helium and then valves 1 and 2 closed, until ready for introducing OF₂ sample into column. Silica gel (30-60 mesh) was used as column

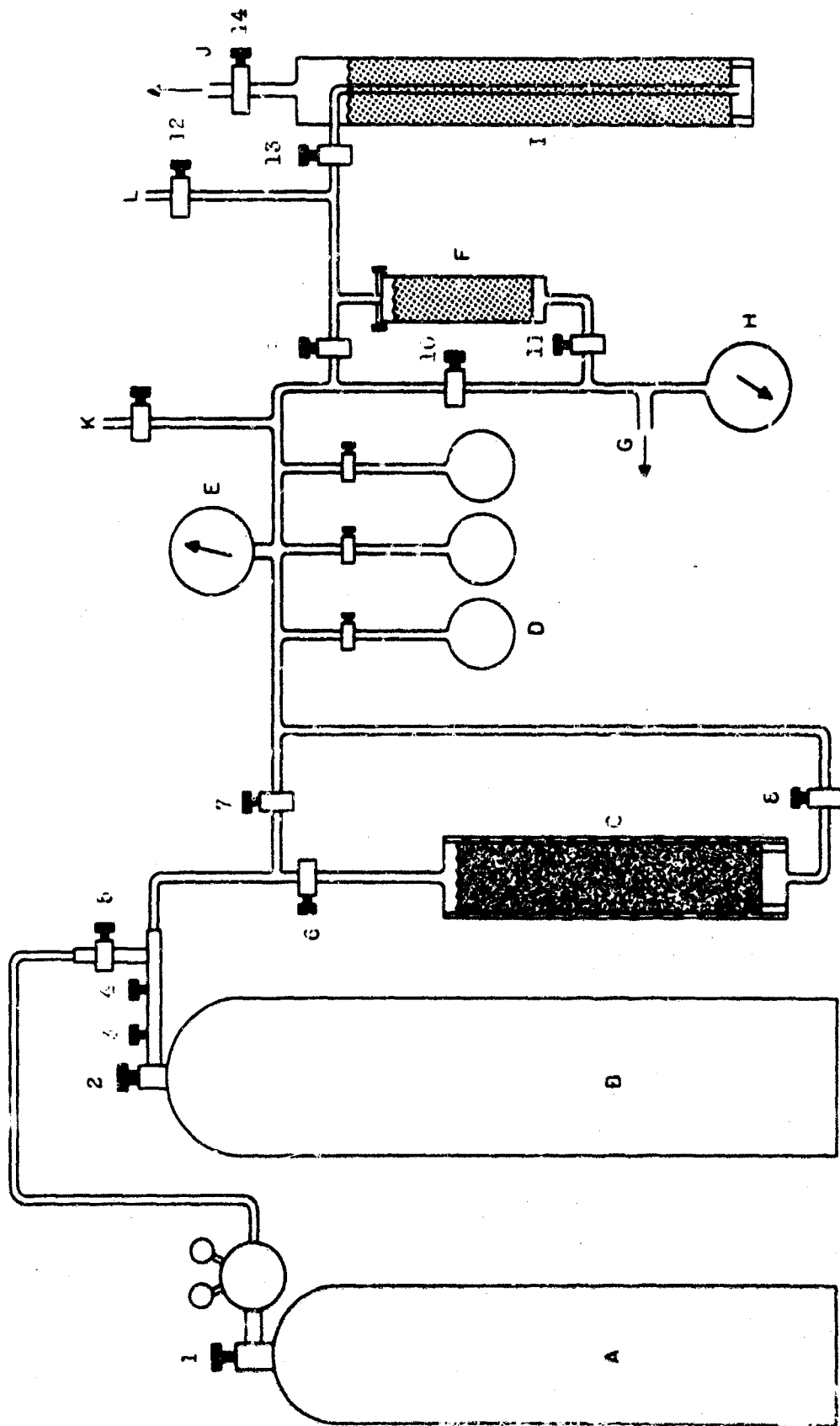


Figure 10 -- Gas Sampling Manifold (F_2 and OF_2)

- | | | |
|--------------------|------------------------------------|----------------------------------|
| A. Nitrogen | E. Pressure Gauge (0-350 p.s.i.g.) | I. Soda-lime Column |
| B. F_2 or OF_2 | F. Soda-lime Column | J. Vent Valve to Hood |
| C. NaF Column | G. Vacuum Source | K, L. To Calorimeter Flow System |
| D. Sample Bulbs | H. Vacuum Gauge (0-30 in.) | |

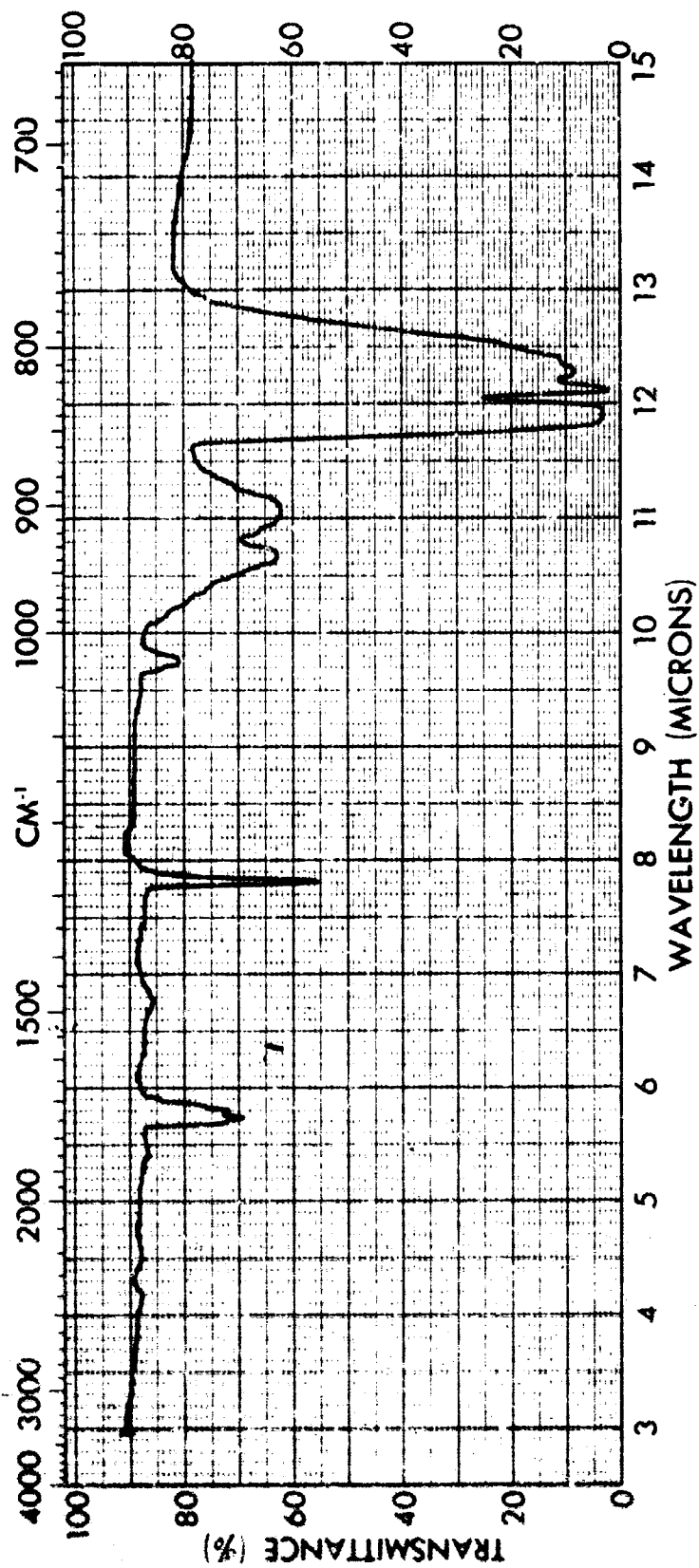


Figure 11 --IR Spectrum of OF₂ Sample

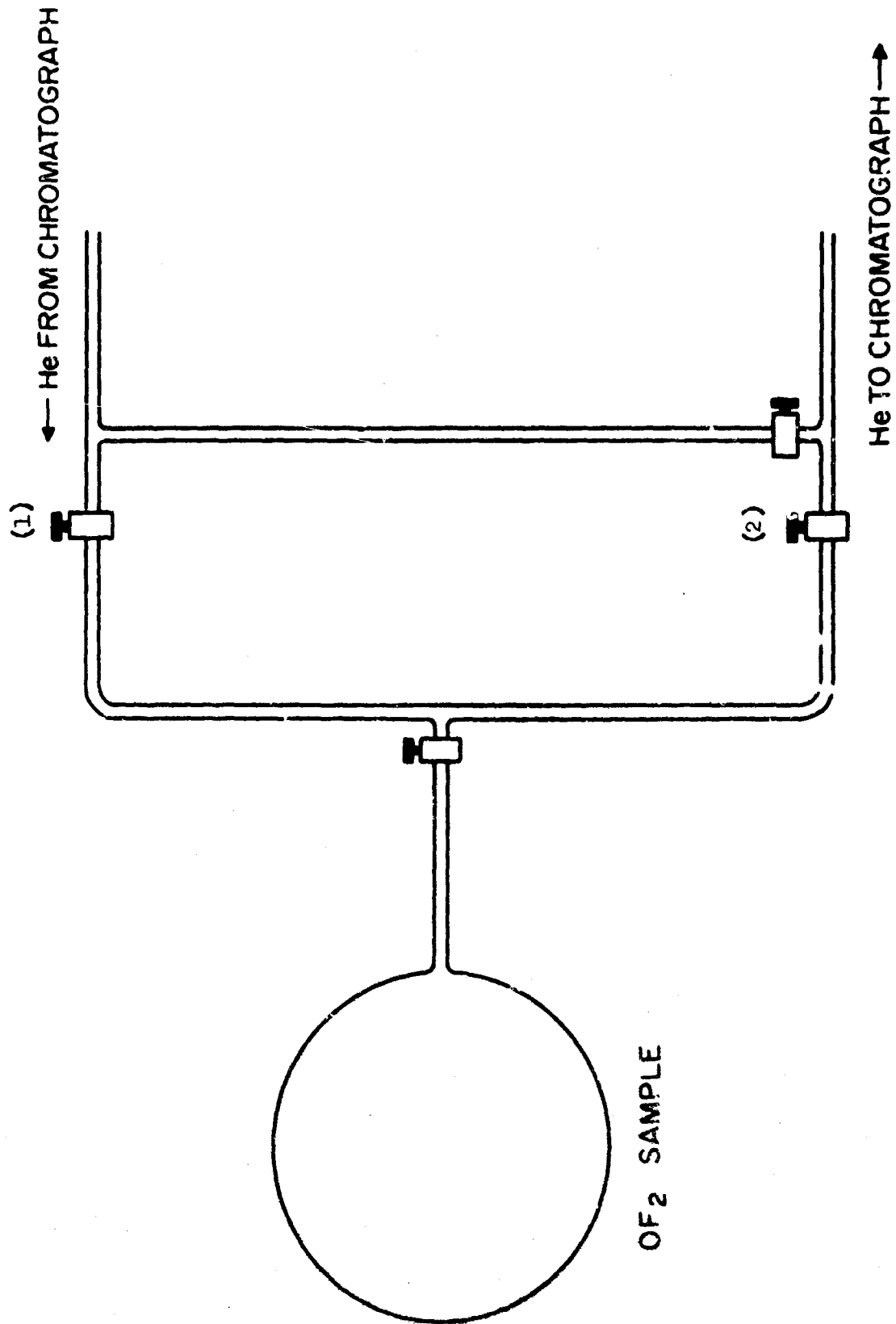


Figure 12 -- Manifold for Introducing OF_2 Sample
Into Chromatograph

material. Prior to the analyses, the column was conditioned at 350° for one hour under a flowing helium atmosphere. Other information on the conditions for the analyses is given on Figures 13 and 14, which show the chromatograms obtained.

In the complete chromatogram, four peaks were obtained. These were verified to be due to O₂ (or air), OF₂, CF₄ and CO₂. Analyses were made with the column temperature at 0° and 50° C. At 0 °C nearly complete separation was achieved between the O₂ and OF₂, but the CO₂ peak was either very slurred or the fraction did not elute at this temperature. At 50 °C, the separation between the O₂ and OF₂ was poor. After elution of the O₂ and OF₂, the column was temperature-programmed to a final temperature of 150 °C to achieve better elution of the CO₂. In agreement with Kesting's et al. [19,20] observations, the CF₄ eluted on the "tail" of the OF₂ fraction. The CF₄ peak was evaluated from chromatograms obtained made on the most sensitive scale, especially for evaluating this peak.

Repeated analyses were made on several bulbs and the results were quite reproducible. We accepted the finding of Kesting, et al., that the peak area percent for the observed components (OF₂, CO₂, O₂, CF₄) was very nearly equal to mole percent. The peak areas were evaluated both analytically and by counting squares. The results from two of the analyses are tabulated below and the average of these two analyses is used to compute the results in weight percent.

	Analysis I	Analysis II	Av.
	Mole %		wt. %
OF ₂	99.07	99.10	99.36
O ₂	.76	.73	.45
CF ₄	.06	.07	.11
CO ₂	.10	.10	.08

For various reasons, several preliminary analyses were carried out before a procedure was accepted for these experiments. First, because of the reactivity of the OF₂, it is conceivable that the OF₂ would react with the silica gel. In carrying out preliminary analyses at various column temperatures, it was noted that extraneous peaks appeared at a temperature of 75°, and also that even at 50°, the mole percent of OF₂ decreased while the mole percent of O₂ increased. The preliminary analyses demonstrated that silica gel is not a generally useful column material for chromatographic analyses of the reactive inorganic fluorides. The tests did show, however, that under the proper conditions, silica gel has good separation efficiency toward OF₂ and the inert component impurities, O₂ and CF₄. Though the O₂ peak appears

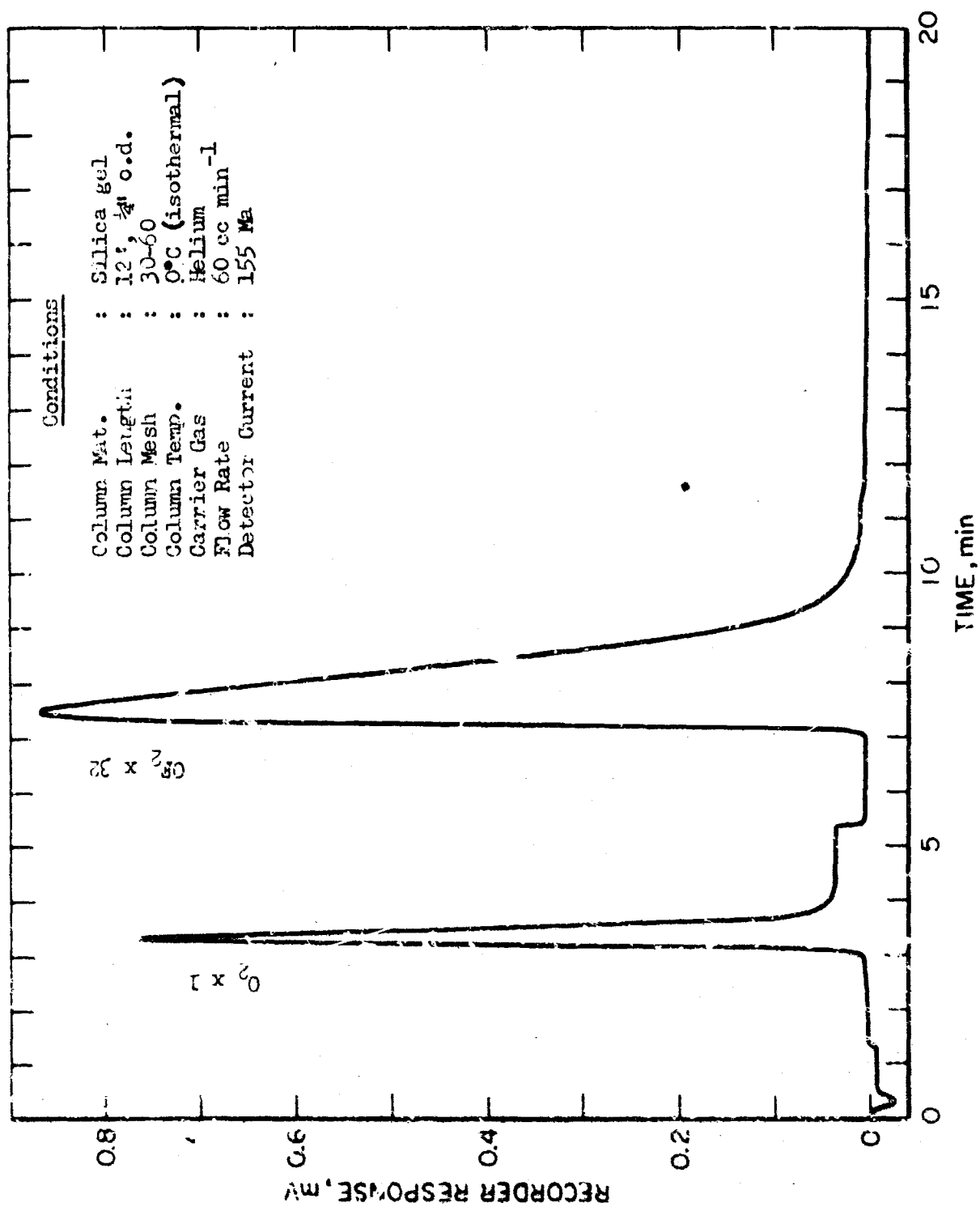


Fig. 13. Chromatogram of OF_2 Sample on Silica Gel (0°C)

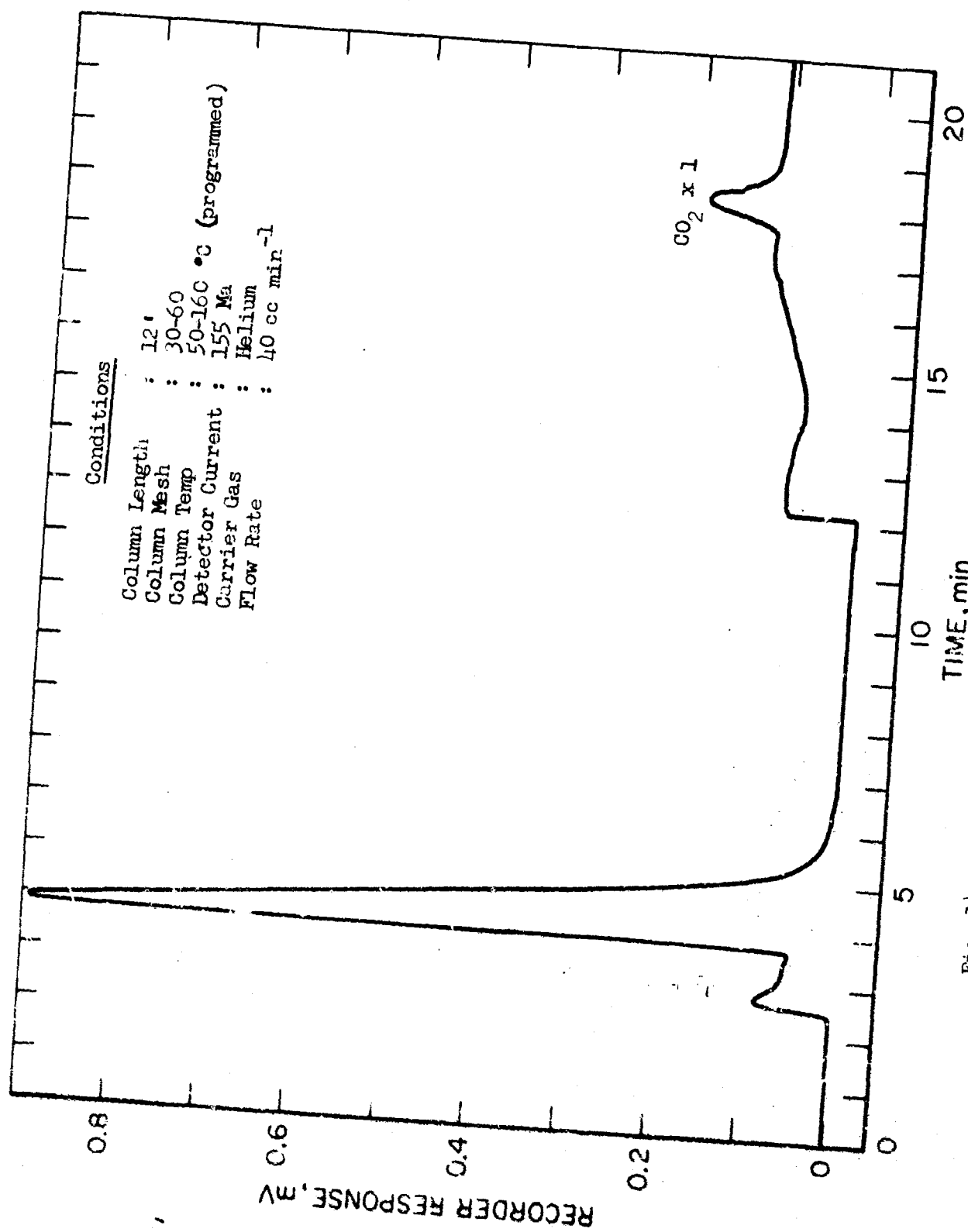


Fig. 14. Chromatogram of OF_2 Sample on Silica Gel (50°C)

to be pure O_2 , there is still some doubt as to whether the peak is due to a mixture of O_2 and N_2 . A method has been developed and will be tested on a sample of the OF_2 to determine whether or not nitrogen is present. An accurate analysis for the oxygen content of the sample is particularly important for the calorimetric portion of the experiments, since under the conditions a correction must be applied for the reaction of the impurity oxygen with the hydrogen.

Hydrogen

The hydrogen used was acquired in a 200 cu. ft. cylinder from the low-temperature calorimetry group in the Heat Division. The hydrogen had been obtained earlier from the Matheson Company. A mass-spectrometric analysis was performed directly on the contents of the cylinder. The composition of the gas was found to be, in mole percent: H_2 , 99.9; H_2O , $0.04 \pm .02$; and N_2 , 0.05 ± 0.01 . The presence of the moisture offered no difficulty in conducting the reactions, because in most of the experiments, the reaction vessel already contained an added quantity of water. However, the nitrogen impurity could conceivably react to give a small amount of NH_3 . No test was made for NH_3 in these experiments. In some earlier calorimetric work on the hydrogen-oxygen reaction, Rossini [23] reported the presence of nitrogen impurity in the oxygen sample. When oxygen was burned in hydrogen he tested the product gases for NH_3 and found the amount present to be negligibly small. On the basis of Rossini's observations, it appears that the nitrogen present in the hydrogen and other materials used in these experiments will produce a negligibly small effect on the results.

3.1.2 Calorimetric Experiments

The oxygen difluoride was introduced at a rate of approximately 80 cc per minute, into a flowing atmosphere of hydrogen of about 360 cc per minute. During the reaction, this gives an excess hydrogen flow of 200 cc per minute. The fuel flow was maintained constant by manual adjustment of the valves in the fuel line near the sample bulb. Several preliminary experiments were carried out. The results from thirteen experiments are reported here. The results are reported as two series, because the first six were carried out before the electrical calibrations and the remaining seven after the calibrations. Otherwise, there is no difference in the procedures used for the two sets of experiments.

3.1.3 Analysis for the Reaction Products

The hydrofluoric acid solution formed in the experiment was analyzed for acid present by titration with standard sodium hydroxide solution. As described earlier most of the product acid solution, with washings, was transferred from the burner to a weighed 250-cc polyethylene bottle. The bottle plus solution was again weighed to 0.1 mg and after

correction for bouyancy effects, the total weight of the acid solution was obtained. Weighed aliquots of this solution were titrated to obtain the amount of acid in the total solution. The acid retained by the polyethylene gas dispersion funnel (see Figure 4) was recovered and titrated separately. Very little acid was found in the secondary solution. The amount ranged from .01 - .10 milli-equivalent. These three measured amounts of acid were combined to give the total observed acid. All of the acid was assumed to have originated from the reaction of hydrogen with the oxygen difluoride sample.

The amounts of HF measured and the amounts theoretically expected are compared in Table 2. The experiment number, the moles of HF arising from CF_2 , $n_{\text{HF}}^{\text{OF}_2}$ (theo); the moles of HF arising from the impurity, $n_{\text{HF}}^{\text{CF}_4}$ (theo); the total moles of HF (theoretical), Σn_{HF} (theo.); the moles of HF measured, n_{HF} (meas.); the ratio of the mole of the measured to the theoretical HF; and the difference between the theoretical and measured amounts of HF, are given in this table. The theoretical amounts of HF are all based on the results from the analyses on the OF_2 sample carried out in this laboratory. Except for three experiments, the results show a consistent loss of HF. Experiment numbers 3 and 4 show a larger amount of measured HF than would be theoretically expected. No good explanation comes to mind for this excess HF. Unless, there was reduction of some metal fluoride like CaF_2 or NiF_2 , to give rise to the "extra" HF, it is believed that the higher recovery is due to some gross error in the titrations for these experiments, rather than a systematic error in the analysis of the oxygen difluoride sample. Experiment number 32 shows an unusually large loss of HF. The reason for this is not clear. On the average, the percentage recovery of HF in the series I was 99.69%, and in series II, 99.30%.

It is assumed that the loss of HF was due to corrosion of the Monel combustion chamber. This assumption is not unreasonable, in view of the fact that the chamber is small (1.12" i.d.) and 2" high, subjected to such a corrosive mixture ($\text{HF-H}_2\text{O}$), and high temperatures. The data in the last column (Δn_{HF}) was tabulated to test whether there was any pattern to the corrosion from one experiment to another. For example, if all the differences were comparable, regardless of amount or length of reaction, one could reason, that a certain amount of HF was needed to condition combustion area and once conditioned, no further corrosion occurred. However, the differences shown vary widely, leading one to believe that the amount of corrosion in a particular experiment depends on the state of the combustion chamber wall after having been exposed to the atmosphere.

Table 2

Reaction Quantities of Oxygen Difluoride

Series I

Expt. No.	$n_{\text{HF}}^{\text{CF}_2}$ (theo.)	$n_{\text{HF}}^{\text{CF}_4}$ (theo.)	Σn_{HF} (theo.)	n_{HF} (meas.)	$\frac{n_{\text{HF}} (\text{meas.})}{n_{\text{HF}} (\text{theo.})}$	Δn_{HF}^a
2	0.10702	0.00016	0.10718	0.10669	0.9954	-0.00049
3	.12648	.00016	.12664	.12602	.9951	- .00062
4	.11360	.00016	.11376	.11280	1.0003	+ .00004
5	.12976	.00016	.12992	.13009	1.0013	+ .00017
6	.12718	.00016	.12734	.12682	.9959	- .00052
7	.12702	.00016	.12718	.12634	.9934	- .00084

AV .9969

Series II

25	.12718	.00016	.12734	.12658	.9940	- .00076
26	.12518	.00016	.12534	.12462	.9942	- .00072
27	.12346	.00016	.12362	.12266	.9922	- .00096
31	.12434	.00016	.12450	.12355	.9924	- .00095
32	.12520	.00016	.12536	.12399	.9890	- .00137
33	.12854	.00016	.12870	.12811	.9954	- .00059
34	.12752	.00016	.12768	.12686	.9936	- .00082

AV .9930

$$\Delta n_{\text{HF}}^a = \Sigma n_{\text{HF}} (\text{theo.}) - n_{\text{HF}} (\text{meas.})$$

3.1.4 Tests for Corrosion of Reaction Vessel

Samples of the product hydrofluoric acid solutions were submitted to the NBS Analytical Chemistry Division for tests for some selected metal ions. Because the combustion chamber was made principally of Monel, and silver-soldered in a few places, the solutions were tested for Ag, Ni, and Cu. Ca was also analyzed for because it was felt that calcium could originate from the CaF_2 disk over the sparking electrode. From one experiment to the next, one could detect a gradual erosion of the disk. The analytical technique used was atomic absorption spectrophotometry [24]. The results from these tests are summarized in Table 3. The blank represents a sample of the demineralized water which is placed in the solution chambers of the reaction vessel for the experiments. The analyst's results in $\mu\text{g/cc}$ solution are shown in the second to fifth columns. The difference between the results on the blank solution and those for the solutions after the experiments shows ions present in the HF solution which must have originated from corrosion products in the combustion chamber that are subsequently dissolved in the solution. The sixth through eighth columns show the weights of ions that would be found in the total solution. The final column gives the equivalents of HF, consumed, assuming the metal was first corroded by either HF or the fuel and then transferred to solution chamber by HF- H_2O mixture. The tests tend to confirm that corrosion does take place, and that the copper and nickel react roughly in the same ratio as they exist in Monel (60 Ni 33 Cu). The experiment #1 is not included in later results because it was carried out mainly for the purpose of conditioning the burner. The corrosion tests show that more corrosion resulted in this experiment than in the others.

Table 3

Tests for Metals Ions in HF Solutions
OF H_2 Expt.

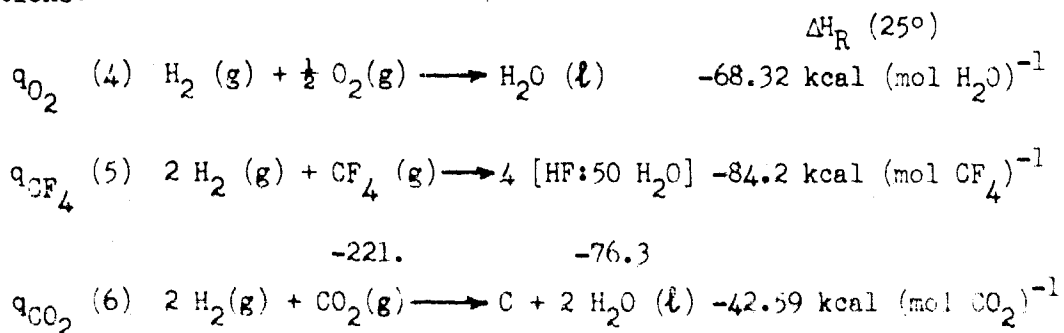
Expt. No.	Metal Ions ug/cc					Total mg.			n_{HF} mol
	As	Ca	Cu	Ni		Ca	Cu	Ni	
1	$0.16 \pm .1$	$0.29 \pm .02$	$5.3 \pm .2$	$10 \pm .4$.06	1.0	2.5	.00011
4	<.02	$0.16 \pm .02$	$4.2 \pm .2$	$6.0 \pm .4$.04	.96	1.4	.00008
7	<.02	$0.16 \pm .02$	$4.6 \pm .2$	$7.4 \pm .4$.04	1.1	1.7	.00009
Blank	<.02	<.02	<.02	<.05					

3.1.5. Heat Measurements for the $\text{OF}_2\text{-H}_2$ Reaction

The over-all heat measurements for the oxygen difluoride-hydrogen reaction are given in Table 4. The first part of the table gives the experiment number; m_g , the mass of the oxygen difluoride sample; ΔR_c , the corrected resistance increase for the thermometer; dR/dt , the factor for converting resistance increase to temperature increase; and $\Delta t_{\text{corr.}}$, the corrected temperature rise of the calorimeter. The average temperature is the mid temperature between the temperature at the beginning of the reaction period, and the temperature at the end of reaction period. The average temperature is taken to be the temperature at which the reaction takes place. $\Delta \epsilon$ is a correction to the energy equivalent for the deviation of the contents of the calorimeter for these reaction experiments from those of the calorimeter for the electrical calibrations. The correction was made for one-half of the HF and water formed in the reaction since this would be the amount present at the average temperature. The heat-capacity data of Thorvaldson and Bailey^[25] were used for making this correction. $\epsilon_{\text{cal, syst.}}$ is the energy equivalent of the calorimeter system for these experiments and $q_{\text{obs.}}$ is the observed heat effect, equivalent to $\epsilon_{\text{cal. syst.}} \times \Delta t_{\text{corr.}}$.

3.1.6. Corrections to the Heat Data

The corrections made to the observed heat data are given in Table 5 and can conveniently be grouped as due to (1) reaction of impurities in OF_2 sample, (2) ignition energy, (3) heat of vaporization of water, and (4) tempering of reacting gases. The impurities corrected for were oxygen, carbon tetrafluoride and carbon dioxide. It was assumed that the reactions with hydrogen took place according to the following equations:



The data for calculating the heats of the reactions were obtained from the compilation by Wagman *et al*^[7]. The ignition energy (q_{ign}) was measured directly and found to be 1.4 joules per second of sparking. The method used was the same as that used by Rossini^[23].

Table 4
Heat Measurements
(CF₂-H₂)

Series I

Temp. °C.	π_s	$\Delta R_{corr.}$	$\frac{dR}{dt}$	$\Delta t_{corr.}$	$t_{av.}$	Δe	$e_{cal syst.}$	$q_{obs.}$
		Ωm	$\Omega m(^{\circ}C)^{-1}$	$^{\circ}C$	$^{\circ}C$	$J(^{\circ}C)^{-1}$	$J(^{\circ}C)^{-1}$	J
2	2.9380	0.235957	0.1005825	2.34591	30.16	+3.8	21891.7	51353
3	3.4370	.279083	.1005762	2.77485	30.37	+4.0	21891.9	60747
4	3.0369	.250550	.1005798	2.49106	30.25	+3.9	21891.8	54234
5	3.5261	.286298	.1005750	2.84661	30.41	+4.0	21891.9	62313
6	3.4550	.280483	.1005757	2.78877	30.38	+3.9	21891.3	61051
7	2.4512	.280094	.1005758	2.73491	30.38	+3.9	21891.8	60967

Series II

23	3.4558	.280495	.1005757	2.78889	30.39	+3.9	21891.8	61054
26	3.4015	.275950	.1005762	2.74369	30.37	+3.9	21891.8	60064
27	3.3549	.272217	.1005763	2.70657	30.37	+3.9	21891.3	59252
31	3.3785	.274271	.1005765	2.72699	30.36	+3.9	21891.8	59599
32	3.4021	.275837	.1005721	2.74267	30.50	+3.9	21891.3	60042
33	3.4929	.283250	.1005739	2.81633	30.45	+4.0	21891.9	61055
34	3.4651	.281155	.1005747	2.79548	30.42	+4.0	21891.9	61193

$e_{cal syst.} = 21887.9 J(^{\circ}C)^{-1} + \Delta e$

Table 5

Corrections to Heat Measurements

(OF₂-H₂)

Series I

Expt. No.	q _{O₂}	-q _{CF₄}	-q _{CO₂}	-q _{ign}	-q _{vap}	-q _{vap}	q _{temp.}	-Σ _{corr.}
	J	J	J	J	J	J	J	J
2	234.3	14.1	8.8	17.1	140.6	31.8	22.8	424
3	274.0	14.1	10.5	18.9	155.0	55.6	36.8	491
4	245.6	14.1	10.5	19.3	130.9	43.6	30.1	434
5	285.8	14.1	10.5	14.0	162.7	45.2	35.6	497
6	274.0	14.1	10.5	21.6	179.1	53.1	22.0	530
7	274.0	14.1	10.5	21.6	169.4	53.1	28.4	514

Series II

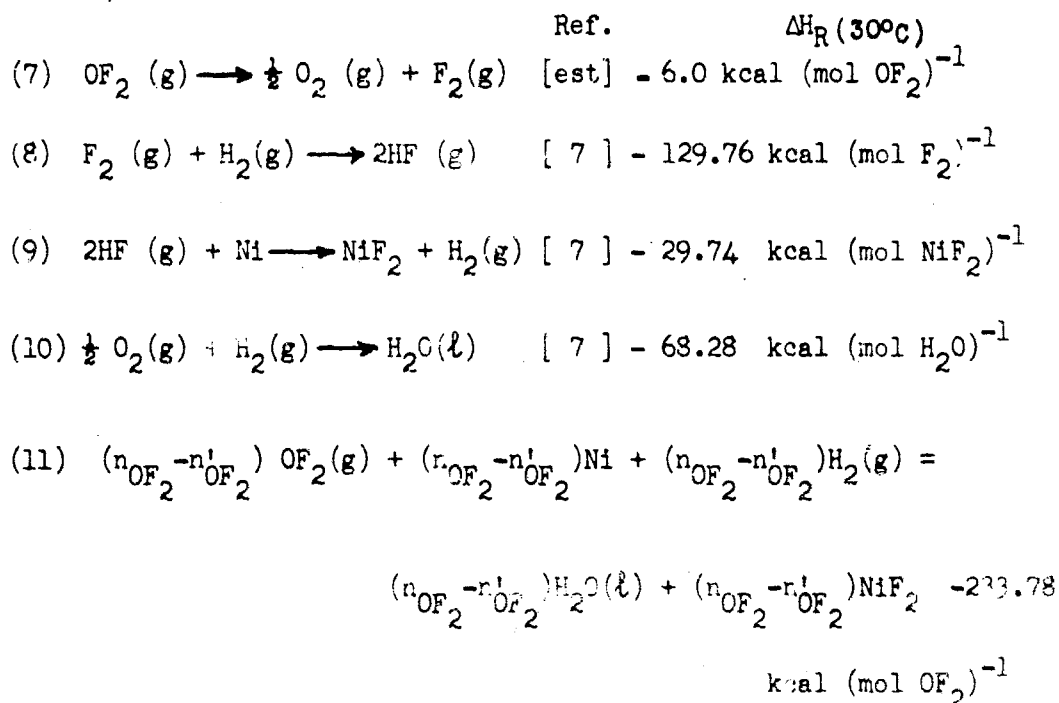
23	274.0	14.1	10.5	16.8	148.1	53.1	38.2	478.
26	271.0	14.1	10.5	19.6	146.1	45.2	42.0	467
27	268.6	14.1	10.5	18.5	143.9	50.6	40.2	466
31	268.6	14.1	10.5	14.8	154.8	50.6	34.2	479
32	268.6	14.1	10.5	14.8	165.7	49.8	29.3	494
33	273.9	14.1	10.5	19.0	156.9	50.6	37.0	494
34	279.9	14.1	10.5	19.9	148.1	50.6	41.5	482

The correction for the heat of vaporization of water arises from two sources. The larger of these corrections, (q'_{vap}), is due to condensation of water in the reaction vessel by the reacting hydrogen. The hydrogen removes the water from the bubbler in the flow line directly preceding the calorimeter. From the room temperature, vapor pressure of water, and volume of hydrogen reacted, the amount of water transported into calorimeter was calculated. q'_{vap} was calculated using the heat of vaporization of water at the average temperature (Table 4) of the calorimeter. q''_{vap} is a correction for the heat of vaporization of water not removed from the calorimeter by the helium used in flushing the fuel line at the end of the reaction period. As shown in Figure 7, helium in fuel flow line is not passed through a bubbler before the calorimeter. As a result, flushing the fuel line with helium causes vaporization of water from the reaction vessel and this occurs after the principal part of the temperature rise has occurred. Also, no helium passes through the fuel line during the initial drift period. Evaporation heat thus influences the final drift rate, but not the initial drift rate. It seems that this situation is analagous to bomb rotation in rotating bomb calorimetry. It is argued there that if bomb rotation is started at time, t_m , no correction needs to be applied for the energy of rotating the bomb [26]. In a flow experiment, t_m is the time at about one-half of the temperature rise. Therefore, if the helium flow were begun at the point where one-half of the temperature rise has occurred, it would not be necessary to correct for the heat of vaporization of water by helium, even if there was no flow in the initial period. On this basis, q''_{vap} corrects for the heat of vaporization of water not evaporated for a time interval equal to one-half reaction time. The volume of helium is calculated from the rate of flow of helium and the temperature of the water is taken to be t_{av} , the average temperature of the calorimeter. q_{temp} is a correction for preheating the reacting gases. The method used for making this correction is explained in the appendix. The sum of the corrections is given in the final column of the table.

3.1.7. Thermal Corrections for Corrosion of Reaction Vessel

As stated in the introduction (equation 3), the object of the study is to measure the heat of reaction of oxygen difluoride with hydrogen to give an aqueous solution of hydrogen fluoride. As shown by the analyses on the product solutions, a discrepancy exists between the amount of oxygen difluoride introduced into the reaction vessel compared to the amount reacted to HF and water. Because of the reactivity of oxygen difluoride and also based on our experiments in the oxygen-hydrogen system, it is assumed that all of the OF_2 released from the sample chamber is reacted with the hydrogen, and the failure to recover the theoretical amount of HF is due to its corrosive effect on the reaction vessel. Using this argument, the observed heat of reaction is corrected for the effects given in Table 4, and is further corrected for the heat of reaction of OF_2 with H_2 , and then subsequent reaction of the product HF with the combustion chamber, which is, principally nickel.

It is assumed that the OF_2 is first thermally decomposed to F_2 and O_2 . In early preliminary experiments, we attempted to burn hydrogen in excess OF_2 . A flame was achieved but an infrared spectrum of the residual gas showed very little OF_2 present, suggesting that the excess OF_2 had thermally decomposed to the elements as a result of the heat from the flame. It is general knowledge that OF_2 does thermally decompose above 250°C [27]. Equations 7-11 presumably show how the subsequent reactions proceed. The over-all heat of the reaction in equation 11 is used to correct for the missing oxygen difluoride. The amount of OF_2 consumed in this manner is the difference between the measured amount of OF_2 (n'_{OF_2}), calculated from the measured product HF, less the HF arising from the CF_4 impurity. This difference is shown only in equation 11.



The data used in making this correction for the loss of OF_2 and also the calculation of the heat of reaction of OF_2 on a molar basis are listed in Table C. n_{OF_2} and n'_{OF_2} are respectively, the theoretical amount of OF_2 reacted determined from the mass of sample, and the amount of OF_2 actually involved in reaction calculated from the measured amount of product HF. $n_{\text{H}_2\text{O}}$ is the number of moles of water added to the reaction vessel (5.55 moles) plus the water formed in the reaction. $\frac{n_{\text{H}_2\text{O}}}{n_{\text{HF}}}$ is the

Table 6

Treatment of Heat Data ($\text{OF}_2\text{-I}_2$)

Series I

Expt. No.	n_{OF_2}	$n_{\text{H}_2\text{O}}$	$\frac{n_{\text{H}_2\text{O}}}{n_{\text{HF}}}$	$-q_{\text{OF}_2}$	$-q_{\text{OF}_2}^1$	$\frac{-q_{\text{OF}_2}}{n_{\text{OF}_2}}$	$\frac{(q_{\text{OF}_2}^1 - q_{\text{OF}_2})}{n_{\text{OF}_2}}$	$\frac{q_{\text{OF}_2}^1 - q_{\text{OF}_2}}{n_{\text{OF}_2}}$
	mol	mol		J	J	J mol ⁻¹	J mol ⁻¹	J mol ⁻¹
2	0.05351	5.60	52.6	50932	240	951822	951784	956290
3	.06324	5.61	44.6	60256	303	952814	952693	957508
4	.05680	5.61	49.4	54100	0	952465	952129	952465
5	.06488	5.62	43.2	61821	0	952851	951678	951678
6	.06359	5.61	44.3	60521	254	951738	951634	955645
7	.06351	5.61	44.4	60453	411	951866	951688	958202

Series II

23	.06359	5.61	44.4	60576	372	952603	952444	958329
26	.06259	5.61	45.1	59597	352	952181	952033	957689
27	.06173	5.61	45.8	58786	469	952308	952114	959771
31	.06217	5.61	45.5	59220	465	952549	952423	959961
32	.05260	5.61	45.3	59548	670	951246	951026	961848
33	.06427	5.61	43.8	61161	288	951626	951537	956039
34	.06376	5.61	44.3	60716	401	952258	952091	958421

water to HF ratio in the solution after the reaction. q_{OF_2} is the observed heat of reaction, corrected for the heat effects given in Table 5. q'_{OF_2} is the thermal correction for corrosion based on equation 11.

For the moment, ignoring the fact that a mass balance was not achieved in most experiments, the heat of reaction per mole of OF_2 is calculated in three different ways. First, it is expressed as

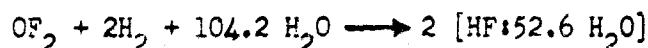
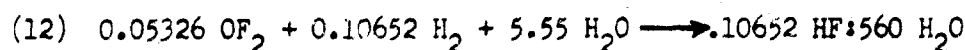
$\frac{q_{OF_2}}{n_{OF_2}}$. This is the ratio of the over-all heat of reaction of OF_2 to the moles of OF_2 introduced into burner. $\frac{q_{OF_2}}{n_{OF_2}}$ is the heat of

reaction per mole of OF_2 , determined from the measured product HF.

$\frac{q_{OF_2} - q'_{OF_2}}{n_{OF_2}}$ is the over-all heat of reaction, corrected for estimated

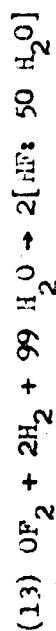
heat effects incurred in the loss of HF, per mole of OF_2 , based on measured HF.

These heats of reaction are for equations with HF:H₂O ratios shown in column 5 of the table. For example the reaction in experiment #2 is Equation 12.



The heats of reaction were adjusted so that the concentration of the HF solution would be HF:50 H₂O. The heats of dilution per mole of OF_2 reacted, and the adjusted heats of reaction are given in Table 7.

Heat of Reaction:



Series I

Expt. no.	ΔH_{dil}	$-\left[\frac{q_{\text{OF}_2}}{n_{\text{OF}_2}} + 2\Delta H_{\text{dil}}\right]$	$-\left[\left(\frac{q_{\text{OF}_2}}{n_{\text{OF}_2}} + 2\Delta H_{\text{dil}}\right)\right]$	$-\left[\left(\frac{q_{\text{OF}_2}}{n_{\text{OF}_2}} + 2\Delta H_{\text{dil}}\right)\right]$
	$J(\text{mol soln.})^{-1}$	$J(\text{mol OF}_2)^{-1}$	$J(\text{mol OF}_2)^{-1}$	$J(\text{mol OF}_2)^{-1}$
2	+17	951788	956324	951750
3	-8	952830	957524	952709
4	-4	952473	952473	952137
5	-17	952835	951885	951712
6	-8	951754	955661	951650
7	-8	951882	958218	951709
Mean		952269	955347	951944
Standard dev. of the mean		213	1116	169
		227.60 \pm .05 Kcal mol ⁻¹	228.33 \pm .27 Kcal mol ⁻¹	227.52 \pm .04 Kcal mol ⁻¹

Series II

23	-8	952619	958345	952460
25	-4	952189	957697	952641
27	-4	952316	959779	952122
31	-4	952557	959969	952431
32	-4	951254	951852	951034
33	-8	951642	956105	951595
34	-8	952274	958437	952107
Mean		952121	958883	951970
Standard dev. of the mean		189	699	131
		227.56 \pm .045 Kcal mol ⁻¹	229.18 \pm .17 Kcal mol ⁻¹	227.53 \pm .05 Kcal mol ⁻¹

^a 1 cal = 4.184 J

3.1.8. Heat of Reaction of Oxygen Difluoride with Hydrogen

Depending on the basis of the amount of reaction, three different values can be derived for the heat of the reaction of oxygen difluoride with hydrogen at 30 °C to give aqueous HF. The values derived from the two series of measurements are averaged and summarized below.

	$-\Delta H_R(30^\circ)$ kcal (mol OF ₂) ⁻¹	standard deviation of the mean
(1) based on n _{OF₂} no correction for corrosion	227.58	0.04
(2) based on n _{OF₂} - no correction for corrosion	228.75	.22
(3) based on n _{OF₂} - corrected for corrosion	227.52	.03

It is to be noted that correcting for corrosion gives a tremendous reduction in the standard deviation of the third value compared to the second value. Also, the first and third values are actually the same considering the standard deviation of mean for each value. This is coincidental because the correction applied for loss (corrosion) of OF₂ is actually comparable to the heat of reaction of OF₂ with hydrogen. It is felt also that the corrections should be applied for corrosion, because the loss of HF (Δn_{HF} in Table 2) is larger than the uncertainty in the analyses for HF in these experiments. On the basis of these observations the latter, [-227.52 kcal (mol OF₂)⁻¹], is the preferred value for the heat of reaction of OF₂ with hydrogen (Equation 13) at 30 °C.

Using heat capacity data for OF₂ [7], H₂ [7], H₂O [7] and HF, aq. [25] from the references indicated, it is found that the heat of reaction at 25 °C is $-227.54 \pm .03$ (.013%) kcal mol⁻¹. Combining the percentage uncertainty in the calibrations (.006%), the percentage uncertainty in the analysis for HF (.05%), and estimated uncertainty in analysis of OF₂ sample (.05%), it is estimated that the over-all uncertainty in this value is $\pm .07\%$, or $\pm .16$ kcal mol⁻¹. The uncertainty was calculated by taking the square root of the sum of the squares of the individual percentage errors.

3.2 The Fluorine-Hydrogen Reaction

3.2.1. Analysis of the Fluorine

The fluorine sample was an ordinary commercial cylinder of gas and was therefore not of the high purity that would be desirable for a definitive study of the hydrogen--fluorine system. The gas was obtained from the Molecular Spectroscopy Section of the Physical Chemistry Division of the National Bureau of Standards. It had earlier been secured from the General Chemical Division of Allied Chemical Company. At the time of these experiments facilities were not available in the laboratory for further purification of the gas by fractional distillation.

The study was continued with the hope that a thorough analysis of the fluorine would yield a reliable basis for the heat measurements, thus resulting in accurate data for the heat of formation of aqueous solutions of hydrogen fluoride from pure liquid water, elemental fluorine, and hydrogen.

The fluorine samples were used from the Monel sample bulbs (Fig. 8), filled to 170 psig. using the same procedure as described for filling the oxygen difluoride sample bulbs. However, the fluorine was subjected to further purification. To remove hydrogen fluoride, it was passed through the NaF trap shown in the manifold in Figure 10.

The fluorine was analyzed by the mercury absorption method to get the total mole percent fluorine [9,28,29]. The residual gas was analyzed by mass spectrometry for the identification and amounts of the impurities present. Since fluorine in these experiments was the fuel or reactant in smaller quantity, it was necessary to have an accurate analysis of the sample. Experience by the earlier investigators has found that the absorption of fluorine by mercury is quite complete. Though Kesting, *et al* [19,20] have devised a method for checking the presence of fluorine in oxygen difluoride and vice versa, there is no way of telling whether or not other reactive gases like NF_3 and OF_2 are present and absorbed in the mercury. Possibly if present in large enough quantity, these gases would exist as impurities and show up on an IR spectrum of the fluorine. Such a spectrum was not obtained in these experiments.

For the most part, the residual gases are usually relatively inert. Because of the accuracy desired in the analysis of the residual gas, a chromatographic method for analyzing the residual gases, independent of the mass spectrometric method, was developed and tested in this study. Earlier reference had been made to the possibility of using chromatography for analysis of the impurities in fluorine [9]. Some investigators have reported on [30] chromatographic methods with which one can analyze the entire

fluorine sample (fluorine inclusive). However, after noting what the impurities were, it appeared an arduous task to find an inert column material with adequate separation efficiency of the fluorine and the contained impurities. Consequently, the mercury absorption method used in conjunction with mass spectrometry and chromatography was adopted for analysis of the fluorine used in this study.

The chromatographic method developed required first the absorption of fluorine with mercury. Then samples of the residual gas were repeatedly injected into the chromatograph. The layout of the equipment used in the chromatography is shown in Figure 15. The chromatographic equipment was identical to that described for analysis of OF_2 to the left of valves, F. The items to the right of valves F are those necessary for extracting the fluorine sample. The flask G, and all connecting flow lines up to flask G are evacuated to 10 microns, by means of vacuum source at L. The vacuum is closed off and the valve to flask G is closed. A small amount of fluorine from container J, is released into flow lines for conditioning, for about 15 minutes. With sample bulb closed, the connecting lines are then re-evacuated through trap K which is filled with soda lime. Afterwards flask G is opened, and filled to one atmosphere with fluorine. The flask is now closed and the fluorine removed from the lines by evacuating through trap, K. Upon contact with the mercury fluorine to give a film, after which little, if any, further reaction takes place, without agitation to break the surface film. The agitation of the mercury is provided by a Teflon covered magnet. The flask is placed on a magnetic stirring motor. Also, as a precaution in case of breakage of flask, it is placed in a large empty evaporating dish (not shown in diagram). To insure complete reaction of fluorine, the valve G was disconnected from line and the flask was vigorously agitated. For these experiments, the 300-cc flask contained about 1000 grams of mercury, much more than is usually used (150 g) for absorption of 1 atm. of fluorine in a 250-cc flask. A large excess of mercury was used because the concentration of impurities necessary for detection on the chromatograph was not known. Conceivably, one could continue to admit and react fluorine sample to build up amounts of the impurities in the flask. Note that after reaction of one atm. of the fluorine with the H, the residual gas in the flask is only about 0.01 atm. Therefore, when the valve to the flask is opened to allow the residual gas to expand into the evacuated sample loop, the sample to be introduced into the chromatograph is also at a pressure of slightly less than .01 atm. The tubing section holding the sample was a 10" long section of .25" o.d. Monel tubing (.032" thick wall). Consequently, from the reaction of one atmosphere of the fluorine gas, the amount of residual gas in the sample loop is quite small. However, it was found that this amount was quite adequate for the chromatographic analyses. After filling the sample loop and closing valves to the flask

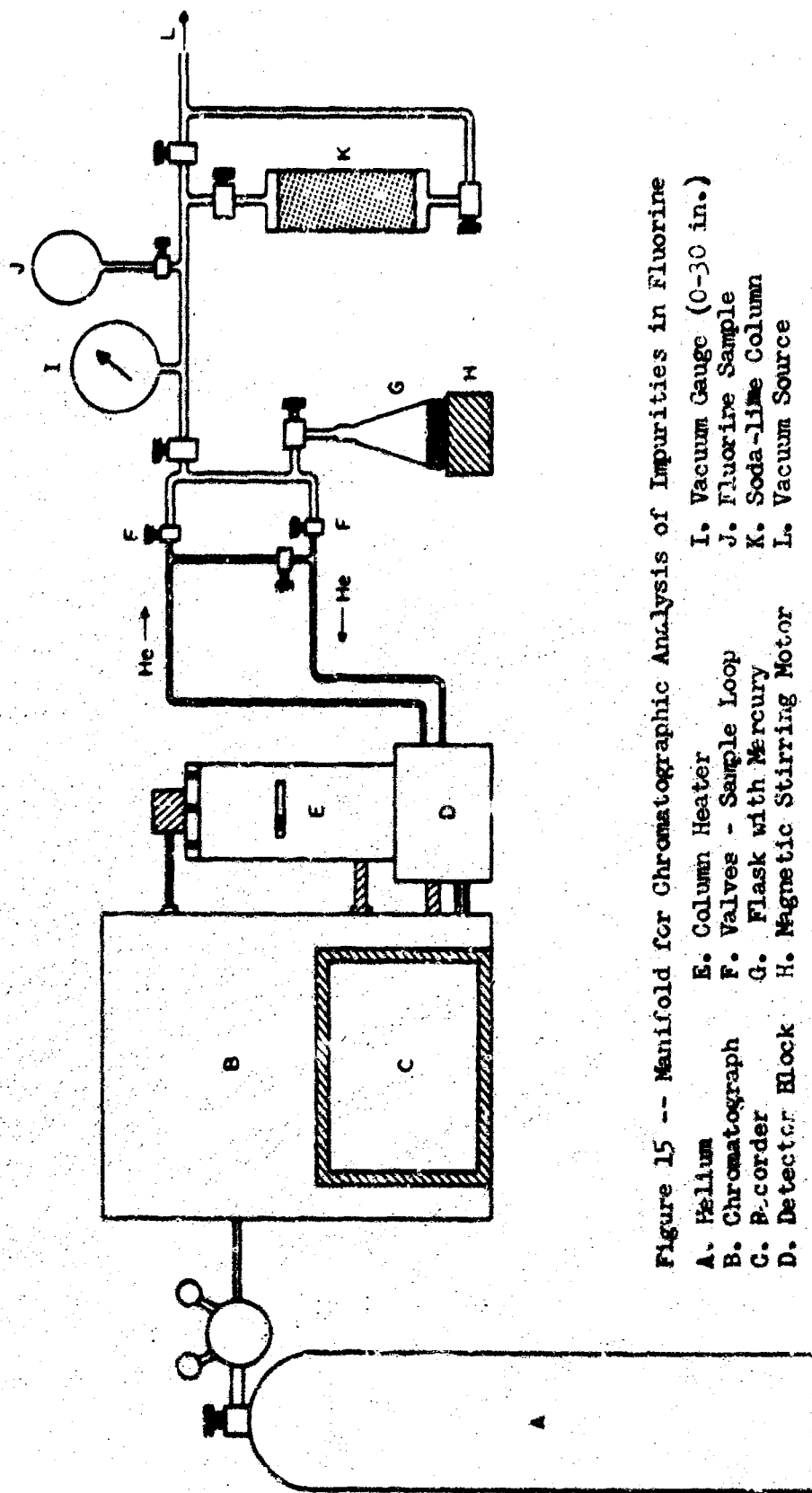


Figure 15 -- Manifold for Chromatographic Analysis of Impurities in Fluorine

- | | | |
|-------------------|----------------------------|----------------------------|
| A. Helium | E. Column Heater | I. Vacuum Gauge (0-30 in.) |
| B. Chromatograph | F. Valves - Sample Loop | J. Fluorine Sample |
| C. B-corder | G. Flask with Mercury | K. Soda-lime Column |
| D. Detector Block | H. Magnetic Stirring Motor | L. Vacuum Source |

and other parts of system, one of the valves F was opened to pressurize the sample with helium from the chromatograph. Immediately the by-pass valve was closed and the second, valve, F, was opened to flush the sample into the chromatograph. After about 20 seconds, the by-pass valve was again opened and the valves, F were closed. Now the loop can be re-evacuated and filled with another sample of the residual gas for a repeat analysis.

An earlier mass spectrometric analysis on the residual gases from commercial fluorine had shown that the major impurities were nitrogen, oxygen, carbon tetrafluoride, and carbon dioxide, with smaller amounts of silicon tetrafluoride, sulfur hexafluoride and fluorocarbons. Using this information the chromatographic column materials were selected. Molecular Sieves, 5A, used by the procedure of Kyriacos and Boord (31) separates nitrogen from oxygen, but shows no separation efficiency toward the other impurities. Silica gel [19] separates oxygen plus nitrogen from the carbon tetrafluoride and carbon dioxide. Chromatograms obtained with these two column materials are shown in Figures 16 and 17, respectively. The conditions for the analyses are given on the chromatograms. The peak components were checked with injections of air, pure carbon tetrafluoride and carbon dioxide.

After the chromatographic analyses, the sample loop was disconnected from the chromatograph at the two valves, F. On one valve a Pyrex break-off tip type ampoule was attached, and the ampoule and connecting lines were evacuated. The valve to the flask was then opened and the ampoule was filled with the residual gas and sealed off. A mass spectrometric analysis was performed on this sample. The results from the two methods are compared in Table 8. Considering that these are two completely different techniques, the results compare rather well. The agreement between the results suggests that the chromatographic method possibly may be developed further and used routinely as a second way of analyzing for the impurities in ordinary commercial fluorine, which is usually reported to be of a purity of not better than 98 percent.

Shown in Table 9 are also the results from mass spectrometric analyses on residual gases from samples of fluorine from sample bulbs which were filled at different times (about two weeks apart). For these analyses, 150 grams of mercury was contained in a 250-cc spherical Pyrex bulb similar in overall design to the bulb shown in Figure 8. The data in Tables 8 and 9 show a difference between the relative amounts of oxygen and nitrogen in the residual gas in the flask used for chromatography, compared to the residual gas used from the spherical bulbs. It is felt that the larger amount of oxygen impurity in the Erlenmeyer flask may have arisen from the mercury, where a much larger amount of mercury was used. There is reason to

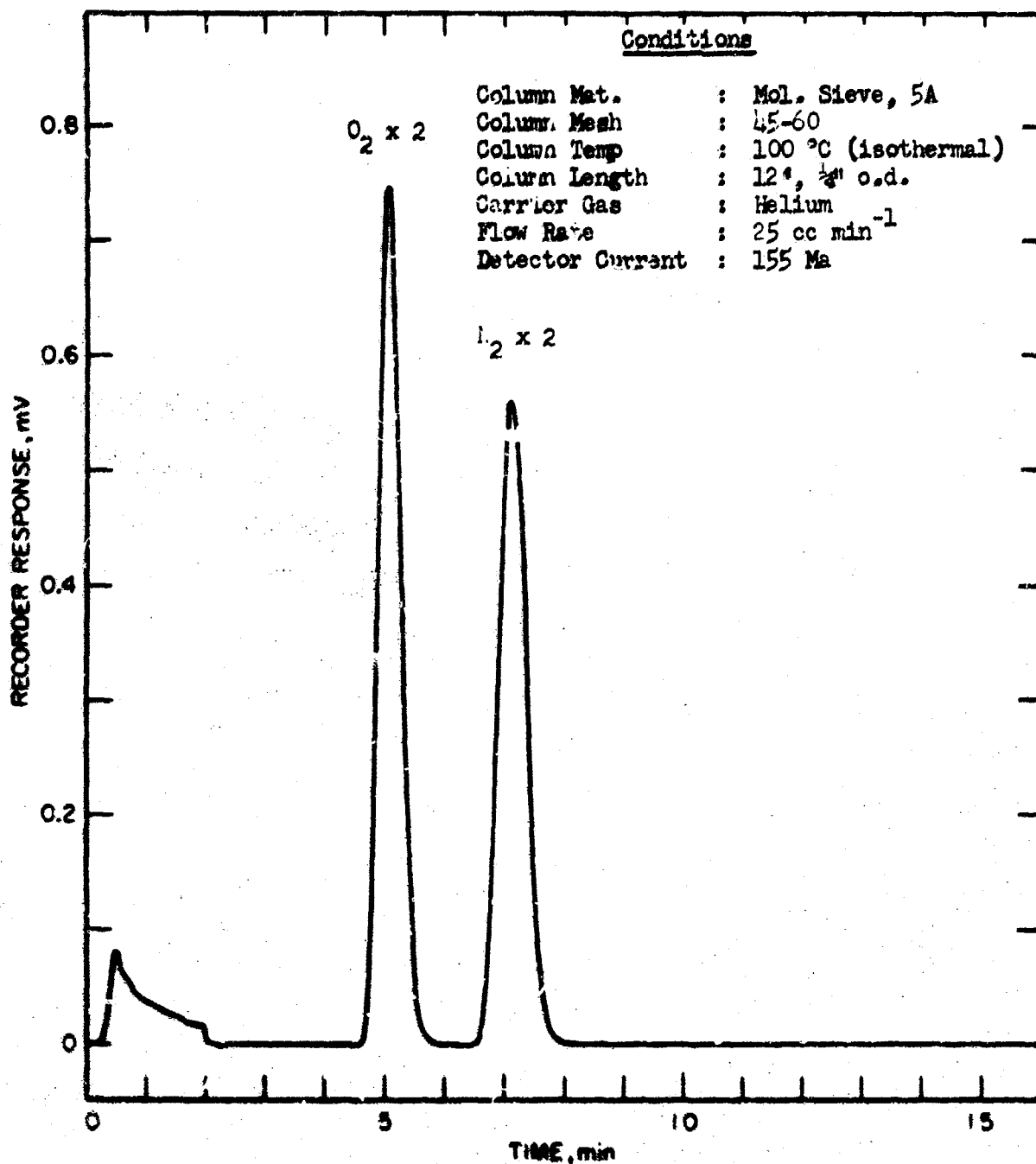


Fig. 16. Chromatogram of Impurities in Fluorine
on Molecular Sieves, 5A

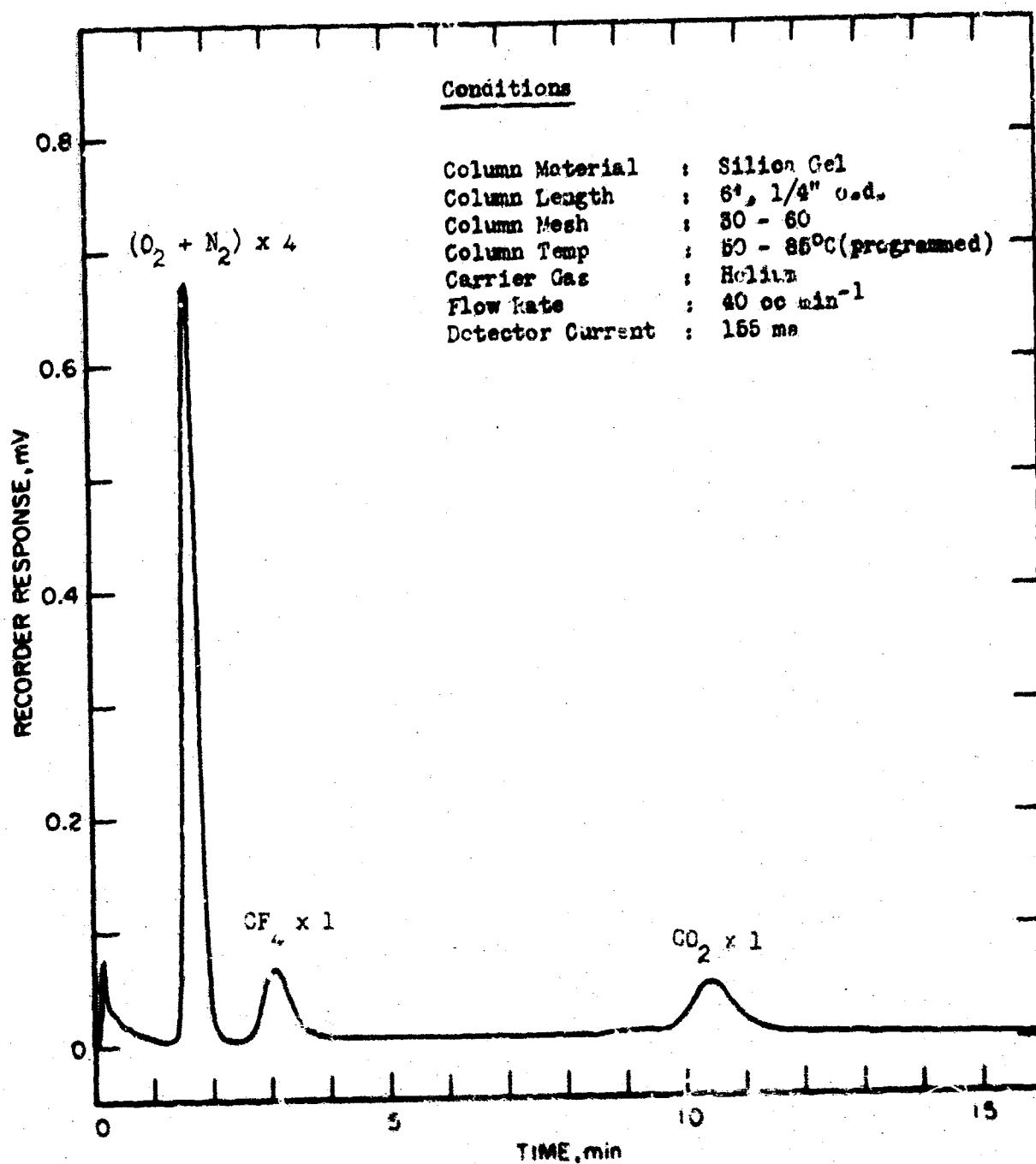


Fig. 17 Chromatogram of Impurities in Fluorine
on Silica Gel

Table 8

Comparison of Chromatographic and Mass Spectrometric
Analyses for Impurities in Fluorine

Component	Mole Percent	
	Chromatography	Mass Spectrometry
N ₂	45.	42.6
O ₂	47.	47.7
CF ₄	3.6	2.8
CO ₂	4.6	5.1
SO ₂ F ₂		.22
Ar		.2
SiF ₄		1.1
C ₂ F ₆		.21
C ₃ F ₈		.04

Table 9

Analysis of Fluorine Sample

Component	Mole Percent of Component in Residual Gas ^a	Mole Percent of Component in Fluorine Sample	Molecular Wt. of Component [32]	Weight percent
	I ^b	II (based on II)		
F ₂		98.75	37.9968	98.92
N ₂	61.8	62.0	28.0134	.54
O ₂	28.6	31.3	31.9988	.25
Ar	0.2	0.2	39.948	.003
CO ₂	3.4	1.2	44.0100	.017
CF ₄	5.0	4.4	88.00475	.128
SiF ₄		0.03	104.0796	.001
SO ₂ F ₂	0.3	.3	102.0596	.010
C ₂ F ₆		.28	138.0128	.013
SF ₆		.08	146.0544	.004
C ₃ F ₈		.08	188.0203	.005
C ₄ F ₈ (unsat.)		.07	200.0320	.005
Remaining Fluoro- carbons	0.6	.06		

^a Mass spectrometric analysis of volatile impurities after removal of F₂ by reaction with mercury

^b Sample pressure of I was factor of ten less than that of II. Analysis of I serves only for comparison of analysis for major impurities.

believe that an improvement in the mercury absorption method for analysis of fluorine would be the following; after evacuation of container, admit a small amount of fluorine to condition the walls of vessel and mercury surface; re-evacuate mercury container and then proceed with analysis by filling vessel to one atmosphere with fluorine. The data given in Table 9 for the analysis of fluorine were used in the calculations for these experiments. The hydrogen used for these experiments was taken from the same cylinder used in the OF_2 - H_2 experiments. The analysis for the hydrogen is given under the description of those experiments.

3.2.2. The Calorimetric Experiments

As implied in the earlier discussion, the principal objective in conducting the reaction is to quantitatively transfer a sample of fuel (F_2) from the sample bulb to the reaction vessel and to react this fuel with hydrogen. Because fluorine is more spontaneously reactive than oxygen difluoride, this objective was more difficult to accomplish for the fluorine-hydrogen reaction than for the similar reaction of OF_2 with hydrogen. In preliminary experiments, several occurrences suggested that, before each experiment, it is necessary to condition the fuel flow line with fluorine. Otherwise there would be a noticeable loss of fluorine during the reaction, making it impossible to achieve a mass balance between the fluorine sample reacted and the HF formed. The most apparent of the corrosive effects of fluorine was the discoloration on the lower part of the Pyrex flow-meter in the fuel line (see Figure 7). This discoloration first appeared yellow in air. But upon exposure to fluorine, it would assume an orange appearance. When exposed again to air, it would be yellow and then orange again in contact with fluorine. In the first experiments, which are grouped as Series I, the fuel line was passivated by flushing with fluorine from the point where the sample bulb is attached to the connector for the burner inlet. In later experiments (Series II) before conditioning, the combustion chamber was assembled, connected to fuel line, and also conditioned with fluorine, up to the end of the platinum tube, to which the polyethylene gas disperser is attached. However, the gas disperser was removed for this conditioning process. When it appeared that the burner had been flushed adequately, the fuel line was then flushed with helium to remove the fluorine remaining in flow line and combustion chamber. The fluorine source was left in place until time to attach the one to be used in the experiment.

After conditioning the burner chamber, it was immediately disconnected from the fuel line, and connected to the solution chambers. The inlet ports of the burner were capped in an attempt to minimize the disturbance to the passivated surfaces.

The calorimeter can with its water, the bubblers, and the magnesium perchlorate absorber were weighed and the remaining procedure was very similar to that already described for the OF_2 experiments. However, the flow rate of fluorine used was considerably higher, approximately 100 cc per minute.

3.2.3. Analysis of the Reaction Product for Hydrogen Fluoride

The procedure used for the analysis of the hydrofluoric acid solutions has already been described, for the oxygen difluoride experiments. Compared to the OF_2 experiments, the recovery of the product hydrogen fluoride in the fluorine experiments was much more erratic, and on the average, there appeared to be a considerably larger loss of hydrogen fluoride. The reason for this is not entirely clear. However, the section on the test for corrosion points out several factors that suggest the fluorine-hydrogen reaction to be more corrosive to the combustion chamber. The analytical results for the solutions are given in Table 10, and compared with the amount of fluorine introduced into the burner. $n_{\text{HF}}^{\text{F}_2}$ (theo) and $n_{\text{HF}}^{\text{CF}_4}$ (theo.) are the moles of hydrogen fluoride theoretically expected from the F_2 and CF_4 in the fluorine sample reacted. Σn_{HF} (theo.) is the total number of moles HF expected and n_{HF} (meas.) is the observed moles of HF. The ratios of these are given in column 7. The data in the last two columns are included for later discussion.

3.2.4. Tests for Corrosion of Combustion Chamber

From visual observation of the combustion chamber after an experiment one could observe that the flame tip was being severely attacked by the reaction. Also, in the center of the lid to the combustion chamber was a blackening that presumably was due to carbon formation from reduction of the fluorocarbons in the fluorine sample. Otherwise, there was a corroded film on the walls of the chamber that did not show any obvious change in appearance after exposure to the atmosphere. However, in view of the varying amounts of HF loss from one experiment to the next, one may claim that the conditioning of the burner was disturbed in varying amounts by exposure to the atmosphere.

It is interesting to note in Table 10 that the two experiments with the smallest amounts of reaction; numbers 53 and 56 show the lowest fractional recovery of HF. In the last four experiments, a consistently larger amount (Δn_{HF}) of hydrogen fluoride was unrecovered. The erraticness of the recovery of the HF is the most puzzling point about the experiments. The loss of hydrogen fluoride shows no trend with the flow rate of fluorine used.

Table 10

Reaction Quantities of Fluorine

Series I

Expt. No.	n_{F_2} mol	$n_{HF}^{F_2}$ (theo.) mol	$n_{HF}^{CF_4}$ (theo.) mol	Σn_{HF} (theo.) mol	n_{HF} (meas.) mol	$\frac{n_{HF} \text{ (meas.)}}{n_{HF} \text{ (theo.)}}$	Δn_{HF} mol	Flow Rate of Fluorine cc min ⁻¹
50	0.09243	0.18486	0.00020	0.18506	.18277	0.9876	.00229	99
51	.07155	.14310	.00016	.14326	.14267	.9959	.00059	101
52	.07051	.14102	.00016	.14118	.13965	.9891	.00153	74
53	.03427	.06854	.00008	.06862	.06706	.9772	.00156	77
54	.07284	.14568	.00016	.14584	.14532	.9964	.00052	119

Series II

49	0.07702	0.15546	0.00016	0.15562	0.15502	0.9961	.00060	90
56	.06410	.12820	.00012	.12832	.12545	.9776	.00287	104
57	.06905	.13810	.00016	.13826	.13596	.9833	.00230	111
58	.08111	.16222	.00016	.16238	.15938	.9815	.00300	102
59	.08864	.17728	.00020	.17748	.17453	.9833	.00295	95
Av. .9844								

On the basis of observations in this study, it is believed that the recovery of hydrogen fluoride can possibly be improved in several ways: (1) A reaction vessel with a larger combustion chamber (of platinum) may be a useful modification. A larger chamber provides more surface area to become corroded; however, this disadvantage is offset by the fact that the gases (HF, in particular) are cooled before reaching the surface. Though platinum is recommended for the material of construction for the combustion chamber, in a preliminary design of the reaction vessel shown in Figure 4, platinum was found to be most unsuitable for the flame tip. After preliminary OF_2 - H_2 experiments with a platinum flame tip, the combustion chamber was always well coated with a black surface, resembling a spray-coat of graphite. It was very obvious that the platinum flame tip was attacked severely. A spectroscopic analysis of the black coating on the burner chamber confirmed the coating to be platinum. (2) Experiments by Priest and Grosse [33] with a hydrogen-fluorine torch suggest that copper may be a satisfactory material for the flame tip. A copper flame tip was not experimented with in the present study. (3) The use of helium to lift the flame from the burner tip may also lessen the reaction of hydrogen fluoride with the flame tip [9].

Tests were made on the aqueous solutions for selected metal ions by means of atomic absorption spectrophotometry [24]. These results are shown in Table 11. A comparison with the same tests for the OF_2 experiments (Table 2) suggests that a smaller amount of the salts resulting from corrosion were transferred to aqueous solution in spite of the fact that a larger loss of HF was observed for the F_2 experiments. The observation raises the questions of how the ions get into the solution in the first place. It can be speculated that in the OF_2 experiments, they are first dissolved in the product $\text{HF}:\text{H}_2\text{O}$ mixture and then washed down into the solution, whereas in the fluorine reaction, the product is dry and the only way salt can be carried into the solution is through evaporation and then flushing down by the effluent gas. As a result one may expect to find more metal ions in the aqueous solutions from the OF_2 experiments than from the fluorine experiments.

3.2.5. Heat Measurements for the F_2 - H_2 Reaction

The data for the over-all heat measurements for the fluorine-hydrogen experiments are given in Table 12. The table gives the experiment number; m , the mass of the fluorine sample; ΔR_c , the corrected resistance change of the thermometer; $\frac{\Delta R_c}{\Delta t}$, the factor for converting resistance change to temperature change; Δt corr., the corrected temperature rise; t_{av} , the average temperature of the calorimeter; Δe , the correction to the energy equivalent for changes

Table 11

Test for Corrosion in F_2-H_2 Experiments

Expt. No.	Ag	Ca ug/cc	Cu	Ni
49	<.02	<.05	$1.9^{+.0.1}$	$4.7^{+.2}$
50	<.02	<.05	$2.3^{+.0.1}$	$3.8^{+.2}$
51	<.02	<.05	$0.55^{+.04}$	$2.1^{+.1}$
52	<.02	<.05	$0.38^{+.04}$	$0.90^{+.04}$
53	<.02	<.05	$0.40^{+.04}$	$1.1^{+.05}$
54	<.02	<.05	$0.80^{+.04}$	$1.9^{+.1}$
56	<.02	$0.1^{+.05}$	$0.15^{+.04}$	$0.93^{+.04}$
57	<.02	<.05	<.02	$1.1^{+.05}$
58	<.02	<.05	$0.30^{+.04}$	$1.8^{+.1}$
59	<.02	<.05	$0.88^{+.04}$	$2.3^{+.1}$

Table 12

Heat Measurements for the $F_2 H_2$ Reaction

Series I

Expt. No.	m g	ΔR_C ohm	$\frac{dR_C}{dt}$ ohm(°C) ¹	$\Delta t_{corr.}$ °C	t _{av.} temp.	Δe J(°C) ¹	$\epsilon_{cal syst.}^A$ J(°C) ¹	q _{obs} J
50	3.5504	.273034	.1005768	2.71469	30.35	+1.8	21889.7	59423.7
51	2.7483	.211629	.1005654	2.10439	30.73	+1.4	21880.3	46063.6
52	2.7084	.208451	.1005656	2.07278	30.73	+1.4	21889.3	45371.7
53	1.3165	.101712	.1005805	1.001125	30.02	+1.0	21888.9	22135.3
54	2.7981	.215627	.1005651	2.14415	30.74	+1.4	21889.3	46933.9

Series II

43	2.9859	.230765	.1005823	2.29429	30.16	+1.6	21887.5	320.9
56	2.4623	.190297	.1005640	1.89230	30.78	+1.6	21889.5	1421.5
57	2.6524	.205160	.1005665	2.04004	30.69	+1.4	21889.3	4655.0
58	3.1136	.240719	.1005721	2.39349	30.51	+1.6	21889.5	52392.3
59	3.4048	.263337	.1005782	2.61823	30.30	+1.8	21889.7	57212.3

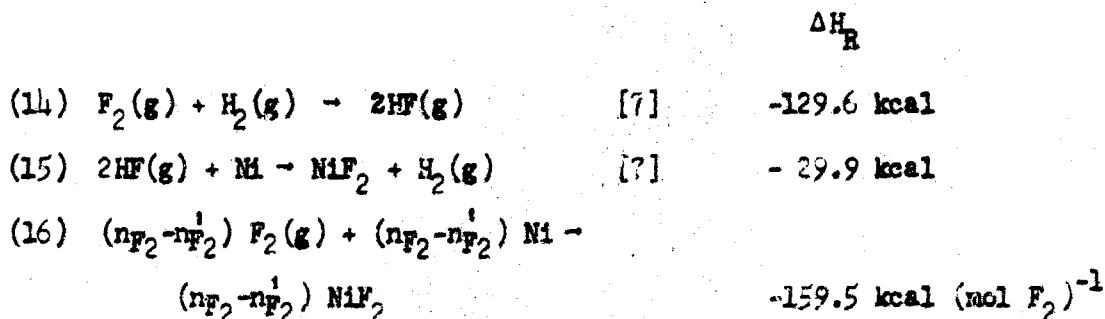
^A $\epsilon_{cal syst.} = \epsilon_{elect. calib.} + \Delta e$

in the content of the calorimeter; $q_{\text{cal syst.}}$, the energy equivalent for the calorimeter system for the F_2 experiment; and $q_{\text{obs.}}$, the observed heat effect. As explained earlier, the experiments are grouped into two series. To the best of our knowledge, the difference between them is the way in which the fuel line and reaction vessel were passivated.

Table 13 gives the corrections for impurities ($q_{O_2}, q_{CF_4}, q_{CO_2}$); ignition, q_{ign} ; vaporization ($q_{\text{vap}}, q'_{\text{vap}}$); and the correction for tempering the reacting gases, q_{temp} . The sum of these corrections is given in the last column. These corrections were applied to the observed heat of reaction ($q_{\text{obs.}}$, Table 12). The corrected heat of reaction, q_{F_2} , is given in Table 14.

3.2.6. Thermal Correction for Corrosion of Reaction Vessel

In making this correction, it was assumed that the unrecovered HF reacted with the reaction vessel. However, in order to arrive at the amount of fluorine actually reacting to give the aqueous solution of hydrogen fluoride with concentrations determined by the analyses, the amount of fluorine equivalent to the unrecovered hydrogen fluoride was subtracted from the theoretical amount of fluorine. Equations 14-16 show how the heat of corrosion was derived.



Using this heat of reaction and Δn_{HF} in Table 10, a correction for the corrosion, $q_{\text{corros.}}$, was calculated and is given in column c of Table 14. $n_{HF}^{F_2}(\text{theo.})$ is the number of moles of HF resulting from the reaction of fluorine in the sample, and n_{HF} is the observed amount of HF in the solution, less the HF arising from the reaction of CF_4 with H_2 to give $HF(\text{aq.})$.

Table 13

Corrections to Heat Data for the F_2-H_2 Reaction

Expt. No.	Series I							
	$-Q_{O_2}$ J	$-Q_{CF_4}$ J	$-Q_{CO_2}$ J	$-Q_{ign}$ J	$-Q'_{vap}$ J	$-Q''_{vap}$ J	$Q_{temp.}$ J	$-S_{Corr.}$ J
50	205.8	17.6	1.7	17.6	122.6	31.4	+15.5	381.2
51	159.8	14.1	1.7	30.0	100.3	24.3	+17.3	312.9
52	159.8	14.1	1.7	14.8	100.3	25.5	+13.8	302.4
53	74.0	6.7	.8	19.6	56.9	14.2	+ 1.5	170.7
54	165.7	14.1	1.7	23.2	90.8	22.4	+25.1	292.8
Series II								
49	177.0	14.1	1.7	22.4	120.9	26.3	+11.1	351.3
56	142.9	10.5	1.7	19.3	89.9	21.4	+15.5	270.2
57	154.4	14.1	1.7	23.8	95.8	21.5	+14.6	296.5
58	182.8	14.1	1.7	30.2	109.2	25.1	+19.2	343.9
59	200.0	17.6	- 1.7	24.1	104.0	30.7	+34.9	343.2

Table 14

Treatment of Heat Data

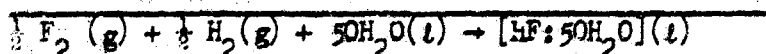
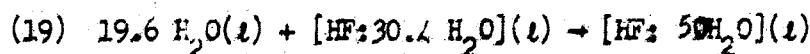
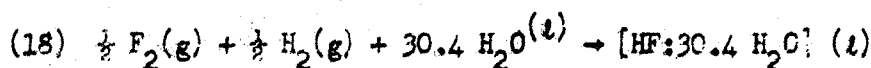
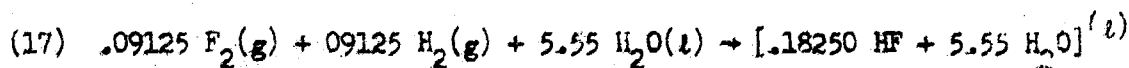


Expt. No.	q_{F_2}	$n_{HF}^{(2)}$ (theo.)	$n_{HF}^{(1)}$ (meas.)	$n_{H_2O}^{(1)}$ (meas.)	$\frac{n_{H_2O}^{(1)}}{n_{HF}^{(1)}}$	$-q_{corros.}$	$\frac{q_{F_2}}{n_{HF}^{(2)}} (theo.)$	$\frac{q_{F_2}}{n_{HF}^{(1)}} (meas.)$	$-q_{F_2} + q_{corros.}$
	J	mol	mol	mol		J	J(mol soln.) ⁻¹	J(mol soln.) ⁻¹	J(mol soln.) ⁻¹
							HF in H ₂ O	HF in H ₂ O	HF in H ₂ O
50	59042.5	0.18486	0.18250	30.4	764	n=50	319390	323520	319334
51	45750.7	.14310	.14251	38.9	197	n=50	319711	321035	319653
52	45069.3	.14102	.13949	39.8	510	n=50	319595	323100	319444
53	21944.6	.06854	.06698	32.9	520	n=50	320404	327928	320104
54	46041.1	.14568	.14516	38.2	173	n=50	320161	321308	320116
Mean									
Standard dev. of the mean									
319882 323396 171 76.45 Kcal mol ⁻¹ 77.29 Kcal mol ⁻¹ 76.42 Kcal mol ⁻¹									
±.04 ±.29 ±.04									
55	59809.0	0.15546	0.15486	35.8	200	n=50	320787	322030	320739
56	41151.3	.12320	.12533	44.3	958	n=50	320993	328343	320700
57	44353.5	.13810	.13580	40.9	767	n=50	321206	326040	320998
58	52048.4	.16222	.15922	34.8	1001	n=50	320851	326896	320609
59	56909.1	.17728	.17433	31.8	984	n=50	321351	326789	321144
Mean									
321072 326179 ±110 76.74 Kcal mol ⁻¹ 77.9 Kcal mol ⁻¹ 76.09									
Standard dev. of the mean									
±.03 ±.25 ±.03									

* $n_{HF}^{(1)}$ (meas.) = total $n_{HF}^{(1)}$ (meas.) - $n_{HF}^{(2)}$ (theo.)

b 1 cal = 4.184 J

Column 5 of Table 13 gives the ratio of the number of moles of HF to that of water in the solution. The heat data (q_{F_2}) were corrected so the data could be based on a solution of concentration, HF: 50 H₂O. An example with the data from experiment No. 50 illustrates how the dilution correction was applied.



The dilution energies were obtained from the literature [7].

3.2.7. Heat of Reaction of Fluorine with Hydrogen

The values measured for the heat of reaction (equation 19) are given in the last three columns of Table 14. $q_{F_2}^{HF}$ (theor.) is the heat of reaction of fluorine, not corrected for corrosion based on the theoretical amount of HF; $\frac{q_{F_2}^{HF}}{n'_{HF}}$ (meas.) is the heat of reaction of

fluorine not corrected for corrosion, based on the observed HF; and

$\frac{q_{F_2}^{HF} - q_{corros.}}{n'_{HF} \text{ (meas.)}}$ is the heat of reaction, based on $q_{F_2}^{HF}$, corrected for $q_{corros.}$, and n'_{HF} (meas.).

We have selected the data from the Series II as most reliable because, we feel that a better procedure, described earlier, was used for conditioning the reaction vessel. However, it is not known whether or not the difference in the conditioning procedures used for the two series of experiments accounts for the differences between the derived heat-of-formation values. Because the uncertainty in the analyses for hydrogen fluoride is considerably less than the hydrogen fluoride unrecovered, one can justifiably apply a correction for the corrosion of the reaction vessel. Mainly on this basis the data in the final column of Table 14 are selected as the most reliable. The average value

for the heat of formation of $[\text{HF}:\text{5OH}_2\text{O}]$ at 30 °C is $-76.69 \pm .03 \text{ Kcal mol}^{-1}$. The $\pm .03$ (.04%) value is the standard deviation of the mean. We believe that the uncertainties in this value arise from the uncertainties in the electrical calibrations (.006%), the uncertainty in the analyses for hydrogen fluoride (.05%), and the uncertainties in the analysis of the fluorine (.03%). The square root of the sum of the squares of the percentage uncertainties is .07%. The heat of formation of $[\text{HF}:\text{5OH}_2\text{O}]$ then becomes $-76.69 \pm .05 \text{ Kcal mol}^{-1}$ at 30 °C. Because of the reactivity of fluorine, and our inability to achieve a mass balance in the reactions, possibly there are several uncalculable sources of error in these experiments. However, our ability to obtain rather precise results does reflect a certain amount of control over the procedures and the method for treating the data. These are some reasons for believing that the value derived may be fairly reliable. Heat-capacity data for F_2 [7], H_2 [7], H_2O [7], and $[\text{HF}:\text{5OH}_2\text{O}]$ [25] were used to calculate ΔH_f° $[\text{HF}:\text{5OH}_2\text{O}]$ at 298.15 °K. ΔH_f° $[\text{HF}:\text{5OH}_2\text{O}]$ equals $-76.68 \pm .05 \text{ Kcal mol}^{-1}$.

3.3. The Oxygen-Hydrogen Reaction

3.3.1. Analysis of the Oxygen

The oxygen was obtained from the Southern Oxygen Company and was reported to be of high purity quality (>99.99 percent pure). Attempts to analyze for the impurities did confirm that the amounts of impurities were too small to be accurately analyzed for by the usual methods. The oxygen was analyzed by mass spectrometry and found to contain 29 ± 10 parts per million argon. The nitrogen was analyzed for according to the chromatographic method of Kyriacos and Boord [31]; Molecular Sieves, 5A, was used for column material. Prior to the analysis, the column was activated at 350° under a flowing helium atmosphere. Other conditions are given on the chromatogram in Figure 18.

For analysis, the oxygen was used from a spherical metal bulb, as shown in Figure 8. The bulb was filled with the manifold previously set-up for filling an oxygen combustion bomb. A vacuum source was provided for evacuating the bulb prior to filling them with oxygen. Although further purification was unnecessary, the gas was passed through a CuO column, heated to 500 °C, and through successive columns of Ascarite and magnesium perchlorate. After evacuating and purging with oxygen, the bulbs were filled to 170-200 p.s.i.g. for the chromatographic and calorimetric experiments. The sample was introduced into the column with a commercially obtained gas sampling valve, which was modified with a loop for a 10-cc sample. Initially one-cc

samples of air were introduced to check the performance of the method. The results shown in Fig. 18 were obtained using a 10 cc sample of oxygen. The slurred peak attributed to nitrogen was quite reproducible. However, attempts to evaluate its area, relative to that of the larger oxygen peak led to rather uncertain results.

On the basis of the analyses, it was estimated that the oxygen sample contained: Oxygen 99.987; nitrogen, .009; and argon .004 weight percent.

Hydrogen. The source and analyses of the hydrogen used have been described for the $\text{OF}_2 - \text{H}_2$ experiments. For most of the $\text{O}_2 - \text{H}_2$ reactions, the hydrogen was used without further purification.

3.3.2. Calorimetric Experiments

This was the only one of the three reactions carried out in which there was the option of using either reactant as fuel, since neither the oxygen nor the hydrogen in excess would react with the water in the solution chamber. The reaction was conducted with hydrogen in excess (oxygen, fuel) because of the higher purity of the oxygen, and also because the oxygen reacted could be weighed with a smaller percentage error in the weighing than the hydrogen. During the reaction, the oxygen was introduced into the burner at a rate of approximately 130 cc per minute. Though it was not needed for forming an HF solution, water was added to the reaction vessel for the first six experiments. The reason for adding the water was to more nearly simulate the condition, used in the electrical calibrations. For the later three experiments, no water was placed in the solution chamber, and the product water was collected to check the mass-balance between the oxygen reacted and the water formed. In these experiments the bubblers preceding the calorimeter were replaced by absorbers containing successive layers of Ascorite and magnesium perchlorate. This absorber removed H_2O from H_2 which otherwise would have interfered with the analysis for the water formed in the reaction. To collect the product water, two magnesium perchlorate absorbers were used; (1) to collect the water flushed out by the effluent gas during the reaction period, and (2) to collect the water from the burner removed by flushing overnight with helium.

The absorbers were corrected for buoyancy by weighing against tares, and were corrected for the displacement of helium upon formation of the hydrate of magnesium perchlorate with the data suggested by Rossini [34].

The reaction quantities of oxygen for all the experiments are given in Table 15. The data given are the experiment number; m_s , the mass of the sample; m_{O_2} , the mass of oxygen; n_{O_2} , the number of moles of oxygen; $m_{\text{H}_2\text{O}}$ (theo.), the mass of water expected; $m_{\text{H}_2\text{O}}$, the measured quantity

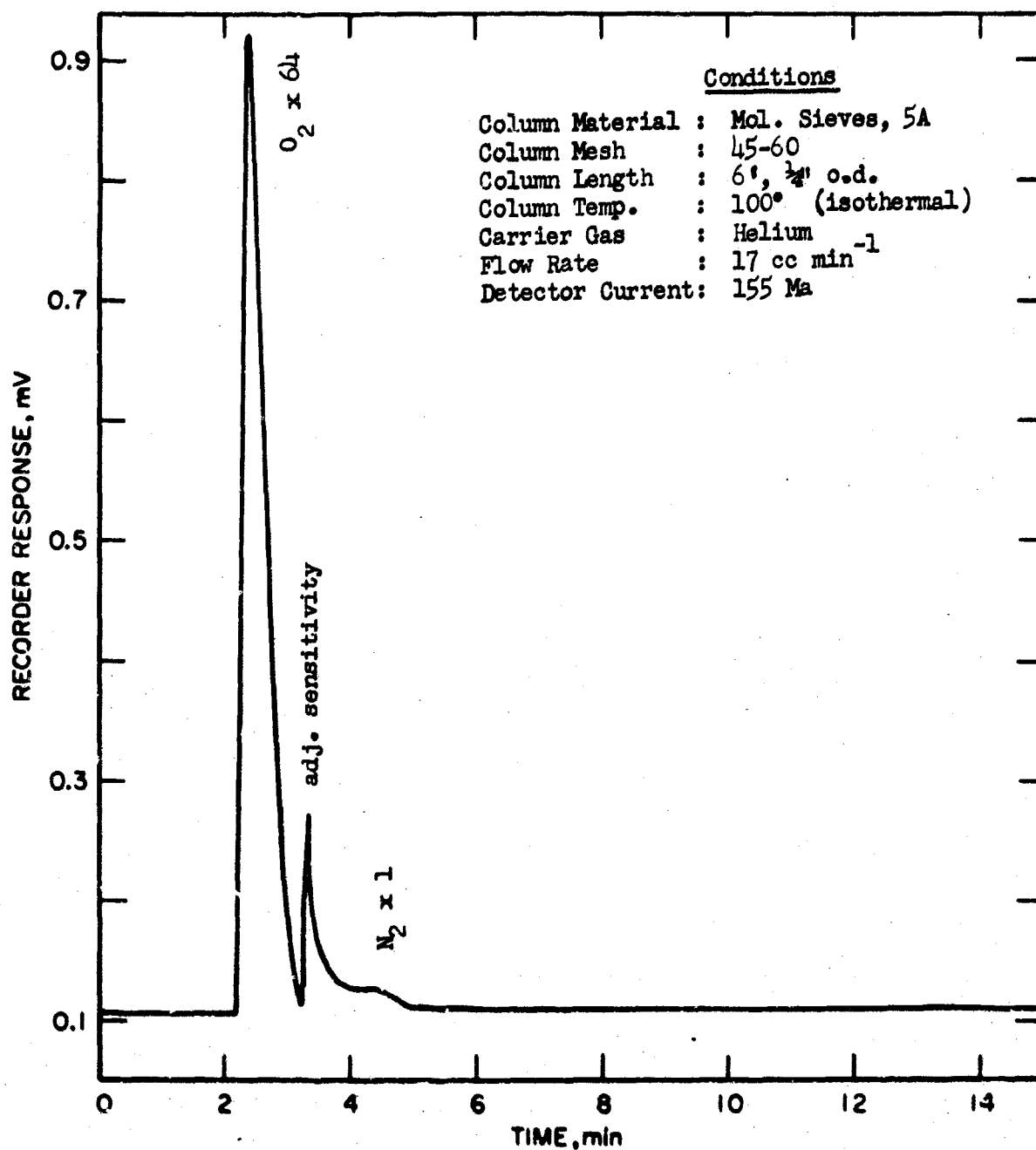


Figure 18 -- Chromatogram of Oxygen on Molecular Sieves, 5A

Table 15
Reaction Quantities in Oxygen-Hydrogen Reactions

Expt. No.	m_s	m_{O_2}	n_{O_2}	m_{H_2O} (theo.)	m_{H_2O} (meas.)	$\frac{m_{H_2O} \text{ (meas.)}}{m_{H_2O} \text{ (theo.)}}$
	g	g	moll	g	g	
35	3.3032	3.3028	.10322	3.7191	a	
36	3.3850	3.3846	.10577	3.8110	a	
37	3.4945	3.4941	.10919	3.9342	a	
40	3.2208	3.2204	.10064	3.6261	a	
41	3.2248	3.2244	.10077	3.6308	a	
42	3.2376	3.2372	.10117	3.6452	a	
44	3.2312	3.2333	.10106	3.6413	3.5417	.10001
45	3.2315	3.2321	.10101	3.6394	b	
46	3.1527	3.1523	.09851	3.5494	3.5517	.10006

a Mass of water not determined because water was present in excess in the reaction vessel.

b Experiment was carried to completion, but attempt to determine m_{H_2O} was unsuccessful.

of water in the latter three experiments; and m_{H_2O} (meas.)/ m_{H_2O} (theo.), ratio of the measured to the expected amounts of water. The analyses for water were completed successfully for two of the experiments, numbers 44 and 46. The ratio, m_{H_2O} (meas.)/ m_{H_2O} (theo.) demonstrates that a reasonably close mass-balance was achieved in the experiments.

3.3.3. Heat Measurements for the $O_2 - H_2$ Reaction

The data for the heat measurements are given in Table 16. The left-hand part of the table shows the experiment numbers; t_{av} , the average temperature of the calorimeter; $R_{corr.}$, the corrected resistance change; dR/dt , the factor for converting resistance change to temperature change, and, $\Delta t_{corr.}$, the corrected temperature rise of the calorimeter. $1/2m_{H_2O}$ is one-half the amount of water formed in the reaction, i.e. the water formed at the average temperature. In the experiments in which the water formed was measured, no water was placed in the solution vessel. This is noted in column 7. Columns 8 and 9 show the correction to the energy equivalent for $1/2m_{H_2O}$ and for the absence of H_2O in the solution chamber for the last three experiments. $C_{cal. syst.}$ is the energy equivalent of the calorimeter system for the oxygen-hydrogen experiments. The observed heat of reaction, ($C_{cal. syst.} \times \Delta t_{corr.}$), is given as $q_{obs.}$.

Table 17 lists the corrections to be applied to the observed heats of reaction for the oxygen-hydrogen system. Given are the experiment number; $q_{obs.}$, the total observed heat; $q_{ign.}$, the ignition energy; $q_{temp.}$, the energy used for preheating the gases, and q'_{vap} and q''_{vap} , the vaporization energies. All of these corrections were derived in the same way and have the same meaning as for the fluorine-hydrogen and oxygen difluoride-hydrogen reactions. q_1^{vap} and q_2^{vap} for experiments numbers 44-46 are respectively, the heat of vaporization (q_1^{vap}) for the water removed from the reaction vessel by the effluent hydrogen during the reaction; and the heat (q_2^{vap}) content of the water vapor in the reaction vessel after the reaction. No corrections were applied for the reaction of impurities. The corrections were applied to the observed heat of reaction, $q_{obs.}$ to give q_{O_2} , the heat of reaction of the oxygen. The number of moles of water, n_{H_2O} formed (Table 17) is based on the number of moles of oxygen reacted. q_{O_2}/n_{H_2O} is the heat of reaction per mole of water at the average temperature of the calorimeter (300.4°K).

Table 16

Heat Measurements ($O_2 H_2$)

Expt. No.	t_{av}	$\Delta R_{corr.}$	$\frac{dR}{dt}$	$\Delta t_{corr.}$	\bar{m}_{H_2O}	Mass of H_2O in Solution Chambers	Ae_1	Ae_2	$e_{cal. syst.}$	q_{cts}
	$^{\circ}C$	ohm	ohms($^{\circ}C$) $^{-1}$	$^{\circ}C$	g	g	J($^{\circ}C$) $^{-1}$	J($^{\circ}C$) $^{-1}$	J($^{\circ}C$) $^{-1}$	J
35	30.36	.272129	0.1005763	2.70570	1.8591	120	7.77	0	21895.7	59243.3
36	30.38	.278901	.1005759	2.77504	1.8015	120	7.53	0	21895.4	60716.8
37	30.43	.288136	.1005744	2.86490	1.9671	120	8.22	0	21896.1	62730.1
40	30.31	.265577	.1005777	2.64052	1.8130	120	7.57	0	21895.5	57815.5
41	30.32	.266234	.1005778	2.64704	1.8258	120	7.58	0	21895.5	57958.2
42	30.32	.266444	.1005777	2.64914	1.8331	120	7.61	0	21895.5	58004.2
44 ^a	30.34	.268911	.1005769	2.67368	1.8208	0	7.61	-492.9	21402.6	57223.7
45 ^a	30.34	.269427	.1005769	2.67882	1.8196	0	7.60	-491.4	21404.1	57337.7
46 ^a	30.47	.262979	.1005730	2.61481	1.7747	0	7.41	-491.4	21403.9	55967.1

^a No H_2O in solution vessel, because product H_2O was measured.

^b Energy Equivalent of standard Calorimeter: 21887.9 ± 1.4 J/ $^{\circ}C$ (1.4 = s.d.m.)

Table 17

Corrections to Heat Data for the O_2-H_2 Reaction

Expt. No.	$Q_{\text{pts.}}$	Ignition Energy q_{ign}	$q_{\text{temp.}}$	$q' \text{ vap.}$	$q' \text{ vap.}$	Q_{O_2}	n_{H_2O}	Heat of Reaction at $t_{\text{av.}}$ $Q_{O_2}^{\text{H}_2O}$	Temp. Corr. to 25°C	Heat of Formation of H_2O at 25°C
	J	J	J	J	J	J	mol	$KJ \text{ mol}^{-1}$	$KJ \text{ mol}^{-1}$	$KJ \text{ mol}^{-1}$
34	59243.3	-23.2	37.5	-36.3	-271.5	58949.8	.20644	285.554	.177	285.725
35	60716.8	-16.0	40.3	-39.6	-278.1	60423.4	.21154	285.636	.171	285.807
36	62730.1	-11.5	25.1	-29.1	-371.1	62343.5	.21898	285.482	.167	285.649
40	57815.5	-19.6	42.0	-26.2	-256.6	57555.1	.20128	285.945	.167	286.112
41	57358.2	-22.4	28.0	-26.1	-279.5	57658.2	.20154	286.088	.167	286.255
42	58004.2	18.2	38.9	-26.1	-265.3	57733.5	.20234	285.339	.167	285.506
							Mean			285.842
							Standard dev.	dev. of the mean		.117
							Mean			68.32 Kcal mol ⁻¹
							Standard dev.	dev. of the mean		.027 " " "
44	57223.7	-16.4	18.4	336.9	33.0	57626.5	.20212	285.110	.167	285.277
45	57337.7	-10.5	45.4	227.6	33.8	57635.0	.20202	285.293	.167	.469
46	57337.7	-17.1	38.5	181.6	33.8	56203.9	.19702	285.270	.176	.446
							Mean			285.397 $KJ \text{ mol}^{-1}$
										-68.21 Kcal mol ⁻¹

The heat capacities of oxygen [7], hydrogen [7], and water [7] were used (columns 10,11) correct the measured heat of reaction to the heat of reaction at 298.15 K.

3.3.4. The Heat of Formation of Water

When conducting the experiments in the same way as used for the calibrations, with water in the solution chamber, a value of $68.32 \pm .03$ Kcal mol⁻¹ is obtained for the heat of formation of water. Without water in the solution chamber, a considerable change in the contents of the calorimeter compared to those for the calibrations, a value of 68.21 is obtained for the heat of formation of water at 298.15 °K. The absence of the water in the solution chambers for the latter experiments may explain the difference between these two values. A comparison between the two burners in Figures 1 and 2 shows that the cooling helix in the earlier burner design is considerably larger than that in the new design. This suggests that without water in the solution chambers in the new burner, some of the heat of the reaction may possibly be lost by insufficient cooling of the effluent gases in the calorimeter. This may explain why the heat of formation value derived from the last three experiments is lower than that from the other experiments. Therefore, $-68.32 \pm .03$ is the preferred value for the heat of formation of water which can be derived from these experiments.

The uncertainty in this figure is presumed to be mainly due to uncertainties as indicated by the standard deviation of the mean of the combustion experiments (.044%), the uncertainty in the analysis of the oxygen sample (.01%), and the uncertainty in the calibration of the calorimeter (.006%). The square root of the sum of the squares of these uncertainties is .046% (.03 Kcal mol⁻¹). Then, the heat of formation of water at 298.15 °K is -68.32 Kcal mol⁻¹ with an overall uncertainty of .03 Kcal mol⁻¹.

4.0 The Heat of Formation of Oxygen Difluoride

The heat of formation of oxygen difluoride is derived by the appropriate combination of the heats of the reactions shown in equations 20-23.

	$\Delta H_{f, 298.15^\circ}$ kcal
(20) $OF_2(g) + 2H_2(g) + 99 H_2O(l) \rightarrow 2[HF \cdot 50H_2O](l)$	-227.54 ±.16
(21 a) $F_2(g) + H_2(g) + 99 H_2O(l) \rightarrow 2[HF \cdot 49.5H_2O](l)$	-153.36 ±.06
(21 b) $H_2O(l) + 2[HF \cdot 49.5H_2O](l) \rightarrow 2[HF \cdot 50H_2O](l)$	
(22) $\frac{1}{2}O_2(g) + H_2(g) \rightarrow H_2O(l)$	-68.32 ±.03
<hr/>	
(23) $F_2(g) + \frac{1}{2} O_2(g) \rightarrow OF_2(g)$	+ 5.86 kcal ±.17 mol ⁻¹

The value derived for $\Delta H_{f, 298.15}(OF_2)$ is $+5.86 \pm .17$ kcal mol⁻¹. The stated uncertainty is a combination (square root of the sum of the squares) of the uncertainties in the heats of the reactions. Because of the factors considered in calculating the uncertainties in the heats of reaction, it is possible that the uncertainty estimate for the heat of formation value does not actually represent the accuracy of the derived value. However, it may be recalled that the main reason for measuring the heats of the auxiliary reactions was to make the derived heat of formation of OF_2 less sensitive to systematic errors which probably exist in the measurements for all three reactions. We shall neither attempt to assess the magnitude of the systematic errors nor to estimate the extent to which they cancel in the heat-of-formation calculation. However, we think that a brief discussion of what we think the principal systematic errors are is in order.

Our inability to achieve the same degree of mass balance in the OF_2-H_2 and F_2-H_2 reactions presents a systematic uncertainty in the amount of success achieved in conducting these two reactions. The recovery of the HF formed was better (99.45%) for the OF_2-H_2 reactions than for the F_2-H_2 reactions (98.44). In the calculations for both reactions, it was assumed that the unrecovered hydrogen fluoride was used in corroding the reaction vessel. A correction was applied for the

heat of corrosion. Referring back to Tables 6 (cols. 9 and 10) and 11 (cols. 10 and 12), the heats of reactions corrected for corrosion based on the measured amounts of HF are much more precise than the uncorrected heats of reaction based on HF measured. However, it is not known whether or not this improvement in precision cancels any errors in the calculations of the heat of formation value, which may arise from our inability to achieve a mass balance.

Another source of systematic error is the placement of the calibration heater in the calorimeter relative to the combustion chamber where the chemical energy is liberated. From the description of the positioning of the electrical calibration heater, one can see that the heater is closer to the side of the calorimeter (nearer the thermometer), whereas the combustion chamber is near the center of the calorimeter. If the calibration of the calorimeter varies with the positioning of the heater, then a systematic error exists in the measured heats of reactions (eqs 20-22), which would be proportional to the difference between the calibrations for the heater positioned in center of calorimeter, and for the heater positioned closer to the side of calorimeter. It seems very likely that in calculating the heat of formation of OF_2 , this particular systematic error would cancel. Although the heat of reaction of oxygen with hydrogen was not measured for the purpose of calibrating the calorimeter, the agreement between the value obtained ($-68.32 \text{ kcal}(\text{mol H}_2\text{O})^{-1}$) in this study and the value ($-68.32 \text{ kcal}(\text{mol H}_2\text{O})^{-1}$) by Rossini [23,7] suggests that the calibration used (Table 1) is reliable.

This discussion of the sources of errors does not give basis for an exact evaluation of the uncertainty in the derived heat of formation of OF_2 . But on the basis of the procedures used and results obtained, it is estimated that the overall uncertainty in the value is not greater than $\pm 0.30 \text{ kcal mol}^{-1}$.

5. The Work of Previous Investigators

5.1. On the Heat of Formation of $\text{OF}_2(\text{g})$

As pointed out in the introduction, several reviewers have already examined earlier experimental work on oxygen difluoride with the hope of deriving a reliable "best" value for the heat of formation of this compound. Therefore, the purpose of this discussion is not to critically examine the reported data but to re-examine the experimental approach, in view of the experience gained in the present study, with more emphasis on the methods of handling the sample, the materials used for apparatus construction, and the analytical methods used. Today these techniques for reactive fluorine compounds are better developed.

A review of their application in the earlier studies may show why the reported values for the heat of formation of this compound vary from +7.6 to -5.2 kcal mol⁻¹.

The reactions studied by von Wartenberg and Klinkott [1] are given in equations 24-26. Shown also are the reported heats of reaction at 191°K and the recalculated $\Delta H_{298.15}^{\circ}(\text{OF}_2)$ [5] based on current data for the auxiliary reactions.

	ΔH_f° kcal mol ⁻¹
(24) $\text{F}_2\text{O}(\text{g}) + 2\text{KOH} (\text{in excess KOH aq. 40\%})$ $= [2\text{KF} + \text{H}_2\text{O}](\text{in aq. KOH}) + \text{O}_2(\text{g})$ $\Delta H_{291}^{\circ} = -125.75 \text{ kcal mol}^{-1} \quad \sigma = 0.75 \text{ kcal mol}^{-1} \quad +6.9$	
(25) $\text{F}_2\text{O}(\text{g}) + [6\text{KI} + 2\text{HF}](\text{in excess aq. sol'n})$ $= [4\text{KF} + 2\text{KI}_3 + \text{H}_2\text{O}](\text{in aq. KI HF sol'n})$ $\Delta H_{291}^{\circ} = -176.55 \text{ kcal mol}^{-1} \quad \sigma = 0.82 \text{ kcal mol}^{-1} \quad +1.4$	
(26) $\text{F}_2\text{O}(\text{g}) + 4\text{HBr} (\text{in excess HBr aq. 45\%})$ $= [2\text{HF} + 4\text{Br}_2] (\text{in aq. HBr})$ $\Delta H_{291}^{\circ} = -134.36 \text{ kcal mol}^{-1} \quad \sigma = 0.51 \text{ kcal mol}^{-1} \quad +8.8$	
	Av. +5.7

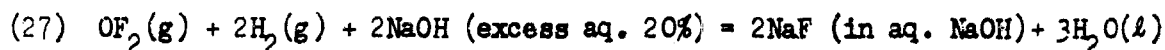
Von Wartenberg investigated the reactivity of OF_2 with several substances and on the basis of the reaction rates, products formed, and heats of reaction, decided that the above three were best for the thermochemical investigation. They prepared the OF_2 used by reaction of fluorine (prepared in their laboratory by electrolysis of $\text{KF} \cdot 3\text{HF}$) with dilute sodium hydroxide. Their analysis of the OF_2 was based on the reaction: $\text{F}_2\text{O} + 4\text{HI} = 4\text{I} + 2\text{HF} + \text{H}_2\text{O}$. Their experimental arrangement for the thermochemical study of the above reactions was the same in each case. A glass spiral (8 turn, 1.5 cm thick tubing) containing the solution for the reaction under study was placed in a 1-liter dewar flask filled with water. OF_2 , in a carrier gas (nitrogen), was bubbled into solution through a narrow opening. The temperature increase of the calorimeter was measured with a calibrated Beckman thermometer and the calorimeter was calibrated with electrical energy.

According to the authors' appraisal of the experiments on the three reactions, the first reaction proved to be less troublesome. Consequently, one could assume that the data for this reaction are more reliable. Little information is given on the purity of the oxygen difluoride sample. From the discussion, it can be assumed that the major impurity is oxygen. It is to be noted that the method of analysis used by these authors does not yield the amount of oxygen present.

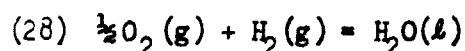
Considering the magnitude of the heats of reactions, it seems possible for one to be able to derive a reliable value for the heat of formation of OF_2 from each one of these reactions. This is assuming that a good analysis is obtained for either the products or reactants and also confirmation is made that well defined products, as indicated by the equations, are obtained. Though the calorimetric measurements may be reliable, lack of detail on the analyses of the OF_2 sample, and of the extent of reactions, makes it difficult to fairly appraise the accuracy of the values derived for $\Delta H_{298.15}(\text{OF}_2)$.

The study of the heat of formation of oxygen difluoride by Ruff and Menzel [2] was designed so that the derived $\Delta H_{298.15}$ of OF_2 would be insensitive to the possible systematic errors. To accomplish this the heats of reaction of O_2 and F_2 were measured in the reaction vessel, using the same procedures as used for the reaction of OF_2 with hydrogen.

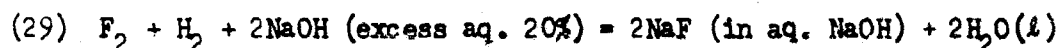
Measurements of Ruff and Menzel [2].



$$\Delta H = -254.9 \text{ kcal mol}^{-1} \quad \sigma = 0.6 \text{ kcal mol}^{-1}$$



$$\Delta H = -68.5 \text{ kcal mol}^{-1} \quad \sigma = 0.1 \text{ kcal mol}^{-1}$$



$$\Delta H = -181.7 \text{ kcal mol}^{-1} \quad \sigma = 1.15 \text{ kcal mol}^{-1}$$

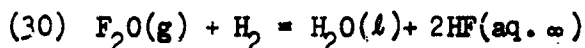
$$\Delta H_{298.15}(\text{OF}_2) = +4.7 \text{ kcal mol}^{-1}$$

These authors prepared OF_2 by reaction of F_2 with dilute aqueous NaOH and through fractional distillation purified the OF_2 to a purity of 98.5 percent. For the OF_2 sample the authors determined the density and analyzed it by gravimetric determination of fluorine and oxidation of acid solution of potassium iodide. The gravimetric determination consisted of first reacting the OF_2 with hot 10% sodium hydroxide, and then precipitating the F^- from an alkaline solution as CaF_2 . From this analysis the gas was 70.12% F_2 compared to theoretical amount of 70.12% F_2 .

For the calorimetric experiments, the reaction vessel was copper with a platinum liner. In an atmosphere of hydrogen, the fuel (OF_2) mixed with nitrogen, ignited by means of a high-voltage spark. The reaction vessel contained a sodium hydroxide solution for reaction with the product hydrogen fluoride. The solution was agitated by a hydrogen flow which also pumped the NaOH to the top of vessel to effect complete solution of the HF. The effluent gases (N_2 , xs hydrogen) were passed through successive columns of concentrated NaOH solution to remove any residual HF brought from reaction vessel, and CaCl_2 and P_2O_5 , to remove water vapor. The O_2 and F_2 experiments were conducted in the same way, mixing the minor reactant with nitrogen, and reacting in a flame with hydrogen.

It is noted that solution of the HF in the sodium hydroxide in the calorimeter increases the magnitude of the over-all heat of reaction for the F_2 and OF_2 experiments. However, this criticism is offset by the fact that such quick trapping of the HF relieves one of the need for correcting for corrosion by HF. One unexplored side reaction in the experiments is the possibility of the reaction of the nitrogen with hydrogen to form ammonia. Tests for ammonium hydroxide and other possible products of reactions would have provided a more thorough characterization of the processes which took place.

The most recent of the previous studies of the $\Delta H_{298.15}^\circ$ (OF_2) is that by Bisbee et al. [3]. By means of bomb calorimetry, they studied the heat of reaction of oxygen difluoride and hydrogen to give an aqueous solution of HF. A heat-of-dilution correction is applied to give the heat of the following reaction:



$$\Delta H_{298}^\circ = -222.93 \text{ kcal mol}^{-1} \pm 0.76 \text{ kcal mol}^{-1}$$

$$\Delta H_{298}^\circ[\text{F}_2\text{O}(\text{g})] = -4.4 \text{ kcal mol}^{-1}.$$

Conceivably, reliable results can be obtained from a bomb calorimetric study of the system. However, omission of details on the (1) analysis of the sample, (2) the technique used to insure mixing of the solution, (3) the corrosion by the product HF, and (4) the quantitative basis for the heat of reaction makes it difficult to evaluate the procedures used in this experimental study, and try to reflect on how these factors may have affected the derived heat-of-formation value. On the basis of the description in the report, it is likely that the OF_2 sample used was not thoroughly analyzed. Oxygen is a usual impurity in the OF_2 produced by the present day method ($\text{F}_2 + \text{NaOH}$) and would certainly react with H_2 under the conditions of these experiments. Therefore, a knowledge of its content in the sample is important for correcting for its heat of reaction with hydrogen. This reflects also a disadvantage of the iodimetric method for analysis of the OF_2 sample.

The measurements were made in a stationary bomb, using a fairly massive internal container for $F_2O(g)$ which was ruptured to initiate reactions with H_2 . The reaction products consisted of H_2O and HF in a condensed phase, formed in the presence of excess $H_2O(l)$. The formation of a homogeneous $HF(aq)$ phase was presumed. However, experience in reactions in which condensation occurs in a stationary bomb indicates that much of the condensation would occur on the walls and would form droplets of a solution quite different from the bulk solution. Mixing these two solutions would evolve heat in addition to that which was measured. The massive F_2O ampoule could also retain significant quantities of heat for an appreciable time and the complete equilibration of the heat distribution was not described. Both of these processes would appear to act in the same direction, causing the measured amount of heat to be less than could have been evolved if equilibrium had been achieved. If any error of these types exists in these experiments, a less negative heat of formation would be indicated for F_2O than was reported.

It was reported that there was some corrosion of the bomb parts by the product HF ; a correction for the heat of corrosion was applied to the data. However, the weight of OF_2 sample used in each experiment is not included among the results. The recovery of HF is reported to be 95%. Therefore, one does not know how the number of moles of OF_2 on which the heat effect is based was derived.

It seems most probable that the OF_2 reacted to completion in the reaction. However, tests on the bomb gases after the reaction would have provided useful documentary data for the study.

Summary of Values for Heat of Formation of OF_2

<u>Study</u>	<u>Year</u>	$\Delta H_{F298.15}$ kcal mol ⁻¹
Ruff and Menzel [2]	1930	+4.7
Wartenberg and Klinkott [1]	1930	+5.7
Bisbee et al. [3]	1965	-4.4
Present study	1967	+5.86

5.2 The Fluorine-Hydrogen Reaction

Since the application of fluorine as an oxidizer in calorimetry, it has become necessary to know accurately the heat of formation of hydrogen fluoride, both in the gaseous and aqueous phases. The reason for the importance of the heat of formation of hydrogen fluoride to the thermochemistry of other compounds, is that reactions of all compounds containing hydrogen with fluorine lead to hydrogen fluoride as a product. Therefore, the accuracy of the heat of formation of a H-containing compound being investigated by either fluorine bomb or fluorine flame calorimetry depends directly on the accuracy of the heat of formation of hydrogen fluoride. This is analagous to the importance of the heat of formation of water in thermochemical studies of reactions involving oxygen and hydrogen. However, a careful study [21] of the heat of formation of water has been conducted so that this value is known accurately.

Several problems have deterred such a study of the heat of formation of hydrogen fluoride. The most prominent of these problems is the polymerization of hydrogen fluoride at ordinary temperatures. A thermochemical study of the fluorine-hydrogen reaction at ordinary temperatures (25-30°C) would lead to the heat of formation of HF in the polymerized state. The equation of state data presently available are not accurate enough to apply a correction to the thermochemical data to yield an accurate value for the heat of formation of monomeric HF. The polymerization of HF decreases rapidly with increasing temperature. However, the corrosive nature of elemental fluorine and hydrogen fluoride increases tremendously with temperature. With the availability of corrosion-resistant materials, a reliable study of this system at high temperatures (~100°C) now seems possible.

The hydrogen-fluorine system is currently the subject of much discussion among investigators who believe that improved thermochemical data for this system would place calorimetry involving fluorine and hydrogen-containing compounds on a much sounder basis. However, such discussion has not been paralleled with experimental work. The earlier study by von Wartenberg and Schütza [35] on the gaseous HF is the most prominent work in which a direct determination of the heat of formation of gaseous HF was attempted. Much later attention was called to the point that the work of von Wartenberg and Schütza in agreement with other work [9] indicated that the heat of formation of gaseous HF should have been more negative than the "best" value selected (-64.2 kcal mol⁻¹) at that time [36]. Shortly thereafter Feder et al. [37] combined the heats of several reactions determined accurately by fluorine bomb calorimetry, and obtained $\Delta H_{298}^0(\text{HF}) = -64.92 \pm .12 \text{ kcal mol}^{-1}$. Today the reported best value for ΔH_{298} is -64.88 kcal mol⁻¹ [7].

Cox and Harrop [38] have recently reported values for $\Delta H_f[\text{HF, aq.}]$ at 298.15°K. The data were derived by Hess' law from measurements of enthalpies of solution of lithium fluoride and lithium hydrogen fluoride, the enthalpy of mixing lithium fluoride solution with hydrofluoric acid, and the enthalpy of dissociation of lithium hydrogen fluoride. These authors combined the heat-of-formation data for gaseous hydrogen fluoride derived by Feder, et al., to obtain the heats of formation for several hydrofluoric acid solutions. Only the value reported for $\Delta H_f^{298.15}(\text{HF} \cdot 50\text{H}_2\text{O})$ will be considered in this discussion. Their value for $\Delta H_f(\text{HF} \cdot 50\text{H}_2\text{O})$ is $-77.422 \text{ kcal mol}^{-1}$. The heat of formation for the same solution, selected by Wagman et al. [7] is $-76.316 \text{ kcal mol}^{-1}$. The value obtained directly in this study, $-76.68 \pm .05 \text{ kcal mol}^{-1}$ lies between the earlier values.

Sinke [39] and Armstrong and Domalski [40,41] have recently derived heats of formation data for aqueous solutions of hydrogen fluoride. Similarly, their values lie between those reported by Cox and Harrop [38] and Wagman, et al [7].

At the present time it appears that additional work is required before the heat of formation of hydrogen fluoride and its aqueous solutions will be accurately known. It is believed that this work must be of two kinds: (1) a review of already existing thermochemical data involving HF; and (2) experimental work designed especially for accurately deriving the heat of formation of HF. In contrast to Cox and Harrop's view we believe that the direct determinations of the heat-of-formation values from F_2 , H_2 , and H_2O should be pursued, in addition to the studies which seek to derive the data using Hess' law. We acknowledge that there are many experimental difficulties in the direct approach, but observations in the present study suggest that reaction vessels can be constructed, and procedures can be developed for a very careful study of the $\text{F}_2\text{-H}_2$ system. However, because of the nature of fluorine and hydrogen, there is a need for conducting direct studies in several laboratories in order to accurately establish the heat of formation of hydrogen fluoride and its aqueous solutions

5.3. The Heat of Formation of $\text{H}_2\text{O}(l)$

The study by Rossini [23] was a carefully done investigation of the heat of formation of water. The study also discusses in detail the earlier similar work carried out for the purpose of deriving the heat of formation. Since Rossini's work, Skinner and Pilcher [42] have used the reaction for calibration of their flame calorimeter. As pointed out in the introduction, the main purpose of the present investigation of this reaction is to provide in the same apparatus the data needed for calculating the heat of formation of oxygen difluoride. The value obtained here ($-68.32 \pm .03 \text{ kcal mol}^{-1}$) compares closely with the accepted value ($-68.32 \text{ kcal mol}^{-1}$) at 298.15 [7] which is based on Rossini's study.

6.0 Appendix

6.1. Vaporization of Water from the Reaction Vessel

The removal of water from the solution chamber does present a problem in using this design of burner-solution reaction vessel. The heat of vaporization of the water is superimposed on the usual drift rate of the calorimeter temperature due to stirring and the temperature difference between the surrounding constant-temperature enclosure. If this heat of vaporization is constant throughout the experiment, it should not affect the true corrected temperature rise of the calorimeter. Realizing this possibility, it was still desirable to eliminate this heat of vaporization as nearly as possible. To achieve this, the hydrogen entering the calorimeter was saturated with water vapor, for which the heat of condensation would compensate for the heat of vaporization of the water vapor removed by the effluent hydrogen.

The amounts of water vapor carried in and removed from the solution vessel were measured by weighing the water bubbler and absorber (magnesium perchlorate) before and after the experiment. The results from these determinations are given in Table 18. m_{H_2O} is the weight of water vapor removed from the solution vessel by the effluent gas and $m_{H_2O}^i$ is the weight of water vapor carried into the vessel by the entering hydrogen. $m_{H_2O}^i - m_{H_2O}$ is the difference between these quantities, where the minus indicates an over-all removal of the H_2O from the solution chamber, and the plus an over-all condensation of H_2O in the reaction vessel. The objective was to make this difference as close to zero as possible.

Several factors in the experiment influence $m_{H_2O}^i$ and m_{H_2O} . (1) $m_{H_2O}^i$ is influenced mainly by the temperature of the room which, as can be seen from the table, underwent considerable variation from day to day, (2) by the fact that the helium flow in the fuel line was not saturated with H_2O before the calorimeter. This resulted in a net removal of water from the solution vessel by the helium. This is observed in the calibrations in which there is a consistent net removal of water from the calorimeter, in spite of the fact that there is no interruption of the hydrogen flow at all during these calibrations. The average calorimeter temperature is higher than the room temperature. This would also cause more water vapor to be removed from the vessel than is brought in. However, it is believed that the principal removal of H_2O from the solution vessel is due to the helium flow in the fuel line.

The values for $m_{H_2O}^i - m_{H_2O}$ vary considerably but are consistent for the O_2-H_2 and F_2O-H_2 reactions in most cases showing an over-all addition of H_2O vapor to calorimeter. (3) It is to be noted that part of the entering hydrogen reacts during the reaction period causing an over-all condensation of water during this part of the experiment. But the helium used for flushing the fuel from the fuel line causes removal of water from solution vessel.

Table 18

 m_{H_2O} Removed From Reaction Vessel

vs

 m'_{H_2O} Condensed In Vessel

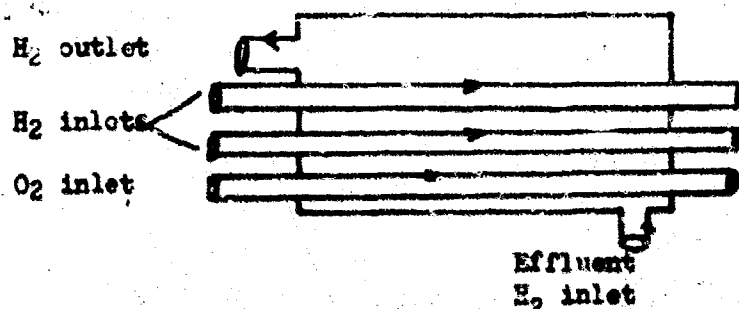
Expt. No.	Room Temp.	Cal. Temp		m_{H_2O}	m'_{H_2O}	$m'_{H_2O} - m_{H_2O}$
	°C	t_1 °C	t_f °C	g	g	g
Electrical Calibrations						
18	26	29.71	31.77	.8033	.5246	-.2787
19	26	28.98	31.77	.8084	.4813	-.3271
20	26.5	28.97	31.79	.7025	.4644	-.2381
21	27.0	28.18	31.78	.7478	.4637	-.2841
Oxygen Hydrogen Reaction						
35	26.2	28.98	31.75	.6680	.6483	-.0197
36	25.7	28.96	31.80	.6483	.7264	+.0781
37	27.4	28.97	31.89	.8313	1.0051	+.1738
40	25.5	28.97	31.66	.8676	.8887	+.0211
41	27.1	28.97	31.67	.9486	.9740	+.0245
42	25.9	28.97	31.67	.9345	.9461	+.0116
Oxygen Difluoride - Hydrogen Reaction						
23	24.5	28.97	31.81	.5466	.5656	+.0190
26	23.8	28.97	31.77	.7458	.7125	-.0323
27	24	28.99	31.75	.7069	.7288	+.0219
31	25	28.97	31.75	.6102	.6803	+.0703
32	25.9	29.11	31.90	.5034	.6186	+.1152
Fluorine - Hydrogen Reaction						
50	26	28.97	31.74	1.4000	1.0715	-.3285
51	27.7	29.66	31.80	1.2908	1.0127	-.2781
52	27.5	29.67	31.78	1.1670	1.0396	-.1274
54	25.0	29.66	31.83	.9910	.8310	-.1591
49	23.5	28.98	31.35	1.0987	1.0397	-.0590
56	26.8	29.82	31.74	.8431	.7853	-.0578
57	27.2	29.66	31.73	1.0606	.9551	-.1055
58	26.5	29.29	31.73	.9137	.8323	-.0814
59	23.8	28.97	31.64	.8322	.7700	-.0622

All of these factors influence $m_{\text{H}_2\text{O}}^i - m_{\text{H}_2\text{O}}^f$ for the $\text{F}_2\text{-H}_2$ reaction, in addition to the fact (5) that per mole fluorine requires for reaction only one mole of hydrogen, causing less water to be condensed in the solution vessel. This larger amount of effluent hydrogen, and the helium used for flushing fluorine from the fuel line, remove an amount of water from the calorimeter which more than compensates for the water condensed by the reacted hydrogen. This results in a net removal of water from the solution vessel. It is believed that, in spite of our inability to adjust $m_{\text{H}_2\text{O}}^i - m_{\text{H}_2\text{O}}^f$ to zero, saturating the entering hydrogen with water does improve the experimental procedures.

The attempt to saturate the hydrogen with water possibly could be improved by (1) thermostating the bubblers at the average temperature of the calorimeter, (2) measuring carefully the amount of helium used, and (3) calibrating the calorimeter, using no gas flow.

6.2. Correction for the Tempering the Gases

The heat exchanger for the inlet and outflowing gases is a simple version of the shell-and-tube heat exchangers which are discussed in various books on heat transfer [43,44]. In these books, heat-exchange equations are derived for more complicated exchangers than the one used on the present reaction vessel. Therefore, these equations are not considered further. To obtain the correction necessary for the tempering or preheating of the gases, each gas used in the experiment is considered separately, on the basis of whether it enters and leaves the calorimeter, or enters the calorimeter and is reacted. During the initial (hydrogen) and final (helium and hydrogen) drift periods, the gases enter and leave the calorimeter without reaction. In the reaction period, the oxygen and part of the hydrogen are reacted. The sketch below shows how the gases enter and leave the exchanger.



(Arrows indicate direction of flow of gases)

The gases at room temperature (t_r) are brought into the calorimeter and preheated or tempered up to the reference temperature ($t_{r,1}$). The reference temperature is the temperature at which the reaction is conducted. It is equivalent to t_{av} , the mid temperature between the

initial and final temperatures of the calorimeter. Upon leaving the calorimeter, the gases are cooled from t_{ref} to some temperature, t_{out} . t_{out} is not measured in the experiment. Here, it is assumed that t_{out} is equal to the temperature of the entering gases at the calorimeter boundary. This means that if a gas enters and leaves the calorimeter, it carries no heat from the calorimeter. In this case, q_{temp} . (See Table 5) is zero for an effluent gas which enters the calorimeter, but is not zero for the reactants, and for the products which are removed from the calorimeter.

In these experiments all of the products remained in the calorimeter. Using the oxygen-hydrogen reaction as an example, q_{temp} . can be derived as follows:

Oxygen:

$n_{O_2}^{reacted}$ - number of moles of oxygen entering calorimeter

$n_{O_2}^{exit}$ - number of moles of oxygen leaving calorimeter = 0

$C_p(O_2)$ - heat capacity of oxygen

t_r - room temperature

t_{ref} - t_{av} . (See Table 4)

$$q_{O_2}^{absorbed} = n_{O_2}^{reacted} \times C_p(O_2) \times (t_{ref} - t_r)$$

$$q_{O_2}^{absorbed} = q_{O_2}^{temp.} \quad (\text{because } n_{O_2}^{exit} = \text{zero})$$

Hydrogen:

$n_{H_2}^{exit}$ - number of moles of effluent hydrogen

$n_{H_2}^{ent}$ - number of moles of hydrogen entering reaction vessel

$C_p(H_2)$ - heat capacity of hydrogen

$q_{H_2}^{rel.}$ - amount of heat released by hydrogen upon leaving the calorimeter

$$q_{\text{absorbed}}^{\text{H}_2} = n_{\text{H}_2}^{\text{out}} \times C_p(\text{H}_2) \times (t_{\text{ref}} - t_r)$$

$$\begin{aligned} q_{\text{rel.}}^{\text{H}_2} &= n_{\text{H}_2}^{\text{exit}} \times C_p(\text{H}_2) \times (t_{\text{ref}} - t_{\text{out}}) \\ &= (n_{\text{H}_2}^{\text{ent}} - n_{\text{H}_2}^{\text{reacted}}) \times C_p(\text{H}_2) \times (t_{\text{ref}} - t_{\text{out}}) \end{aligned}$$

$$\begin{aligned} q_{\text{absorbed}}^{\text{H}_2} - q_{\text{rel.}}^{\text{H}_2} &= q_{\text{temp.}}^{\text{H}_2} \\ &= n_{\text{H}_2}^{\text{reacted}} \times C_p(\text{H}_2) \times (t_{\text{ref}} - t_r) \end{aligned}$$

The number of moles of hydrogen reacted is calculated from the quantity of oxygen reacted, which is measured.

References

- [1] H. V. Wartenberg and G. Z. Klinkott, Z. anorg. u. allgem. Chem. 193, 409 (1930).
- [2] O. Ruff and W. Menzel, Z. anorg. u. allgem. Chem. 190, 257 (1930).
- [3] W. R. Bisbee, J. V. Hamilton, R. Rushworth, T. J. Houser, and J. M. Gerhauser, Advan. Chem. Ser. 54, 215 (1965).
- [4] W. H. Evans, T. R. Munson, and D. D. Wagman, J. Research Natl. Bur. Standards 55, 147 (1955).
- [5] Natl. Bur. Standards Report 9389, July 1, 1966.
- [6] JANAF Thermochemical Tables, Dow Chemical Co., Midland, Michigan, (Clearinghouse for Federal Scientific and Technical Information Springfield, Va., Aug. 1966).
- [7] D. D. Wagman, W. H. Evans, I. Halow, V. B. Parker, S. M. Bailey, and R. H. Schumm, "Selected Values of Chemical Thermodynamic Properties, Part 1. Tables for the First Twenty-Three Elements in the Standard Order of Arrangement," NBS Tech. Note 270-1, (U. S. Government Printing Office, Washington, D. C., 1965).
- [8] P. Lebeau and A. Damiens, Compt. rend 185, 652 (1927); 188, 1253 (1929).
- [9] G. T. Armstrong, Chapter 7, Experimental Thermochemistry, Vol. II., ed. H. A. Skinner (Interscience Publishers, Inc., New York, N. Y., 1962).
- [10] J. C. Brosheer, F. A. Lenfesty, and K. L. Ellmore, Ind. and Eng. Chem. 39, 423 (1947).
- [11] H. C. Dickinson, Bull. Bur. Standards 11, 189 (1914).
- [12] E. J. Prosen, W. H. Johnson, and F. Y. Pergiel, J. Research Natl. Bur. Standards 62, 43 (1959).
- [13] R. S. Jessup, Precise Measurement of Heat of Combustion with a Bomb Calorimeter, NBS Mono. 7, Feb. 26, 1960.
- [14] E. D. West and D. C. Ginnings, The Review of Scientific Instruments 28, 1070 (1957).
- [15] D. C. Ginnings and E. D. West, The Review of Scientific Instruments 35, 965 (1964).

- [16] N. S. Osborne, H. F. Stimson and D. C. Ginnings, J. Research Natl. Bur. Standards 23, 197 (1939).
- [17] K. L. Churney and G. T. Armstrong, manuscript to be published.
- [18] H. C. Shomate, "Computer Calculations of Combustion Bomb Calorimetric Data," Technical Progress Report 327, NOTS TP 3288, U. S. Naval Ordnance Test Station, China Lake, Calif., August 1963.
- [19] W. R. Kesting, General Chemical Division, Allied Chem. Corp., Baton Rouge, La., private communication.
- [20] W. R. Kesting, J. E. Crosslin, and B. W. Bridwell, "Analysis of Oxygen Difluoride," Report of the Analytical Chemistry Working Group, 22nd Meeting, ed. John W. Gunn, Jr. (Chemical Propulsion Information Agency, Nov. 3, 1965.)
- [21] H. I. Bernstein, and J. Powling, J. Chem. Phys. 18, 685 (1950).
- [22] E. A. Jones, J. S. Kirby-Smith, P. J. H. Woltz, and A. H. Nielsen, J. Chem. Phys. 19, 337 (1951).
- [23] F. D. Rossini, J. Research Natl. Bur. Standards 6, 1 (1931).
- [24] O. Menis, ed. "Analytical Coordination Chemistry: Titrimetry, Gravimetry, Flame Photometry, Spectrophotometry, Gas Evolution and Isotopic Preparation", Natl. Bur. Standards Tech. Note 402, (U.S. Govt. Printing Office, Washington, D.C., 1966).
- [25] T. Thorvaldson and E. C. Bailey, Can. J. of Research 24, 51 (1946).
- [26] G. Waddington, S. Sunner, and W. N. Hubbard, Chapter 7, Experimental Thermochemistry, Vol. I, ed. F. D. Rossini (Interscience Publishers, Inc., New York, N.Y. 1956).
- [27] Anton B. Burg, "Volatile Inorganic Fluorides", Fluorine Chemistry, Vol. I, ed. J. H. Simons (Academic Press, Inc., N. Y. 1950).
- [28] L. A. Bigelow, Chem. Revs. 40, 110 (1947).
- [29] H. Schuler and H. J. Schumacher, Z. anorg. u. allgem. Chem. 245, 221, (1940).
- [30] R. L. Harris, Union Carbide Corp., Nuclear Division, Paducah, Kentucky, private communication.
- [31] G. Kyriacos and C. E. Boord, Anal. Chem. 29, 787 (1957).

- [32] A. E. Cameron and E. Wichers, J. Am. Chem. Soc. 84, 4175 (1962).
- [33] H. F. Priest and A. V. Grosse, Ind. and Eng. Chem. 39, 431 (1947).
- [34] F. D. Rossini, Chapter 4, Experimental Thermochemistry, ed. F. D. Rossini (Interscience Publishers, Inc. New York, N.Y. 1956).
- [35] H. V. Wartenberg and H. Schütza, Z. anorg. u. allgem. Chem. 206, 65 (1932).
- [36] F. D. Rossini, D. D. Wagman, W. H. Evans, S. Levine, and I. Jaffe, Selected Values of Chemical Thermodynamic Properties, NBS Circular 500, (U. S. Govt. Printing Office, Washington, D.C. 1952).
- [37] H. M. Feder, W. N. Hubbard, S. S. Wise, and J. L. Margrave, J. Phys. Chem. 67, 1148 (1963).
- [38] J. D. Cox and D. Harrop, Trans. Faraday Soc. 61, 1328 (1965).
- [39] G. C. Sinke, J. Phys. Chem. 71, 359 (1967).
- [40] E. S. Domalski and G. T. Armstrong, J. Research Natl. Bur. Standards 71A, No. 2 Issue, 1967, (in press).
- [41] E. S. Domalski and G. T. Armstrong, J. Research Natl. Bur. Standards 71A, No. 3 Issue, 1967, (in press).
- [42] G. Pilcher, H. A. Skinner, A. S. Pell, and A. E. Pope, Trans. Faraday Soc. 59, 316 (1963).
- [43] M. Jakob, Heat Transfer, pp. 227-260, (John Wiley and Sons, Inc. New York, 1957).
- [44] William McAdams, Heat Transmission, pp. 230, 346, (McGraw-Hill Book Co., New York, 1942).

DOCUMENT CONTROL DATA - R&D

<p>(Security classification of title, body of abstract and indexing annotation must be entered when the overall report is classified.)</p> <p>1. ORIGINATING ACTIVITY (Corporate author) National Bureau of Standards B3C Physics Building Washington, D. C. 20234</p>			<p>2A. REPORT SECURITY CLASSIFICATION <input checked="" type="checkbox"/> Unclassified Other - Specify _____</p> <p>2B. GROUP _____</p>		
<p>3. REPORT TITLE PRELIMINARY REPORT ON THE THERMODYNAMIC PROPERTIES OF SELECTED LIGHT-ELEMENT AND SOME RELATED COMPOUNDS</p>					
<p>4. DESCRIPTIVE NOTES (Type of report and inclusive dates) <input checked="" type="checkbox"/> Scientific Report <input type="checkbox"/> Final Report <input type="checkbox"/> Journal Article <input type="checkbox"/> Proceedings <input type="checkbox"/> Book <input type="checkbox"/> Interim</p>					
<p>5. AUTHOR(S) (Last name, first name, initial) Charles W Beckett Thomas B Douglas</p>					
<p>6. REPORT DATE AS PRINTED 1 January 1967</p>		<p>7A. TOTAL NO. OF PAGES 237</p>		<p>7B. NO. OF REFS 245</p>	
<p>8A. CONTRACT OR GRANT NO. ISSA-65-8</p>		<p>9A. ORIGINATOR'S REPORT NUMBER(S) (if given) NBS Report 9500</p>			
<p>B. PROJECT NO. 9713-02</p>		<p>9B. OTHER REPORT NO. (if any other numbers than 9A. are associated with this report) AFOSR 67-0891 AD</p>			
<p>C. 61415014</p>		<p>D. 681308</p>			
<p>10. AVAILABILITY/LIMITATION NOTICES Distribution of this document is restricted <i>Statement</i> <i>2</i> <input type="checkbox"/> Available from DDC <input type="checkbox"/> Available from CFSTI <input type="checkbox"/> Available from Source <input type="checkbox"/> Available Commercially</p>					
<p>11. SUPPLEMENTARY NOTES (Citation) TECH, OTHER</p>			<p>12. SPONSORING MILITARY ACTIVITY AF Office of Scientific Research (SREP) Office of Aerospace Research Washington, D. C. 20333</p>		
<p>13. ABSTRACT Thermodynamic and related properties of substances important in current high-temperature research and development activities are being investigated under contract with the U.S. Air Force Office of Scientific Research (USAF Order No. OAR ISSA 65-8) and the Advanced Research Projects Agency (ARPA Order No. 20). This research program is a direct contribution to the Interagency Chemical Rocket Propulsion Group, Working Group on Thermochemistry, and, often simultaneously, to other organizations oriented toward acquiring the basic information needed to solve not only the technical problems in propulsion but also those associated with ballistics, reentry, and high-strength high-temperature materials. For given substances this needed basic information comprises an ensemble of closely related properties being determined by a rather extensive array of experimental and theoretical techniques. Some of these techniques, by relating thermodynamic properties to molecular or crystal structure, make it possible to tabulate these properties over far wider ranges of temperature and pressure than those actually employed in the basic investigations. (U) This report presents improved values for the heats of formation and some other thermodynamic properties of a number of light-element substances -- resulting from recent NBS experimental studies (calorimetric, vaporization, and spectroscopic) and critical literature review. Methods, results, and earlier published values are discussed critically and in detail. The standard heat of formation of $\text{BF}_3(\text{g})$ was determined by direct combination of the elements in a bomb calorimeter and with an estimated error of $\pm 0.5 \text{ kcal mol}^{-1}$. $\text{OF}_2(\text{g})$ was found to be endothermic ($+5.86 \pm 0.3 \text{ kcal mol}^{-1}$) from flame calorimetry on the reactions of OF_2, O_2, and F_2 with H_2.</p>					

Security Classification

KEY WORDS

Experimental Research
Literature Reviews and Critical Data Analysis
Thermodynamic Properties
Light-element Compounds
Propulsion-combustion Products
Calorimetry, Equilibrium Studies and Spectroscopy
High Temperatures and Fast Measurements
Mass Spectrometry

[illegible]

INSTRUCTIONS

1. **ORIGINATING ACTIVITY:** Enter the name and address of the contractor, subcontractor, grantee, Department of Defense activity or other organization (corporate author) issuing the report.

- REPORT SECURITY CLASSIFICATION: Enter the overall security classification of the report. Indicate whether "Restricted Data" is included. Marking is to be in accordance with appropriate security regulations.

- GROUP: Automatic downgrading is specified in DoD Directive 5200.10 and Armed Forces Industrial Manual. Show the group number. Also, when applicable, show that signal markings have been used for Group 3 and Group 4 authorized.

- REPORT TITLE:** Enter the complete report title in all capital letters. Titles in all cases should be unclassified. A meaningless title cannot be selected without classification. Show title classification in all capitals in parenthesis immediately following the title.

1. **DESCRIPTIVE NOTES:** If appropriate, enter the type of report, e.g., interim, progress, summary, annual, or final. Give the inclusive dates when a specific reporting period is covered.

5. **AUTHOR(S):** Enter the name(s) of author(s) as shown on
in the report. Enter last name, first name, middle initial.
of military, show rank and branch of service. The name of
the principal author is an absolute minimum requirement.

1. **REPORT DATE:** Enter the date of the report as day, month, year, or month, year. If more than one date appears in the report, use date of publication.

13. TOTAL NUMBER OF PAGES: The total page count should follow normal pagination procedures, i.e., enter the number of pages containing information.

16. NUMBER OF REFERENCES: Enter the total number of references cited in the report. 12

12. **CONTRACT OR GRANT NUMBER:** If appropriate, enter the applicable number of the contract or grant under which the report was written.

- 3b. 3c. A 2d. **PROJECT NUMBER:** Enter the appropriate military department identification, such as project number, sub-project number, 57 ten numbers, task number, etc.

14. ORIGINATOR REPORT NUMBER(S) Enter the official report number by which the document will be identified and controlled by the originating activity. This number must be unique to this report.

10. OTHER REPORT NUMBER(S): If the report has been assigned any other report numbers (either by the originator or by the sponsor), also enter this number(s).

9. AVAILABLE CITATION NOTICES. Enter any limitations on the citation of the report, other than

those imposed by security classification using standard statements such as:

- (1. "Qualified requesters may obtain copies of this report from DDC."

- (2) "Foreign announcement and dissemination of this report by DDC is not authorized."

- (3) "U. S. Government agencies may obtain copies of this report directly from DDC. Other qualified DDC users, at all request through

- (4) "U. S. military agencies may obtain copies of this report directly from DDC. Other qualified users shall request through

- (S) "All distribution of this report is controlled. Only authorized DDC users shall request through

If the report has been furnished to the Office of Technical Services, Department of Commerce, for sale to the public, indicate this fact and enter the price, if known.

11. SUPPLEMENTARY NOTES: Use for additional explanatory notes.

12. **SPONSORING MILITARY ACTIVITY** Enter the name of the departmental project office or laboratory sponsoring (or proposing) the research, and development. Include address.

13. **ABSTRACT:** Enter an abstract giving a brief and factual summary of the document indicative of the report, even though it may also appear elsewhere in the body of the technical report. If additional space is required, a continuation sheet shall be attached.

It is highly desirable that the abstract of classified reports be unclassified. Each paragraph of the abstract shall end with an indication of the military security classification of the information in the paragraph, represented as (GS), (S), (C), or (U).

There is no limitation on the length of the abstract. However, the suggested length is from 150 to 225 words.

14. **KEY WORDS:** Key words are technically meaningful terms or short phrases that characterize a report and may be used in index entries for cataloging the report. Key words must be selected so that no security classification is required. Identifiers, such as equipment model designation, trade name, military project code name, geographic location, may be used as key words but will be followed by an indication of technical context. The assignment of links, roles, and weights is optional.

UNCLASSIFIED

Section 5 Classifications

Best Available Copy

UNCLASSIFIED

DD FORM 1473, 1 Jan 64

13 ABSTRACT

(CONTINUED)

The results of a precise entrainment (transpiration) study of the sublimation of $AlF_3(c)$ were combined with published data to give new values for the thermodynamic properties of $AlF_3(g)$ and $AlF_6(g)$. A final revised report on high-temperature mass spectrometry of the BeO - BeF_2 system discusses interfering ion intensities, and evaluates the heat of sublimation of $BeF_2(g)$ and the standard heat of formation of $Be_2OF_2(g)$. A quadrupole mass spectrometer appears to have shown that liquid Al_2O_3 loses oxygen and becomes non-stoichiometric, a result consistent with the earlier NBS discovery of an irreversible change in sublimed $Al_2O_3(c)$. To illustrate light-element hydroxide molecules, $CsOH(g)$ and $CsOD(g)$ showed high-temperature microwave spectra indicative of a linear or near-linear molecule, a low-frequency large-amplitude bending vibration producing an unusual variation in the rotational constant, and a highly ionic Cs-O bond. The dipole moment also was derived. From the current revision of NBS Circular 500, recommended values of ΔH_{298}° for 39 Be-containing substances (including different states) of special interest are given, together with discussions of the underlying published data. Recent design and experimental studies have led to a proposed feasible procedure for automatic power measurement to complement the existing NBS automatic temperature measurement in precise low-temperature heat-capacity calorimetry. (U)